



CLIMATE CHANGE IMPACT ON THE PHOTODEGRADATION OF POLYCYCLIC AROMATIC HYDROCARBONS IN SOILS

Montserrat Marquès Bueno

ADVERTIMENT. L'accés als continguts d'aquesta tesi doctoral i la seva utilització ha de respectar els drets de la persona autora. Pot ser utilitzada per a consulta o estudi personal, així com en activitats o materials d'investigació i docència en els termes establerts a l'art. 32 del Text Refós de la Llei de Propietat Intel·lectual (RDL 1/1996). Per altres utilitzacions es requereix l'autorització prèvia i expressa de la persona autora. En qualsevol cas, en la utilització dels seus continguts caldrà indicar de forma clara el nom i cognoms de la persona autora i el títol de la tesi doctoral. No s'autoritza la seva reproducció o altres formes d'explotació efectuades amb finalitats de lucre ni la seva comunicació pública des d'un lloc aliè al servei TDX. Tampoc s'autoritza la presentació del seu contingut en una finestra o marc aliè a TDX (framing). Aquesta reserva de drets afecta tant als continguts de la tesi com als seus resums i índexs.

ADVERTENCIA. El acceso a los contenidos de esta tesis doctoral y su utilización debe respetar los derechos de la persona autora. Puede ser utilizada para consulta o estudio personal, así como en actividades o materiales de investigación y docencia en los términos establecidos en el art. 32 del Texto Refundido de la Ley de Propiedad Intelectual (RDL 1/1996). Para otros usos se requiere la autorización previa y expresa de la persona autora. En cualquier caso, en la utilización de sus contenidos se deberá indicar de forma clara el nombre y apellidos de la persona autora y el título de la tesis doctoral. No se autoriza su reproducción u otras formas de explotación efectuadas con fines lucrativos ni su comunicación pública desde un sitio ajeno al servicio TDR. Tampoco se autoriza la presentación de su contenido en una ventana o marco ajeno a TDR (framing). Esta reserva de derechos afecta tanto al contenido de la tesis como a sus resúmenes e índices.

WARNING. Access to the contents of this doctoral thesis and its use must respect the rights of the author. It can be used for reference or private study, as well as research and learning activities or materials in the terms established by the 32nd article of the Spanish Consolidated Copyright Act (RDL 1/1996). Express and previous authorization of the author is required for any other uses. In any case, when using its content, full name of the author and title of the thesis must be clearly indicated. Reproduction or other forms of for profit use or public communication from outside TDX service is not allowed. Presentation of its content in a window or frame external to TDX (framing) is not authorized either. These rights affect both the content of the thesis and its abstracts and indexes.



UNIVERSITAT
ROVIRA I VIRGILI

Climate change impact on the photodegradation of polycyclic aromatic hydrocarbons in soils

MONTSE MARQUÈS BUENO



DOCTORAL THESIS

2017

Montse Marquès Bueno

CLIMATE CHANGE IMPACT ON THE PHOTODEGRADATION OF POLYCYCLIC AROMATIC HYDROCARBONS IN SOILS

DOCTORAL THESIS

Supervised by

Prof. Josep Lluís Domingo

Dr. Montse Mari

Dr. Martí Nadal

Department of Chemical Engineering



UNIVERSITAT ROVIRA I VIRGILI

Tarragona, 2017



Department of Chemical Engineering
Països Catalans, 26
43007 Tarragona

Dr. Martí Nadal, Dr. Montse Mari and Prof. Josep Lluís Domingo, researchers at the Laboratory of Toxicology and Environmental Health, Universitat Rovira i Virgili

CERTIFY

That the present doctoral thesis, entitled "Climate change impact on the photodegradation of polycyclic aromatic hydrocarbons in soils" presented by Montse Marquès Bueno for the award of the degree of Doctor, has been carried out under our supervision at the Department of Chemical Engineering at Universitat Rovira i Virgili, and it fulfills all the requirements to be eligible for the Distinction of International Doctor.

Tarragona, April 2017

Prof. Josep Lluís Domingo

Dr. Montse Mari

Dr. Martí Nadal

*Als meus pares,
i als meus avis que ja no hi són.*

AKNOWLEDGEMENTS/AGRAÏMENTS

Si n'és de complicat donar-vos les gràcies a tots els que m'heu acompanyat en aquesta carrera de fons... de tot cor: GRÀCIES, GRÀCIES i més GRÀAAAACIES a TOTS! Aquesta tesi també és de tots i cadascun de vosaltres.

Primer de tot, vull agrair a la Marta Schuhmacher que m'obris les portes de l'AGA el dia que vaig anar a parlar amb ella interessant-me per fer el treball final de màster, i la possibilitat de continuar amb el doctorat. Gràcies per posar-me en contacte amb el Martí Nadal, el que es va acabar convertint amb el meu director de tesi. Gràcies Martí per confiar en mi per treballar en el marc del projecte del Ministeri. Per donar-me la possibilitat de formar-me dins i fora del grup, i per trobar sempre diners per finançar els experiments i nombrosos congressos que he assistit al llarg de la tesi. Gràcies per la teva consideració i per apretar amb els *deadlines*, si no hagués estat així estic segura de que no haguéssim arribat a on estem. Infinites gràcies a la Montse Mari, per tenir tanta paciència i aguantar les meves crisis quan les coses no sortien bé al principi. Per aconsellar-me sempre que ho he necessitat i valorar tot el que he aconseguit al llarg de la tesi. Ha estat molt guai ser la teva primera doctorand! Gràcies al Jordi, el director moral. Per ser un pou de ciència i de qualitat humana. Gràcies per haver estat sempre disposat a assegurar-me a entendre els resultats, per tot el que m'has ensenyat i has aportat a aquesta tesi.

Gràcies als *jefes* Francesc Castells (de l'AGA juntament amb la Marta), i el Dr. Domingo (TecnATox), també director d'aquesta tesi, per acollir-me a "casa" vostra.

Thanks Roland for giving me the opportunity to perform the stay in The University Centre in Svalbard (UNIS) and The Norwegian University of Life Science (NMBU). Living in the Arctic is the most amazing experience that I have had!

I a tots els que ens veiem cada dia: gràcies per la vostra empatia, per aconseguir que desconnecti quan fem el "café" i arreglem el món plegats. A la galleguinha Carminha, un placer estirar el cuello y verte entre pantalla y estantería ;-). Gracias por entenderme siempre tan bien, querida! Al Quim, perquè estàs sempre disposat a donar un cop de mà. A Vikas, no dejes nunca de explicarnos tantas cosas en el *Coffebook*. A la Gemma, gràcies per pensar sempre en els doctorands, per ser una mina de convocatòries i defensora del que és just. Tornem a Nantes a fer una *galette*?

A Renato *du Brasil*, por enseñarme que no todo es trabajar, que también hay que disfrutar! ;-) Gracias por estar ahí estos últimos meses de estrés máximo, y por tu ayuda en la recta final experimental. Estoy segura de que te echaremos todos muchíiiiisimo de menos! ☺ To all PhD students from AGA: Fran, Noelia, Raju and Venkat. Good luck in your last year. Although I am really stressed it's so grateful to see how you reap the benefits of your hard work. So, come on! You all are almost PhD already! ☺. Gracias Fran por competir conmigo a ver quién es más gafe ;-) y a Noelia, gracias por todos los momentos compartidos entre reuniones, muestreos, triaje... y conversaciones de cremas antiarrugas para contrarestar los efectos de la tesis. Raju, it is a pleasure to have you as a lab mate. Thanks for being always so kind. Venkat, you will be the next presenting thesis ;-) I a les dues més noves, reusenques d'adopció: María Ángeles i Neus. Molta força en aquesta etapa que fa poc que heu començat! Espero que, tot i que hi ha moments de tot al llarg de la tesi, gaudiu de la recerca com ho faig jo.

Thank you to Tatiana for sharing our crying moments when working with PAHs. Sampling in Pyramiden was so funny! Jessica, thanks for the technical assistance during my stay in Svalbard.

A tots els companys de l'AGA que ja no hi són: gràcies nois! Fatima, thanks for introducing me to the scientific world and become more than my master thesis supervisor. I was so lucky and I'm still missing you so much! ☺ A la Neus, gràcies per haver estat sempre al meu costat dins i fora de l'AGA. Per preocupar-te per com m'anaven els experiments, i evidentment, per venir a Svalbard ;-). Al Francesc, per ensenyar-me a fer columnes aquell juliol del 2013... i per la calma i harmonia que vas aportar al grup. A l'Amores, per totes les converses entre carmanyoles. A l'Ana Passuello, l'any que ve tornes a venir per Santa Tecla? To Sofia, for sharing all your knowledge about PAHs, and also some glasses of wine in Bordeaux. To Eskinder, it was short but nice to have the workplace next to you. A les exreusenques: Isabel, Gemma Perelló i Lolita. I a tots els visitants que heu passat per l'AGA-TecnATox: gràcies per la vostra companyia i per internacionalitzar-nos! En especial al Dani, un plaer supervisar el teu TFM.

A la Irene Maijó dels SRCiT, moltíssimes gràcies per tot el suport i incondicional ajuda. Per la teva paciència i ensenyar-me tant sobre cromatografia. Per trobar

sempre un forat a l'apretada agenda del GC-MS per analitzar les meves mostres, per contestar les meves infinites preguntes i per tenir tan bon rotllo. A la Rosa Ras, gràcies per la teva amabilitat, eficàcia i qualitat treballant.

Al Borràs per ser com el "papa" dels laboratoris de recerca i trobar sempre solucions a tots els nostres problemes, especialment per la teva implicació en totes les "baralles" que hem tingut amb comercials. Ana Montero, gracias por abrirme siempre el 301 y dejarme la mufla. Y por visitarnos cuando hacemos triaje. I a la Susana, per també deixar-me la mufla quan la de docència em va resultar petita. Ja veus que gastem vidre de bona qualitat! A veure quan repetim una sortida amb la família al complet ;-)

A la Pepa, gràcies per ser una més del grup a efectes socials. Per preocupar-te sempre de que les nostres panxes estiguin contentes. A la Carme Audí, per tenir tanta energia i ensenyar-me què és treballar de valent i amb rigor. Gràcies per preocupar-te sempre tant per la tesi com per mi.

Infinites gràcies amics i família. Segurament sou els que us heu emportat la pitjor part d'aquesta tesi: discursos inacabables sobre els PAHs, cabòries, absència... quines ganes que tinc de disposar de més temps lliure per gaudir-vos de veritat!

Moltiiiiissimes gràcies a les meves amigues de tota la vida: Sònia, Pàmies i Gal-la (des dels 3!), i també l'Elena i l'Alba (que ja fa una bona colla d'anys que ens coneixem). Per animar-me sempre i estar tan contentes com jo quan he anat recollint els fruits d'aquests darrers anys. Gràcies al *Consejo* i als *Rumberos*, per amenitzar molts caps de setmana amb uns bons sopars de pedres, vi i música. En especial a la Marta per escoltar-me sempre i seguir com anaven sortint els resultats de ben a prop. Menuda amiga friki que tienes! A la Sílvia, per ser tan generosa i ser-hi quan t'he necessitat, a la Natàlia, per contagiar la teva alegria fins i tot quan he estat en crisi doctoral-existencial, i a Paula: la bondat en persona que està pendent de tot i de tothom. Valeu el vostre pes en or! A les de la carrera, en especial a la Laura, l'Angie i l'Ester, que tot i estar geogràficament disperses la trobada anual no falla. I la pregunta de: "Quan defenses la tesi, Montse?" tampoc. A la Sandra i l'Alba perquè per temps que passi sempre és com si ens haguéssim vist ahir. El que va unir el MEAPS que no ho separi ningú! També gràcies a la colla de l'Oriol per preguntar-me sempre pel doctorat. En especial a la Maria pels teus consells, i a la Neus, no ens n'adonarem que ja seràs doctora tu també!

A l'Eduard, per estar orgullós de les teves nebodes científiques. Per totes les converses de canvi climàtic, fotografia, Svalbard, Lofoten, Féroes... jo de gran vull ser com tu! Quan dius que anem al restaurant del far de Cap de Creus? ;-)

I finalment, gràcies papa i mama. Gràcies per l'educació que m'heu donat dins i fora de casa que m'ha capacitat per anar per aquest món. Per respectar que sigui perseverant, perfeccionista, i fins i tot obsessiva en els estudis/feina. Gràcies per tenir tanta paciència quan estic ofuscada. A la Maria del Mar, encara que has viscut la tesi estant físicament lluny, gràcies per escoltar-me i assessorar-me quan t'ho he demanat. I al Xavi, gràcies per enrecordar-te'n sempre del teu *corazón*.

Oriol, gràcies per intentar entendre els PAHs, la fotodegradació i què passava amb les columnes quan es trencaven. Gràcies per la canya quan ha estat necessària i pels quilòmetres recorreguts en busca de desconexió. Que els dos estiguem escrivint la tesi a la mateixa època ha estat bonic i complicat a la vegada. Ànims que ja queda poc, Dr. Casanovas-Marsal!

**IT ALWAYS SEEMS
IMPOSSIBLE
UNTIL IT'S DONE**

Nelson Mandela

TABLE OF CONTENTS

SUMMARY	XV
SUMMARY	XVII
RESUM	XXIII
INTRODUCTION	1
1. Climate change and POPs	3
2. PAHs	5
2.1 Physicochemical properties	7
3. PAHs in the environment	8
3.1 Emission sources	8
3.2 PAHs fate	8
3.3 PAHs in surface soils	10
3.4 PAHs in water and sediments	10
3.5 PAHs in biota	11
4. Environmental transformation and degradation of PAHs	11
4.1 Biological degradation	12
4.2 Chemical degradation	13
4.3 Photodegradation	14
HYPOTHESIS & OBJECTIVES	17
CHAPTER 1	21
ABSTRACT	23
INTRODUCTION	24
CLIMATE CHANGE IMPACT ON POPs	28
CONCLUSIONS	42
REFERENCES	43
DISCUSSION CHAPTER 1	50
CHAPTER 2	51
ABSTRACT	53
INTRODUCTION	54
MATERIALS AND METHODS	55

RESULTS AND DISCUSSION	60
CONCLUSIONS	69
REFERENCES	70
DISCUSSION CHAPTER 2	74
CHAPTER 3	75
ABSTRACT	77
INTRODUCTION	78
MATERIALS AND METHODS.....	79
RESULTS AND DISCUSSION	83
CONCLUSIONS	91
REFERENCES	92
DISCUSSION CHAPTER 3	95
CHAPTER 4	97
ABSTRACT	99
INTRODUCTION	100
MATERIALS AND METHODS.....	102
RESULTS AND DISCUSSION	106
CONCLUSIONS	121
REFERENCES	122
DISCUSSION CHAPTER 4	127
CHAPTER 5	129
ABSTRACT	131
INTRODUCTION	132
MATERIALS AND METHODS.....	133
RESULTS AND DISCUSSION	136
CONCLUSIONS	151
REFERENCES	152
DISCUSSION CHAPTER 5	157
CHAPTER 6	159
ABSTRACT	161
INTRODUCTION	162

MATERIALS AND METHODS.....	163
RESULTS AND DISCUSSION	166
CONCLUSIONS	179
REFERENCES	180
DISCUSSION CHAPTER 6	186
GENERAL DISCUSSION	189
CONCLUSIONS	195
REFERENCES	199
ANNEX.....	207
ANNEX 1 – Supporting information chapter 2.....	209
ANNEX 2 – Supporting information chapter 3.....	213
ANNEX 3 – Supporting information chapter 4.....	215
ANNEX 4 – Supporting information chapter 5.....	219
ANNEX 5 – Supporting information chapter 6.....	225

SUMMARY

SUMMARY

Due to the increasing emission of greenhouse gases, the Earth's climate is substantially changing faster according to the periodic assessments of the Intergovernmental Panel on Climate Change (IPCC). It has been confirmed that the global mean temperature increased by $0.6\pm 0.2^{\circ}\text{C}$ during the 20th century, while it is projected to increase up to $1.8\text{-}4.0^{\circ}\text{C}$ by the end of the 21st century, under a range of probable greenhouse gas emission scenarios. Moreover, the increase in the surface UV-B radiation, induced by ozone depletion, has received wide attention as an environmental issue of great concern. High latitude regions, such as Arctic or Antarctic, are those more severely affected. However, the Mediterranean region is also pointed out as a vulnerable zone, because it lays in the transition between high and low latitude processes. Therefore, the impact of climate change on the environment has become a topic of notable concern, not only globally but also locally.

Temperature and UV-B radiation are key parameters that may alter the fate and behavior of a wide range of chemicals, such as persistent organic pollutants (POPs). Because of their toxicity, resistance to degradation, potential to be bioaccumulated and ability to be transported over long distances POPs are chemicals of concern. Other semi-volatile organic compounds (SVOCs) have also received wide attention, such as polycyclic aromatic hydrocarbons (PAHs). In addition to their potential toxicity and environmental occurrence, they have a photosensitive nature, and therefore, are vulnerable to climate change.

The present thesis was aimed at studying the impact of an increase of temperature and light intensity on the fate of PAHs in Mediterranean soils. The monitoring of PAHs concentrations and ecotoxicity, as well as the identification of PAHs photodegradation by-products, was carried out at laboratory scale by the simulation of 2 climate scenarios: current and extreme climate change (RCP 8.5) for the Mediterranean region according to IPCC. In addition, a field experiment was also performed to assess the PAHs degradation under real Mediterranean conditions. Finally, PAHs levels were determined in soils collected in the Arctic, another vulnerable region to climate change.

In Chapter 1, the state of the art of the impact of climate change on environmental concentrations of POPs, as well as on human health risks, was reviewed. Climate change and POPs are of broad and current interest, for which further attention should be paid not only by scientists, but also by policy makers to adapt outdated regulations. Most of the studies performed so far were found to be focused on legacy POPs, such as polychlorinated dibenzo-*p*-dioxins and dibenzofurans (PCDD/Fs), polychlorinated biphenyls (PCBs) and pesticides. However, the number of investigations assessing the impact of climate change on the environmental levels of PAHs was limited. Some studies pointed out that as a result of the special photosensitivity of PAHs, more toxic photodegradation byproducts may be formed in the future, resulting in adverse health effects. This has become an unquestionable gap, which deserves further investigations.

Chapter 2 presents the results of a study on PAHs photodegradation in soils under the current Mediterranean climate scenario. Arenosol and fine-textured Regosol soils, representative of the typical Mediterranean soils, were spiked with PAHs and exposed to controlled conditions of temperature (20°C) and low light intensity (9.6 W m⁻²) for up to 28 days. Concentrations of PAHs were further monitored and supported with a Microtox® ecotoxicity assessment. In addition, hydrogen (H) isotopes of benzo(*a*)pyrene were analyzed to confirm its degradation. Photodegradation was found to be dependent on exposure time, specific physicochemical properties of each hydrocarbon, and soil texture. Sorption and photodegradation processes were more enhanced in fine-textured soil in comparison to Arenosol soil. Significant photodegradation rates were detected for a number of PAHs, namely phenanthrene, anthracene, benzo(*a*)pyrene, and indeno(123-*cd*)pyrene. Benzo(*a*)pyrene, commonly used as an indicator for PAH pollution, was below the limit of detection after 7 days of light exposure. The ecotoxicity assessment, showed a higher detoxification trend in fine-textured soil than in Arenosol soil, being in agreement with its higher photodegradation rates. Reported differences between both soils were mostly attributed to the higher content of metal oxides in fine-textured Regosol soil, as they may act as potential PAHs photocatalysts. Finally, the strong isotopic effect observed in benzo(*a*)pyrene suggested, on one hand, that compound-specific isotope analysis (CSIA) may be a powerful tool to monitor *in situ* degradation of PAHs, and on the other

hand, evidenced an unknown degradation process of benzo(*a*)pyrene simultaneously occurring in the darkness.

Chapter 3 was aimed at explaining the differences in PAHs photodegradation rates found between Arenosol and fine-textured soil in chapter 2. It was hypothesized that the main difference could be related to the photocatalysis caused by the joint impact of light exposure and Fe₂O₃ presence in soils. The catalysis contribution was mostly attributed to Fe₂O₃ because it is the most abundant metal oxide in both tested soils, being higher in Regosol than in Arenosol. Reported results showed that Fe₂O₃ had a significant effect on in the photocatalysis of fluorene, phenanthrene and benzo(*a*)pyrene. Therefore, Fe₂O₃ would not be the only responsible for the higher degree of PAHs photodegradation in fine-textured Regosol soil than in Arenosol soil. Soil is a complex matrix containing a number of elements, such as a wide range of metal oxides, humic acids, presenting a specific texture. Each one of these parameters has a specific role on PAHs fate.

In chapter 4, the potential impact of the temperature and light intensity increase on the fate of PAHs in surface soils was assessed. The environmental temperature was increased 4°C, according to IPCC RCP 8.5 scenario, while it was set a high light intensity (24 W m⁻²), being samples exposed during 28 days. As expected, low molecular weight PAHs were rapidly volatilized when increasing both temperature and light intensity. However, photodegradation of medium and high molecular weight PAHs increased in the coarse-textured Arenosol soil under the climate change scenario, while those rates did not show any variation in fine-textured Regosol soil, regardless the climate scenario. The lower content of metal oxides in Arenosol soil requires a higher temperature and light intensity to achieve a full photodegradation of PAHs, pointing out the potential impact of climate change. In turn, H isotopes confirmed that benzo(*a*)pyrene was degraded in the climate change scenario, not only under light but also in the darkness, as previously occurred in the current climate scenario. Finally, the number of by-products and required time to be formed was enhanced by the increase of temperature and light intensity. Consequently, in an expected climate change scenario, the human exposure to PAHs might decrease while that to PAHs degradation by-products, which might be even more toxic than native compounds, may increase.

Chapter 5 provides the evaluation of PAHs photodegradation in surface soil caused by solar radiation exposure. Solar intensity was up to 20-times higher than that emitted by common light lamps used for photodegradation studies at lab scale. Soil samples spiked with PAHs were deployed in a methacrylate box, and exposed to solar radiation for 7 days, meaning a total solar energy of 102.6 MJ m^{-2} . As hypothesized, individual PAHs were volatilized, sorbed and/or photodegraded, depending on their physicochemical properties and soil characteristics. Low and medium molecular weight PAHs were more sorbed and photodegraded in fine-textured Regosol soil, while a higher volatilization was observed in the coarse-textured Arenosol soil. In contrast, high molecular weight PAHs were more photodegraded in Arenosol soil, probably because of an enhanced light penetration in the coarse-textured soil. Specially high photodegradation rates and low half-lives were noted for anthracene, pyrene and benzo(*a*)pyrene, which had already been found to be the most sensitive to light exposure at laboratory scale. In addition to oxidation products of PAHs previously found at laboratory scale, new oxy-, as well as nitro- and hydro- PAHs, were also identified in the field study. The toxic and mutagenic potential of these PAHs by-products is usually higher than that of the 16 US EPA priority PAHs commonly monitored.

Finally, in chapter 6 results of a monitoring study to determine PAH concentrations in Arctic soils are presented. Pyramiden (Central Spitsbergen, Svalbard Archipelago) was selected because it is a potential contaminated site due to: i) the Long Range Atmospheric Transport (LRAT), ii) coal deposits, iii) previous coal-mining extraction, and iv) the current operating coal and diesel-based power plants in this settlement. Furthermore, trace elements were analyzed for further confirmation of anthropogenic pollution. PAHs profiles and molecular diagnostic ratios (MDRs) mostly indicated a common pyrogenic source: combustion in local power plants. However, the contribution of petrogenic sources due to the local geology should not be disregarded. The highest levels of PAHs and trace elements were found in soils close to power plants and those exposed to prevailing winds. Although PAH levels were higher than those found in the scientific literature, they only exceeded target concentrations in three sampling sites. Concentrations of trace elements were generally lower than threshold levels, with only a few exceptions (e.g., Be, Co, Hg, Mn,

Ni and Zn) punctually above them. The most polluted sites showed a higher organic matter content, highlighting a relevant role on retaining pollutants in soils. These unexpected high PAH levels found in Pyramiden demonstrated the importance of environmental monitoring programs in remote areas of the planet. In addition, in those regions there is a potential seasonal effect since the photodegradation of PAHs and the formation of oxy- and nitro- PAHs might be enhanced during the continuous light exposure of midnight sun season. The remobilization and formation of PAHs photodegradation products might be progressively enhanced in a climate change context.

Photodegradation is here reported as an important degradation pathway for PAHs in soil surface in highly irradiated areas, such as the Mediterranean regions, and under a climate change context. Further attention needs to be paid on changes on human health risk, mainly in terms of toxic degradation products. Although PAHs photodegradation will lead to a decrease of PAHs in soils, the oxidation and nitrification reactions will simultaneously cause the formation of oxy- and nitro-PAHs. These chemicals have lower lipophilicity, and therefore, higher potential mobility, bioavailability, toxicity, and even mutagenicity and carcinogenicity nature than their parent PAHs. Furthermore, there is no regulation regarding and consequently, they are not usually monitored in environmental surveillance programs. In addition, there is a lack of standardized analytical methods for most PAHs by-products which also difficults this monitoring and surveillance. Altogether, these findings highlight the need to update the list of 16 US EPA priority PAHs commonly monitored, and also to implement a regulation for PAHs derivatives.

RESUM

Les avaluacions del Panell Intergovernamental del Canvi Climàtic han evidenciat que l'augment de les emissions de gasos amb efecte hivernacle ha causat un accelerament del canvi climàtic. Hi ha diversos estudis que confirmen que la temperatura mitjana global ha incrementat entre $0.6\pm 0.2^{\circ}\text{C}$ durant el segle XX, i s'espera que ho faci entre 1.8 i 4.0°C a finals del segle XXI, segons diferents escenaris d'emissió de gasos. A més a més, s'ha prestat més atenció al forat de la capa d'ozó i a l'increment de radiació UV-B que se n'ha derivat. Les regions situades en latituds altes, com per exemple l'Àrtic i l'Antàrtida, són les més severament afectades. Tot i així, la zona mediterrània també és una regió vulnerable ja que està en una àrea de transició afectada pels processos de les latituds altes i baixes. Conseqüentment, l'impacte del canvi climàtic és un tema que genera gran preocupació, no només a escala global, sinó també local.

Es preveu que l'esperat augment de temperatura i radiació UV-B impacti sobre el comportament de diversos contaminants, com per exemple els contaminants orgànics persistents (COPs). Els COPs són compostos químics que desperten interès i preocupació per la seva toxicitat, resistència a la degradació, potencial per ser bioacumulats i capacitat per viatjar a grans distàncies de les fons a través dels corrents atmosfèrics i oceànics. També s'ha prestat atenció en altres compostos orgànics semivolàtils, com per exemple els hidrocarburs aromàtics policíclics (HAPs). A més de la seva toxicitat i ubiqüitat en el medi ambient, també són fotosensibles, i conseqüentment, potencialment vulnerables al canvi climàtic.

L'objectiu d'aquesta tesi és estudiar l'impacte de l'increment de la temperatura i la intensitat de la llum en el comportament dels HAPs després de ser dipositats en dos sòls típicament mediterranis. Primerament, es va simular un escenari climàtic actual i un de canvi climàtic extrem (RCP 8.5) per aquesta regió segons les prediccions de l'IPCC. Es va analitzar la tendència de les concentracions dels HAPs i l'ecotoxicitat dels sòls, a la vegada que s'identificaren els subproductes derivats de la fotodegradació dels HAPs. A més a més, es va dur a terme un experiment en el camp per tal d'avaluar la degradació dels HAPs en condicions ambientals reals de la zona mediterrània.

Finalment, els nivells d'HAPs van ser determinats en una altra zona potencialment vulnerable al canvi climàtic: l'Àrtic.

En el capítol I, es va fer una revisió bibliogràfica de l'impacte del canvi climàtic en les concentracions ambientals de COPs i riscos per la salut humana. El canvi climàtic i els COPs són un tema candent sobre el qual no només els científics hi haurien de prestar més atenció, sinó que també ho haurien de fer els responsables polítics per tal d'adaptar les legislacions ambientals. La majoria dels estudis es centren en els COPs que ja han estat prohibits o regulats, i que són una herència del passat, com les dioxines perclorades i furans (PCDD/Fs), bifenils perclorats (PCBs) i pesticides. Contràriament, el nombre d'investigacions avaluant l'impacte del canvi climàtic en nivells ambientals d'HAPs és limitat. Tot i així, els HAPs són potencialment vulnerables al canvi climàtic per la seva especial fotosensibilitat. A més a més, alguns estudis assenyalen que com a resultat de la seva fotodegradació es podrien formar en el futur subproductes més tòxics causant efectes adversos sobre la salut. Conseqüentment, aquest buit inqüestionable requereix ser avaluat.

El capítol II presenta els resultats de l'estudi de la fotodegradació dels HAPs en sòls en condicions climàtiques actuals per la zona mediterrània. Es recolliren sòls Arenosol i Regosol de textura fina, escollits com a representants dels sòls típicament mediterranis, per contaminar amb concentracions conegudes d'HAPs, i posteriorment, es van incubar en una cambra climàtica a condicions controlades de temperatura (20°C), humitat (40%) i intensitat de llum baixa (9.6 W m⁻²) durant 28 dies. Seguidament, es va analitzar les concentracions dels HAPs, a la vegada que es va avaluar l'ecotoxicitat dels sòls mitjançant el test Microtox®. A més a més, per tal de confirmar la probable degradació dels HAPs, es van analitzar els isòtops d'hidrogen (H) mitjançant la tècnica d'anàlisi d'isòtops de compostos específics. Els resultats van demostrar que la fotodegradació dels HAPs depèn del temps d'exposició, les propietats fisicoquímiques de cada HAP i el tipus de sòl. Els processos d'adsorció i fotodegradació van ser més notables en el sòl de textura fina, essent el fenantrè, antracè, benzo(a)pirè i indeno(123-cd)pirè significativament fotodegradats. En concret, el benzo(a)pirè, utilitzat habitualment com indicador de contaminació d'HAPs, va ser totalment degradat després de 7 dies d'exposició a la llum. L'avaluació de l'ecotoxicitat va mostrar una tendència a la detoxificació al llarg del temps, essent

més gran en el sòl de textura fina que en l'Arenosol. Aquest fet coincideix amb els resultats de concentracions en que els HAPs mostraren índex de fotodegradació més elevats en aquest tipus de sòl. Una probable explicació podria ser el contingut més elevat d'òxids metàl·lics en el sòl Regosol de textura fina que en l'Arenosol, els quals podrien haver-se comportat com a fotocatalitzadors dels HAPs. Finalment, l'elevat efecte isotòpic que va mostrar el benzo(a)pirè va suggerir, per una banda, que l'anàlisi d'isòtops de compostos específics podria ser una valuosa eina per monitoritzar la degradació dels HAPs, tant a nivell de laboratori com en el camp, i d'altra banda, va evidenciar que el benzo(a)pirè en la foscor experimentà un procés de degradació inesperat i desconegut.

L'objectiu del capítol III va ser explicar els diferents nivells de fotodegradació dels HAPs trobats en el sòl Arenosol i el Regosol de textura fina, diferències detectades en el capítol II. És a dir, confirmar la hipòtesi del rol fotocatalitzador dels òxids metàl·lics. Concretament, la contribució de la catàlisi va ser majoritàriament atribuïda a l'òxid de ferro (III) (Fe_2O_3), ja que tot i ser el més abundant en els dos sòls estudiats, el seu contingut era molt més elevat en el sòl de textura fina que en l'Arenosol. Els resultats van mostrar que el Fe_2O_3 afavoreix de manera significativa la fotocatalisi del fluorè, fenantrè i benzo(a)pirè. Conseqüentment, sembla ser que el Fe_2O_3 no seria l'únic causant de la fotodegradació més elevada en el sòl Regosol de textura fina que en l'Arenosol. De fet, el sòl és una matriu complexa amb diversos elements, com un ampli rang d'òxids metàl·lics, a més a més d'àcids húmics i una textura específica, tenint cada un d'ells un rol específic en el comportament dels HAPs.

En el capítol IV, es va avaluar l'impacte de l'increment de la temperatura i la intensitat de la llum en el comportament dels HAPs en sòls. La temperatura es va augmentar 4°C , d'acord amb l'escenari RCP 8.5 de l'IPCC 2013 per la regió mediterrània, mentre que es va fixar la llum a alta intensitat (24 W m^{-2}), i la humitat (40%). L'exposició dels HAPs en la superfície dels sòls Arenosol i Regosol de textura fina es va dur a terme durant 28 dies. Tal i com era d'esperar, l'augment de la temperatura i la intensitat de la llum va causar una volatilització més ràpida dels HAPs de baix pes molecular. Pel que fa als HAPs de mig i alt pes molecular, la fotodegradació va augmentar en el sòl de textura grollera (Arenosol), mentre que no mostraren diferències significatives en el sòl de textura fina Regosol. En efecte, l'augment de la

temperatura i la intensitat de la llum podria haver provocat que els òxids metàl·lics presents en el sòl Arenosol s'activessin, donant lloc a la reacció completa de la fotodegradació dels HAPs, i assenyalant el possible impacte del canvi climàtic. D'altra banda, l'anàlisi d'isòtops va confirmar la degradació del benzo(a)pirè en l'escenari de canvi climàtic, no només quan els HAPs es van exposar a la llum, sinó que també en la foscor, tal i com havia succeït en l'escenari climàtic actual. Finalment, el nombre de subproductes i temps necessari per formar-se va augmentar en incrementar la temperatura i la intensitat de la llum. D'aquesta manera, com a conseqüència del canvi climàtic, l'exposició als HAPs podria disminuir segons el tipus de sòl, però a la vegada, podria augmentar l'exposició a derivats de la degradació dels HAPs, els quals podrien ser més tòxics que els compostos nadius.

En el capítol V es va dur a terme l'avaluació de la degradació dels HAPs causada per la radiació solar en condicions reals de la zona mediterrània. La radiació solar té una intensitat 20 vegades més elevada que la que s'emet per làmpades típicament utilitzades en els experiments de fotodegradació a nivell de laboratori. Conseqüentment, el rol de la llum en la fotodegradació dels HAPs podria haver estat subestimat, a la vegada que es va omplir un buit en la recerca dels HAPs i fotodegradació ja que tal avaluació no s'havia dut a terme fins a dia d'avui. Les mostres del mateix tipus de sòls contaminades al laboratori amb HAPs es van dipositar en una caixa de metacrilat i van ser exposades a la radiació solar durant 7 dies, el que va significar una energia solar de 102.6 MJ m^{-2} . La temperatura, humitat, precipitació i radiació solar es van monitoritzar de manera contínua. Al llarg de l'experiment els HAPs van volatilitzar-se, adsorbir-se al sòl i/o fotodegradar-se, segons les seves propietats fisicoquímiques i les del sòl. Els HAPs de baix i mig pes molecular es van adsorbir i fotodegradar més en el sòl Regosol de textura fina, mentre que el sòl Arenosol de textura grollera va afavorir la seva volatilització. Per contra, els HAPs d'alt pes molecular es van fotodegradar més en el sòl Arenosol, possiblement per l'elevada intensitat provinent dels rajos solars, la qual va penetrar més fàcilment entre les partícules del sòl. Concretament, es van trobar índex de fotodegradació elevats i temps de vida mitja baixos en l'antracè, pirè i benzo(a)pirè, HAPs que ja havien mostrat ser més sensibles a la llum en els experiments de laboratori. A part dels productes de reaccions d'oxidació que ja s'havien detectat prèviament, es van

identificar altres oxi-, nitro- i hydro- HAPs en aquest experiment de camp, els quals han mostrat tenir un potencial tòxic i mutagènic més elevat que els propis 16 HAPs prioritaris de l'EPA que s'avaluen normalment.

Finalment, el capítol VI mostra els resultats d'un estudi de monitoratge ambiental per determinar les concentracions d'HAPs en sòls de l'Àrtic. Pyramiden (Centre de Spitsbergen, arxipèlag de Svalbard) va ser escollit per ser un lloc possiblement contaminat degut a: i) el transport atmosfèric de llarg recorregut, ii) els dipòsits de carbó degut a la geologia local, iii) la prèvia extracció minera de carbó, iv) les actuals plantes elèctriques en funcionament. A més dels nivells d'HAPs es van analitzar metalls per tal de confirmar el possible origen antropogènic de la contaminació. Tant els perfils d'HAPs com els índex de diagnòstic molecular van indicar fonts de contaminació pirogèniques a la majoria de les mostres, esdevenint la combustió de carbó i dièsel de les plantes de producció d'electricitat locals les fonts més probables. De totes maneres, la contribució amb origen petrògenic no es va descartar. Encara que els nivells d'HAPs van ser més alts de l'esperat, només hi ha tres punts que excediren els nivells de referència. En general, els metalls van estar per sota dels nivells de referència, només amb algunes excepcions. Els nivells més elevats d'HAPs i metalls es van trobar en sòls propers a les plantes i en aquells exposats a les direccions dels vents predominants. A més a més, aquests sòls tenien un contingut en matèria orgànica més elevat, deixant entreveure que aquesta podria estar retenint els contaminants en els sòls. Els nivells notables i inesperats d'HAPs demostraren la importància dels programes de monitoratge ambiental en regions remotes del planeta. A la vegada, la llum contínua durant el període de sol de mitjanit podria provocar un efecte estacional causant un increment en la fotodegradació dels HAPs i formació d'oxi- i nitro- HAPs. Aquesta tendència a l'alça es podria veure progressivament remarcada en un context de canvi climàtic.

La fotodegradació és una via important de degradació dels HAPs en la superfície de sòls en zones amb elevada irradiació, com la regió mediterrània, i en un context de canvi climàtic. S'hauria de prestar més atenció als potencials canvis sobre els riscos per la salut humana, principalment derivats de la formació de productes de la degradació d'aquests compostos. Encara que la fotodegradació dels HAPs provocarà una disminució de les concentracions en sòls, les reaccions d'oxidació i nitrificació

causaran la formació simultània d'oxi- i nitro- HAPs. Aquests compostos són més hidròfils, i consegüentment, més mòbils, biodisponibles, tòxics i fins i tot més mutagènics que els propis HAPs. A més a més, no hi ha cap tipus de regulació que els tingui en compte, i consegüentment, no s'acostumen a considerar en els programes de control ambiental actuals. En efecte, la manca de mètodes analítics estandarditzats per la majoria de derivats dels HAPs també dificulta el seu control. Els resultats de la present tesi destaquen la necessitat d'una nova legislació dels HAPs, actualitzant els considerats actualment com a prioritaris, i incloent els seus subproductes.

INTRODUCTION

1. Climate change and POPs

The reconstruction of the Earth's historical climate trends has demonstrated that climate is constantly changing, showing peculiar oscillations at different time scales. However, a particular climate change acceleration has been observed over the last decades. The assessments of the Intergovernmental Panel on Climate Change (IPCC) have evidenced that, due to increasing greenhouse gases, the Earth's climate is substantially changing (IPCC, 2013). The air temperature is projected to increase 1.8-4.0°C by the end of the 21st century, under a range of probable greenhouse gas emission scenarios, being high latitudes those more severely affected (Noyes et al., 2009).

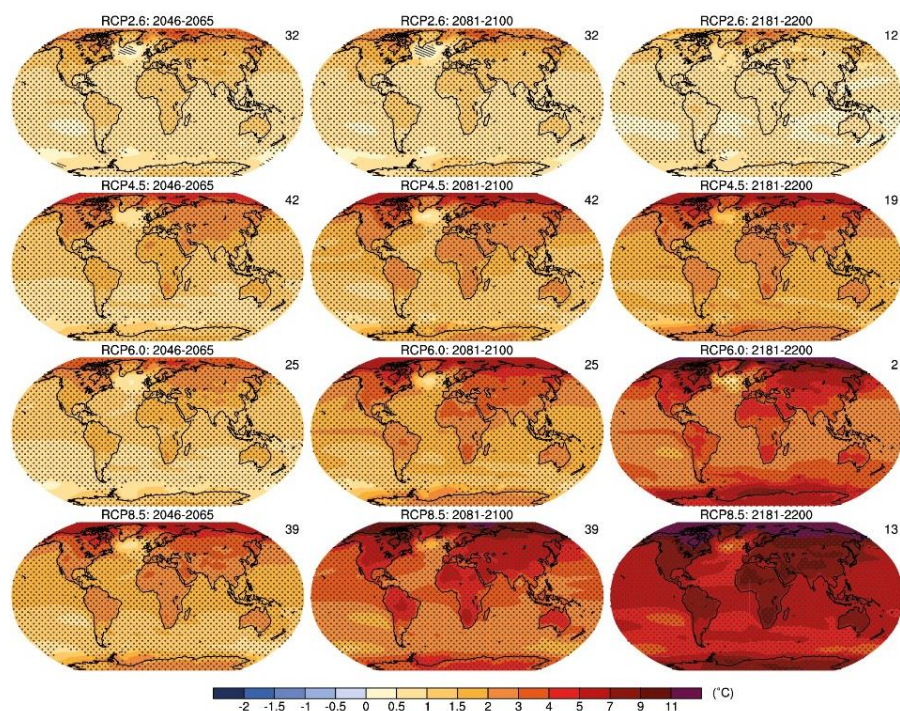


Fig. 1. Projected changes in global average temperatures under four emissions pathways (rows) for three different time periods (columns). Changes in temperatures are relative to 1986-2005 averages. RCP2.6 is a very low emissions pathway, RCP4.5 is a medium emissions pathway, RCP6.0 is a medium-high emissions pathway, and RCP8.5 is the high emissions pathway. Source: IPCC, 2013.

Instrumental observations suggest that the Arctic has been changing faster than any other region on the Northern hemisphere over the past decades (Serreze and Barry, 2011; van der Bilt et al., 2015). This change is specially evidenced after melting of ice caps and glaciers, the rise of sea level and temperature increase (Jayawardena, 2014). Moreover, the Mediterranean basin is considered one of the most vulnerable regions of the world to climate change, where according to IPCC (2013), air temperature is expected to increase up to 4°C in 2100 (Bangash et al., 2012; Sánchez-Canales et al., 2012; Schröter et al., 2005; Terrado et al., 2014). This region is lying in a transition zone between the arid climate of North Africa and the temperate and rainy climate of central Europe, being therefore affected by interactions between mid-latitude and tropical processes (Giorgi and Lionello, 2008).

Persistent organic pollutants (POPs) have become chemicals of concern during the last decades due to: i) their considerable resistance to degradation, ii) their ability to be transported over long distances from sources by air and ocean currents, in a process known as Long Range Atmospheric Transport (LRAT), iii) their potential to be bioaccumulated through terrestrial and aquatic food webs, to levels that may result in adverse health effects for animals and humans (Hung et al., 2013), and iv) their potential toxic effects such as immunotoxicity, neurotoxicity, developmental toxicity, carcinogenicity, mutagenicity, and endocrine disruption (Chao et al., 2014; Domingo, 2012; Gascón et al., 2013; Grandjean and Landrigan, 2006; Kim et al., 2013).

One of the consequences of climate change that has recently attracted some interest is its potential to alter the environmental distribution and biological effects of chemical toxicants (Noyes et al., 2009). Environmental variables such as temperature, wind speed, precipitation, and solar radiation, have some influence, either directly or indirectly, on the environmental fate and transport of POPs (Gusev et al., 2012). As climate change will obviously alter most of those factors to varying degrees, it is generally accepted that climate change can influence every step along the fate, transport and distribution pathways of POPs and other semi-volatile organic chemicals (SVOCs), such as polycyclic aromatic hydrocarbons (PAHs) (Cai et al., 2014; Kallenborn et al., 2012; Schiedek et al., 2007; Teran et al., 2012). Although PAHs are not considered POPs, and consequently, they are not included in the Stockholm Protocol, the executive body of the United Nations Economic Commission for Europe (UNECE)

included four PAHs (benzo(*a*)pyrene, benzo(*b*)fluoranthene, benzo(*k*)fluoranthene and indeno(123-*cd*)pyrene) in the Protocol on POPs, signed in 1998 in Aarhus (Denmark).

2. PAHs

Polycyclic aromatic hydrocarbons (PAHs) are organic compounds composed of carbon and hydrogen atoms arranged in fused aromatic rings (linear, cluster or angular structures). PAHs form a family of over 200 ubiquitous environmental pollutants with toxic, mutagenic, and carcinogenic properties.

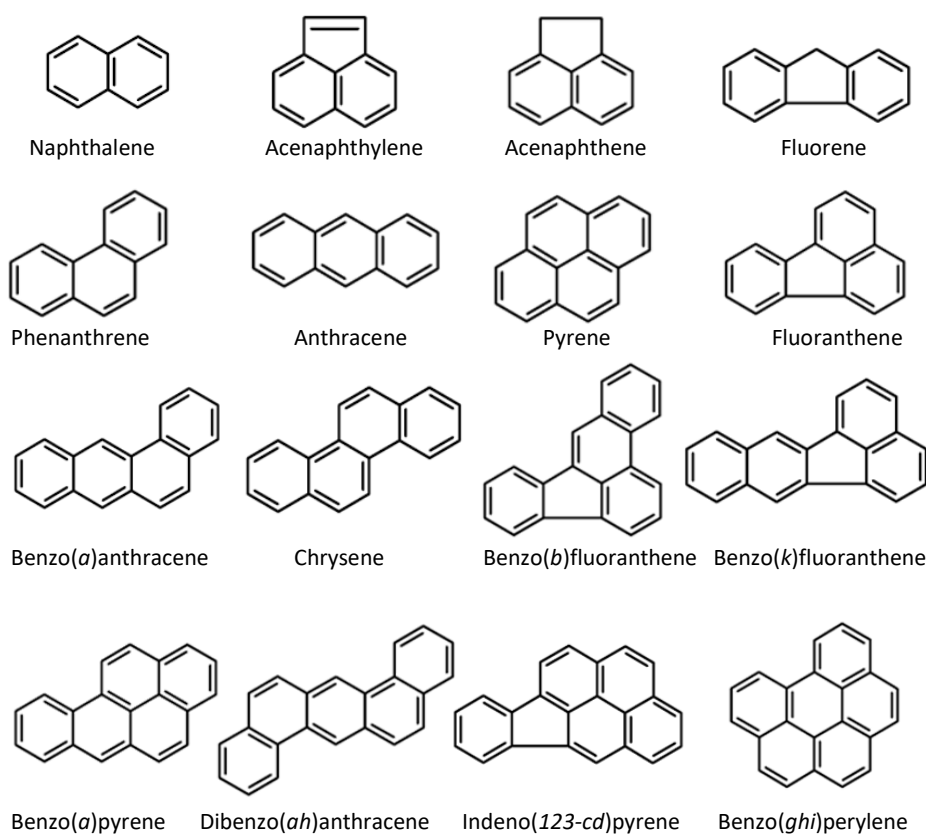


Fig. 2. Chemical structure of 16 US EPA priority PAHs.

Due to their frequency and/or risk, 16 PAHs were selected as priority pollutants by the United States Environmental Protection Agency (US EPA) in the 1970s (Ma et

al., 2009; Siciliano et al., 2010; Thavamani et al., 2011) (Fig. 1). In 2005, the European Commission (EC) recommended the monitoring of 15 EU priority PAHs along with an additional PAH highlighted by the Joint FAO/WHO Expert Committee on Food Additives (JECFA). Those 15+1 EU priority PAHs include benzo(*a*)anthracene, cyclopenta(*cd*)pyrene, chrysene, 5-methylchrysene, benzo(*b*)fluoranthene, benzo(*k*)fluoranthene, benzo(*j*)fluoranthene, benzo(*a*)pyrene, indeno(123-*cd*)pyrene, dibenzo(*ah*)anthracene, benzo(*ghi*)perylene, dibenzo(*al*)pyrene, dibenzo(*ae*)pyrene, dibezo(*ai*)pyrene, dibenzo(*ah*)pyrene + benzo(*c*)fluorene (European Commission, 2005). Up to eight PAHs are found in both United States and European priority lists. However, the 16 US PAHs identified by the US EPA are the most commonly used in monitoring programs.

In terms of toxicity, the International Agency for Research on Cancer (IARC) classifies PAHs according to their carcinogenicity. Benzo(*a*)pyrene is considered as carcinogenic to humans (Group 1), dibenzo(*ah*)anthracene as probably carcinogenic (Group 2A), and naphthalene, benzo(*a*)anthracene, chrysene, benzo(*b*)fluoranthene, benzo(*k*)fluoranthene and indeno(123-*cd*)perylene as possibly carcinogenic to humans (Group 2B). The remaining PAHs, with the exception of acenaphthylene, which is not yet considered by IARC, are not classifiable as to its carcinogenicity to humans (Group 3) (IARC, 2017).

The European Union only regulates PAHs levels in air, food and drinking water. Thus, the 4th European Daughter Directive on Air Quality (European Union, 2004) established a target value for benzo(*a*)pyrene of 1 ng m⁻³ in air. Regarding to PAHs levels in foodstuffs, PAH4 (benzo(*a*)pyrene, benzo(*a*)anthracene, benzo(*b*)fluoranthene and chrysene) levels are regulated by the Commission Regulation (EU) No. 835/2011 (European Commission, 2011), an amendment to Regulation No. 1881/2006 (European Commission, 2006). Finally, benzo(*a*)pyrene has been limited in drinking water to 0.01 µg mL⁻¹, while the sum of benzo(*b*)fluoranthene, benzo(*k*)fluoranthene, benzo(*ghi*)perylene and indeno(123-*cd*)pyrene should be lower than 0.10 µg mL⁻¹, according to the Council Directive 98/83/EC (European Commission, 1998).

2.1 Physicochemical properties

PAHs are lipophilic compounds which tend to be rapidly adsorbed to particulate organic matter, rather than vaporized or dissolved in water (Stogiannidis and Laane, 2014). However, they present a varying chemical structure, from 2 to 6 (and more) aromatic rings, leading to different physicochemical properties. Table 1 shows the molecular weight (MW), solubility in water, Log K_{ow} and vapour pressure of 16 US EPA priority PAHs. According to that, PAHs can be classified into Low Molecular Weight (LMW), Medium Molecular Weight (MMW) and High Molecular Weight (HMW) PAHs (Gao et al., 2016). LMW PAHs are naphthalene, acenaphthene and acenaphthylene, MMW PAHs include fluorene, phenanthrene, anthracene, fluoranthene and pyrene, while HMW PAHs comprises benzo(*a*)anthracene, chrysene, benzo(*b*)fluoranthene, benzo(*k*)fluoranthene, benzo(*a*)pyrene, dibenzo(*ah*)anthracene, benzo(*ghi*)perylene and indeno(*123-cd*)pyrene. Generally, the electrochemical stability, persistence, resistance toward biodegradation, and carcinogenic potential of PAHs, increase with the increase of aromatic rings, structural angularity, and hydrophobicity, while volatility tends to be inversely proportional to molecular weight (Ghosal et al., 2016). These physicochemical properties control the fate and transport of these chemicals once they are released to the natural environment (Amjadian et al., 2016).

Table 1. Physicochemical properties of 16 US EPA priority PAHs.

Compound	MW	Solubility in water (mg L ⁻¹)	Log K_{ow} (at 25°C)	Vapor pressure (mm Hg)
Naphthalene	128	31	3.37	0.087
Acenaphthylene	152	16	4.00	9.12x10 ⁻⁴
Acenaphthene	154	3.8	3.92	2.5x10 ⁻³
Fluorene	166	1.9	4.18	3.2x10 ⁻⁴
Phenanthrene	178	1.1	4.57	1.21x10 ⁻⁴
Anthracene	178	0.045	4.54	2.67x10 ⁻⁶
Pyrene	202	0.13	5.18	4.5x10 ⁻⁶
Fluoranthene	202	0.26	5.22	9.22x10 ⁻⁶
Benzo(<i>a</i>)anthracene	228	0.011	5.91	1.54x10 ⁻⁷
Chrysene	228	0.006	5.91	6.23x10 ⁻⁹
Benzo(<i>b</i>)fluoranthene	252	0.0015	5.80	5.0x10 ⁻⁷
Benzo(<i>k</i>)fluoranthene	252	0.0008	6.00	9.7x10 ⁻¹⁰
Benzo(<i>a</i>)pyrene	252	0.0038	5.91	5.49x10 ⁻⁹
Dibenzo(<i>ah</i>)anthracene	278	0.006	6.75	9.55x10 ⁻¹⁰
Indeno(<i>123-cd</i>)pyrene	276	0.00019	6.50	1.3x10 ⁻¹⁰
Benzo(<i>ghi</i>)perylene	276	0.00026	6.50	1.0x10 ⁻¹⁰

3. PAHs in the environment

3.1 Emission sources

PAHs naturally occur in coal, crude oil and gasoline, while they are also produced due to the incomplete combustion of organic matter (EPA, 2017). In turn, sources can be both natural (e.g., plant synthesis, organic matter diagenesis, and forest fires) and anthropogenic (e.g., industrial activities, residential heating, power generation, incineration, and traffic). Furthermore, industrial food processing from some domestic cooking practices can be another source of PAHs (Zelinkova and Wenzl, 2015). Finally, there is some evidence for biogenic PAHs formation in the environment. Overall, it is largely stated that anthropogenic sources are predominant (Cabrerizo et al., 2011).

PAHs are always emitted as a mixture, being the relative molecular concentration ratios characteristic of a given emission source (Tobiszewski and Namieśnik, 2012). Since the anthropogenic input to the environment far exceeds the natural sources, PAHs tend to be in greater concentrations in urban environments. However, the emission of PAHs, combined with global transport phenomena, result in a worldwide distribution (Ghosal et al., 2016). Therefore, PAHs are ubiquitous in the environment.

In an interesting study, Zhang and Tao (2009) investigated PAHs emissions on a global scale. The global emissions of 16 PAHs were estimated in 520 Gg in 2004. The contributions of residential biomass burning and deforestation wildfires were 56.7 and 17.0%, respectively. China (114 Gg), India (90 Gg) and USA (32 Gg) were the three countries with the highest total emissions. In 2007, PAHs global emissions increased in 1 Gg according to data provided by Tao et al. (2012). A parallel study carried out in China during 2012 quantified PAHs emissions in 121 Gg, which agrees well with the slightly global increase. European countries accounted for 9.5% of the total PAH emissions annually (Mu et al., 2015), being Spain the highest contributor (210 Mg), followed by Germany (177 Mg) and Poland (144 Mg). By contrast, EU-27 countries showed a decreasing trend during the last decades (58% between 1990-2011, and 6.1% between 2010 and 2011) (IARC, 2013).

3.2 PAHs fate

Once PAHs are released to the atmosphere, they can be present in the vapour phase or associated to the particulate phase, according to their specific

physicochemical properties. Thus, LMW PAHs, with two and three aromatic rings, are mainly found in the gas phase, while MMW PAHs can be found in both gaseous and particulate phases. By contrast, HMW PAHs, with 4 or more rings, tend to be sorbed to particulates (Cuadras et al., 2016; Nielsen et al., 2015).

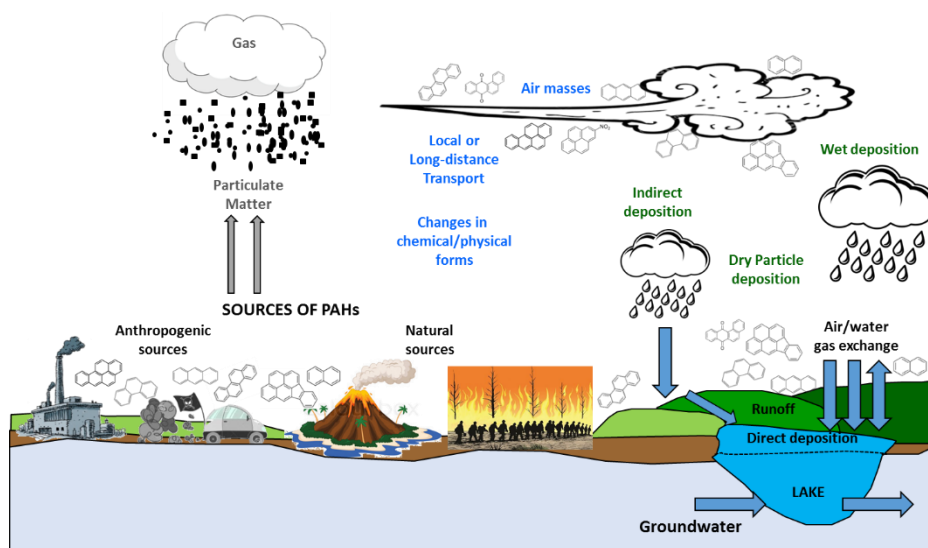


Fig. 3. Environmental fate of PAHs.

Air transport routes, including air-to-soil and soil-to-air exchange, are key processes in the environmental fate of PAHs, at both regional and global scales. Air-to-soil transport occurs primarily through the deposition of aerosols via gravitational effects, wet deposition, and adsorption to soil constituents. In addition, soil-to-air occurs through the volatilization of deposited PAHs, which take place at different degrees depending on physicochemical properties of PAHs and soil characteristics, as well as other concurrent environmental parameters. Wind currents, storms and low-pressure systems contribute to the transport of PAHs far from the sources, mainly placed in urban and industrial regions, to urban peripheries, rural regions, open seas, semi-rural areas and even open plateaus (Manzetti, 2013). As a consequence of that high mobility of both gaseous and particulate phases, PAHs are able to be deposited even in Polar regions, becoming therefore a transboundary environmental problem

(Ma et al., 2013). Finally, although PAHs are widely present as contaminants in air, aquatic environments, sediments, surface water and groundwater (Ghosal et al., 2016), the soil is one of the major sinks of atmospheric PAHs (Nadal et al., 2011; Wang et al., 2014), playing therefore a key role in the fate of these pollutants.

3.3 PAHs in surface soils

PAHs fate in soils includes volatilization, adsorption on soil particles, leaching, microbial degradation, chemical oxidation, and photo-oxidation (Haritash and Kaushik, 2009), being physicochemical properties key parameters controlling their behavior. The heavier the molecular weight, the more likely to be deposited in soil surface (Nadal et al., 2004), becoming more resistant to soil-air exchange, and consequently, being accumulated in the top layer of soil (Majumdar et al., 2017). The lipophilic nature of PAHs, inherently, enhance PAHs sorption to organic matter, and in addition, hinder their leaching. This favours their occurrence in the top-layer of soil.

Most PAHs in soil are bound to soil particles. Therefore, soil texture and physicochemical properties of PAHs have been identified as the most important factors influencing PAHs sorption and mobility. Furthermore, organic content, K_{ow} coefficient and conductivity have a key role on PAHs movement. Briefly, as the K_{ow} increases, and the aqueous solubility decreases, the tendency for sorption to a particular soil increases (Abdel-Shafy and Mansour, 2016).

3.4 PAHs in water and sediments

Similar processes controlling PAHs deposition to surface soil affect their deposition to water and sediments. In urban areas and surrounding areas, sediments are influenced by atmospheric deposition of PAHs. They also get inputs of PAHs from storm, urban and industrial sewer effluents, and roadway runoff. On the other hand, in rural areas, PAHs sorbed to atmospheric particles can settle on the surface of lakes, streams and oceans by dry or wet deposition. As PAHs are hydrophobic nature, they rapidly tend to stick with particulate/organic matter in aquatic environments. Ocean currents are responsible of their dispersion and eventually become integrated with

the sediment, becoming immobilized due to their own non-polar structures (Abdel-Shafy and Mansour, 2016). Sediments are the most important reservoir of PAHs in the marine environment, especially those PAHs coming from pyrolysis processes, which are more resistant to microbial degradation than PAHs with petrogenic origin (Perra et al., 2009).

3.5 PAHs in biota

Air, soil, water and even sediments are potential pathways of PAHs intake by biota. For instance, lichens, which are symbioses of fungi and algae and/or cyanobacteria, have the remarkable ability to uptake and accumulate PAHs. Consequently, they are being considered potential air-PAHs biomonitors (Augusto et al., 2013; Vingiani et al., 2015). However, when referred to PAHs in biota, studies are mostly focused on aquatic organisms and the concentration of pollutants directly from water and sediments. In addition, the distribution among different trophic levels shows the PAHs capacity of bioaccumulation and biomagnification, leading to human health risks due to the consumption of contaminated aquatic organisms (Zhang et al., 2015). Thus, mussels are generally used in marine monitoring programs to assess PAHs levels, while commercial fish species are further analyzed to understand the risk to the human food chain Law et al. (2014). Several biological effects of PAHs are associated to their exposure, such as tissue and genetic alterations, cancer, effects on growth and development and effects of immune function. Specifically, different fish species have shown increased levels of PAH metabolites, CYP1A, DNA-adducts and liver cancer, cardiotoxicity and reduced growth (Grung et al., 2016).

4. Environmental transformation and degradation of PAHs

Biological, chemical and photochemical processes are responsible of the transformation of PAHs during combustion processes or once they are in the environment. The reactivity of each PAH depends on its ionization potential (Jia et al., 2014), which measures the difficulty of removing an electron or the strength by which

an electron is bound. Thus, the higher the ionization potential, the more difficult is to remove an electron. In addition, transformation reactions are highly regioselective, being those carbon positions with the highest electron density the most reactive regions (L-regions). For example, the L-regions of anthracene and benzo(*a*)anthracene are 9- and 10-positions, and 7- and 12-positions, respectively (Fig. 4) (Fu et al., 2012). Depending on the molecular structure, PAHs can also own different regions named K, M, N and bay region. Vijayalakshmi and Suresh (2008) reported that K and M regions are activating, while L region is deactivating the carcinogenic potential of PAHs.

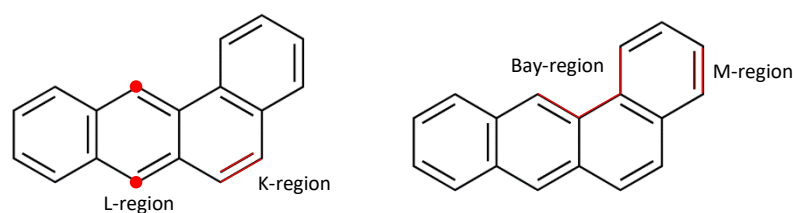


Fig. 4. Location of L, K, M and bay regions exemplified with benzo(*a*)anthracene.

4.1 Biological degradation

Algae, bacteria and fungus are microorganisms capable to cause PAHs degradation in terrestrial and aquatic ecosystems. Organisms produce the breakdown of organic compounds into less complex metabolites, through mineralization into inorganic minerals, H₂O, CO₂ (aerobic) or CH₄ (anaerobic). The rate of microbial degradation depends on the kind of microorganisms, the nature and chemical structure of the PAHs, and even the environmental conditions. As an example, Fig. 5 shows the chlorination and methoxylation of anthracene through fungal degradation. Those microorganisms are usually used under controlled conditions to degrade or detoxify contaminated soils by means of a technique called bioremediation. In turn, plants and their associated microorganisms are capable to extract, sequester and/or detoxify PAHs from contaminated sites.

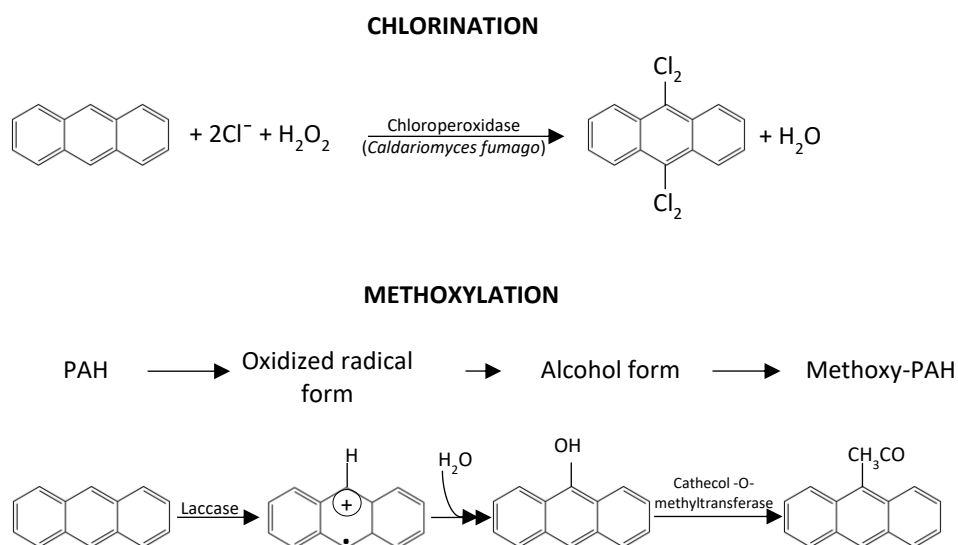


Fig. 5. Typical spontaneous PAH-degradation processes exemplified on anthracene through fungal degradation. Adapted from Manzetti (2013).

4.2 Chemical degradation

The chemical reactions occurring during the transformation and degradation of PAHs are particularly catalyzed by sunlight. They involve oxidation, nitration and/or other chemical processes taking place as a result of the interaction between PAHs and any environmental matrix (atmosphere, soil and aqueous environments) (Manzetti, 2013). Although chemical reactions can occur in different matrices, they are more significant in air, either gas or particulate phase. Gas phase reactions with OH^- , NO_3 and O_3 provide a significant pathway for atmospheric PAHs. Fig. 6 displays a set of reactions that take place during the oxidation and nitration of anthracene, leading to its corresponding quinone and nitro derivative. The joint interaction of sunlight and O_2 with the presence of a PAH, generates a quinone-PAH by effect of oxidation. On the other hand, the established mechanism of PAH reactions with the OH^- involves the formation of a PAH-OH adduct, followed by a further reaction with NO_2 or O_3 . In air, particled PAHs are adsorbed on different solid substrates, including carbonaceous aerosol (graphite, diesel exhaust, kerosene flame soot or ethylene flame soot) and mineral particles (silica or MgO). The reaction between OH, $\text{N}_2\text{O}_5/\text{NO}_3$ and O_3 drives

to heterogeneous and less comprehensive rates although depending on the reactant and also on the nature of the substrate (Keyte et al., 2013).

4.3 Photodegradation

As it has been mentioned, PAHs can be directly degraded after the absorption of sunlight radiation by direct chemical photooxidation. All PAHs are usually reported to absorb UV-A (320-400 nm), and those with five or more aromatic rings have also the capacity to absorb visible light (>400 nm) (Fu et al., 2012; Yu, 2002). On the other hand, although UV-B (280-300 nm) has a contribution of less than 1% of the total solar energy that reaches the Earth's surface, it has been found to have a potential role due to its high photonic energy (Li et al., 2011; Nadal et al., 2006).

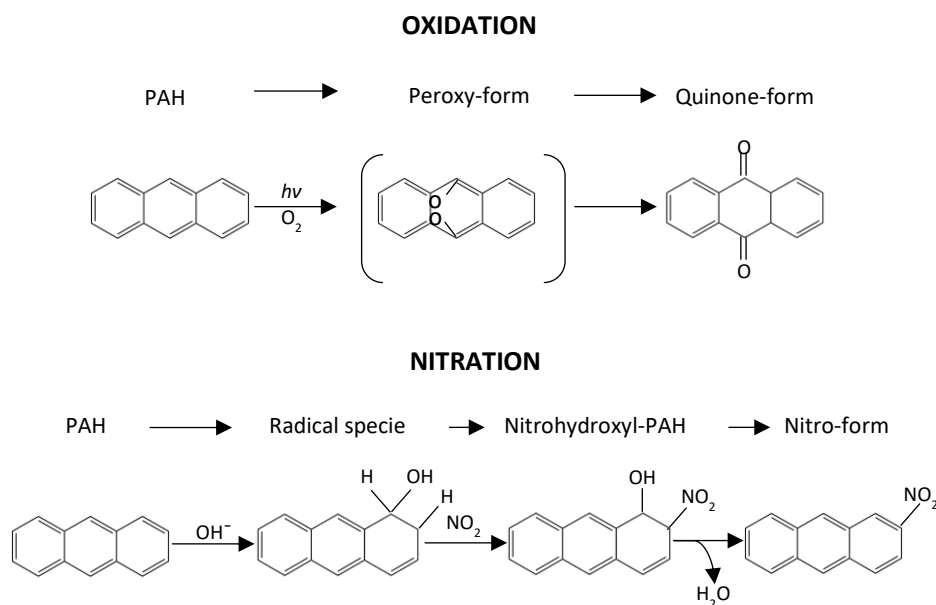


Fig. 6. Typical spontaneously PAH-degradation processes exemplified on anthracene. Adapted from Manzetti (2013).

During photooxidation, chemical transformation can simultaneously occur at different rates depending on sunlight intensity, overlapping spectral characteristics of solar radiation. This degradation pathway is called direct photodegradation (Fig. 7). In

turn, PAHs deposited on surface soil are capable to suffer indirect photodegradation. This process occurs through the sorption of sunlight energy by other substances, such as clay and soil organic matter. Afterwards, the energy is transmitted to PAHs through electron orbital interactions (Pierzynski et al., 2000) (Fig. 7).

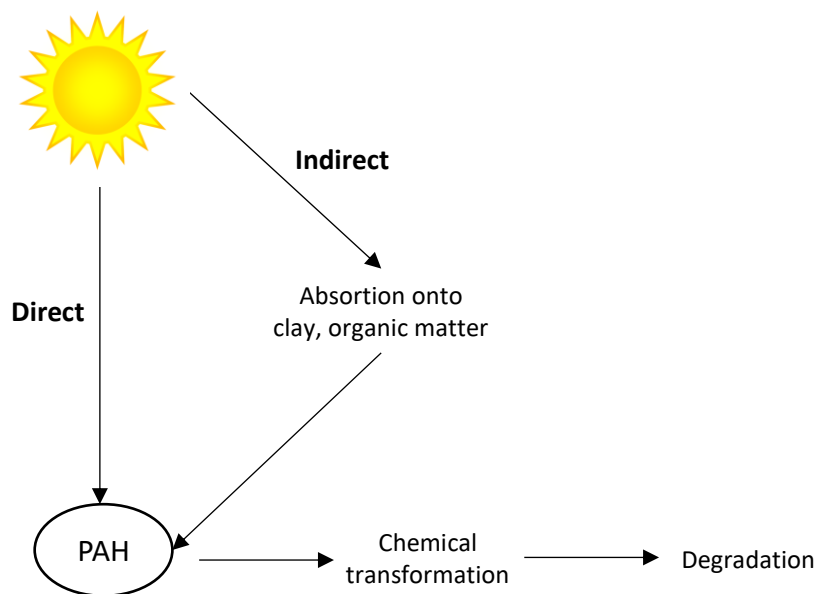


Fig. 7. Direct and indirect photo-reactions of PAHs in soils exposed to sunlight.

Photodegradation, both direct and indirect, are important transformation pathways for most PAHs in the environment (Zhang et al., 2006). This process has been mainly studied in water (Bertilsson and Widenfalk, 2002; de Bruyn et al., 2012; Fasnacht and Blough, 2003; García-Martínez et al., 2005; Jacobs et al., 2008; Jing et al., 2014; Luo et al., 2014; Rivas et al., 2000; Shemer and Linden, 2007; Singh et al., 2013; Xia et al., 2009), and at laboratory scale by means of artificial light (Gupta and Gupta, 2015; Zhang et al., 2008; Zhang et al., 2010; Zhang et al., 2006). In turn, natural sunlight, whose intensity is notably higher than that emitted by laboratory lamps, has been used to study the photodegradation in air of different organic compounds, such as organophosphate pesticides (Borrás et al., 2015), aromatic compounds (Pereira et al., 2015), organochlorines (Vera et al., 2015), and herbicides (Muñoz et al., 2014).

Unfortunately, the knowledge of PAHs photodegradation in soils at laboratory scale is rather limited, with only few investigations (Balmer et al., 2000; Frank et al., 2002; Gong et al., 2001; Xiaozhen et al., 2005). Furthermore, PAHs photodegradation has not been yet extensively studied under solar radiation, either in soils or any other environmental matrix.

HYPOTHESIS

&

OBJECTIVES

According to IPCC climate change projections, the average temperature is expected to raise up to 4°C in the Mediterranean region, as a consequence of the increasing trend of greenhouse gases emissions during the last century. In turn, the ozone layer depletion will cause an increase of solar radiation intensity, especially of the UV-B spectrum.

Changes in environmental parameters, such as temperature and solar radiation, as a consequence of the climate change, are expected to alter the fate of pollutants, such as PAHs. These substances are known to be seasonal dependent, not only because of changes on emission patterns, but also for their sensitivity to temperature and light, which eventually cause their degradation. Despite of this, potential climate change impact on PAHs fate has not been deeply assessed, especially in surface soil which acts as a sink of these environmental pollutants.

It is here hypothesized that the increase of temperature and light intensity in a climate change context may increase the photodegradation of PAHs found in surface soils. Changes on their environmental concentrations may ultimately have a significant impact on the human exposure to PAHs and the associated decreases.

General objective:

To assess the joint impact of temperature and light intensity increase derived from climate change on PAHs in soils surface under different climate scenarios.

Specific objectives:

- To review the state of the art of climate change and POPs.
- To assess the photodegradation of PAHs over time under a current Mediterranean climate scenario (20°C and low light intensity) in two soils with different properties.
- To assess the role of Fe₂O₃ as photocatalyst of PAHs reactions to understand differences between Arenosol and fine-textured Regosol soils.
- To assess the photodegradation of PAHs over time under a RCP 8.5 climate change scenario (24°C) and high light intensity in two typical soils.
- To assess the photodegradation of PAHs caused by solar radiation through a field experiment performed in the Mediterranean region.

- To determine the contamination with PAHs in Arctic soils, as a potential polluted and very vulnerable region to climate change.

CHAPTER 1

Climate change and environmental concentrations of POPs: A review

Martí Nadal ^a, Montse Marquès ^{a,b}, Montse Mari ^{a,b},

José L. Domingo ^a

^a Laboratory of Toxicology and Environmental Health, School of Medicine, IISPV, Universitat Rovira i Virgili, Sant Llorenç 21, 43201 Reus, Catalonia, Spain.

^b Environmental Engineering Laboratory, Departament d'Enginyeria Química, Universitat Rovira i Virgili, Avinguda Països Catalans 26, 43007 Tarragona, Catalonia, Spain.

Environmental Research 143 (2015) 177-185.

ABSTRACT

In recent years, the climate change impact on the concentrations of persistent organic pollutants (POPs) has become a topic of notable concern. Changes in environmental conditions such as the increase of the average temperature, or the UV-B radiation, are likely to influence the fate and behaviour of POPs, ultimately affecting human exposure. The state of the art of the impact of climate change on environmental concentrations of POPs, as well as on human health risks, is here reviewed. Research gaps are also identified, while future studies are suggested. Climate change and POPs are a hot issue, for which wide attention should be paid not only by scientists, but also and mainly by policymakers. Most studies reported in the scientific literature are focused on legacy POPs, mainly polychlorinated dibenzo-*p*-dioxins and dibenzofurans (PCDD/Fs), polychlorinated biphenyls (PCBs) and pesticides. However, the number of investigations aimed at estimating the impact of climate change on the environmental levels of polycyclic aromatic hydrocarbons (PAHs) is scarce, despite of the fact that exposure to PAHs and photodegradation byproducts may result in adverse health effects. Furthermore, no data on emerging POPs are currently available in the scientific literature. In consequence, an intensification of studies to identify and mitigate the indirect effects of the climate change on POP fate is needed to minimize the human health impact. Furthermore, being this a global problem, interactions between climate change and POPs must be addressed from an international perspective.

Keywords: climate change, persistent organic pollutants (POPs), environmental fate and transport, polycyclic aromatic hydrocarbons, legacy POPs, scientific literature

INTRODUCTION

The reconstruction of the Earth's historical climate trends has demonstrated that climate is constantly changing, showing peculiar oscillations at different time scales. However, in recent years a particular climate acceleration has been observed over the last decades. The assessments of the Intergovernmental Panel on Climate Change (IPCC) have evidenced that, due to increasing greenhouse gases, the Earth's climate is substantially changing (IPCC, 2013). A number of studies have confirmed that the global mean temperature increased by $0.6\pm 0.2^{\circ}\text{C}$ during the 20th century (IPCC, 2001). In addition, the air temperature is projected to increase $1.8\text{-}4.0^{\circ}\text{C}$ by the end of the 21st century, under a range of probable greenhouse gas emission scenarios, being high latitudes those more severely affected (Noyes et al., 2009). The Mediterranean region is a vulnerable zone, where a number of climate-related events, such as higher sea levels, increased frequency of extreme climatic events including intense storms, heavy rainfall events and droughts (Kusangaya et al., 2014; McBean and Ajibade, 2009) are probably going to occur. Moreover, the increase in the surface UV-B radiation induced by ozone depletion has received wide attention as an environmental issue of great concern (Watanabe et al., 2011). Hence, climate change is an increasingly urgent problem, with wide consequences for the environment and life on Earth (Kim et al., 2014). The global change effects will impact not only animal species and ecosystem processes (Moe et al., 2013), but they will also alter the degree of human exposure to pollutants, changing the risks in the future (Balbus et al., 2013). A number of studies have identified the expected degree of these impacts in various regions. Instrumental observations suggest that the Arctic has been changing faster than any other region on the Northern hemisphere over the past decades (Serreze and Barry, 2011; van der Bilt et al., 2015), being evidenced by melting of ice caps and glaciers, as well as the rise of sea level and temperature (Jayawardena, 2014). Moreover, the Mediterranean basin is considered one of the most vulnerable regions of the world to climate change. According to IPCC (2013), air temperature is expected to increase up to 4°C (Sánchez-Canales et al., 2012; Schröter et al., 2005; Bangash et al., 2012; Marquès et al., 2013; Terrado et al., 2014). This region is lying in a transition zone between the arid climate of North Africa and the temperate and rainy climate of central Europe, being therefore

affected by interactions between mid-latitude and tropical processes (Giorgi and Lionello, 2008).

Persistent organic pollutants (POPs) have become chemicals of concern during the last decades due to: a) their considerable resistance to degradation, b) their ability to be transported over long distances from sources by air and ocean currents, in a process known as Long Range Atmospheric Transport (LRAT), c) their potential to be bioaccumulated through terrestrial and aquatic food webs, to levels that may result in adverse health effects for animals and humans (Hung et al., 2013), and d) their potential toxic effects such as immunotoxicity, neurotoxicity, developmental toxicity, carcinogenicity, mutagenicity, and endocrine disruption (Chao et al., 2014; Domingo, 2012a; Gascón et al., 2013; Gasull et al., 2013; Kim et al., 2013). In 2001, the Stockholm Convention on Persistent Organic Pollutants elaborated a first list of POPs whose emissions and/or production must be eliminated, or at least notably reduced. That list included a variety of POP candidates: organochlorine pesticides (DDT, aldrin, chlordane, dieldrin, endrin, heptachlor, hexachlorobenzene (HCB), mirex, and toxaphene), as well as polychlorinated biphenyls (PCBs) and polychlorinated dibenzo-*p*-dioxins and dibenzofurans (PCDD/Fs) (commonly known as 'dioxins'). However, this is a dynamic list, and therefore, more compounds with similar properties have been added throughout time. In May 2009, a new set of chemicals, including other pesticides (chlordecone, α -hexachlorocyclohexane, β -hexachlorocyclohexane, lindane, pentachlorobenzene and pentachlorobenzene), polybrominated biphenyls (PBBs) (hexabromobiphenyl, hexabromodiphenyl ether and heptabromodiphenyl ether, tetrabromodiphenyl ether and pentabromodiphenyl ether), as well as perfluoroalkyl substances (perfluorooctanesulfonic acid (PFOS) and its salts, and perfluorooctanesulfonyl fluoride (PFOSF)), were also included in the list. Furthermore, endosulfan and hexabromocyclododecane were added in the Fifth and Sixth Conference of Parties, held in 2011 and 2013, respectively (Jennings and Li, 2015).

Parallel initiatives have highlighted the PBT properties of other chemical pollutants. For instance, the Executive Body of the United Nations Economic Commission for Europe (UNECE) included four polycyclic aromatic hydrocarbons (PAHs) (benzo(*a*)pyrene, benzo(*b*)fluoranthene, benzo(*k*)fluoranthene, and indeno(123-*cd*)pyrene) in the Protocol on POPs, signed in 1998 in Aarhus (Denmark).

PAHs were also included in the original list of POPs by the UNECE's Convention on Long-Range Transboundary Air Pollution (CLRTAP). The above 4 PAHs are persistent, bioaccumulative, toxic, and can be transported to long distances through the air (LRAT). Consequently, they can be also considered as POPs. Thus, they were included in a list of 16 priority substances by the 1998 Aarhus Protocol on POPs together with eleven pesticides, two industrial chemicals, as well as two other by-products/contaminants (UNECE, 2014). The Protocol banned the production of some substances (aldrin, chlordane, chlordecone, dieldrin, endrin, hexabromobiphenyl, mirex and toxaphene), while others (DDT, heptachlor, hexachlorobenzene, PCBs) were scheduled for elimination at a later stage. Moreover, the use of some products such as DDT, hexachlorocyclohexanes (HCHs) and PCBs, is severely restricted and provisions for dealing with the wastes of substances that will be banned are included. Finally, the Protocol obliges Parties to reduce their emission of PCDD/Fs, PAHs and HCB below their levels in 1990.

The fate and behavior of POPs have attracted considerable political and scientific interest, particularly when local releases have resulted in dispersed contamination far from source regions (Paul et al., 2012). The transport distance and the number of air-surface exchange episodes depend on the surface characteristics (e.g. soil, water, vegetation, etc.), as well as the physical-chemical properties of the compound. Thus, persistent chemicals, with a lower vapor pressure, will be preferably deposited in areas closer to the emission source, while those with a higher vapor pressure are more easily transported far away. In addition, there are other mechanisms and factors which influence the distribution of POPs in the atmosphere. These are the capacity of the environmental compartments to accumulate or degrade POPs, the general atmospheric patterns, and the kinetic of the air-surface exchange, among others.

One of the consequences of climate change that has recently attracted some interest is its potential to alter the environmental distribution and biological effects of chemical toxicants (Noyes et al., 2009). Environmental variables such as temperature, wind speed, precipitation, and solar radiation, have influence, either directly or indirectly, on the environmental fate and transport of POPs (Gusev et al., 2012). As climate change will obviously alter most of those factors to varying degrees, it is generally accepted that climate change can influence every step along the fate,

transport and distribution pathways of semi-volatile organic chemicals, including PAHs and POPs (Cai et al., 2014; Kallenborn et al., 2012; Schiedek et al., 2007; Teran et al., 2012). Temperature is one of the key meteorological parameters that is able to impact more severely the global distribution of POPs in the environment (Dalla Valle et al., 2007). According to the results of multicompartiment chemistry-transport models, the degradation rates of POPs in the environment are estimated to increase by a factor of two to three for every 10°C increment (Lammel, 2001; Macdonald et al., 2005). Therefore, global warming is probably influencing the environmental behavior of POPs. It enhances the volatilization from primary and secondary sources, and influencing their partitioning between soil, sediment, water and atmosphere, including air-surface exchange and wet/dry deposition (Noyes et al., 2009; Teran et al., 2012; Armitage et al., 2011). An increase of rainfall can cause a raise of POP deposition onto soil. The more frequent storm surges may enhance the mobilization of chemicals stored in the soil compartment, which can be transported by land runoffs, making them available to the aquatic organisms (Dalla Valle et al., 2007). In turn, cold temperatures can induce their deposition and accumulation in Arctic environmental media, resulting in the so-called cold-trapping effect (Rahn and Heidam 1981; Perrie et al., 2012). It has been also observed in other recent studies that the fate of POPs depends on the meteorological conditions, and therefore climate change will modify their concentrations and trends in the Arctic (Perrie et al., 2012), ultimately affecting the rest of the world. In addition to the Arctic, which is already experiencing substantial changes (Armitage and Wania, 2013), other world areas such as the Alps or the Mediterranean, are also sensitive to POP deposition. For instance, the central and eastern Mediterranean is a receptor area for POPs emitted in western, central and Eastern Europe, particularly during summer (Mulder et al., 2015). Furthermore, the role of climate change and eutrophication on POP dynamics is a topic that needs further consideration by scientists (Wania and Mackay, 1999).

Despite of the lack of knowledge of climate change impacts on the POP occurrence, it has been suggested that the temperature increases should cause a faster degradation of these chemicals in the aquatic ecosystem, resulting in a reduction of the dietary exposure to POPs (McKone et al., 1996; Macdonald et al., 2005; Ma et al., 2004; Bard 1999)). However, these pollutants could be also

transported to higher latitude areas where wet deposition would lead to a potentially elevated POP dietary intake among exposed northern and indigenous communities (Sonne et al., 2014). Health impacts of POPs are not immediate. They have usually resulted from chronic, cumulative and long-term exposure to one or more substances, being the major exposure route non-atmospheric. Hence, POPs do not usually cause respiratory health effects. In contrast, ingestion and bioaccumulation are routes of concern. Dietary exposure seems to be the most contributive exposure pathway for POPs and other semi-volatile chemical contaminants (Domingo et al., 2008, 2012b,c; Martí-Cid et al., 2010; Martorell et al., 2012; Perelló et al., 2015). Moreover, although toxic effects of POPs are elucidated at multiple endpoints, they are not well defined when evaluating mixtures of POPs (Hung et al., 2013).

In the present paper, we have reviewed the state of the art regarding the influence of climate change on the environmental concentrations of POPs. This paper was aimed at gathering publicly available information on this topic. It should help to identify research gaps in the design of future environmental and health studies, considering plausible changes in human health risks, which are associated to global warming.

CLIMATE CHANGE IMPACT ON POPs

The scientific literature on the potential effect of climate change on POPs was reviewed by using the Scopus database (www.scopus.com). A first selection of papers was performed by using the terms: “climate change and POPs” or “global warming and POPs” in their title, abstract, or keywords. Afterwards, a specific choice was carried out by using, as keywords, “climate change” or “global warming”, as well as the name of each individual chemical. POPs were selected considering the current list addressed in the Stockholm Convention.

Finizio et al. (1998) reported for the very first time the potential impact of climate change on POPs, and more specifically on some organochlorine pesticides (DDT, HCHs, chlordane, toxaphene, aldrin). Other halogenated chemicals such as PCDD/Fs and PCBs, were also mentioned. The authors remarked that the long-range transport of POPs in the environment was largely dependent on the environmental conditions, particularly air temperature, particulate air matter and wind direction/speed.

Consequently, a change of conditions might mean notable consequences for POP distribution. It was concluded that a change in the global atmospheric conditions, and therefore the average condition for a region, can influence the biogeochemical cycle of POPs and then their presence in a specific ecosystem. According to Finizio et al. (1998), there were no studies reporting these interactions at that moment. However, they suggested that some scenarios could be simulated with the use of “global chemodynamic models” as those previously developed by Wania and Mackay (1995).

Pesticides

Pesticides form the larger group of POPs included in the Stockholm Convention. Consequently, a considerable number of data from different perspectives are currently available. Ma and Cao (2010) aimed at quantifying the perturbations of POPs as result of the climate change. A perturbed air-surface coupled model was developed to simulate and predict perturbations of POP concentrations in various environmental media under several climate change scenarios. The selected chemicals were α - and γ -HCHs, as well as HCB and PCB-153 congener. All POPs exhibited a strong response to specified climate change scenarios, as shown by their high concentrations perturbations in air. In the air-soil system, the model predicted 4-50% increases in the air concentrations of these chemicals associated to a potential increase of 0.05-0.1°K/yr in the air temperature. The authors estimated that a 20% increase/decrease in precipitation may result in a 53% and 4% decrease/increase, in perturbed air concentration of γ -HCH and α -HCH, respectively (Ma and Cao, 2010).

Wöhrschimmel et al. (2013) applied a global-scale multimedia fate model to analyze and quantify the impact of climate change on emissions and fate of POPs, and their transport to the Arctic. Two climate scenarios (base-scale and IPCC-based SRES-A2) were used to characterize the evolution over time of two well-characterized POPs (α -HCH and PCB) after an air temperature increase of 2.0-5.4°C. Regarding to climate change, four different spatially and temporally resolved generic emission scenarios were defined, covering the period 2020–2050. The model was run from the first year of emission (around 1950s) until 2100. The temporal evolution followed a plausible pattern for substances that were thought to be introduced in 2020, and successfully merchandised up to the saturation of the market in 2035, and then phased out over

the following 15 years. This phase-out would be linked to concerns on their hazard for the human health and/or the environment, or to their replacement in the market. These scenarios were used after considering both current climate conditions and with the climate change parameterization of *BETR Research model* described by MacLeod et al. (2011). Beyond temperature, other parameters of the model were air, land, and ocean surface temperatures, precipitation, atmospheric and oceanic circulation, land-ice and sea-ice cover, and organic carbon content in soils. Reported results from the simulation showed that, in the atmosphere, according to the simulations, the maximum α -HCH value was 10^3 pg/m³ in 1980, decreasing to 10^{-4} pg/m³ in 2100. Reported α -HCH concentrations in ocean waters had a similar behavior, showing their maximum level around 1990, with a reported concentration of 1 ng/L. In turn, the minimum value (10^{-5} ng/L) was estimated to occur in 2010.

Sun et al. (2005) attributed the increase of HCHs in coastal sediments to the glaciers meltwater derived from the regional warming from the early 1970s. Accumulation flux profiles and temporal trends of HCHs were determined through the analysis of two lake cores (NR and AX) collected from Niudu Lake in King George Island (West Antarctica). NR was a core under the influence of glacier meltwater, while AX was the control core. With respect to DDT, NR core showed an abnormal peak around 1980s in addition to the expected one in 1960s. On the other hand, the accumulation flux of DDT in AX core showed a gradual decline after the 1960s peak. This difference was most probably caused by regional climate warming and the resulted discharge of the DDT stored in the Antarctic ice cap, into the lakes in the Antarctic glacier frontier.

The revolatilization of α -HCH, DDT and cis-chlordane deposited in water and ice sinks was investigated by Ma et al. (2011). The records of their concentrations in Arctic air since the early 1990s were analyzed, and further compared with results from modelled simulations of the climate change effect. A correlation analysis was used to detect any evidence of POP revolatilization in the Arctic linked to regional warming. Strong correlations between POP air concentrations and mean surface air temperatures/sea-ice extent indicated the potential volatilization from secondary emission sources/reservoirs in water, snow, ice and land across the Arctic. POPs had been remobilized into the Arctic atmosphere over the past two decades as a result of

climate change, confirming that the Arctic warming could undermine global efforts to reduce environmental and human exposure to these toxic chemicals.

To assess time trends and recycling of DDTs and HCHs, Cheng et al. (2014) analyzed the levels of these pollutants in lake sediment cores from five critical regions in the Tibetan Plateau. A recent increase of both chemicals was found, likely due to the retreat of glaciers in response to climate warming. In the past 30 years, and because of the climate warming, glaciers have shrunk more than 6606 km² on the entire Tibetan Plateau, with the greatest retreat since the mid-1980s. Hence, glacier and snow melt due to climate warming is able to release stored contaminants accumulated during years of higher transport of such pollutants to this region. Consequently, a warmer climate is expected to enhance the amount of glacial water discharge into lakes and depositing more DDTs into lake sediments. In fact, these closed-basin lakes fed mainly by glacier meltwater in particular became a more sensitive monitor of global warming, in terms of temporal trends of organochlorine pesticides (OCPs).

Bogdal et al. (2009) also reported a decrease in the usage and emissions of the OCPs in Switzerland in recent decades. The main reason was the ban of DDT in that country in 1972, and that of HCB and γ -HCH, dieldrin and heptachlor in 1986. Results obtained by means of sediment cores from Lake Oberaar (Switzerland) indicated low fluxes of pesticides in the deepest sediment sample, dated from the early 1950s. From late 1990s onwards, the fluxes of pesticides, as well as those of other compounds (PCDD/Fs, PCBs, as well as polychlorinated naphthalenes) clearly increased. When assessing the supposed accelerated release of DDT in lake Oberaar due to ice and snow melting, the same authors found similar results to other POPs, such as PCDD/Fs (Bogdal et al., 2010).

Similar findings were also reported in different mountainous watersheds across a broad latitudinal, longitudinal and altitudinal range in the Canadian Cordillera in British Columbia and the Yukon, western Canada (Elliott et al., 2012). This bioaccumulation study investigated the temporal trends of DDT concentration in osprey eggs from those areas, which were in agreement with some modeled predictions of release from melting glaciers due to climate change. Predictions from the modeled dynamics of POPs released by a Swiss glacier were coincident with the

apparent temporal trends observed in ospreys (Bogdal et al., 2010), indicating that previous glacial melting might have been a factor influencing contaminant trends in western Canada.

Studies on the effects of the climate change on POP dynamics in the marine environment also exist. Borgå et al. (2010) applied a bioaccumulation model to calculate the effect of two different climate change scenarios on the pelagic marine food web of the Arctic. The authors introduced a factor of change (i.e., the ratio of pollutant levels in a future climate scenario vs. current levels) to describe bioaccumulation and contaminant concentration changes in a projected future climate for each food web organism, and for 3 different pollutants (γ -HCH, PCB-52, and PCB-153). Two different scenarios were defined: 1) temperature in water and air increased by 2.0°C, and 2) raise of 4.0°C in both parameters. It was found that γ -HCH did not biomagnify. In turn, PCB-52 showed a higher degree of biomagnification. In addition, the modeled and measured biomagnification values of PCB-153 were even higher than those corresponding to PCB-52, with values increasing with the trophic position. γ -HCH showed the lowest and least spread in magnitude of the individual process rates and parameters. The effect of increased temperature on the octanol-water (K_{ow}) and octanol-air (K_{oa}) partitioning coefficients, as well as the decreased lipid content, were the two most influential parameters resulting in reduced bioaccumulation on a wet weight basis. It was concluded that increased temperature would reduce the overall bioaccumulation of PCBs in Arctic marine food web.

Hallanger et al. (2011) assessed the differences between Arctic and Atlantic fjord systems on the bioaccumulation of POPs in zooplankton. Samples of zooplankton and seawater were collected from Liefdefjorden and Kongsfjorden, Svalbard, Norway. In zooplankton, the predatory species tended to have higher values of POPs than other species, while the lowest concentrations of POPs were found in the herbivorous *Calanus* species. Σ PCBs and Σ pesticides were higher in Kongsfjorden than in Liefdefjorden. Differences in POP concentrations were assumed to be due to fjord specific characteristics, such as ice cover and timing of snow/glacier melt. Hence, it was difficult to conclude where there were Arctic vs. Atlantic specific differences, and to extrapolate these results to possible climate change effects on accumulation of POPs in zooplankton.

McKinney et al. (2015) reviewed the ecological impacts of global climate change on the pathways of POPs and mercury, as well as their exposure in Arctic marine ecosystems. Most of the reviewed studies reported changes in POP concentrations in biological tissues linked to climate change-induced changes in species trophic interactions, particularly in relation to sea ice changes. However, the influence of changing trophic interactions on POP levels and trends varied widely in both magnitude and direction.

Recently, O'Driscoll et al. (2014) simulated, by means of HAMSOM and FANTOM models, the fate and cycling of γ -HCH and PCBs in the North Sea in the 21st century. Sediment concentrations of γ -HCH were estimated to be reduced in 2015, with respect to 2005 values as a consequence of the lower dry gas deposition. Although these authors concluded that the influence of climate change on those two POPs was small, the increased number and magnitude of storms in the 21st century will give place to POP resuspension and revolatilization processes. On the other hand, Morselli et al. (2014) created a combination of a dynamic fate model, and a hydrological module, capable of estimating water discharge and snow/ice melt contributions on an hourly basis. The resulting model, which was applied to the case study of the Frodolfo glacier-fed stream (Italian Alps), was fed with levels of PCBs and p,p'-DDE in stream water, being available four macroinvertebrate groups. The model showed to be appropriate to estimate pollutant concentrations under diverse climate change scenarios.

According to climate change predictions, it is well established that the probabilities of flooding will increase (Wu et al., 2015). Flood events will make easier the sediments resuspension. It means that contaminants contained in polluted sediments will be more easily transferred to the surrounding water. Smit et al. (2009) carried out a laboratory experiment where flood events were simulated in a reactor to estimate the desorption of dieldrin from field aged sediments. The authors concluded that the concentration gradient plays a major role in desorption, while mass transfer was kinetically hindered within the sediment particles.

Riou et al. (2012) assessed the influence of the increase of salinity in an estuary, as a consequence of the severe droughts induced by climate change in presence of waterborne DTT in a Tilapia species. The experiment was conducted with young adults

of *Sarotherodon melanotheron*, hatched and grown in constantly aerated freshwater at 29°C. *S. melanotheron* was reported to be very resistant to waterborne DDT contamination. However, it was brought clear evidence that this pesticide affects the gill multi-functionality at different salinities. Although it seemed very resistant to short-term waterborne DDT contamination, the resulting alterations of the gill issue, cells and enzymes, might affect longer term respiration, toxicant depuration, and/or osmoregulation in highly fluctuating salinities.

In a recent investigation, Komprda et al. (2013) assessed the influence of climate and land use change on the potential re-emission of organochlorine pesticides (HCB and DDE, as the prevalent DDT metabolite) from background and agricultural soils of the Czech Republic. The studied region presented a relatively large portion of the land covered by forest (32.6%). Regarding the influence of temperature change on POP emissions, an increase of air temperature by 1°C resulted in an increase of the total yearly volatilization flux by approximately 7.8% and 8.5%, for HCB and DDE, respectively, in all land use types. Data about the influence of land use change on POP emissions showed that the arable-to-grassland scenario had a strong influence on volatilization fluxes, resulting in a decline of secondary emission of -7.5%, for both POPs, at all altitudes. These results showed that the potential increase of emissions associated with increased temperature under climate change can be completely neutralized by projected changes in land use. The study also indicated that an increase of 1°C in air temperature would produce an increase of 8% in the averaged total volatilization flux. However, this effect could be neutralized by a change of land use of 10% of the arable lands to grassland or forest (Komprda et al., 2013).

Land use aspects are highlighted as an important issue to be considered in future assessments of climate change impacts on POP fate and distribution. The first outcomes of EU ArcRisk project on human health impacts in the Arctic owing to climate-induced changes in contaminant cycling were reported by Pacyna et al. (2015). They highlighted the need to characterize better the primary and secondary sources of POPs, as well as to quantify current and future releases of POPs from these sources, for a better prediction of the environmental exposure to these contaminants. Furthermore, not only direct effects of climate change (e.g., changes in temperature, ice and snow cover, precipitation, wind speed and ocean currents) on contaminants

fate and behavior but also indirect effects (e.g., alterations in carbon cycling, catchment hydrology, land use, vegetation cover, etc.) should be considered. It has been stated that the climate change has the potential to impact on the usage patterns of chemicals (e.g. pesticides) through land-use change (Paul et al., 2012). For example, agricultural land use may be forced to migrate due to alterations in temperature, precipitation or sea level, which may indirectly change the amount and dose of chemicals applied in the field.

Polychlorinated dibenzo-*p*-dioxins and dibenzofurans (PCDD/Fs)

Dalla Valle et al. (2007) applied a dynamic multimedia model to selected POP congeners to simulate the effects of different climate change scenarios on their distribution and fluxes over the next 50 years in the Venice Lagoon (Italy). A level IV dynamic model (Mackay, 2001), considering five compartments (air, soil, sediment, water, and suspended particulate matter), was developed and applied to this area. 2,3,7,8-tetrachlorodibenzofuran (2,3,7,8-TCDF) and 1,2,3,4,7,8-hexachlorodibenzofuran (1,2,3,4,7,8-HxCDF) were the selected PCDD/F congeners. Three different climate change scenarios (A, B, C) were tested, in accordance to the climate change scenarios envisaged by the 2001 IPCC climate change assessment report. Potential differences of PCDD/F concentrations in sediments and suspended particulate matter were observed among the three scenarios, showing a factor of around two between final levels in the two extreme scenarios. In turn, water concentrations of PCDD/Fs decreased in the same way, independently of the climatic conditions. Modelling results suggested that although global warming may have the potential of reducing the environmental levels of these chemicals, probably it enhances their mobility, and hence, their potential for long-range atmospheric transport.

Focused on the water compartment, Carere et al. (2011) predicted the effects of climate change on the chemical quality in lakes species. The results showed an enhanced capacity of bioaccumulation of PCDD/Fs and dioxin-like PCBs (dl-PCBs) in an expected warming world. Thus, concentrations of POPs in fishes showed significant temperature correlations. An important aspect of POP cycling in these environments concerned the extent to which these pollutants may be remitted to atmosphere in the

snow/ice pack, or percolated to soils and water bodies, particularly during snow melt. Temperature was found to be an important driver to the global cycling of POPs, through its influence on emissions from primary and secondary sources, gas-particle distributions, reaction rates, air-surface exchange, and global transport.

Regarding freshwater, Bogdal et al. (2009) hypothesized about a possible release of legacy pollutants from melting Alpine glaciers and their relevance. Two sediment cores retrieved in 2006 from Lake Oberaar (Switzerland) were extracted and further analyzed for PCDD/Fs, PCBs, DDT and their transformation products. The results revealed a consistent trend for all persistent organochlorinated compounds, showing a peak in 70s and an increase since 2000. In a subsequent investigation performed by the same research group, the release of POPs from Alpine glaciers was assessed in Lake Oberaar (Switzerland) by using a dynamic multimedia mass balance model (Bogdal et al., 2010). It was concluded that the effects of the climate warming will accelerate the release of previously deposited POPs.

The results of one of the most meaningful studies on climate change effects over the fate and transport of PCDD/Fs were recently reported (Chi et al., 2013). Specifically, extreme weather events (winter monsoon, southeast biomass burning, and tropical cyclone -typhoon-) were explored in Taiwan. During the winter monsoon period, the quantity of PCDD/Fs absorbed onto air total suspended particles was found to increase. Therefore, the monsoon was not only found to bring cold air, but also to transport air pollutants and dust over long distances, from mainland China to Taiwan. The authors demonstrated the effect of typhoon events on the long-term remobilization of PCDD/Fs, as well as supported the hypothesis that such events would have the potential to remobilize previously deposited pollutants. Consequently, climate change will alter the primary and secondary release of PCDD/Fs, mainly because of higher wind speeds. Stronger air circulation will increase the airborne transport to downwind locations (e.g., Taiwan) from the main emission areas of the Asian continent. The possibility of an enhanced frequency and intensity of extreme weather events will also lead to increased release and a higher risk of remobilization of PCDD/Fs from soils, sediments, and other reservoirs of PCDD/Fs.

Polychlorinated biphenyls (PCBs)

In addition to PCDD/Fs, Dalla Valle et al. (2007) also reported the reduction of the environmental concentrations of PCB-118 and PCB-180 congeners in a moderate climate change scenario. Concentration changes of POPs in sediments, water and suspended particulate matter of the Venice Lagoon (Italy), between 2000 and 2050, were simulated and compared to a baseline situation. The authors noted that environmental concentrations might differ by a factor of two in a moderate climate change scenario, compared to a situation with stable climate from 2000 to 2050. However, these results also suggested that global warming might have the potential of reducing the environmental levels of these chemicals, enhancing their mobility and their potential for long-range atmospheric transport.

Wöhrnschimmel et al. (2013) applied a global-scale multimedia fate model to analyze and quantify the impact of climate change on the emissions and fate of POPs, and their transport to the Arctic, being PCB-153 the selected pollutant. Based on the model, there will be an atmospheric reduction from 5 to 10^{-3} pg/m³ between 1980 and 2100. According to the simulations, in ocean waters, PCB-153 concentration will be also decreased in 2100 with respect to data of 1980. Recently, Cabrerizo et al. (2013) assessed how changes in soil biogeochemistry driven by climate perturbations may increase to a larger degree the soil fugacity capacity of POPs. The potential perturbations of climate change on the remobilization and reservoirs of PCBs in the Antarctica, were explored. A climate change related increase of 1°C in air temperature was estimated to increase the Antarctic atmospheric burdens of PCBs by 21-45%. In addition, a concurrent increase of 0.5% of solid organic matter will counteract the influence of warming by reducing the POP fugacity in soil. A 1°C increase in Antarctic temperatures will induce an increase of soil-vegetation organic carbon and associated POP pools by 25%, becoming a net sink of POPs. Therefore, up to 70 times more POPs than the amount remobilized to the atmosphere, will be trapped.

Lamon et al. (2012) developed and applied a Level III fugacity model to estimate the current mass balance of PCBs in the Adriatic Sea, and to examine the effects of climate change on the distribution of these pollutants. The model, which differentiated 3 bulk compartments (sediment, coastal water, and atmosphere), assessed the influence in the variation of up to 8 environmental parameters on the

environmental fate and transport of PCBs 52, 138 and 153. Two scenarios were considered: 20CE (1990 as 20th Century Scenario) and A1B (2100, as forecast under conditions described in the Special Report on Emission Scenarios by IPCC). Modeled fugacities of PCBs in air, water and sediments of the Adriatic Sea were in good agreement with experimental observations. Under the A1B climate scenario, modeled fugacities resulted to be higher because higher temperatures reduce the fugacity capacity of chemicals in air, water and sediments, and because diffusive sources to air are stronger.

Ma and Cao (2010) also quantified the perturbations of PCBs (28 and 153), in addition to HCHs and HCB, as result of the precipitation decrease related to climate change. PCB-28 exhibited a trend similar to that of α -HCH, showing a concentration increase of 2%.

Carrie et al. (2010) assessed the influence of climate change on the concentrations of PCBs in Mackenzie River (Canada) burbot (*Lota lota*), in which PCB levels were analyzed. Lipid-corrected concentrations over the period 1988-2008 for Σ hexa-PCB and Σ hepta-PCB showed a progressive increase with a minimum in early 2000, and a maximum in 2008. A strong temporal correlation between increasing primary productivity and PCBs in burbot was found, suggesting that warming temperatures and reduced ice cover might lead to an increased exposure to these contaminants in high trophic level Arctic freshwater biota.

Bogdal et al. (2009) also measured PCBs, which started to be globally produced in the 1930s and dramatically increased in the 1960s. PCBs were banned in Switzerland for open applications in 1972, while in 1986 a complete ban for all applications was established. However, PCB fluxes clearly increased again from 1990s to 2005. The same research group also considered PCBs in the forecast of POP melting release in an expected warming world (Bogdal et al., 2010). The amount of PCBs incorporated into the glacier between 1930-2006 was 335 g, following an increasing temporal trend.

To assess the bioaccumulation of PCBs, Borgå et al. (2010) applied a bioaccumulation model to calculate the effect of two different climate change scenarios on the pelagic marine food web of the Arctic. Based on the results of this group of pollutants, PCB-52 showed intermediate changes in the bioaccumulation compared to γ -HCH and PCB-153. Due to the temperature effect on K_{ow} and K_{oa} , there

was a higher reduction in the bioaccumulation of PCB-52 than that of PCB-153. This was a consequence of the temperature effect on growth rate, which was less influential for PCB-52 than for PCB-153. The former congener showed the largest reduction in bioaccumulation, and a large spread in direction and magnitude of influential parameters and processes.

Ng and Gray (2011) coupled bioenergetic and bioaccumulation models to investigate the biological and chemical effects of climate change into three Great Lakes (US and Canada) fish species (round gobies, mottled sculpin, and lake trout). The accumulation of PCBs was calculated under four climate scenarios for Lake Erie and Lake Superior scenarios. Round goby and lake trouts showed the highest PCB concentration in Lake Superior under a 100-year projection (temperature increase of 5°C). In turn, mottled sculpin did not show an important distinction in concentration terms between scenarios. In turn, Elliott et al. (2012) also reported temporal trends for PCB concentration in osprey eggs in different mountainous watersheds in western Canada, being coincident with some modeled predictions of release from melting glaciers. ΣPCB concentrations in eggs and plasma were up to 1420 and 28.2 ng/g, respectively. Similarly to other POPs, it was concluded that there would be lower levels of PCBs in relatively small lakes draining areas of large watersheds in the future.

Recently, Hansen et al. (2015) applied The Danish Eulerian Hemispheric Model (DEHM) to investigate how projected climate changes will affect the atmospheric transport of 13 POPs -10 PCB congeners and 3 HCHs- to the Arctic and their environmental fate within that Ocean. Under the applied climate and emission scenarios, the total mass of all compounds was predicted to be up to 55% lower across the Northern Hemisphere, at the end of the 2090s, than in the 1990s. The mass of HCHs within the Arctic was predicted to be up to 38% higher, while the change in mass of the PCBs was predicted to range from 38% lower to 17% higher, depending on the congener and the applied initial environmental concentrations.

MacLeod et al. (2005) developed the Berkeley-Trent Global model (BETR-Global) and evaluated its performance in describing atmospheric concentrations of individual PCB congeners and the dependence of these concentrations on large-scale climate variability. The role of the variability in global-scale climate conditions was proved to be very important. More specifically, they estimated that the maximum variability in

atmospheric PCB concentrations attributable to the North Atlantic Oscillation variability is approximately a factor of 2. In contrast, Kong et al. (2013) reported that the uncertainty in chemical properties (e.g., degradation half-life), and not the uncertainty associated to the climate change, dominates the variance of modelled absolute fate of POPs. These findings were reported when evaluating the influence of input data to multimedia models, on the modelled fate of 6 PCB congeners under various climate and emission scenarios. Long-term average environmental concentrations of PCBs were forecasted to change in a factor of 2, when comparing present conditions with those estimated for the period 2080-2099 (Kong et al., 2013). In another investigation (Kong et al., 2014), the same group of researchers calculated the steady-state concentrations of hypothetical perfectly persistent chemicals in the Baltic Sea water column under two alternative climate change scenarios (IPCC A2 and B2), being compared to results for a baseline climate scenario. The application of the POPCYCLING-Baltic multimedia chemical fate model highlighted temperature as the most influential individual climate parameter, being more relevant than precipitation, wind speed and particulate organic carbon.

In a modelling study of the concentrations of PCB-153 in the North Sea during the 21st century, O'Driscoll et al. (2014) found that the total mass of PCB-153 in sediments will decrease because of degradation, erosion and subsequent volatilization during storms. In contrast to γ -HCH, which was identified as a net depositional compound at the North Sea surface, PCB-153 was noted to be "volatilizational". However, the influence of the climate change on PCB-153 was suggested to be small, while trends in emissions from primary and secondary sources will remain as the key driver. In turn, the net export of PCB-153 out of the Arctic was suggested to increase under future climate conditions, according to the estimations of Octaviani et al. (2015) when studying the long-term atmospheric cycling and fate of POPs. These data contrasted with those found for DDT, for which a trend of decreasing net Arctic import would reverse to an increasing trend, 100 years after peak emission (Octaviani et al., 2015). Surface exchange (water/air and soil/air) is much more important for the cycling of PCB-153 than that of PCB-28 (because of short atmospheric lifetimes) and of DDT (because of very low volatility).

Polycyclic aromatic hydrocarbons (PAHs)

The number of investigations focused on the effect of climate change on PAHs is very scarce, with a certainly limited number of approaches. The only two areas where the climate change impact on the fate of PAHs has been studied, are South Korea and the Arctic. Cai et al. (2014) quantitatively assessed the predicted impacts of the climate change on the transport and fate of PAHs within and across environmental media in South Korea. Simulations were conducted for the period from 2000 to 2049 under the A1B scenario, being compared with a non-climate change scenario. Similarly to recent investigations on other POPs (Gouin et al., 2013; Kong et al., 2013), changes within a factor of 2 for the average concentration of PAHs in air, soil and water, were estimated. Degradation rate would play a leading role in the change of PAH levels in soils, while in water, runoff and degradation would be the key processes.

On the other hand, the effects of PAH emissions for the period 2000-2050 and the climate change on the atmospheric transport of three PAHs (phenanthrene, pyrene, and benzo(*a*)pyrene) were investigated by Friedman et al. (2014). The GEOS-Chem model, coupled to meteorology from a general circulation model, was used. The study was focused on impacts to Northern hemisphere midlatitudes and the Arctic. A small 2050 “climate penalty” for volatile PAHs, and “climate benefit” for particle-bound PAHs, was estimated. Deposition and surface-to-air fluxes of the 3 analyzed PAHs were suggested to be the critical factors for the increase or decrease of environmental PAHs in air.

In another study not entirely focused on the links between climate change and PAHs, Brinkmann et al. (2010) assessed how flood events will affect rainbow trout as a consequence of biomarker cascade, after exposure to PAH-contaminated sediment suspensions. The main motivation was the fact that temperatures of German rivers frequently exceed 25°C during summer, because of the recent changes in climate. Effects of re-suspension of sediments on biota under elevated temperature regimes are likely to differ from those under lower temperature regimes. On the other hand, Nadal et al. (2006) assessed the joint impact of UV-B radiation and temperature on the photodegradation of PAHs. This approach was experimentally performed by means of comparison of two different environments: Atlantic (Lancaster, UK) and Mediterranean (Tarragona, Catalonia, Spain) climatic conditions. A significant faster

photodegradation rates were detected, specially for light PAHs, suggesting some kind of synergistic effect when both temperature and UV-B dose increased. This synergism might have a great implication on the long-range transport of environmental organic pollutants, taking into account that low-latitude areas are the hottest and most irradiated of the planet.

CONCLUSIONS

Legacy POPs (pesticides, PCBs and PCDD/Fs) are the compounds to which researchers have paid more attention, when studying the influence of climate change on their environmental behavior. In general terms, it is estimated that the global change will alter the environmental concentrations of POPs within a factor of 2-3. In turn, information on PAHs is particularly scarce, even being likely to be significantly affected by the climate change. Moreover, few investigations have focused on PAHs and metabolites, whose incidence may be even higher than parent compounds. Furthermore, data on the effect of climate change on the environmental fate of emerging contaminants, such as polybrominated diphenyl ethers (PBDEs) and perfluoroalkyl substances (PFASs), are not currently available. Consequently, more information is clearly necessary (Pacyna et al., 2015).

Nonetheless, global modeling studies do not agree on whether climate change acts to reduce or increase environmental concentrations of POPs in the Arctic (Hansen et al., 2015), the area where the linking between the global change and the occurrence of POPs has been more extensively studied in recent years. Furthermore, as modeling uncertainty plays a key role, interpretation or speculation from data coming from the application of multimedia environmental fate models should be treated with caution (Gouin et al., 2013). Although very preliminary, a number of studies have remarked the effect of melting glaciers, as well as some extreme events, such as floods and droughts, on the remobilization and bioaccumulation of POPs. The influence of temperature increase and precipitation decrease, on the fate and transport of POPs, has been also investigated. However, studies considering the expected increase of UV-B radiation as a consequence of ozone layer depletion have not been found. Sensitive areas, such as the Arctic, the Alps or the Mediterranean, should be particularly considered, as they are more exposed to variations resulting of the global warming.

Furthermore, the generation and toxicity of byproducts, as well as their potential interaction, deserves further attention. Finally, the lack of studies focused on assessing potential changes of health risks associated to the exposure to POPs, as a consequence of the climate change, needs also to be addressed.

Acknowledgments

This study was financially supported by the Spanish Ministry of Economy and Competitiveness, through the project CTM2012-33079. Montse Marquès also received a PhD fellowship from AGAUR (Commissioner for Universities and Research of the Department of Innovation, Universities and Enterprise of the “Generalitat de Catalunya” and the European Social Fund).

References

- Armitage, J.M., Quinn, C.L., Wania, F., 2011. Global climate change and contaminants - An overview of opportunities and priorities for modelling the potential implications for long-term human exposure to organic compounds in the Arctic. *J. Environ. Monit.* 13, 1532-1546.
- Armitage, J.M., Wania, F., 2013. Exploring the potential influence of climate change and particulate organic carbon scenarios on the fate of neutral organic contaminants in the Arctic environment. *Environ. Sci. Process. Impact.* 15, 2263-2272.
- Balbus, J.M., Boxall, A.B., Fenske, R.A., McKone, T.E., Zeise, L., 2013. Implications of global climate change for the assessment and management of human health risks of chemicals in the natural environment. *Environ. Toxicol. Chem.* 32, 62-78.
- Bangash, R.F., Passuello, A., Hammond, M., Schuhmacher, M., 2012. Water allocation assessment in low flow river under data scarce conditions: A study of hydrological simulation in Mediterranean basin. *Sci. Total Environ.* 440, 60-71.
- Bard, S.M., 1999. Global transport of anthropogenic contaminants and the consequences for the Arctic marine ecosystem. *Mar. Pollut. Bull.* 38, 356-379.
- Bogdal, C., Schmid, P., Zennegg, M., Aselmetti, F.S., Schering, M., Hungerbühler, K., 2009. Blast from the past: Melting glaciers as a relevant source for Persistent Organic Pollutants. *Environ. Sci. Technol.* 43, 8173-8177.
- Bogdal, C., Nikolic, D., Lüthi, M.P., Schenker, U., Scheringer, M., Hungerbühler, K., 2010. Release of legacy pollutants from melting glaciers: Model evidence and conceptual understanding. *Environ. Sci. Technol.* 44, 4063-4069.
- Borgå, K., Saloranta, T.M., Ruus, A., 2010. Simulating climate change-induced alterations in bioaccumulation of organic contaminants in an arctic marine food web. *Environ. Toxicol. Chem.* 29, 1349-1357.

- Brinkmann, M., Hudjetz, S., Cofalla, C., Roger, S., Kammann, U., Giesy, J.P., Hecker, M., Wiseman, S., Zhang, X., Wölz, J., Schüttrumpf, H., Hollert, H., 2010. A combined hydraulic and toxicological approach to assess re-suspended sediments during simulated flood events. Part I-multiple biomarkers in rainbow trout. *J. Soil. Sediment.* 10, 1347-1361.
- Cabrerizo, A., Dachs, J., Barceló, D., Jones, K.C., 2013. Climatic and biogeochemical controls on the remobilization and reservoirs of persistent organic pollutants in Antarctica. *Environ. Sci. Technol.* 47, 4299-4306.
- Cai, J.J., Song, J.H., Lee, Y., Lee, D.S., 2014. Assessment of climate change impact on the fates of polycyclic aromatic hydrocarbons in the multimedia environment based on model prediction. *Sci. Total Environ.* 470-471, 1526-1536.
- Carere, M., Miniero, R., Cicero, M.R., 2011. Potential effects of climate change on the chemical quality of aquatic biota. *TrAC Trends Anal. Chem.* 30, 1214-1221.
- Carrie, J., Wang, F., Sanei, H., Macdonald, R.W., Outridge, P.M., Stern, G.A., 2010. Increasing contaminant burdens in an arctic fish, burbot (*Lota lota*), in a warming climate. *Environ. Sci. Technol.* 44, 316-322.
- Chao, H.R., Huang, H.L., Hsu, Y.C., Lin, C.W., Lin, D.Y., Gou, Y.Y., Chen, K.C., 2014. Impact of brominated POPs on the neurodevelopment and thyroid hormones of young children in an indoor environment-A review. *Aerosol Air Qual. Res.* 14, 1320-1332.
- Cheng, H., Lin, T., Zhang, G., Liu, G., Zhang, W., Qi, S., Jones, K.C., Zhang, X., 2014. DDTs and HCHs in sediment cores from the Tibetan Plateau. *Chemosphere* 94, 183-189.
- Chi, K.H., Lin, C.Y., Ou Yang, C.F., Hsu, S.C., Chen, Y.F., Luo, S., Kao, S.J., 2013. Evaluation of environmental fate and sinks of PCDD/Fs during specific extreme weather events in Taiwan. *J. Asian Earth Sci.* 77, 268-280.
- Dalla Valle, M., Codato, E., Marcomini, A., 2007. Climate change influence on POPs distribution and fate: A case study. *Chemosphere* 67, 1287-1295.
- Domingo, J.L., Martí-Cid, R., Castell, V., Llobet, J.M., 2008. Human exposure to PBDEs through the diet in Catalonia, Spain: Temporal trend. A review of recent literature on dietary PBDE intake. *Toxicology* 248, 25-32.
- Domingo, J.L., 2012a. Polybrominated diphenyl ethers in food and human dietary exposure: A review of the recent scientific literature. *Food Chem. Toxicol.* 50, 238-249.
- Domingo, J.L., Perelló, G., Nadal, M., Schuhmacher, M., 2012b. Dietary intake of polychlorinated dibenzo-p-dioxins and dibenzofurans (PCDD/Fs) by a population living in the vicinity of a hazardous waste incinerator. Assessment of the temporal trend. *Environ. Int.* 50, 22-30.
- Domingo, J.L., Jogsten, I.E., Eriksson, U., Martorell, I., Perelló, G., Nadal, M., van Bavel, B., 2012c. Human dietary exposure to perfluoroalkyl substances in Catalonia, Spain. Temporal trend. *Food Chem.* 135, 1575-1582.
- Elliott, J.E., Levac, J., Guigueno, M.F., Shaw, D.P., Wayland, M., Morrissey, C.A., Muir, D.C.G., Elliott, K.H., 2012. Factors influencing legacy pollutant accumulation in Alpine Osprey: Biology, topography, or melting glaciers? *Environ. Sci. Technol.* 46, 9681-9689.
- Finizio, A., Di Guardo, A., Cartmale, L., 1998. Hazardous Air Pollutants (HAPs) and their effects on biodiversity: An overview of the atmospheric pathways of Persistent Organic Pollutants (POPs) and suggestions for future studies. *Environ. Monit. Assess.* 49, 327-336.

- Friedman, C.L., Zhang, Y., Selin, N.E., 2014. Climate change and emissions impacts on atmospheric PAH transport to the Arctic. *Environ. Sci. Technol.* 48, 429-437.
- Gascón, M., Morales, E., Sunyer, J., Vrijheid, M., 2013. Effects of persistent organic pollutants on the developing respiratory and immune systems: A systematic review. *Environ. Int.* 52, 51-65.
- Gasull, M., Pumarega, J., Rovira, G., López, T., Alguacil, J., Porta, M., 2013. Relative effects of educational level and occupational social class on body concentrations of persistent organic pollutants in a representative sample of the general population of Catalonia, Spain. *Environ. Int.* 60, 190-201.
- Giorgi, F., Lionello, P., 2008. Climate change projections for the Mediterranean region. *Global Planet Change* 63, 90-104.
- Gouin, T., Armitage, J.M., Cousins, I.T., Muir, D.C., Ng, C.A., Reid, L., Tao, S., 2013. Influence of global climate change on chemical fate and bioaccumulation: The role of multimedia models. *Environ. Toxicol. Chem.* 32, 20-31.
- Gusev, A., MacLeod, M., Bartlett, P., 2012. Intercontinental transport of persistent organic pollutants: A review of key findings and recommendations of the task force on hemispheric transport of air pollutants and directions for future research. *Atmos. Pollut. Res.* 3, 463-465.
- Hallanger, I.G., Ruus, A., Warner, N.A., Herzke, D., Evenset, A., Schøyen, M., Gabrielsen, G.W., Borgå, K., 2011. Differences between Arctic and Atlantic fjord systems on bioaccumulation of persistent organic pollutants in zooplankton from Svalbard. *Sci. Total Environ.* 409, 2783-2795.
- Hansen, K.M., Christensen, J.H., Geels, C., Silver, J.D., Brandt, J., 2015. Modelling the impact of climate change on the atmospheric transport and the fate of persistent organic pollutants in the Arctic. *Atmos. Chem. Phys.* 15, 6549-6559.
- Hung, H., MacLeod, M., Guardans, R., Scheringer, M., Barra, R., Harner, T., Zhang, G., 2013. Toward the next generation of air quality monitoring: Persistent organic pollutants. *Atmos. Environ.* 80, 591-598.
- IPCC, 2001. Summary for Policymakers (SPM). Third Assessment Report of Working Group I of the Intergovernmental Panel on Climate Change, Shanghai, China.
- IPCC, 2013. Fifth Assessment Report: Climate Change 2013 (AR5). Intergovernmental Panel on Climate Change.
- Jayawardena, A.W., 2014. Climate change - is it the cause or the effect? *KSCE J. Civil Eng.* 19, 359-365.
- Jennings, A.A., Li, Z., 2015. Residential surface soil guidance applied worldwide to the pesticides added to the Stockholm Convention in 2009 and 2011. *J. Environ. Manage.* 160, 226-240.
- Kallenborn, R., Halsall, C., Dellong, M., Carlsson, P., 2012. The influence of climate change on the global distribution and fate processes of anthropogenic persistent organic pollutants. *J. Environ. Monit.* 14, 2854-2869.
- Kim, S., Park, J., Kim, H.J., Lee, J.J., Choi, G., Choi, S., Kim, S., Kim, S.Y., Moon, H.B., Kim, S., Choi, K., 2013. Association between several persistent organic pollutants and thyroid hormone levels in serum among the pregnant women of Korea. *Environ. Int.* 59, 442-448.
- Kim, K.H., Kabir, E., Ara Jahan, S., 2014. A review of the consequences of global climate change on human health. *J. Environ. Sci. Health C. Environ. Carcinog. Ecotoxicol. Rev.* 32, 299-318.

- Komprda, J., Komprdová, K., Sáňka, M., Možný, M., Nizzetto, L., 2013. Influence of climate and land use change on spatially resolved volatilization of persistent organic pollutants (POPs) from background soils. *Environ. Sci. Technol.* 47, 7052-7059.
- Kong, D., MacLeod, M., Li, Z., Cousins, I.T., 2013. Effects of input uncertainty and variability on the modelled environmental fate of organic pollutants under global climate change scenarios. *Chemosphere* 93, 2086-2093.
- Kong, D., MacLeod, M., Cousins, I.T., 2014. Modelling the influence of climate change on the chemical concentrations in the Baltic Sea region with the POPCYCLING-Baltic model. *Chemosphere* 110, 31-40.
- Kusangaya, S., Warburton, M.L., Archer van Garderen, E., Jewitt, G.P.W., 2014. Impacts of climate change on water resources in southern Africa: A review. *Phys. Chem. Earth Parts A/B/C* 67-69, 47-54.
- Lammel, G.F.J., Leip, A., Semeena, V.S., 2001. Long-range transport and environmental fate of modern pesticides - Model development and application. Proceedings of the International Workshop 'Slowly degradable organics in the atmospheric environment and air-sea exchange'. Edited by Gerhard Lammel. Hamburg, Germany, 2001.
- Lamon, L., MacLeod, M., Marcomini, A., Hungerbühler, K., 2012. Modeling the influence of climate change on the mass balance of polychlorinated biphenyls in the Adriatic Sea. *Chemosphere* 87, 1045-1051.
- Ma, J., Cao, Z., 2010. Quantifying the perturbations of persistent organic pollutants induced by climate change. *Environ. Sci. Technol.* 44, 8567-8573.
- Ma, J., Hung, H., Blanchard, P., 2004. How do climate fluctuations affect Persistent Organic Pollutant distribution in North America? Evidence from a decade of air monitoring. *Environ. Science Technol.* 38, 2538-2543.
- Ma, J., Hung, H., Tian, C., Kallenborn, R., 2011. Revolatilization of persistent organic pollutants in the Arctic induced by climate change. *Nature Clim. Change* 1, 255-260.
- Macdonald, R.W., Harner, T., Fyfe, J., 2005. Recent climate change in the Arctic and its impact on contaminant pathways and interpretation of temporal trend data. *Sci. Total Environ.* 342, 5-86.
- Mackay, D., 2001. *Multimedia Environmental Models: The Fugacity Approach*. Second edn., Boca Raton, FL, USA.
- MacLeod, M., Riley, W.J., McKone, T.E., 2005. Assessing the influence of climate variability on atmospheric concentrations of polychlorinated biphenyls using a global-scale mass balance model (BETR-global). *Environ. Sci. Technol.* 39, 6749-6756.
- Marquès, M., Bangash, R.F., Kumar, V., Sharp, R., Schuhmacher M., 2013. The impact of climate change on water provision under a low flow regime: A case study of the ecosystems services in the Francolí river basin. *J. Hazard. Mater.* 263, 224-232.
- Martí-Cid, R., Huertas, D., Nadal, M., Linares, V., Schuhmacher, M., Grimalt, J.O., Domingo, J.L., 2010. Dietary exposure to organochlorine compounds in Tarragona Province (Catalonia, Spain): Health risks. *Hum. Ecol. Risk Assess.* 16, 588-602.
- Martorell, I., Nieto, A., Nadal, M., Perelló, G., Marcé, R.M., Domingo, J.L., 2012. Human exposure to polycyclic aromatic hydrocarbons (PAHs) using data from a duplicate diet study in Catalonia, Spain. *Food Chem. Toxicol.* 50, 4103-4108.

- McBean, G., Ajibade, I., 2009. Climate change, related hazards and human settlements. *Curr. Opin. Environ. Sust.* 1, 179-186.
- McKinney, M. A., Pedro, S., Dietz, R., Sonne, C., Fisk, A.T., Roy, D., Jenssen, B.M., Letcher, R.J., 2015. A review of ecological impacts of global climate change on persistent organic pollutant and mercury pathways and exposures in arctic marine ecosystems. *Curr. Zool.* 61, 617-628
- McKone, T.E., Daniels J.I., Goldman M., 1996. Uncertainties in the link between global climate change and predicted health risks from pollution: Hexachlorobenzene (HCB) case study using a fugacity model. *Risk Anal.* 16, 377-393.
- Moe, S.J., De Schamphelaere, K., Clements, W.H., Sorensen, M.T., Van den Brink, P.J., Liess M., 213. Combined and interactive effects of global climate change and toxicants on populations and communities. *Environ. Toxicol. Chem.* 32, 49-61.
- Morselli, M., Semplice, M., Villa, S., Di Guardo, A., 2014. Evaluating the temporal variability of concentrations of POPs in a glacier-fed stream food chain using a combined modeling approach. *Sci. Total Environ.* 493, 571-579.
- Mulder, M.D., Heil, A., Kukučka, P., Kuta, J., Přibyllová, P., Prokeš, R., Lammel, G., 2015. Long-range atmospheric transport of PAHs, PCBs and PBDEs to the central and eastern Mediterranean and changes of PCB and PBDE congener patterns in summer 2010. *Atmos. Environ.* 111, 51-59.
- Nadal, M., Wargent, J.J., Jones, K.C., Paul, N.D., Schuhmacher, M., Domingo, J.L., 2006. Influence of UV-B radiation and temperature on photodegradation of PAHs: Preliminary results. *J. Atmos. Chem.* 55, 241-252.
- Ng, C.A., Gray, K.A., 2011. Forecasting the effects of global change scenarios on bioaccumulation patterns in great lakes species. *Global Change Biol.* 17, 720-733.
- Noyes, P.D., McElwee, M.K., Miller, H.D., Clark, B.W., Van Tiem, L.A., Walcott, K.C., Erwin, K.N., Levin, E.D., 2009. The toxicology of climate change: Environmental contaminants in a warming world. *Environ. Int.* 35, 971-986.
- Octaviani, M., Stemmler, I., Lammel, G., Graf, H.F., 2015. Atmospheric transport of persistent organic pollutants to and from the arctic under present-day and future climate. *Environ. Sci. Technol.* 49, 3593-3602.
- O'Driscoll, K., Mayer, B., Su, J., Mathis, M., 2014. The effects of global climate change on the cycling and processes of persistent organic pollutants (POPs) in the North Sea. *Ocean Sci.* 10, 397-409.
- Pacyna, J.M., Cousins, I.T., Halsall, C., Rautio, A., Pawlak, J., Pacyna, E.G., Sundseth, K., Wilson, S., Munthe, J., 2015. Impacts on human health in the Arctic owing to climate-induced changes in contaminant cycling - The EU ArcRisk project policy outcome. *Environ. Sci. Policy* 50, 200-213.
- Paul, A.G., Hammen, V.C., Hickler, T., Karlson, U.G., Jones, K.C., Sweetman, A.J., 2012. Potential implications of future climate and land-cover changes for the fate and distribution of persistent organic pollutants in Europe. *Global Ecol. Biogeogr.* 21, 64-74.
- Perelló, G., Díaz-Ferrero, J., Llobet, J.M., Castell, V., Vicente, E., Nadal, M., Domingo, J.L., 2015. Human exposure to PCDD/Fs and PCBs through consumption of fish and seafood in Catalonia (Spain): Temporal trend. *Food Chem. Toxicol.* 81, 28-33.
- Perrie, W., Long, Z., Hung, H., Cole, A., Steffen A., Dastoor, A., Durnford, D., Ma, J., Bottenheim, J.W., Netcheva, S., Staebler, R., Drummond, J.R., O'Neill, N.T., 2012. Selected topics in arctic atmosphere and climate. *Clim. Change* 115, 35-58.

- Rahn, K.A., Heidam, N.Z., 1981. Progress in Arctic air chemistry, 1977-1980: A comparison of the first and second symposia. *Atmos. Environ.* 15, 1345-1348.
- Riou, V., Ndiaye, A., Budzinski, H., Dugué, R., Le Ménach, K., Combes, Y., Bossus, M., Durand, J.D., Charmantier, G., Lorin-Nebel, C., 2012. Impact of environmental DDT concentrations on gill adaptation to increased salinity in the tilapia *Sarotherodon melanotheron*. *Comp. Biochem. Physiol. C. Pharmacol. Toxicol. Endocrinol.* 156, 7-16.
- Sánchez-Canales, M., López Benito, A., Passuello, A., Terrado, M., Ziv, G., Acuña, V., Schuhmacher, M., Elorza, F.J., 2012. Sensitivity analysis of ecosystem service valuation in a Mediterranean watershed. *Sci. Total Environ.* 440, 140-153.
- Schiedek, D., Sundelin, B., Readman, J.W., Macdonald, R.W., 2007. Interactions between climate change and contaminants. *Mar. Pollut. Bull.* 54, 1845-1856.
- Schröter, D., Cramer, W., Leemans, R., Prentice, I.C., Araújo, M.B., Arnell, N.W., Bondeau, A., Bugmann, H., Carter, T.R., Gracia, C.A., De La Vega-Leinert, A.C., Erhard, M., Ewert, F., Glendining, M., House, J.I., Kankaanpää, S., Klein, R.J.T., Lavorel, S., Lindner, M., Metzger, M.J., Meyer, J., Mitchell, T.D., Reginster, I., Rounsevell, M., Sabaté, S., Sitch, S., Smith, B., Smith, J., Smith, P., Sykes, M.T., Thonicke, K., Thuiller, W., Tuck, G., Zaehle, S., Zierl, B., 2005. Ecology: Ecosystem service supply and vulnerability to global change in Europe. *Science* 310, 1333-1337.
- Serreze, M.C., Barry, R.G., 2011. Processes and impacts of Arctic amplification: a research synthesis. *Global Planet. Change* 77, 85-96.
- Smit, M.P.J, Grotenhuis, T., Bruning, H., Rulkens, W.H, 2009. Modeling desorption kinetics of a persistent organic pollutant from field aged sediment using a bi-disperse particle size distribution. *J. Soil. Sediment.* 10, 119-126.
- Sonne, C., Gustavson, K., Rigét, F.F., Dietz, R., Krüger, T., Bonefeld-Jørgensen, E.C., 2014. Physiologically based pharmacokinetic modeling of POPs in Greenlanders. *Environ. Int.* 64, 91-97.
- Sun, L.G., Yin, X.B., Pan, C.P., Wang, Y.H., 2005. A 50-years record of dichloro-diphenyl-trichloroethanes and hexachloro-cyclohexanes in lake sediments and penguin droppings on King George Island, Maritime Antarctic. *J. Environ. Sci.* 17, 899-905.
- Teran, T., Lamon, L., Marcomini, A., 2012. Climate change effects on POPs' environmental behaviour: A scientific perspective for future regulatory actions. *Atmos. Pollut. Res.* 3, 466-476.
- Terrado, M., Acuña, V., Ennaanay, D., Tallis, H., Sabater, S., 2014. Impact of climate extremes on hydrological ecosystem services in a heavily humanized Mediterranean basin. *Ecol. Indic.* 37, 199-209.
- UNECE, 2014. The 1998 Aarhus Protocol on Persistent Organic Pollutants (POPs). http://www.unece.org/env/lrtap/pops_h1.html. Accessed 24 September 2014.
- van der Bilt, W.G.M., Bakke, J., Vasskog, K., D'Andrea, W.J., Bradley, R.S., Ólafsdóttir, S., 2015. Reconstruction of glacier variability from lake sediments reveals dynamic Holocene climate in Svalbard. *Quat. Sci. Rev.* 126, 201-218.
- Wania, F., Mackay, D., 1995. A global distribution model for persistent organic chemicals. *Sci. Total Environ.* 160-161, 211-232.
- Wania, F., Mackay, D., 1999. The evolution of mass balance models of persistent organic pollutant fate in the environment. *Environ. Pollut.* 100, 223-240

- Watanabe, S., Sudo, K., Nagashima, T., Takemura, T., Kawase, H., Nozawa, T., 2011. Future projections of surface UV-B in a changing climate. *J. Geophys. Res. Atmos.* 116, D16118.
- Wöhrnschimmel, H., Macleod, M., Hungerbühler, K., 2013. Emissions, fate and transport of persistent organic pollutants to the arctic in a changing global climate. *Environ. Sci. Technol.* 47, 2323-2330.
- Wu, C.H., Huang, G.R., Yu, H.J., 2015. Prediction of extreme floods based on CMIP5 climate models: A case study in the Beijiang River basin, South China. *Hydrol. Earth Syst. Sci.* 19, 1385-1399.

DISCUSSION CHAPTER 1

In recent years, the impact of climate change on the concentrations of POPs has become a topic of notable concern. Changes in the environmental conditions such as the increase of the average temperature or the UV-B radiation, are likely to influence the fate and behaviour of POPs, ultimately affecting human exposure. In addition, the way that climate especially can change biomagnification and exposure of wildlife and humans is via changes in the food web dynamics. Legacy POPs (pesticides, PCBs and PCDD/Fs) are the compounds to which researchers have paid more attention when studying the influence of climate change on their environmental behavior. In general terms, it is estimated that the global change will alter the environmental concentrations of POPs within a factor of 2-3. However, the number of investigations aimed at estimating the impact of climate change on the environmental levels of PAHs is scarce. Because of PAHs are potentially sensitive to sunlight, the impact of climate change on the fate and behaviour of PAHs deserves further attention.

CHAPTER 2

Photodegradation of polycyclic aromatic hydrocarbons in soils under a climate change base scenario

Montse Marquès ^{a,b}, Montse Mari ^{a,b}, Carme Audí-Miró ^c,
Jordi Sierra ^{b,d}, Albert Soler ^c, Martí Nadal ^{a*},
José L. Domingo ^a

^a Laboratory of Toxicology and Environmental Health, School of Medicine, IISPV, Universitat Rovira i Virgili, Sant Llorenç 21, 43201 Reus, Catalonia, Spain.

^b Environmental Engineering Laboratory, Departament d'Enginyeria Química, Universitat Rovira i Virgili, Av. Països Catalans 26, 43007 Tarragona, Catalonia, Spain.

^c Grup de Mineralogia Aplicada i Geoquímica de Fluids, Departament de Cristal·lografia, Mineralogia i Dipòsits Minerals, Facultat de Geologia, SIMGEO UB-CSIC, Universitat de Barcelona UB, Martí Franquès s/n, 08028 Barcelona, Spain.

^d Laboratory of Soil Science, Faculty of Pharmacy, Universitat de Barcelona, Av. Joan XXIII s/n, 08028 Barcelona, Catalonia, Spain.

ABSTRACT

The photodegradation of polycyclic aromatic hydrocarbons (PAHs) in two typical Mediterranean soils, either coarse- or fine- textured, was here investigated. Soil samples, spiked with the 16 US EPA priority PAHs, were incubated in a climate chamber at stable conditions of temperature (20°C) and light (9.6 W m⁻²) for 28 days, simulating a climate change base scenario. PAH concentrations in soils were analyzed throughout the experiment, and correlated with data obtained by means of Microtox® ecotoxicity test. Photodegradation was found to be dependent on exposure time, molecular weight of each hydrocarbon, and soil texture. Fine-textured soil was able to enhance sorption, being PAHs more photodegraded than in coarse-textured soil. According to the EC₅₀ values reported by Microtox®, a higher detoxification was observed in fine-textured soil, being correlated with the outcomes of the analytical study. Significant photodegradation rates were detected for a number of PAHs, namely phenanthrene, anthracene, benzo(*a*)pyrene, and indeno(123-*cd*)pyrene. Benzo(*a*)pyrene, commonly used as an indicator for PAH pollution, was completely removed after 7 days of light exposure. In addition to the PAH chemical analysis and the ecotoxicity tests, a hydrogen isotope analysis of benzo(*a*)pyrene was also carried out. The degradation of this specific compound was associated to a high enrichment in ²H, obtaining a maximum δ²H isotopic shift of +232‰. This strong isotopic effect observed in benzo(*a*)pyrene suggests that compound-specific isotope analysis (CSIA) may be a powerful tool to monitor in situ degradation of PAHs. Moreover, hydrogen isotopes of benzo(*a*)pyrene evidenced a degradation process of unknown origin occurring in the darkness.

Keywords: polycyclic aromatic hydrocarbons (PAHs), photodegradation, soil, ecotoxicity, hydrogen isotopes.

INTRODUCTION

Polycyclic aromatic hydrocarbons (PAHs) are a large group of semi-volatile organic compounds composed of two or more fused aromatic rings. Although these chemicals are mostly released to air, soil is considered as one of the major sinks of atmospheric PAHs (Nadal et al., 2011; Wang et al., 2014), being deposited via dry and wet processes (Nadal et al., 2004). PAH fate in the environment includes volatilization, adsorption on soil particles, leaching, microbial degradation, chemical oxidation, and photo-oxidation (Hartiash and Kaushik, 2009). Photodegradation is an important transformation pathway for most PAHs in the environment (Zhang et al., 2006), having been largely studied in water (Bertilsson and Widenfalk, 2002; de Bruyn et al., 2012; Fasnacht and Blough, 2003; García-Martínez et al., 2005; Jacobs et al., 2008; Jing et al., 2014; Luo et al., 2014; Rivas et al., 2000; Shemer and Linden, 2007; Singh et al., 2013; Xia et al., 2009). In contrast, the knowledge regarding the photodegradation process of PAHs in soils is rather limited (Balmer et al., 2000; Frank et al., 2002; Gong et al., 2001; Xiaozhen et al., 2005). It has been reported that soil depth has an important role in the photodegradation of these chemicals, enhancing the resistance of PAHs to be photodegraded. In addition, temperature, soil particle size and humic acids also have a significant influence on photodegradation in soils under UV-B radiation (Zhang et al., 2010). Photodegradation of PAHs in soils has been shown to be not only limited by the light penetration capacity in soils, but also by its wavelength (Cavoski et al., 2007; Xiaozhen et al., 2005). Consequently, photodegradation depends on a number of variables, such as soil type, thickness of the soil layer, as well as light absorption spectrum of each compound (Zhang et al., 2010). This degradation process may play a key role on the fate of PAHs in areas such as the Mediterranean region, with high sunlight presence during the whole year. In turn, some PAH metabolites, which can even be more toxic than their parental compounds, may be generated during the degradation process. Overall, although PAH levels might be reduced in soils exposed to sunlight, toxicity may be increased (Huang et al., 1995; Mallakin et al., 1999; McConkey et al., 1997).

Compound-specific isotope analysis (CSIA) is a very valuable tool, which can be used to monitor in situ degradation processes of chemical pollutants, and as a source identification technique (Elsayed et al., 2014; Imfeld et al., 2014). CSIA is capable of

discriminating degradation from other attenuation processes naturally occurring in the environment, that do not generate destruction of pollutants, such as dispersion, volatilization or sorption. CSIA is based on the isotopic effect produced during a degradation process, which is known as isotopic fractionation (Meckenstock et al., 2004). This effect is based on the enrichment of heavy isotopes in the reacting compound, which is linked to the different strength of the bonds that contain heavy and light isotopes. Since nondestructive natural attenuation processes frequently do not entail significant isotope fractionation, a significant enrichment of the heavy isotope of organic pollutants confirms that a degradation process is occurring. Unfortunately, research on the hydrogen isotopic fractionation of PAHs during degradation is very scarce. To the best of our knowledge, the only precedent is the study of Bergmann et al. (2011), who reported a high hydrogen isotopic shift of naphthalene in two different microbial cultures.

The present investigation aimed at assessing the photodegradation of 16 US EPA priority PAHs in two types of Mediterranean soils. Laboratory experiments were conducted in a climate chamber to simulate the current Mediterranean environmental conditions, keeping temperature and sunlight stable. Temporal changes of PAH concentrations and ecotoxicity levels were investigated, and jointly evaluated. Moreover, hydrogen isotopic analysis of benzo(*a*)pyrene, considered one of the most toxic PAHs and probably carcinogenic to humans (Aina et al., 2006), was complementarily performed to verify the findings.

MATERIALS AND METHODS

Soil characteristics

Two common Mediterranean soils were selected to perform the photodegradation experiments. Physicochemical properties of both soils are given in Table 1. Soil samples were collected from the A horizon of remote areas of Catalonia (NE of Spain). The Arenosol soil, with granitic origin, is an acidic and coarse-textured soil that can be classified as Haplic Arenosol, according to the (FAO-UNESCO, 1998). It is commonly used for ecotoxicity tests in terrestrial environments. In turn, Regosol soil is an alkaline calcareous fine-textured soil formed of sedimentary materials, being

classified as Calcaric Regosol (FAO-UNESCO, 1998). Both soils are characterized by owing a low organic matter content (Table 1). In order to quantify titanium, iron, aluminum and manganese oxides, ammonium oxalate was used as extractant, according to the method described by Drees and Ulery (2008).

Experimental design

Photodegradation experiments were carried out in a Binder KBWF 240 climate chamber (Binder GmbH, Tuttlingen, Germany) with constant lighting, temperature and humidity. Temperature and daylight were set at 20°C and 9.6 W m⁻², respectively, as current environmental conditions in the Mediterranean area. Because photodegradation reactions occur mainly in the surface, soil was air-dried. Consequently, to avoid the presence of water and any potentially associated biodegradation process, humidity was kept constant at 40%. Ten grams of air-dried soil were deployed in uncovered glass Petri dishes forming a thick layer of 1 mm of soil. A stock solution containing 16 US EPA priority PAHs at 2000 µg mL⁻¹ in dichloromethane:benzene was provided by Supelco® (99.0% purity, Bellefonte, PA, USA). Each sample was 10-times spiked with 25 µL of this stock solution diluted with an hexane/dichloromethane (1:1) mixture (Scharlau Chemie S.A., Barcelona, Spain; hexane: 96% purity, dichloromethane: 99.5% of purity) to an individual PAH concentration of 100 µg mL⁻¹, leading to a Σ16 PAHs concentration of 40 µg g⁻¹ in soil. Afterwards, samples were incubated inside the climate chamber. In order to differentiate concentration decreases due to slow sorption and/or volatilization processes from photodegradation, a number of dark control samples covered with aluminum foil were exposed to the same environmental conditions. Duplicates of irradiated samples and dark controls of each soil were removed from the climate chamber after 1, 2, 3, 4, 5, 6, 7, 14, and 28 days. To verify the lack of any biotic reactions, before the experiment was initiated, soils were incubated at the same conditions in manometric respirometers (Oxitop®, WTW). Negligible oxygen consumption was observed during the incubation period, discarding biotic processes. Ten grams of soil without any spiking of PAHs were used as blank soil samples.

Table 1. Physico-chemical properties of the selected Mediterranean soils.

	Arenosol soil	Regosol soil
pH	5.8	8.0
Electrical conductivity at 25°C (dS m ⁻¹) ^a	0.06	0.13
Organic C (%) ^b	0.71	1.70
Total Kjeldahl N (%)	0.07	0.18
C/N	10.1	9.44
CaCO ₃ (%)	0.10	23.20
Texture: sand/silt/clay (%) ^c	74.1/14.0/11.9	43.4/22.3/34.3
Cation exchange capacity (meq 100 g ⁻¹) ^d	12.60	18.23
Exchangeable calcium (mg CaO kg ⁻¹) ^d	4.80	12.55
TiO ₂ (mg kg ⁻¹)	429	41.3
MnO ₂ (mg kg ⁻¹)	573	648
Al ₂ O ₃ (mg kg ⁻¹)	3008	6070
Fe ₂ O ₃ (mg kg ⁻¹)	6686	13492

Analytical methods: ^aAqueous extracts 1:2.5; ^bOxidizable C by Walkley-Black method; ^cRobinson Pipette method; ^d1 N ammonium acetate extracts.

PAH analysis

Prior to analysis, PAHs were extracted from soil samples by using 30 mL of a mixture of hexane/dichloromethane (1:1) (Scharlau Chemie S.A., Barcelona) in a Milestone Start E Microwave Extraction System (Milestone s.r.l., Sorisole, Italy), according to the US EPA method 3546. Subsequently, samples were filtered, concentrated to 1 mL and further evaporated with a gentle stream of purified N₂. Since any interference with target analytes was found, cleanup was discarded in order to achieve suitable recoveries for low molecular weight PAHs. Regarding the quality control, d₁₀-fluorene (98.3% purity, Supelco[®]) was used as surrogate, while d₈-naphthalene (99.8% purity, Supelco[®]) and d₁₂-benzo(*a*)pyrene (98.5% purity, Supelco[®]) were used as internal standards. Dried samples were dissolved with a solution of internal standards at 50 µg mL⁻¹ concentration in hexane/dichloromethane (1:1) mixture (Scharlau Chemie S.A., 99.5% of purity). Blank soil samples were also extracted following the same procedure in order to assure that collected soils were PAH-free. All samples were analyzed by means of gas chromatography-mass spectrometry (GC-MS) in accordance to the US EPA method 8270. A Hewlett-Packard G1099A/MSD5973 equipment with an HP-5MS 5% Phenyl Methyl Siloxane column (20 m x 0.25 mm x 0.25 µm) was used to quantify the content of the 16 PAHs under study

in soil. The final experimental conditions were: 1 μL injection at 310°C in split-splitless, and pulsed splitless mode at 35 psi (for 0.05 min). Transfer line temperature was set at 280°C. Ultra-pure (99.9999%) helium was used as carrier gas, at a total flow rate of 1.4 mL min^{-1} . The GC oven temperature started at 80°C, being consecutively increased at 15°C min^{-1} until 180°C, at 8°C min^{-1} until 250°C, and at 3°C min^{-1} up to 300°C. At the end of each ramp, temperature was held for 1 min. Finally, an increase of 20°C min^{-1} was executed until reaching 320°C, holding this temperature for 6 min. The detector was set to quantify the analytes covering specific masses ranging from 40 to 600 atomic mass units. The mass spectrometer and source temperatures were 150°C and 230°C, respectively. Samples were quantified using a six-point calibration curve (5, 10, 25, 50, 60, 80 $\mu\text{g mL}^{-1}$). Sample preparation for the PAH analyses was performed at the “Laboratory of Environmental Engineering” of the Universitat Rovira i Virgili (URV), while concentrations were determined at the “Servei de Recursos Científics i Tècnics” of the same institution (SRCiT-URV).

Statistical analysis

Results were statistically evaluated using XLSTAT Statistical Software for Excel. Repeated measures of the ANOVA were used to state significant differences between irradiated and non-irradiated samples through the time. A regression analysis was also executed to study the relationship between concentrations and time. Probability levels were considered as statistically significant at $p < 0.05$.

Ecotoxicological tests

Soils were extracted by using an ultrasonic bath mixture (1:1) of n-hexane 95% (UV-IR-HPLC) PAI-ACS (Panreac, Castellar del Vallès, Barcelona, Spain) and acetone (Reag. Ph. Eur) PA-ACS-ISO (Panreac), following the US EPA method 3550C. Blank soil samples were simultaneously extracted following the same procedure. Afterwards, soil extracts were filtered, and the solvent was completely dried with a rotatory evaporator, being finally reconstituted with 2 mL of dimethyl sulfoxide (UV-IR-HPLC-GPC) to a concentration of 2-4% in Microtox® diluent (2% NaCl of aqueous solution). Ecotoxicity values were quantified by means of the Microtox® 500 Analyser (SDI, USA),

following the ISO 11348-1:2007 norm. The bioluminescent bacteria *V. fischeri* was used to measure the inhibition of light emission when organisms were exposed to soil extract samples. EC₅₀ values were estimated as the sample concentration causing 50% of light inhibition on the test organisms (Roig et al., 2013). Sample preparation and Microtox® test were performed at the “Laboratory of Environmental Engineering” of the URV.

Hydrogen isotope analysis of benzo(a)pyrene

For hydrogen isotope analysis, soil samples were also extracted with the same Milestone Start E Microwave Extraction System (Milestone s.r.l., Sorisole, Italy), according to the US EPA method 3546. The extract was treated by following the same procedure used to analyze PAH levels. Once the extract was completely dried, it was dissolved in 62.5 µL of dichloromethane (99.5%, Scharlau Chemie S.A.) free of any deuterated PAHs that could interfere in δ²H analysis. The hydrogen isotope composition of benzo(a)pyrene was analyzed using a gas chromatography-pyrolysis-isotope ratio mass spectrometry system (GC-Pyr-IRMS) consisting of a Trace GC Ultra equipped with a split/splitless injector, coupled to a Delta V Advantage IRMS (Thermo Scientific GmbH, Bremen, Germany), through a combustion interface.

The GC/Pyr/IRMS system was equipped with an Agilent Technologies DB-1 column (30 m × 0.25 mm, 1.0 µm film thickness; Santa Clara, CA, USA). The oven temperature program was kept at 50°C for 1 min, heated again until 160°C at a rate of 25°C min⁻¹, then up to 320°C at a rate of 3°C min⁻¹, being finally held at 320°C for 20 min. The injector was set to splitless mode at a temperature of 280°C. Helium was used as a carrier gas with a gas flow rate of 1.0 mL min⁻¹.

Hydrogen isotope ratios are reported relative to an international standard (Vienna Standard Mean Ocean Water, VSMOW), using the delta notation:

$$\delta^2\text{H} (\text{‰}) = (R/(R_{\text{std}} - 1)) \times 1000$$

where R and R_{std} are the isotope ratios (H²/H¹) of the sample and the standard, respectively. All the measurements were run in duplicate, and the standard deviations of the δ²H values obtained were below ±10‰. The analytical system was daily verified using PAH control standards with known hydrogen isotope ratios, which were previously determined using a Carlo-Erba 1108 (Carlo-Erba, Milano, Italy) elemental

analyzer (EA) coupled in continuous flow to a Delta Plus XP isotope ratio mass spectrometer (Thermo Fisher Scientific, Bremen, Germany). The samples were prepared for the isotopic analyses in the “Mineralogia Aplicada i Geoquímica de Fluids” Research Group laboratory and analyzed at the “Centres Científics i Tecnològics” of the Universitat de Barcelona (CCiT-UB).

RESULTS AND DISCUSSION

Photodegradation of PAHs in soils

The trends in the levels of naphthalene, phenanthrene, pyrene, benzo(*a*)pyrene, and benzo(*ghi*)perylene in Arenosol and Regosol soils, are depicted in Fig. 1. Those compounds were selected as representatives of 2-, 3-, 4-, 5- and 6-ringed PAHs, respectively. The results for other PAHs are shown in Annex 1 (Fig. S1).

A different behavior for the 16 PAHs in coarse- and fine-textured soils over the time was observed, leading to different photodegradation rates, which were calculated considering the difference between irradiated samples and dark controls (Table 2). Statistical significances for the different exponential and linear rates are shown in Table 3. Three main processes might be related to the concentration decreases: volatilization (Wang et al., 2015), sorption (Liu et al., 2007; Zhang et al., 2014), and photodegradation (EL-Saeid et al., 2015). However, the contribution of each process was different according to the physicochemical properties of each compound (SI, Table S1), as well as to the texture of each soil. In general terms, higher photodegradation rates were noted in some compounds for fine-textured soil, when comparing irradiated samples and dark controls. As expected, the lowest PAH recoveries were found for the most volatile compounds (naphthalene, acenaphthylene and acenaphthene). PAH recoveries 1 h after soil contamination were found to be higher in fine-textured Regosol soil (14%-127%) than in heterogeneous coarse-textured Arenosol soil (7%-92%). The latter has lower organic matter content, as well as a lower amount of fine fraction, causing a weaker retention of PAHs.

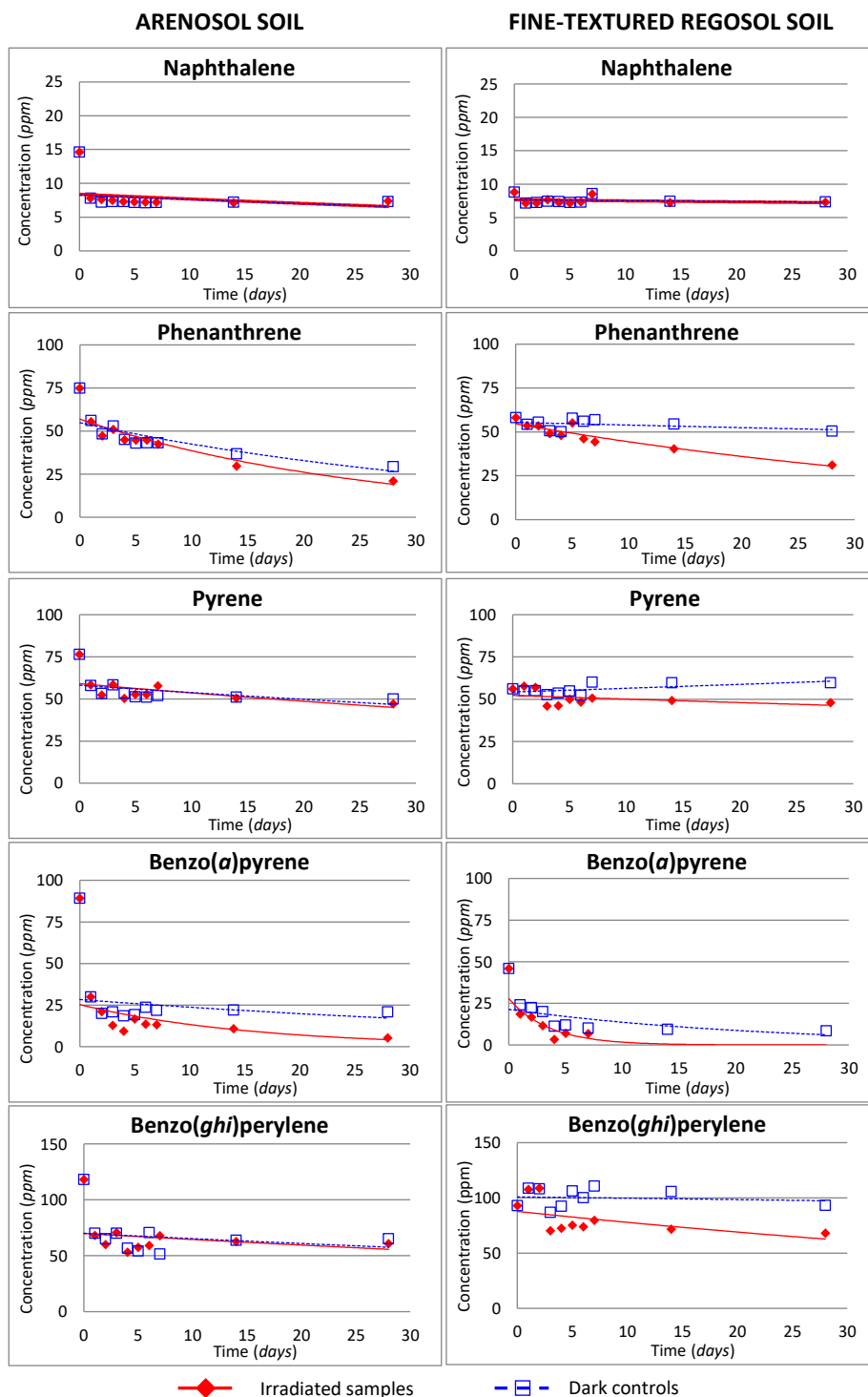


Fig. 1. Concentration of various PAHs in irradiated and dark control soil samples in Arenosol soil (left) and fine-textured Regosol soil (right).

Volatilization was probably the most significant process for 2- and 3-ringed PAHs. No differences of naphthalene concentrations were found between irradiated and dark control samples, indicating that naphthalene was not photodegraded in any soil, either Arenosol or Regosol. Because of its high vapor pressure, the decreasing content of naphthalene (85%) observed during the first hour after being spiked (SI, Table S1) could be related to volatilization processes (Liu et al., 2011). Similar results were also obtained for acenaphthylene, being 80% decreased in the same period of time elapsed. Regarding acenaphthene, similar and constant concentrations were noted for irradiated and dark control samples over the time, with slight decreasing rates in Arenosol and Regosol soils (1.5% and 2%, respectively). Consequently, a significant decrease of the concentration of this compound was not observed ($p > 0.05$), indicating that photodegradation did not occur.

Fluorene, phenanthrene, anthracene and fluoranthene showed higher decreasing concentration rates in Regosol than in Arenosol soil. In Regosol soil, phenanthrene and anthracene exhibited photodegradation rates of 33% and 40%, respectively, after 28 days of light exposure, being the differences between controls and irradiated samples statistically significant after 2 days.

In Arenosol soil, pyrene, benzo(*a*)anthracene, chrysene and benzo(*b+k*)fluoranthene kept their concentrations constant in both irradiated samples and dark controls, suggesting lack of photodegradation. In contrast, decreasing concentrations of the same 4-ringed PAHs were found in fine-textured Regosol soil. Decreasing rates were up to 30% for these compounds at the end of the experiment. In turn, pyrene concentration was only slightly decreased (17%) over the experiment. This ratio is 10% lower than that reported by (Zhang et al., 2010) for pyrene in soil samples irradiated using UV lamps with a wavelength of 254 nm. However, no significant differences were noted in the current study between irradiated and control samples ($p > 0.05$).

Benzo(*a*)pyrene was sorbed to soil during the first day according to the fast concentration decrease, in both soils and both irradiated and non-irradiated samples. A decreased rate of 23% was estimated in coarse-textured Arenosol soil, which is in agreement with the findings of Zhang et al. (2006). In turn, higher rates were observed in fine-textured Regosol soil, showing a complete removal of benzo(*a*)pyrene after 7

days of incubation. Zhang et al. (2008) reported that titanium dioxide (TiO₂) under UV light, accelerates the photodegradation process of phenanthrene, pyrene and benzo(*a*)pyrene on surface soil, being benzo(*a*)pyrene the most quickly degraded. Although the TiO₂ content in fine-textured Regosol soil is lower than that in Arenosol soil, the higher content of other photocatalysts (e.g., Fe₂O₃, Al₂O₃, MnO₂, or TiO₂) in the fine-textured soil, as well as the higher fine fraction due to its clay content, might be responsible of this complete degradation (Gupta and Gupta, 2015; Zhang et al., 2006; Zhao et al., 2004).

Table 2. Photodegradation rates (%) of the 16 PAHs under study in Arenosol and Regosol soils.

	Arenosol soil	Regosol soil
Naphthalene	0	0
Acenaphthylene	0	0
Acenaphthene	1.5	2
Fluorene	3	9.5
Phenanthrene	11.2	33.2
Anthracene	19.7	39.8
Fluoranthene	0	12.5
Pyrene	0	17.1
Benzo(<i>a</i>)anthracene + chrysene	0	30
Benzo(<i>b+k</i>)fluoranthene	0	30
Benzo(<i>a</i>)pyrene	23	4.9*
Benzo(<i>ghi</i>)perylene	3.6	24.6
Dibenzo(<i>ah</i>)anthracene	2	28.3
Indeno(<i>123-cd</i>)pyrene	11.7	68.9

*completely degraded after 7 days of light exposure.

As a consequence of the high constant concentrations in irradiated samples and dark controls, it can be confirmed that dibenzo(*ah*)anthracene tended to be less adsorbed than other PAHs in both soils, since concentrations in dark controls were constant over the experiment. This compound seemed to suffer a slight photodegradation in the coarse-textured soil, while the degradation rate was substantially higher in fine-textured soil (<5% and 28%, respectively) over the experiment. After 28 days of exposure, only 12% of the indeno(*123-cd*)pyrene was photodegraded in Arenosol soil, while up to 69% was removed in fine-textured Regosol soil. Benzo(*ghi*)perylene was adsorbed more quickly in the coarsed soil,

finding a slightly higher decrease of its concentration in dark controls over the experiment when comparing to dibenzo(*ah*)anthracene. The photodegradation of benzo(*ghi*)perylene started in the 14th day of exposure, being the photodegradation rate <5% after 28 days. Contrastingly, this PAH was less adsorbed in Regosol soil, where a photodegradation of up to 25% was noted at the end of the experiment.

Phenanthrene, pyrene, benzo(*a*)pyrene and benzo(*ghi*)perylene showed a concentration decrease in dark conditions in Arenosol soil, indicating that unknown degradation processes, other than photodegradation, could be also occurring in the dark conditions for this type of soil. In contrast, in the Regosol soil, these same compounds showed constant concentrations in dark conditions, being therefore different from the levels observed under light conditions.

Table 3. Statistical significance (*p*) of the regression associated to the photodegradation of PAHs.

Compound	Arenosol soil		Regosol soil		
	regression	<i>p</i>	regression	<i>p</i>	
Naphthalene	exponential	0.277	exponential	0.955	
Acenaphthylene	exponential	0.571	exponential	0.023	
Acenaphthene	exponential	0.005	exponential	<0.0001	
Fluorene	exponential	0.006	exponential	<0.0001	
Phenanthrene	exponential	<0.0001	exponential	<0.0001	
Anthracene	exponential	<0.0001	exponential	<0.0001	
Fluoranthene	exponential	0.548	exponential	0.152	
Pyrene	exponential	0.06	linear	0.134	
Benzo(<i>a</i>)anthracene	+	exponential	0.137	linear	0.095
chrysene					
Benzo(<i>b+k</i>)fluoranthene	exponential	0.039	linear	0.454	
Benzo(<i>a</i>)pyrene	exponential	0.017	exponential	0.114	
Benzo(<i>ghi</i>)perylene	exponential	0.409	exponential	0.120	
Dibenzo(<i>ah</i>)anthracene	exponential	0.058	exponential	0.131	
Indeno(<i>123-cd</i>)pyrene	linear	0.289	exponential	0.004	

In bold, statistically significant regression.

Focusing on the differences between soil textures, our findings agree with those previously reported by Xiaozhen et al. (2005). These authors found that the photolysis rate of antrazine and the photolytic depth increased gradually from sand through silt to clay. Therefore, photochemical reactions may be accelerated when soil particles are smaller. This is likely related to the increase of the surface area per mass, hence showing a greater catalytic capability. By contrast, Zhang et al. (2010) found that the increase of soil particle size allows a higher scattering and permeation of light, therefore speeding up any photodegradation process. It must be stated that the current experiment was performed with the top soil layer (1 mm of depth), since the objective was to analyze the PAH photodegradation in soils due to atmospheric deposition. Consequently, in the present study the role of light penetration is discarded. Several studies have also highlighted the active function of Fe_2O_3 , MnO and TiO_2 to boost photodegradation processes. Zhao et al. (2004) found that the addition of $\alpha\text{-Fe}_2\text{O}_3$ or TiO_2 enhanced the photocatalytic degradation of gamma-hexachlorocyclohexane ($\gamma\text{-HCH}$) in the soil surface. Similarly, Zhang et al. (2006) stated that the content of Fe_2O_3 and other semiconductor oxides, such as TiO_2 and MnO_2 , in soils improved the photodegradation of benzo(a)pyrene. Notwithstanding, the presence of oxides available in fine-textured Regosol soil, as well as its clay content, might have some influence on the high photodegradation rates, even in the PAHs of high molecular weight. Nadal et al. (2006) reported that high molecular weight PAHs could not be photodegraded in an organic solvent after one week of UV-B exposure. In contrast, Guieysse et al. (2004) confirmed found out that UV-photolysis acts preferentially on large PAHs. In any case, the complexity of soils could give place to an enhancement and acceleration of photodegradation reactions.

Effect of photodegradation over ecotoxicity of PAHs

Microtox[®] has been established as a fast, useful and sensitive method to assess the toxicity of soils spiked with PAHs (Khan et al., 2012). According to Salizzato et al. (1997), 5 min.- EC_{50} values were found to be suitable for these organic compounds. In the present study, blank samples in Arenosol and Regosol soils, showed ecotoxicity values of 113 and 182 mg of soil mL^{-1} Microtox[®] diluent, respectively. These results are 10-times higher than toxicity results found in spiked soil samples before any

irradiation, showing values of 12.9 and 15.6 mg of soil mL⁻¹ Microtox® diluent, in Arenosol and Regosol soil samples, respectively.

The EC₅₀ values of irradiated samples and dark controls in Arenosol and fine-textured Regosol soils are depicted in Fig. 2. The coefficient of determination (R²) of EC₅₀ vs. Σ16 PAH concentrations over the time was 0.75 and 0.78 in coarse- and fine-textured soils, respectively. Both irradiated samples and dark controls tended to increase their EC₅₀ over time. This slow detoxification would be mainly consequence of the volatilization, sorption and/or photodegradation of PAHs. In Arenosol samples, EC₅₀ of irradiated and control samples showed a very similar trend. Therefore, no ecotoxicity differences were found, independently on the exposure to light, being in full agreement with the findings from the chemical analysis of PAHs. In contrast, EC₅₀ in irradiated and dark control samples of fine-textured soils showed a different pattern (Fig. 2). Excluding data regarding one day after incubation, the EC₅₀ curve of irradiated samples was more pronounced than that of dark controls, indicating a lower toxicity. Taking into account that irradiated and dark control samples were exposed to the same conditions, excepting light exposure, it is clear that light enhances the detoxification of fine-textured Regosol soil. Similarly to Arenosol soil findings, the current toxicity results also agree with the high photodegradation rates observed in the analytical experiment. Those 3-, 4-, 5- and 6-ringed PAHs, which were highly photodegraded, could be the responsible of the toxicity decrease. In the period of time elapsed between day 1 and before 2 and 3 days after incubation time in Regosol and Arenosol soils, respectively, the toxicity of irradiated samples was higher than in dark controls. This could be linked to the potential formation of metabolites, such as some oxygenated PAHs, even more toxic than the parental compounds (Bandowe et al., 2014; Knecht et al., 2013; Lundstedt et al., 2007). Anyhow, this finding deserves further investigation, which should confirm the relationship between the generation of by-products and the ecotoxicological status of soil.

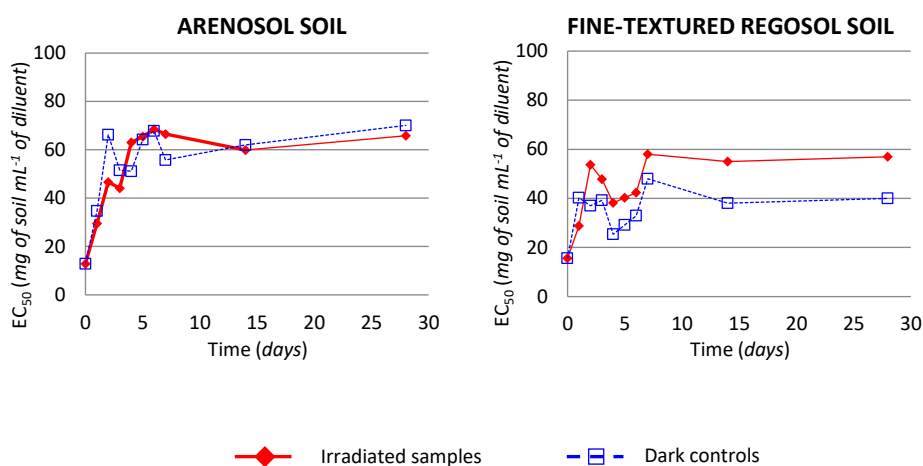


Fig. 2. Ecotoxicity of Arenosol (left) and Regosol (right) soil samples spiked with 16 PAHs.

The results of the Microtox® ecotoxicity test demonstrated that the light, together with other mechanisms such as sorption, volatilization, and abiotic degradation, enhances PAH detoxification on surface soil. This process is especially remarkable in fine-textured soils, which contain materials capable to act as photocatalysts. Anyway, although photodegradation and detoxification occurred, spiked soil samples did not achieve toxicity levels of blank samples 28 days after light exposure. Consequently, a longer exposure time, or an increase of light intensity, would be required to completely remove PAHs from soils. However, the outcomes of both chemical and ecotoxicological analyses indicate that photodegradation is an important process of PAH removal in soil.

Hydrogen isotope effects on benzo(a)pyrene

The hydrogen isotopic composition of benzo(a)pyrene in irradiated samples and dark controls is shown in Fig. 3. In Arenosol soil, benzo(a)pyrene of irradiated samples experienced a change in its hydrogen isotopic composition (after only 5 days of experiment) from -39‰ to +193‰. In agreement with data on PAH levels, this high isotopic shift clearly confirms degradation of benzo(a)pyrene under the selected climate conditions. Due to their too low concentrations, $\delta^2\text{H}$ could not be obtained from the subsequent samples. Unexpectedly, a hydrogen isotopic change of

benzo(*a*)pyrene was also observed in dark control samples. Therefore, unknown degradation processes could be also occurring in absence of light (Fig. 3). Under darkness conditions, benzo(*a*)pyrene in Arenosol suffered a progressive enrichment in $\delta^2\text{H}$. Despite being slower than in irradiated samples, it increased from -39‰ to +181‰ after 28 days of incubation in the dark. It is suggested that there could be some abiotic degradation of benzo(*a*)pyrene, which would be the result of its reaction with organic and/or mineral phases of the soil. The hydrogen isotope results of benzo(*a*)pyrene in Regosol soil samples were similar to those corresponding to Arenosol soil. Benzo(*a*)pyrene hydrogen isotopic composition changed from -39‰ to +68‰ after only 3 days of experiment (Fig. 3). Five days after starting, a decrease in the $\delta^2\text{H}$ value was observed, most likely as a result of reversible sorption processes, which might have released benzo(*a*)pyrene molecules with a lower degradation degree, and consequently, with a lower $\delta^2\text{H}$. However, this isotopic shift also confirms that benzo(*a*)pyrene in Regosol soil is degraded under the same climate conditions. Dark controls also showed a slow degradation, with an isotopic change from -39‰ to +35‰ after 28 days of experiment. Similarly to Arenosol soil samples, dark controls of Regosol soil showed a slower isotopic enrichment in ^2H with respect to irradiated samples, confirming that the same process of PAH loss might be occurring. The evolution of the hydrogen isotopic composition of the dark controls shows fluctuations over the time that could be linked to sorption/desorption effects. Consequently, the hydrogen isotope analysis also seems to confirm that sorption processes of PAHs in soil were present, which is in agreement with the data from the chemical analysis of PAHs. Notwithstanding, since the relationship between the lack of hydrogen isotopic fractionation of PAHs with sorption processes in soil has not been described in the scientific literature, this hypothesis cannot be confirmed yet. Our results corroborate that benzo(*a*)pyrene is not only photodegraded, but also that this degradation is associated to a significant isotopic change. Moreover, they highlight the great potential of CSIA to be used as a powerful tool to monitor in situ PAH degradation. Furthermore, the abiotic degradation of benzo(*a*)pyrene without light intervention was proved to be a potentially relevant pathway of PAH loss in soil. However, further studies are still necessary to confirm the mechanisms of PAH degradation in dark conditions.

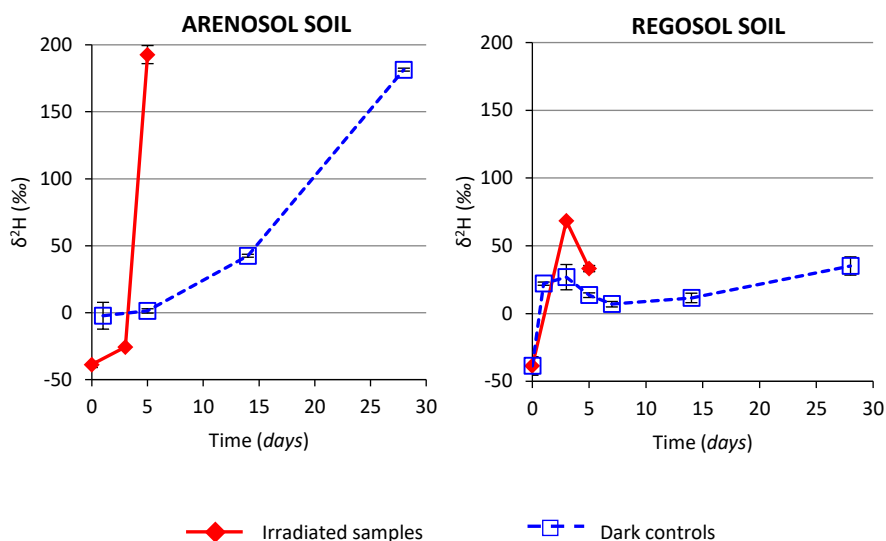


Fig. 3. Hydrogen isotopic composition of benzo(a)pyrene in Arenosol and Regosol soils in irradiated and dark control experiments.

CONCLUSIONS

The photodegradation of PAHs in soils is highly dependent on the exposure time, the molecular weight of each hydrocarbon, and the soil texture. Low molecular weight PAHs are more influenced by volatilization and sorption, while medium and high molecular weight PAHs are able to undergo different photodegradation ratios. Soil properties (texture and metal oxides) were found to influence on volatilization, sorption and photodegradation of PAHs. Photodegradation in soils is a mechanism that mostly occurs in soil surface, being able to partially detoxify soil. Moreover, this process can be enhanced by solid phase soil composition, especially in soils with a finer fraction, as well as by the presence of semiconductor minerals, such as metal oxides. The evolution of 16 PAH concentrations over the time agrees well with Microtox[®] results, with a faster detoxification in fine-textured Regosol soil. However, after 28 days of incubation, soil samples were not completely detoxified. It is important to note that photodegradation is not the only process of PAH loss in soils. Other mechanisms, such as biodegradation and sorption, may also have important roles on the PAH behavior in soils. Moreover, in a climate change context, where an

increase of solar radiation is expected, photodegradation could become a very important process in PAH dynamics in soils.

Finally, the complementary analyses of hydrogen isotopes of benzo(*a*)pyrene confirmed, at a molecular level, that this compound is degraded not only under light conditions, but also in the darkness. Furthermore, the strong isotopic effect observed in benzo(*a*)pyrene makes the CSIA a potentially suitable technique to give evidence of PAH degradation. Since its degradation involves a high hydrogen isotopic variation, CSIA is also a powerful tool to quantify in situ the degradation efficiency.

Acknowledgments

This study was financially supported by the Spanish Ministry of Economy and Competitiveness, through the projects CTM2012-33079 and CGL2011-29975-C04-01, and by the Catalan Government, through the projects 2014SGR90 and 2014SGR1456. Montse Marquès received a PhD fellowship from AGAUR (Commissioner for Universities and Research of the Department of Innovation, Universities and Enterprise of the “Generalitat de Catalunya” and the European Social Fund). The authors are indebted to Josep Maria Mateo-Sanz for his excellent assistance in statistics analysis.

References

- Aina, R., Palin, L., Citterio, S., 2006. Molecular evidence for benzo(*a*)pyrene and naphthalene genotoxicity in *Trifolium repens* L. *Chemosphere* 65, 666-673.
- Balmer, M.E., Goss, K.-U., Schwarzenback, R.P., 2000. Photolytic transformation of organic pollutants on soil surfaces an experimental approach. *Environ. Sci. Technol.* 34, 1240-1245.
- Bandowe, B.A.M., Bigalke, M., Boamah, L., Nyarko, E., Saalia, F.K., Wilcke, W., 2014. Polycyclic aromatic compounds (PAHs and oxygenated PAHs) and trace metals in fish species from Ghana (West Africa): Bioaccumulation and health risk assessment. *Environ. Int.* 65.
- Bergmann, F.D., Abu Laban, N.M.F.H., Meyer, A.H., Elsner, M., Meckenstock, R.U., 2011. Dual (C, H) isotope fractionation in anaerobic low molecular weight (Poly)aromatic hydrocarbon (PAH) degradation: potential for field studies and mechanistic implications. *Environ. Sci. Technol.* 45, 6947-6953.
- Bertilsson, S., Widenfalk, A., 2002. Photochemical degradation of PAHs in freshwaters and their impact on bacterial growth – influence of water chemistry. *Hydrobiologia.* 469, 23-32.

- Cavoski, I., Caboni, P., Sarais, G., Cabras, P., Miano, T., 2007. Photodegradation of rotenone in soils under environmental conditions. *J. Agric. Food Chem.* 55, 7069-7074.
- de Bruyn, W.J., Clark, C.D., Ottelle, K., Aiona, P., 2012. Photochemical degradation of phenanthrene as a function of natural water variables modeling freshwater to marine environments. *Mar. Pollut. Bull.* 64, 532-538.
- Drees, L.R., Ulery, A.L., 2008. *Methods of Soil Analysis. Part 5. Mineralogical Methods.* Soil Science Society of America, 677 S. Segoe Road, Madisom, WI 53711, USA.
- EL-Saeid, M.H., Al-Turki, A.M., Nadeem, M.E.A., Hassanin, A.S., Al-Wabel, M.I., 2015. Photolysis degradation of polyaromatic hydrocarbons (PAHs) on surface sandy soil. *Environ. Sci. Pollut. Res.* 22, 9603–9616.
- Elsayed, O.F., Maillard, E., Vuilleumier, S., Nijenhuis, I., Richnow, H.H., Imfeld, G., 2014. Using compound-specific isotope analysis to assess the degradation of chloroacetanilide herbicides in lab-scale wetlands. *Chemosphere* 99, 89-95.
- FAO-UNESCO, *World Reference Base for Soil Resources.* FAO, Rome, 1998.
- Fasnacht, M.P., Blough, N.V., 2003. Mechanisms of the aqueous photodegradation of Polycyclic Aromatic Hydrocarbons. *Environ. Sci. Technol.* 37, 5767-5772.
- Frank, M.P., Graebing, P., Chib, J.S., 2002. Effect of soil moisture and sample depth on pesticide photolysis. *J. Agric. Food Chem.* 50, 2607-2614.
- García-Martínez, M.J., Canoira, L., Blazquez, G., Da Riva, I., Alcántara, R., Llamas, J.F., 2005. Continuous photodegradation of naphthalene in water catalyzed by TiO₂ supported on glass Raschig rings. *Chem. Eng. J.* 110, 123-128.
- Gong, A., Ye, C., Wang, X., Lei, Z., Liu, J., 2001. Dynamics and mechanism of ultraviolet photolysis of atrazine on soil surface. *Pest Manage. Sci.* 57, 380-385.
- Guieysse, B., Viklund, G., Toes, A.C., Mattiasson, B., 2004. Combined UV-biological degradation of PAHs. *Chemosphere* 55, 1493-1499.
- Gupta, H., Gupta, B., 2015. Photocatalytic degradation of polycyclic aromatic hydrocarbon benzo(a)pyrene by iron oxides and identification of degradation products. *Chemosphere* 138, 924–931.
- Hartiash, A.K., Kaushik, C.P., 2009. Biodegradation aspects of Polycyclic Aromatic Hydrocarbons (PAHs): A review. *J. Hazard. Mater.* 169, 1-15.
- Huang, X., Dixon, D.G., Greenberg, B.M., 1995. Increased polycyclic aromatic hydrocarbon toxicity following their photomodification in natural sunlight: Impacts on the duckweed *Lemna gibba* L. G-3. *Ecotoxicol. Environ. Saf.* 32, 194-200.
- Imfeld, G., Kopinke, F.D., Fischer, A., Richnow, H.H., 2014. Carbon and hydrogen isotope fractionation of benzene and toluene during hydrophobic sorption in multistep batch experiments. *Chemosphere* 107, 454-461.
- Jacobs, L.E., Weavers, L.K., Chin, Y., 2008. Direct and indirect photolysis of polycyclic aromatic hydrocarbons in nitrate-rich surface waters. *Environ. Toxicol. Chem.* 27, 1643-1648.
- Jing, L., Chen, B., Zhang, B., Zheng, J., Liu, B., 2014. Naphthalene degradation in seawater by UV irradiation: The effects of fluence rate, salinity, temperature and initial concentration. *Mar. Pollut. Bull.* 81, 149-156.
- Khan, M., Cheema, S.A., Tang, X., Shen, C., Sahi, S.T., Jabbar, A., Park, J., Chen, Y., 2012. Biototoxicity assessment of pyrene in soil using a battery of biological assays. *Arch. Environ. Contam. Toxicol.* 63, 503-512.

- Knecht, A.L., Goodale, B.C., Truong, L., Simonich, M.T., Swanson, A.J., Matzke, M.M., Anderson, K.A., Waters, K.M., Tanguay, R.L., 2013. Comparative developmental toxicity of environmentally relevant oxygenated PAHs. *Toxicol. Appl. Pharmacol.* 271, 266-275.
- Liu, G., Yu, L., Li, J., Liu, X., Zhang, G., 2011. PAHs in soils and estimated air-soil exchange in the Pearl River Delta, South China. *Environ. Monit. Assess.* 173, 861-870.
- Liu, L., Tindall, J.A., Friedel, M.J., 2007. Biodegradation of PAHs and PCBs in soils and sludges. *Water Air Soil Pollut.* 181, 281-296.
- Lundstedt, S., White, P.A., Lemieux, C.L., Lynes, K.D., Lambert, I.B., Oberg, L., Haglund, P., Tysklind, M., 2007. Sources, fate, and toxic hazards of oxygenated polycyclic aromatic hydrocarbons (PAHs) at PAH-contaminated sites. *Ambio.* 36, 475-485.
- Luo, L., Wang, P., Lina, L., Luana, T., Keb, L., Fung Yee Tam, N., 2014. Removal and transformation of high molecular weight polycyclic aromatic hydrocarbons in water by live and dead microalgae. *Process Biochem.* 49, 1723-1732.
- Mallakin, A., McConkey, B.J., Miao, G., McKibben, B., Snieckus, V., Dixon, D.G., Greenberg, B.M., 1999. Impacts of structural photomodification on the toxicity of environmental contaminants: anthracene photooxidation products. *Ecotoxicol. Environ. Saf.* 43, 204-212.
- McConkey, B.J., Duxbury, C.L., Dixon, D.G., Greenberg, B.M., 1997. Toxicity of PAH photooxidation product to the bacteria *Photobacterium Phosphoreum* and the duckweed *Lemna Gibba*: effects of phenanthrene and its primary photoproduct, phenanthrenequinone. *Environ. Toxicol. Chem.* 16, 892-899.
- Meckenstock, R.U., Morasch, B., Griebler, C., Richnow, H., 2004. Stable isotope fractionation analysis as a tool to monitor biodegradation in contaminated aquifers. *J. Contam. Hydrol.* 75, 215-255.
- Nadal, M., Schuhmacher, M., Domingo, J.L., 2004. Levels of PAHs in soil and vegetation samples from Tarragona County, Spain. *Environ. Pollut.* 132, 1-11.
- Nadal, M., Schuhmacher, M., Domingo, J.L., 2011. Long-term environmental monitoring of persistent organic pollutants and metals in a chemical/petrochemical area: Human health risks. *Environ. Pollut.* 159, 1769-1777.
- Nadal, M., Wargent, J.J., Jones, K.C., Paul, N.D., Schumacher, M., Domingo, J.L., 2006. Influence of UV-B radiation and temperature on photodegradation of PAHs: Preliminary results. *J. Atmos. Chem.* 55, 241-252.
- Rivas, F.J., Beltran, F.J., Acedo, B., 2000. Chemical and photochemical degradation of acenaphthylene. Intermediate identification. *J. Hazard. Mater.* B75, 89-98.
- Roig, N., Sierra, J., Rovira, J., Schuhmacher, M., Domingo, J.L., Nadal, M., 2013. In vitro tests to assess toxic effects of airborne PM10 samples. Correlation with metals and chlorinated dioxins and furans. *Sci. Total Environ.* 443, 791-797.
- Salizzato, M., Rigioni, M., Pavoni, B., Volpi Ghirardini, A., Ghetti, P.F., 1997. Separation and quantification of organic micropollutants (PAH, PCB) in sediments. Toxicity of extracts towards *Vibrio fischeri*. *Toxicol. Environ. Chem.* 60, 183-200.
- Shemer, H., Linden, K.G., 2007. Aqueous photodegradation and toxicity of the polycyclic aromatic hydrocarbons fluorene, dibenzofuran, and dibenzothiophene. *Water Res.* 41, 853-861.

- Singh, P., Mondal, K., Sharma, A., 2013. Reusable electrospun mesoporous ZnO nanofiber mats for photocatalytic degradation of polycyclic aromatic hydrocarbon dyes in wastewater. *J. Colloid Interface Sci.* 394, 208-215.
- Wang, C., Wang, X., Gong, P., Yao, T., 2014. Polycyclic aromatic hydrocarbons in surface soil across the Tibetan Plateau: Spatial distribution, source and air-soil exchange. *Environ. Pollut.* 184, 138-144.
- Wang, Y., Luo, C., Wang, S., Liu, J., Pan, S., Li, J., Ming, L., Zhang, G., Li, X., 2015. Assessment of the Air-Soil Partitioning of Polycyclic Aromatic Hydrocarbons in a Paddy Field Using a Modified Fugacity Sampler. *Environ. Sci. Technol.* 49, 284-291.
- Xia, X., Li, G., Yang, Z., Chen, Y., Huang, G.H., 2009. Effects of fulvic acid concentration and origin on photodegradation of polycyclic aromatic hydrocarbons in aqueous solution: Importance of active oxygen. *Environ. Pollut.* 157, 1352-1359.
- Xiaozhen, F., Boa, L., Aijun, G., 2005. Dynamics of solar light photodegradation behavior of atrazine on soil surface. *J. Hazard. Mater.* B117, 75-79.
- Zhang, L., Li, P., Gong, Z., Li, X., 2008. Photocatalytic degradation of polycyclic aromatic hydrocarbons on soil surfaces using TiO₂ under UV light. *J. Hazard. Mater.* 158, 478-484.
- Zhang, L., Li, P., Gong, Z., Oni, A., 2006. Photochemical behavior of benzo(a)pyrene on soil surfaces under UV light irradiation. *J. Environ. Sci.* 18, 1226-1232.
- Zhang, L., Xua, C., Chena, Z., Li, X., Li, P., 2010. Photodegradation of pyrene on soil surfaces under UV light irradiation. *J. Hazard. Mater.* 173, 168-172.
- Zhang, X., Wu, Y., Hu, S., Lu, C., Yao, H., 2014. Responses of kinetics and capacity of phenanthrene sorption on sediments to soil organic matter releasing. *Environ. Sci. Pollut. Res.* 21, 8271-8283.
- Zhao, X., Quan, X., Zhao, Y., Zhao, H., Chen, S., Chen, J., 2004. Photocatalytic remediation of γ -HCH contaminated soil induced by α -Fe₂O₃ and TiO₂. *J. Environ. Sci.* 16, 938-941.

DISCUSSION CHAPTER 2

When simulating a current Mediterranean climate scenario, PAHs deposited on surface soil showed a different behavior, depending on the exposure time, molecular weight of each PAH and soil properties.

LMW PAHs were more easily sorbed and volatilized, while MMW and HMW PAHs were able to undergo different photodegradation degrees. Fine-textured soil enhanced sorption, being PAHs more photodegraded than in coarse-textured soil. In both soils, significant photodegradation rates were detected for a number of PAHs, namely phenanthrene, anthracene, benzo(*a*)pyrene, and indeno(123-*cd*)pyrene after 28 days of exposure. Benzo(*a*)pyrene, commonly used as an indicator for PAHs pollution, was completely removed after 7 days of light exposure in fine-textured Regosol soil. Surprisingly, a remarkably decrease of benzo(*a*)pyrene concentrations in the darkness was observed, probably due to unknown degradation processes.

Microtox[®] and hydrogen isotopes analysis were carried out in order to complement the results of PAHs monitoring. The decreasing trend of $\Sigma 16$ PAHs concentrations over time agreed well with Microtox[®] findings, showing a faster detoxification in fine-textured soil. However, a complete detoxification was not observed. Despite there was a detoxification trend over time in both tested soils, particular oscillations of EC₅₀ in irradiated samples and dark controls might indicate the formation of intermediate products with a high toxicity. The analyses of hydrogen isotopes of benzo(*a*)pyrene confirmed the degradation of this compound, not only under light conditions but also in the darkness.

These suggested the need to analyze in more depth the potential role of iron oxide as catalyzer of the photodegradation of PAHs. In addition, toxicity oscillations reported by Microtox[®] test pointed out the need to further investigate the generation of PAHs by-products. Finally, as a result of the strong isotopic effect observed, CSIA was recognized as a powerful tool to assess PAHs degradation, and therefore, it was again applied in other experiments.

CHAPTER 3

The role of iron oxide on the photodegradation of PAHs: trends and toxicity

Montse Marquès ^{a,b}, Daniel Cervelló^b, Montse Mari ^{a,b},

Jordi Sierra ^{b,c}, Marta Schuhmacher ^b, Martí Nadal ^a,

José L. Domingo ^a

^a Laboratory of Toxicology and Environmental Health, School of Medicine, IISPV, Universitat Rovira i Virgili, Sant Llorenç 21, 43201 Reus, Catalonia, Spain.

^b Environmental Engineering Laboratory, Departament d'Enginyeria Química, Universitat Rovira i Virgili, Av. Països Catalans 26, 43007 Tarragona, Catalonia, Spain.

^c Laboratory of Soil Science, Faculty of Pharmacy, Universitat de Barcelona, Av. Joan XXIII s/n, 08028 Barcelona, Catalonia, Spain.

For submission to *Polycyclic Aromatic Compounds*.

ABSTRACT

Laboratory experiments were conducted to study the photocatalytic capability of amorphous α - Fe_2O_3 to degrade polycyclic aromatic hydrocarbons (PAHs). Solutions containing 16 US EPA priority PAHs were spiked with Fe_2O_3 and incubated in a climate chamber at stable conditions of temperature (20°C) and light (9.6 W m⁻²) for 28 days. In addition, samples without Fe_2O_3 were also incubated. PAHs levels were monitored by means of GC-MS, and their toxicity was assessed using Microtox[®] bioassay. Low and medium molecular weight PAHs were more influenced by a quick volatilization and photodegradation, while photodegradation was especially relevant for some heavier compounds. The Fe_2O_3 had a significant photocatalytic effect on fluorene, phenanthrene and benzo(*a*)pyrene. On the other hand, photolysis was more notable than photocatalysis for benzo(*a*)anthracene and dibenzo(*ah*)anthracene. Anthracene presented the same photodegradation, regardless of the Fe_2O_3 content. Remaining PAHs were not photodegraded either with or without Fe_2O_3 . These results indicated that, in some cases, Fe_2O_3 might act as a shield for PAHs. Other factors, such as the presence of the own soil matrix components (i.e. humic acid, other metals oxides, texture) or the chemical structure of the Fe_2O_3 may also play a role. Photodegradation trends were supported by changes of EC₅₀ values. A higher detoxification was observed under light exposure when Fe_2O_3 was absent, while EC₅₀ results suggested the formation of toxic or more bioavailable by-products, when Fe_2O_3 was used as a photocatalyst.

Keywords: polycyclic aromatic hydrocarbons, photodegradation, photocatalysis, iron oxide, *Vibrio fischeri*, Microtox[®].

INTRODUCTION

Polycyclic aromatic hydrocarbons (PAHs) are a class of semi-volatile organic compounds (SVOC), which are ubiquitous in the environment. The origin of PAHs may be either natural, such as petroleum or coal deposits, volcanic eruptions and forest fires, or anthropogenic, such as industrial production, residential heating, motor vehicle exhaust, waste incineration, and agriculture (Guo et al., 2011). PAHs, and especially those with four or more rings and their metabolites, are considered as hazardous pollutants because of their toxicity, mutagenicity and/or carcinogenicity, being classified as compounds with significant human health risk (Li et al., 2008; Yan et al., 2004).

Due to their hydrophobic nature and low solubility, PAHs are resistant to biodegradation. They can be bioaccumulated in the environment, especially in soils where they are easily sorbed to the organic matter, eventually reaching the food chain (Nadal et al., 2004; Nadal et al., 2011). The environmental fate of PAHs include a number of processes, being the most relevant volatilization, microbiological degradation, photo-oxidation, chemical oxidation, adsorption on soil particles and leaching (Lehto et al., 2000; Rababah and Matsuzawa, 2002; Siddiqi et al., 1994). Low molecular weight PAHs are more readily volatilized and biodegraded. In contrast, however, high molecular weight PAHs are recalcitrant, being biological degradation rather ineffective (Ukiwe et al., 2013). For this reason, researchers have recently paid attention to several chemical technologies, such as photodegradation, for bioremediation of soils contaminated by PAHs (Karaca and Tasdemir, 2013; Kohtani et al., 2005). Balmer et al. (Balmer et al., 2000) and Wang et al. (Wang et al., 2009) reported that temperature, soil particle size, humic acids, soil depth and light wavelength affect the nature of PAHs photoreactions in soils. Iron, zinc, titanium, aluminium, manganese and magnesium oxides, as well as oxalic and humic acids, also have been reported to directly and/or indirectly photocatalyse PAHs degradation in soils (Gupta et al., 2016; Marquès et al., 2016b; Vela et al., 2012; Zhang et al., 2008). Iron oxides are natural minerals found in soils and rocks, lakes and rivers, on the seafloor, and in air and organisms (Wang et al., 2009). Goethite (α -FeOOH), hematite (α -Fe₂O₃) (IO), lepidocrocite (γ -FeOOH), and maghemite (γ -Fe₂O₃) are the most common iron oxides. Iron oxides have been found to be potential natural

photocatalysts for the degradation of organic pollutants in the environment (Li et al., 2007; Wang et al., 2009).

It has been demonstrated that the Mediterranean region is characterized by a high solar radiation. In the nature, solar radiation plays a key role in the photodegradation of PAHs in soil (Marquès et al., 2017). Content of oxides in soil is a significant parameter, as these substances may cause a photocatalytic effect. Specifically, a significant role was attributed to Fe_2O_3 because it was the most abundant (Marquès et al., 2016a; Marquès et al., 2016b). However, there is a gap regarding the influence with respect to other factors. The present study was aimed at investigating the photocatalytic degradation of 16 US EPA priority PAHs caused by iron (III) oxide (Fe_2O_3). The photocatalytic capability of Fe_2O_3 , considered as indirect photodegradation, was compared to the photolytic effect of light, as direct photodegradation. Furthermore, concentration changes were additionally supported by Microtox® tests to correlate any variations in PAHs concentrations with ecotoxicity values.

MATERIALS AND METHODS

Chemicals

A stock solution containing 16 US EPA priority PAHs (99% of purity) at a concentration of $2000 \mu\text{g mL}^{-1}$ in dichloromethane:benzene was obtained from Supelco® (Bellefonte, PA, USA). Hexane ($\geq 96\%$ of purity) and dichloromethane ($\geq 99.5\%$ of purity) were purchased from Scharlau Chemie S.A. (Barcelona, Spain). Amorphous alpha Iron(III) oxide ($\geq 97\%$ of purity) was provided by Sigma Aldrich (Saint Louis, MO, USA). A mixture of six labelled hydrocarbons containing d_4 -1,4-dichlorobenzene ($\geq 99.8\%$ of purity), d_8 -naphthalene ($\geq 96.3\%$ of purity), d_{10} -acenaphthene ($\geq 99.8\%$ of purity), d_{10} -phenanthrene ($\geq 99.3\%$ of purity), d_{12} -chrysene ($\geq 99.8\%$ of purity), and d_{12} -perylene ($\geq 99.5\%$ of purity) at a concentration of $2000 \mu\text{g mL}^{-1}$ was provided by Supelco® (Bellefonte, PA, USA). Finally, two individual internal standards, d_{10} -fluorene ($\geq 98.3\%$ of purity) and d_{12} -benzo(a)pyrene ($\geq 98.5\%$ of purity), were supplied by Supelco® (Bellefonte, PA, USA).

For the Microtox[®] ecotoxicological test, acetone ($\geq 99.5\%$ of purity) and dimethyl sulfoxide (DMSO) ($\geq 99.5\%$ of purity) were obtained from Panreac (Castellar del Vallès, Spain), while both, Microtox[®] diluent (2% NaCl in ultra-pure water) and Microtox[®] Reactive (*Vibrio fischeri*), were provided as a freeze-dried reagent by Azur Environment (Workingham, England). The latter reagent was stored at -20°C and rehydrated prior to the test performance.

Characterization of iron oxide

The iron oxide images and qualitative microanalysis were obtained by FE-SEM microscope (Thermal field Emission Electron Microscope with energy dispersive X-ray spectroscopy analysis) JEOL JSM-7100F (Akishima, Tokyo, Japan).

Photodegradation experimental design

A solution containing 16 US EPA priority PAHs at $100\ \mu\text{g mL}^{-1}$ in hexane/dichloromethane (1:1), diluted down from the parent solution, was 10-times spiked with $25\ \mu\text{L}$ on uncovered glass Petri dishes (80 mm diameter) for two different tests: 1) iron oxide absence (OA); and 2) iron oxide presence (OP) by spreading a thin layer of amorphous Fe_2O_3 (total weight: 0.2 g). Petri dishes were incubated inside a Binder KBWF 240 climate chamber (Binder GmbH, Tuttlingen, Germany) setting constant temperature, light intensity and humidity (20°C , $9.6\ \text{W m}^{-2}$ and 40%, respectively). Dark control samples subjected to the same conditions were set by covering the petri dishes with aluminium foil. In order to assess any potential contamination, blank samples were prepared by following the same steps. Triplicates of irradiated samples and dark controls for both tests (OA and OP) were removed from the climate chamber after 0, 1, 2, 3, 6, 7, 9, 10, 14, and 28 days of incubation.

PAH extraction

PAHs were recovered for GC-MS analysis by cleaning glass Petri dishes with 20 mL of hexane/dichloromethane (1:1). The extract was filtered (cellulose filter, Filter-Lab), and further concentrated down with a rotary evaporator and a gentle flow of N_2 (99.9999% of purity). In order to control the efficiency of each sample extraction, 25

μL of 6 labelled hydrocarbons mixture (d_4 -1,4-dichlorobenzene, d_8 -naphthalene, d_{10} -acenaphthene, d_{10} -phenanthrene, d_{12} -chrysene, and d_{12} -perylene) were 10-times spiked before PAHs extraction. Finally, a solution containing both internal standards (d_{10} -fluorene and d_{12} -benzo(*a*)pyrene) in hexane/dichloromethane (1:1) was added to samples prior GC-MS analyses.

Analysis by GC-MS of PAH

The quantification of PAHs was performed on a Hewlett-Packard (HP) G1099A/MSD5973 gas chromatograph (GC) coupled to a mass spectrometer (MS) according to the US method 8270 (EPA, 2007). The routine GC column was a DB-5 (5%-Phenyl)-methylpolysiloxane capillary column (60 m \times 0.25 mm id \times 0.25 μm thickness). One μL of sample was injected in splitless mode at an injector temperature of 310°C. The temperature program for the GC was as follows: it was initiated at 90°C, being then increased at a rate of 15°C min^{-1} up to 200°C, changed at 6°C min^{-1} until 320°C, and finally left at 320°C for 20 min. The transfer line temperature was set at 280°C. The carrier gas was ultra-pure (99.9999%) helium, at a total flow rate of 1.4 mL min^{-1} . The analysis was performed using a mass selective detector set to monitor specific masses ranging from 40 to 350 atomic mass units (AMU). The mass spectrometer and source temperatures were 150°C and 230°C, respectively. PAH quantification was performed through the construction of a five-point calibration curve (20, 30, 50, 70 and 80 $\mu\text{g mL}^{-1}$).

Calculations

The photodegradation rate was obtained by applying the following equation:

$$L = \frac{C_N - C_I}{C_0} \cdot 100 \quad (\text{Eq. 1})$$

where L is the photodegradation rate (%) at time t , C_0 is the original concentration of the individual PAH, C_N is the concentration of the same PAH in non-irradiated soil sample at time t , and C_I is the concentration of the individual PAH in the irradiated sample at time t .

In order to determine the half-life of each compound, the following formulas were used:

$$\ln \frac{C_0}{C_t} = k \cdot t \quad (\text{Eq. 2})$$

$$t_{1/2} = \ln \frac{2}{k} \quad (\text{Eq. 3})$$

where C_0 and C_t are the individual PAH concentration at $t=0$ and t , respectively, and k is the apparent constant reaction rate of the pseudo first order (1/day).

Statistical analysis

Results were statistically evaluated using XLSTAT Statistical Software for Excel. Repeated measures of the ANOVA were firstly used to state significant differences between irradiated and non-irradiated samples through the time, which indicated that photodegradation occurred. Subsequently, photodegradation rates for each single PAH and test (with Fe_2O_3 and without Fe_2O_3) were further calculated. Afterwards, ANOVA test was applied again to state significant differences between the photodegradation of each single PAH and test. Probability levels were considered as statistically significant at $p < 0.05$.

Ecotoxicological test

For the Microtox[®] ecotoxicological test, another set of irradiated and dark controls in presence/absence of Fe_2O_3 were incubated in the climate chamber. A batch of samples was also prepared. Samples were removed from the climate chamber after 0, 1, 3, 5, 7, 14, and 28 days of exposure. PAHs were extracted with 20 mL of acetone, filtered and dried with a rotary evaporator. Dried samples were reconstituted with 2 mL of DMSO.

The acute toxicity was measured by means of Microtox[®] M500 analyzer (SDI Europe, UK) according to the Microtox[®] User Manual (*Microtox[®] Acute Toxicity Test-Standard procedure*, 1998) and ISO 11348-3:2007. Dilution series of the extract in DMSO were prepared. *V. fischeri* were exposed to 2-4% of those dilutions in Microtox[®]

diluent, and after 5, 15 and 20 minutes of exposure at 15°C light emission was monitored. Results after 5 min were reported in terms of the effective concentration (EC_{50}) of exposed PAHs that causes a 50% of decrease in the bioluminescence of the bacteria (Domingo et al., 2015; Marquès et al., 2016b; Roig et al., 2013).

RESULTS AND DISCUSSION

Fe_2O_3 effect on PAH photodegradation

The electronic images (Fig. 1) indicated that iron oxides were a homogeneous agglomeration of globular structures, and the amorphous structure instead of a crystalline structure was confirmed. EDX patterns depicted the elemental composition, confirming the presence of Fe and O.

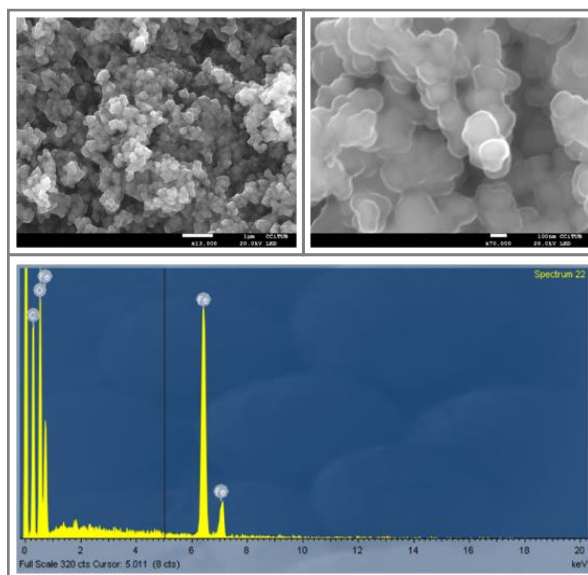


Fig. 1. Field Emission Scanning Electron Microscopy (FE-SEM) images and Energy Dispersive X-Ray Analysis (EDX) patterns of iron oxide.

The concentration trends of 5 PAHs (anthracene, benzo(*a*)anthracene, chrysene, benzo(*a*)pyrene and dibenzo(*ah*)anthracene), selected as representatives of 2-, 3-, 4-, 5-, and 6-ringed PAHs, in presence (OP) and absence (OA) of Fe_2O_3 , are shown in Fig. 2. Data about the remaining PAHs are included in Supplementary data (Fig. S1). The photodegradation rates of the same PAHs subjected to light radiation for 28 days,

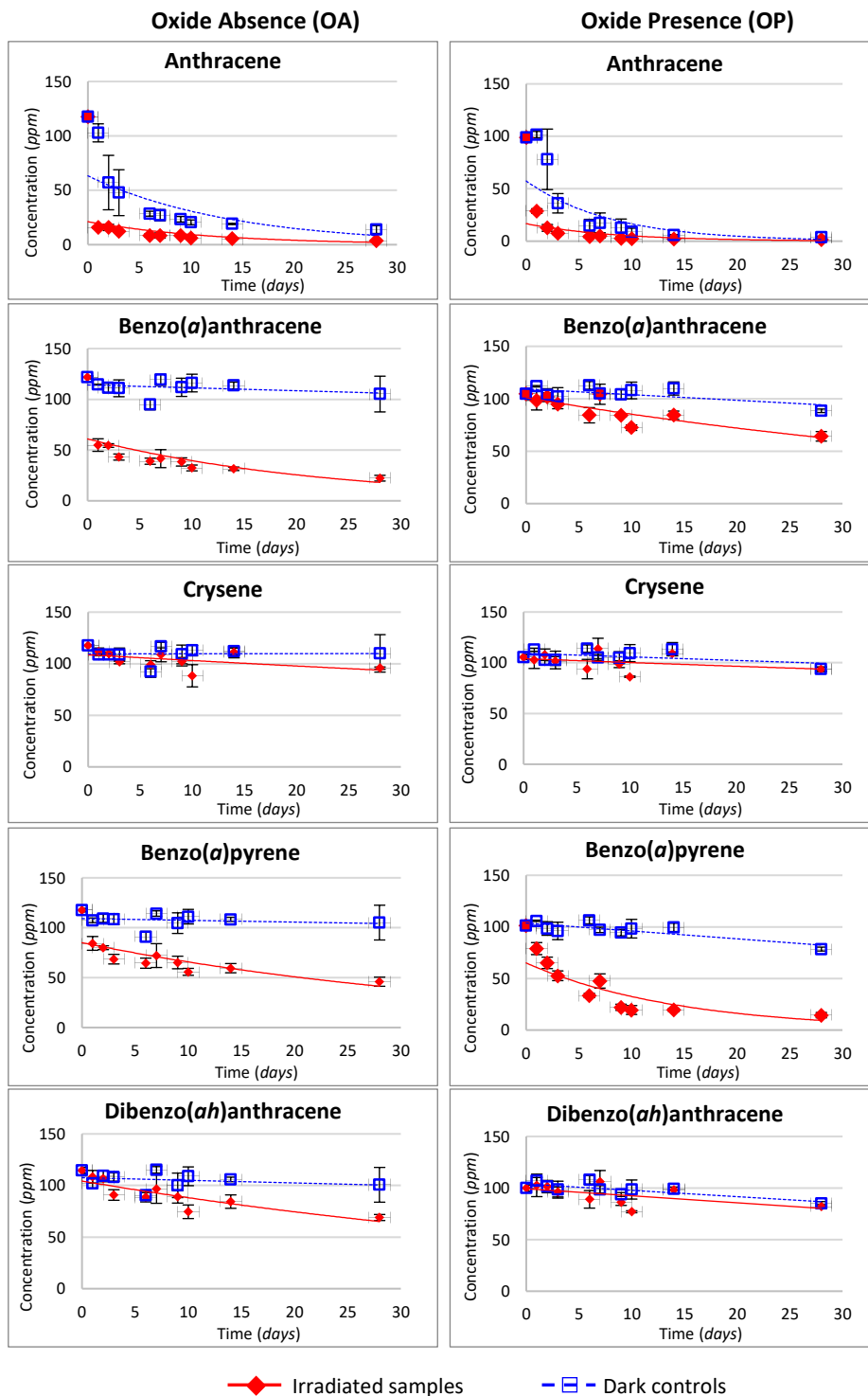


Fig. 2. Concentration trend of some 3-, 4-, 5-, and 6-ringed PAH in the absence (OA) and presence (OP) of Fe_2O_3 . Error bars represent the average standard deviations (SD) of triplicates.

with and without Fe_2O_3 , and together with the statistical significances between both groups are shown in Table 1.

Finally, half-lives of PAHs exposed to light in OP and OA are shown in Fig. 3.

Because of the total volatilization at the beginning of the experiment, naphthalene, acenaphthylene and acenaphthene could not be recovered. Consequently, they were excluded from data analysis. The recoveries of the remaining PAHs ranged between 87% and 108% in OA test while similar values were found in OP test (92%-109%). Due to the lack of any matrix, such as soil, PAHs concentration trends might be associated to two main processes: volatilization and photodegradation. However, the individual contribution of each process was different according to the physicochemical properties of each compound, the incubation time, as well as the presence of Fe_2O_3 .

For 2-, 3-, and some 4-ringed PAHs, volatilization was the most relevant process for concentration decrease. In contrast, chrysene, as well as other 5- and 6-ringed PAHs, were not volatilized, remaining their levels in dark controls constant. Differences between irradiated samples and dark controls in both tests were due to the impact of light exposure. However, photodegradation rates were only reported when the differences between PAH concentrations of irradiated samples and dark controls were statistically different. Thus, they were calculated for fluorene, phenanthrene, anthracene, benzo(*a*)anthracene and benzo(*a*)pyrene, with and without Fe_2O_3 , and also dibenzo(*ah*)anthracene without Fe_2O_3 .

For fluorene, phenanthrene and benzo(*a*)pyrene photodegradation was statistically higher in presence of Fe_2O_3 than in its absence. In contrast, for benzo(*a*)anthracene it was significantly higher when Fe_2O_3 was absent than when it was present. Finally, the photodegradation of anthracene was similar either in presence and absence of Fe_2O_3 ($p > 0.05$)

Although fluorene presented a low recovery (49% - 58%), most probably due to its quick volatilization, its trend was clear. Fluorene decreased up to 94% in dark controls after the 1st day of exposure and it was undetected after the 2nd day of exposure. Although volatilization had a great impact on fluorene, photodegradation also had a role on PAH loss. Differences observed between irradiated and dark control samples on the 1st day of exposure indicated a quick photodegradation in both groups

of samples, with and without Fe₂O₃ (Fig. S1, Supplementary data). A higher volatilization was noted in samples with no oxides, suggesting that Fe₂O₃ could be retaining PAHs by hindering PAHs volatilization, and therefore enhancing their photodegradation. This behaviour was not noted only for fluorene, but also for phenanthrene and anthracene (Fig. 2). As they were also quickly volatilized in both irradiated samples and dark controls, photodegradation rates were also calculated according to data from 1st day of exposure. Phenanthrene and anthracene showed a similar trend as fluorene, being volatilization a relevant process. However, recoveries were nearly 100%, indicating that volatilization was a slow process in contrast to fluorene. Regarding anthracene, although kinetics differed considerably between OA and OP, photodegradation rates remained similar. Photodegradation rates here reported for fluorene, phenanthrene and anthracene were slightly higher than those found in a previous experiment conducted by using different soil matrices (Marquès et al., 2016b). The higher photodegradation rates might be related to the absence of soil, which enhances light exposure and, boosts estimated here the photodegradation of these compounds. After one day of exposure, photodegradation of fluorene and phenanthrene was significantly higher with Fe₂O₃ than without Fe₂O₃, while that reported for anthracene was statistically the same in both groups of samples.

Table 1. Photodegradation rates of PAHs in absence and presence of Fe₂O₃.

	Fe ₂ O ₃ absence	Fe ₂ O ₃ presence	p
Fluorene*	5.9	85	<0.001
Phenanthrene*	42.5	63	0.014
Anthracene*	74	70	>0.05
Fluoranthene	n.c	n.c	-
Pyrene	n.c	n.c	-
Benzo(a)anthracene	68	25	0.003
Chrysene	n.c	n.c	-
Benzo(b)fluoranthene	n.c	n.c	-
Benzo(k)fluoranthene	n.c	n.c	-
Benzo(a)pyrene	50	71	0.008
Benzo(ghi)perylene	n.c	n.c	-
Dibenzo(ah)anthracene	23	n.c	-
Indeno(123-cd)pyrene	n.c	n.c	-

* Calculated at the 1st exposure day

n.c = photodegradation rate is not calculated because irradiated samples and dark controls are not statistically different (p>0.05)

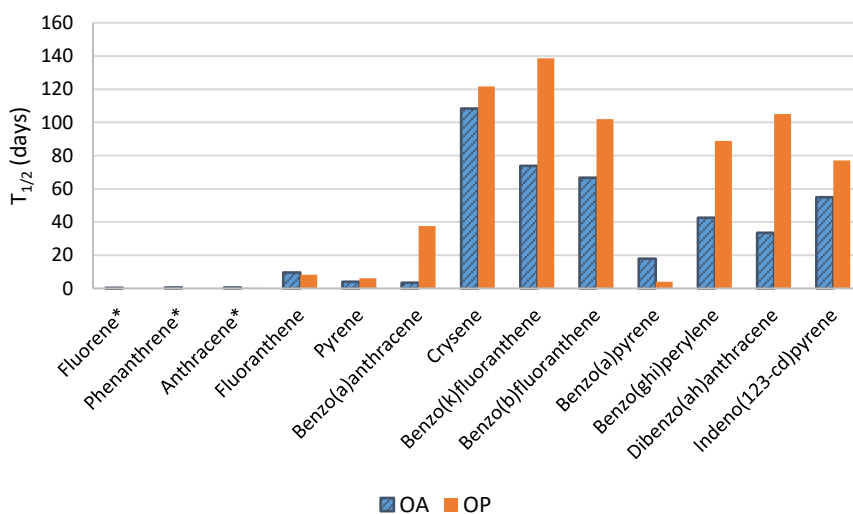
The concentration of benzo(*a*)anthracene, and other heavy molecular weight compounds, remained constant throughout the experiment in dark controls since volatilization had a lower effect on the decrease of concentration. Regarding benzo(*a*)anthracene, a photodegradation rate of 68% was estimated when Fe₂O₃ was lacked, being attributed to its photolysis. In contrast, photodegradation was 25% when the photocatalyst was present, being this rate statistically lower than that reported without Fe₂O₃. It suggests that Fe₂O₃ had no photocatalytic effect on benzo(*a*)anthracene, and it even hindered photolysis. A possible explanation for the low degradation rate in samples with Fe₂O₃ may be related to the scattering by catalyst particles on PAHs, which might attenuate their light absorption (Zhang et al., 2008).

Benzo(*a*)pyrene was the PAH with highest photodegradation at the end of the experiment, with rates of 50% and 71%, in absence and presence of Fe₂O₃, respectively. Statistical differences between these photodegradation rates confirmed that Fe₂O₃ has a very active photocatalytic role on the photodegradation of benzo(*a*)pyrene. Similar results were observed in a previous study, performed under the same climate conditions and time lapse but on the soil matrix (Marquès et al., 2016b). Very interestingly, in the present study, benzo(*a*)pyrene had not been completely degraded after 28 days, remaining between 14% and 39% of benzo(*a*)pyrene in the petri dishes (OP and OA, respectively). In turn, benzo(*a*)pyrene was completely degraded under light when using soils. Furthermore, an extreme decrease was noted in the darkness. It denotes that the combination of other soil components, such as humic acids and other oxides, may be capable to enhance not only photoreactions in irradiated samples, but also unknown degradation reactions in the darkness.

Chrysene, benzo(*b*)fluoranthene, benzo(*k*)fluoranthene, benzo(*ghi*)perylene, dibenzo(*ah*)anthracene and indeno(123-*cd*)pyrene presented a similar pattern, characterized by a lack of volatilization. However, photodegradation only occurred for dibenzo(*ah*)anthracene without Fe₂O₃, showing a rate of 23%. Light protection caused by Fe₂O₃ particles on PAHs is therefore greater than the joint impact of potential photolysis and photocatalysis. No significant differences were found when comparing concentrations of chrysene, benzo(*b*)fluoranthene, benzo(*k*)fluoranthene and

benzo(*ghi*)perylene in irradiated samples and dark controls. These results are in agreement with previous findings performed in soils (Marquès et al., 2016b).

The most volatile compounds (e.g., fluorene, phenanthrene and anthracene) showed the lowest half-lives, mainly because of the important role of volatilization. Although they own a higher molecular weight and lower vapor pressure, fluoranthene and pyrene, both belonging to the group of 4-ringed PAHs, also showed low half-lives, due to their notable volatilization. Similarly, benzo(*a*)anthracene was significantly photodegraded presenting a low half-life. Chrysene showed the highest half-life. Contrasting with other 5-, and 6-ringed PAHs, which were not or poorly degraded, benzo(*a*)pyrene presented a very low half-life, in accordance to its important photodegradation.



*Completely removed after 1 day of light exposure

Fig. 3. Half-lives of 16 priority PAHs exposed to light with (OP) and without (OA) Fe₂O₃.

In general terms, volatilization was found to be a key process in the behaviour of PAHs, not only for low but also for medium molecular weight PAHs. Volatilization of those compounds was even higher than that reported previously after an experimental study with soils (Marquès et al., 2016b). Therefore, it is evidenced that soils may trap PAHs and prevent their volatilization. Although fluoranthene and pyrene have a high molecular weight and low vapour pressure, their concentration in dark conditions decreased, irrespectively of the presence/absence of Fe₂O₃. Only 10%

and 41%, respectively, remained at the end of the experiment. These results agree with previous data Marquès et al., 2016b, suggesting the effect of some unknown degradation processes in the darkness, in addition to photodegradation and volatilization. In turn, the concentration decrease in samples with no Fe_2O_3 and light exposure might be only attributed to their potential volatilization enhanced by the lack of matrix. Photodegradation has been identified as a key process of PAH loss. However, direct photodegradation, caused only by the impact of light, is not always more important than photodegradation by the joint impact of light and Fe_2O_3 . Benzo(a)pyrene showed a different pattern in comparison to similar PAHs, as photodegradation was clearly accelerated in samples with Fe_2O_3 . The photodegradation of benzo(a)pyrene followed well a pseudo first-order kinetics, being our results in agreement with others found in the scientific literature (Gupta and Gupta, 2015; Gupta et al., 2016; Marquès et al., 2016b; Zhang et al., 2008). However, the incomplete degradation found in this study suggests that photodegradation of PAHs in soils may be enhanced by the combination of iron oxide with other photocatalysts, such as aluminium, titanium and manganese oxides, commonly found in soils. In addition, the effects of soil texture and humic acids should not be disregarded. Balmer et al., 2000 found that soil texture has an important role in the degradation of organic pollutants. Although the present study was designed with absence any soil, it was noted that the presence of any matrix (e.g., Fe_2O_3 particles) may prevent volatilization, and even photodegradation of some PAHs.

Despite commercially and laboratory- synthesized pure iron oxides are commonly used in catalytic studies (Gupta and Gupta, 2015; Wang et al., 2009; Zhang et al., 2008; Zhao et al., 2004), it is hypothesized that the Fe_2O_3 used in the present study, with an homogeneous amorphous structure (Fig. 1), is probably less reactive than heterogeneous materials usually found in the environment. However, this needs further investigation.

Toxicity assessment

In addition to the chemical analysis some bioassays were also conducted to assess the toxic effects of PAHs. Based on the literature, *Vibrio fischeri* inhibition test

is the most sensitive, rapid, cost-effective, easy to operate, reproducible test, while it avoids ethical problems related to the use of higher organisms, such as fish and rat (Parvez et al., 2006). Moreover, it was reported that Microtox[®] is an accurate test to assess the toxicity of PAHs (Khan et al., 2012; Salizzato et al., 1998).

Despite DMSO was used as a co-solvent, an unusual behaviour of the dose-effect curves was observed, most probably due to the polarity of PAHs. It was noted that the longer is the contact time (from 5 min to 20 min) between the toxic compound and the bacterium, the lower the toxicity is (Fig. S2, Supplementary data). This might be related to the low aqueous solubility of PAHs in addition to the fact that the saline solution (2% of NaCl) might exacerbate its solubility. In an aqueous media, aromatic hydrocarbons tend to precipitate, even using DMSO and the low concentrations of PAHs (2-4%). Hence, although usually the EC₅₀ values for Microtox[®] are collected at 15 minutes of contact, some studies indicate that the 5-min EC₅₀ is also suitable for this kind of organic compounds (Salizzato et al., 1998). Thus, 5-min EC₅₀ values were here provided.

Blank samples with and without Fe₂O₃ showed toxicity values of 329 and 751 mL of extract mL⁻¹ Microtox[®] diluent, respectively. It was confirmed that DMSO and Fe₂O₃ did not confer an additional toxicity, compared with PAH- spiked samples.

The evolution of toxicity throughout the incubation period, expressed as EC₅₀, is depicted in Fig. 4. Initially (t=0), toxicity of samples spiked with PAHs was markedly higher because of the lack of any volatilization or photodegradation process. Initial EC₅₀ values for samples with Fe₂O₃ (OP), were slightly higher than those without Fe₂O₃ (OA), suggesting that some PAHs could have been sorbed to Fe₂O₃, which would lower the toxicity.

In general terms, a global decrease of the toxicity was observed irrespective of the content of Fe₂O₃. Toxicity of samples without Fe₂O₃ decreased with time until the 3rd day of exposure, when EC₅₀ remained stable until the end of the experiment. It would be related to the volatilization and photodegradation of PAHs. In contrast, toxicity of irradiated samples was lower than that of dark controls from the 1st day of exposure, which could be due to the quick photodegradation of some PAHs (e.g., fluorene, phenanthrene, and anthracene). After three days of incubation onwards, irradiated samples and dark controls did not show toxicity differences.

Irradiated samples and dark controls with Fe_2O_3 presented the same toxicity until the 1st day of exposure. However, irradiated samples presented higher toxicity than dark controls from the 3rd day until the end of the experiment. The higher toxicity of samples exposed to light could be associated to the potential formation of more soluble PAHs by-products (e.g. oxygenated PAHs). The higher the solubility of a compound is, the higher the bioavailability of that compound is, and therefore, a greater uptake by organisms occurs (Cochran et al., 2012; Ge et al., 2016).

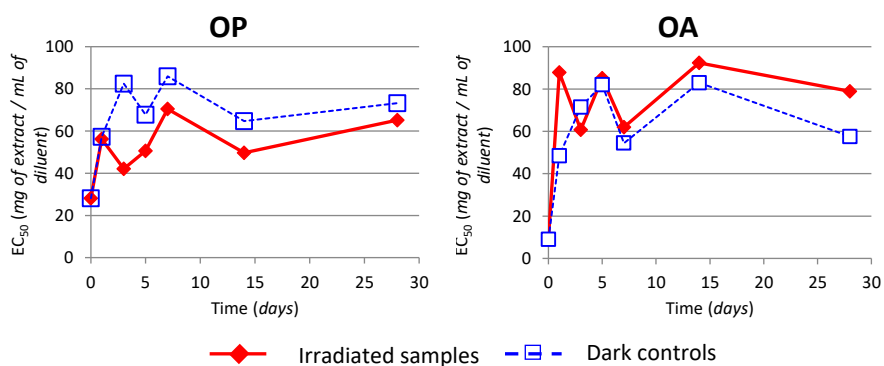


Fig. 4. Toxicity trends of samples with (OP) and without (OA) Fe_2O_3 , exposed to light and in the darkness.

CONCLUSIONS

The role of iron oxide Fe_2O_3 as a potential catalyser for PAH photodegradation was here analysed. Low and medium molecular weight PAHs were more influenced by a quick volatilization and photodegradation, while photodegradation was especially relevant for some heavier compounds. Fluorene, phenanthrene and benzo(*a*)pyrene showed significant higher photodegradation rates when Fe_2O_3 was present than when it was absent. The most relevant long-term photocatalytic effect of Fe_2O_3 was noted for benzo(*a*)pyrene. Photodegradation rate of benzo(*a*)pyrene was 71% when there was Fe_2O_3 , and 50% when Fe_2O_3 was lacked. In contrast, the photodegradation of benzo(*a*)anthracene and dibenzo(*ah*)anthracene was significantly higher without Fe_2O_3 than when it was present. For the remaining PAHs, the lack of differences between irradiated samples and dark controls indicated that photodegradation, either photolysis or photocatalysis, did not occur. This fact suggests that, the presence of Fe_2O_3 may hinder the volatilization of LMW PAHs, enhancing their fast photocatalysis.

Oppositely, Fe_2O_3 may hamper the light to reach the PAHs, therefore preventing its photolysis. It also points out that other parameters, besides Fe_2O_3 , may have been involved in the photocatalysis of PAHs. Furthermore, the reactivity of Fe_2O_3 may be different depending on the chemical structure of the oxide which can be either homogeneous (e.g., commercial products) or heterogeneous (e.g., natural). These results highlight the different behavior of apparently similar compounds. It is especially relevant for benzo(a)pyrene, which is often used as a single indicator of PAH pollution. In this specific case, benzo(a)pyrene clearly cannot be used as standard for other PAHs when evaluating Fe_2O_3 as a photocatalyzer.

PAH concentrations trends agreed well with bioassay tests. A general detoxification was found to some extent, mainly as a result of volatilization and photodegradation. However, after 28 days of exposure, samples were not completely detoxified, agreeing with the traces of PAHs. The increase of toxicity in irradiated samples containing Fe_2O_3 , in comparison with dark controls, suggested that more bioavailable and toxic PAH by-products may be generated through photocatalysis. In order to increase the knowledge on the mechanisms involved in PAHs environmental fate, further investigations on the formation of PAH derivatives formation should be conducted.

Acknowledgments

This study was supported by the Spanish Ministry of Economy and Competitiveness (Mineco), through the project CTM2012-33079. Montse Marquès received a PhD fellowship from AGAUR (Commissioner for Universities and Research of the Department of Innovation, Universities and Enterprise of the “Generalitat de Catalunya” and the European Social Fund). The authors are indebted to Dr. Irene Maijó for her excellent guidance and assistance in GC-MS analysis.

References

- Balmer, M. E., Goss, K.-U., Schwarzenbach, R. P., 2000. Photolytic transformation of organic pollutants on soil surfaces - An experimental approach. *Environ. Sci. Technol.* 34, 1240-1245.

- Cochran, R. E., Dongari, N., Jeong, H., Beránek, J., Haddadi, S., Shipp, J., Kubátová, A., 2012. Determination of polycyclic aromatic hydrocarbons and their oxy-, nitro-, and hydroxy-oxidation products. *Anal. Chim. Acta* 740, 93-103.
- Domingo, J. L., Marquès, M., Mari, M., Schuhmacher, M., Sierra, J., Nadal, M., 2015. Climate change impact on the PAH ecotoxicity in Mediterranean soils. *Toxicol. Lett.* 238S, S56-S383.
- Ge, L., Na, G., Chen, C.-E., Li, J., Ju, M., Wang, Y., Li, K., Zhang, P., Yao, Z., 2016. Aqueous photochemical degradation of hydroxylated PAHs: Kinetics, pathways, and multivariate effects of main water constituents. *Sci. Total Environ.* 547, 166-172.
- Guo, Y., Wu, K., Huo, X., Xu, X., 2011. Sources, distribution, and toxicity of polycyclic aromatic hydrocarbons. *J. Environ. Health* 73, 22-25.
- Gupta, H., Gupta, B., 2015. Photocatalytic degradation of polycyclic aromatic hydrocarbon benzo(a)pyrene by iron oxides and identification of degradation products. *Chemosphere* 138, 924-931.
- Gupta, H., Kumar, R., Park, H.-S., Jeon, B.-H., 2016. Photocatalytic efficiency of iron oxide nanoparticles for the degradation of priority pollutant anthracene. *Geosystem Engineering* 20, 21-27.
- Karaca, G., Tasdemir, Y., 2013. Effects of temperature and photocatalysts on removal of polycyclic aromatic hydrocarbons (PAHs) from automotive industry sludge. *Polycyclic Aromat. Compd.* 33, 380-395.
- Khan, M. I., Cheema, S. A., Tang, X., Shen, C., Sahi, S. T., Jabbar, A., Park, J., Chen, Y., 2012. Biototoxicity Assessment of Pyrene in Soil Using a Battery of Biological Assays. *Arch. Environ. Contam. Toxicol.* 63, 503-512.
- Kohtani, S., Tomohiro, M., Tokumura, K., Nakagaki, R., 2005. Photooxidation reactions of polycyclic aromatic hydrocarbons over pure and Ag-loaded BiVO₄ photocatalysts. *Appl. Catal., B* 58, 265-272.
- Lehto, K.-M., Vuorimaa, E., Lemmetyinen, H., 2000. Photolysis of polycyclic aromatic hydrocarbons (PAHs) in dilute aqueous solutions detected by fluorescence. *J. Photochem. Photobiol. A Chem.* 136, 53-60.
- Li, F. B., Li, X. Z., Liu, C. S., Liu, T. X., 2007. Effect of alumina on photocatalytic activity of iron oxides for bisphenol A degradation. *J. Hazard. Mater.* 149, 199-207.
- Li, X., Li, P., Lin, X., Zhang, C., Li, Q., Gong, Z., 2008. Biodegradation of aged polycyclic aromatic hydrocarbons (PAHs) by microbial consortia in soil and slurry phases. *J. Hazard. Mater.* 150, 21-26.
- Marquès, M., Mari, M., Audí-Miró, C., Sierra, J., Soler, A., Nadal, M., Domingo, J. L., 2016a. Climate change impact on the PAH photodegradation in soils: Characterization and metabolites identification. *Environ. Int.* 89-90, 155-165.
- Marquès, M., Mari, M., Audí-Miró, C., Sierra, J., Soler, A., Nadal, M., Domingo, J. L., 2016b. Photodegradation of polycyclic aromatic hydrocarbons in soils under a climate change base scenario. *Chemosphere* 148, 495-503.
- Marquès, M., Mari, M., Sierra, J., Nadal, M., Domingo, J. L., 2017. Solar radiation as a swift pathway for PAH photodegradation: A field study. *Sci. Total Environ.*
- Nadal, M., Schuhmacher, M., Domingo, J. L., 2004. Levels of PAHs in soil and vegetation samples from Tarragona County, Spain. *Environ. Pollut.* 132, 1-11.
- Nadal, M., Schuhmacher, M., Domingo, J. L., 2011. Long-term environmental monitoring of persistent organic pollutants and metals in a chemical/petrochemical area: Human health risks. *Environ. Pollut.* 159, 1769-1777.

- Parvez, S., Venkataraman, C., Mukherji, S., 2006. A review on advantages of implementing luminescence inhibition test (*Vibrio fischeri*) for acute toxicity prediction of chemicals. *Environ. Int.* 32, 265-268.
- Rababah, A., Matsuzawa, S., 2002. Treatment system for solid matrix contaminated with fluoranthene. II—Recirculating photodegradation technique. *Chemosphere* 46, 49-57.
- Roig, N., Sierra, J., Rovira, J., Schuhmacher, M., Domingo, J. L., Nadal, M., 2013. In vitro tests to assess toxic effects of airborne PM10 samples. Correlation with metals and chlorinated dioxins and furans. *Sci. Total Environ.* 443, 791-797.
- Salizzato, M., Bertato, V., Pavoni, B., Ghirardini, A. V., Ghetti, P. F., 1998. Sensitivity limits and EC₅₀ values of the *Vibrio fischeri* test for organic micropollutants in natural and spiked extracts from sediments. *Environ. Toxicol. Chem.* 17, 655-661.
- Siddiqi, M. A., Ye, D., Elmarakby, S. A., Kumar, S., Sikka, H. C., 1994. Microbial Metabolism of Polycyclic Aromatic Hydrocarbons (PAH) and Aza-PAH. *Polycyclic Aromat. Compd.* 7, 115-122.
- Ukiwe, L. N., Egereonu, U. U., Njoku, P. C., Nwoko, C. I. A., Allinor, J. I., 2013. Polycyclic Aromatic Hydrocarbons degradation techniques: A review. *Int. J. Chem.* 5, 43-55.
- Vela, N., Martínez-Menchón, M., Navarro, G., Pérez-Lucas, G., Navarro, S., 2012. Removal of polycyclic aromatic hydrocarbons (PAHs) from groundwater by heterogeneous photocatalysis under natural sunlight. *J. Photochem. Photobiol. A Chem.* 232, 32-40.
- Wang, Y., Liu, C. S., Li, F. B., Liu, C. P., Liang, J. B., 2009. Photodegradation of polycyclic aromatic hydrocarbon pyrene by iron oxide in solid phase. *J. Hazard. Mater.* 162, 716-723.
- Yan, J., Wang, L., Fu, P. P., Yu, H., 2004. Photomutagenicity of 16 polycyclic aromatic hydrocarbons from the US EPA priority pollutant list. *Mutat. Res.* 557, 99-108.
- Zhang, L., Li, P., Gong, Z., Li, X., 2008. Photocatalytic degradation of polycyclic aromatic hydrocarbons on soil surfaces using TiO₂ under UV light. *J. Hazard. Mater.* 158, 478-484.
- Zhao, X., Quan, X., Zhao, Y.-Z., Zhao, H.-M., Chen, S., Chen, J.-W., 2004. Photocatalytic remediation of gamma-HCH contaminated soil induced by alpha-Fe₂O₃ and TiO₂. *Journal of Environmental Science (China)* 16, 938-941.

DISCUSSION CHAPTER 3

As highlighted in the chapter 2, an experimental study was performed to assess the role of metal oxides in soils as PAHs photocatalysts. For that purpose, an experiment was designed to discriminate the direct (photolysis) from the indirect (photocatalysis) photodegradation caused by iron (III) oxide (Fe_2O_3). It was chosen because a more significant photodegradation of PAHs was observed in Regosol soil, whose Fe_2O_3 content was higher than in coarse-textured Arensol soil.

LMW PAHs (e.g., fluorene, phenanthrene and anthracene) were highly impacted by volatilization. For fluorene, phenanthrene and benzo(*a*)pyrene, photodegradation was significantly higher in the presence of Fe_2O_3 than in its absence. Anthracene was also photodegraded, although statistical differences were not found between both groups of samples (absence and presence of Fe_2O_3). In turn, photodegradation only occurred when dibenzo(*ah*)anthracene was without Fe_2O_3 . All the remaining PAHs were not photodegraded since irradiated samples and dark controls were not statistically different. Consequently, it seems that Fe_2O_3 was not the only responsible for the enhancement of photodegradation found in Regosol. Soil is a complex matrix with texture, humic acids, wide range of metal oxides, and other components. Each soil component has probably a specific contribution to PAHs fate in soil. In turn, matrix differences between both experiments should be considered. In fact, in this experiment the lack of matrix in samples without Fe_2O_3 might have enhanced volatilization of LMW and MMW PAHs, while in turn, heavier PAHs in spiked dishes were completely exposed to light. In contrast, Fe_2O_3 particles might have protected PAHs from light, leading to a higher photodegradation of some PAHs (e.g., benzo(*a*)anthracene and dibenzo(*ah*)anthracene) in samples without photocatalyst.

Microtox[®] data confirmed that co-occurrence of PAHs, Fe_2O_3 and light leads to a higher toxicity than if they are lacked. These results suggest that, in any case, iron (III) oxide is responsible for the formation of more bioavailable, and toxic, PAHs degradation by-products.

Very interestingly, benzo(*a*)pyrene showed a different behavior with respect to other HMW PAHs. It highlights the importance of studying different PAHs, avoiding the performance of tests in single PAHs.

CHAPTER 4

Climate change impact on the PAH photodegradation in soils: Characterization and metabolites identification

Montse Marquès ^{a,b}, Montse Mari ^{a,b}, Carme Audí-Miró ^c, Jordi Sierra ^{b,d},
Albert Soler ^c, Martí Nadal ^{a,*}, José L. Domingo ^a

Environment International 89-90 (2016) 155-165.

Climate change impact on the PAH ecotoxicity in Mediterranean soils

José L. Domingo ^a, Montse Marquès ^{a,b}, Montse Mari ^{a,b},
Jordi Sierra ^{b,d}, Martí Nadal ^a

Toxicology Letters 238S (2015) S56-S383.

^a Laboratory of Toxicology and Environmental Health, School of Medicine, IISPV, Universitat Rovira i Virgili, Sant Llorenç 21, 43201 Reus, Catalonia, Spain.

^b Environmental Engineering Laboratory, Departament d'Enginyeria Química, Universitat Rovira i Virgili, Av. Països Catalans 26, 43007 Tarragona, Catalonia, Spain.

^c Grup de Mineralogia Aplicada i Geoquímica de Fluids, Departament de Cristal·lografia, Mineralogia i Dipòsits Minerals, Facultat de Geologia, SIMGEO UB-CSIC, Universitat de Barcelona UB, Martí Franquès s/n, 08028 Barcelona, Spain.

^d Laboratory of Soil Science, Faculty of Pharmacy, Universitat de Barcelona, Av. Joan XXIII s/n, 08028 Barcelona, Catalonia, Spain.

ABSTRACT

Polycyclic aromatic hydrocarbons (PAHs) are airborne pollutants that are deposited on soils. As climate change is already altering temperature and solar radiation, the global warming is suggested to impact the environmental fate of PAHs. This study was aimed at evaluating the effect of climate change on the PAH photodegradation in soils. Samples of Mediterranean soils were subjected to different temperature and light radiation conditions in a climate chamber. Two climate scenarios were considered according to IPCC projections: 1) a base (B) scenario, being temperature and light intensity 20°C and 9.6 W m⁻², respectively, and 2) a climate change (CC) scenario, working at 24°C and 24 W m⁻², respectively. As expected, low molecular weight PAHs were rapidly volatilized when increasing both temperature and light intensity. In contrast, medium and high molecular weight PAHs presented different photodegradation rates in soils with different texture, which was likely related to the amount of photocatalysts contained in both soils. In turn, the hydrogen isotopic composition of some of the PAHs under study was also investigated to verify any degradation process. Hydrogen isotopes confirmed that benzo(*a*)pyrene is degraded in both B and CC scenarios, not only under light but also in the darkness, revealing unknown degradation processes occurring when light is lacking. Potential generation pathways of PAH photodegradation by-products were also suggested, being a higher number of metabolites formed in the CC scenario. Microtox® results showed a higher detoxification in irradiated samples as temperature and light intensity increase. However, toxicity oscillations of those samples exposed to the light might be related to PAHs photodegradation byproducts, as it happened with the occurrence of naphthalic anhydride. Consequently, in a more or less near future, although humans might be less exposed to PAHs, they could be exposed to new metabolites of these pollutants, which might be even more toxic.

Keywords: climate change, polycyclic aromatic hydrocarbons (PAHs), photodegradation, metabolites, hydrogen isotopes

INTRODUCTION

The reconstruction of Earth's past climate conditions has demonstrated that climate has been continuously changing. However, past changes have rarely been as quick as nowadays, with human influence playing a key role (Cubasch et al., 2013; Lamon et al., 2009; Wu et al., 2016). Human-caused greenhouse gases (GHG) are leading to an increase of the global temperature, which is usually known as climate change. Climate-induced changes strongly differ throughout the globe, especially along latitudinal gradient (Philippart et al., 2011). Although the high latitude regions will suffer the greatest warming (Noyes et al., 2009), the Mediterranean basin has been identified as one of the most vulnerable regions, since it lies in a transition zone between arid and temperate/rainy climates (Bangash et al., 2012; Marquès et al., 2013; Sánchez-Canales et al., 2012; Schröter et al., 2005; Terrado et al., 2014). Moreover, it is pointed out as one of the world's regions where projected future increases in greenhouse gases concentrations are most likely to cause significant changes in climate during the 21st century, with a high degree of consistency among different projections (Giorgi, 2006; Mariotti et al., 2015). The Fifth Assessment Report of the Intergovernmental Panel on Climate Change (IPCC) predicted an increase of the mean global temperature by 1 to 1.5°C in the period 2016–2035, resulting in an increase of up to 4.8°C at the end of the century with respect to temperatures registered between 1850 and 1900 (IPCC, 2013).

One of the consequences of climate change is its potential to alter the environmental fate and transport of semi-volatile organic compounds (SVOCs) at environmentally relevant levels of human exposure (Armitage et al., 2011; Nadal et al., 2015). Temperature has a large influence on the partitioning of environmental pollutants in the atmosphere, as well as in soil and water (Manciocco et al., 2014; Noyes et al., 2009). Moreover, the increase of the temperature may enhance the mobilization of organic contaminants from reservoirs such as natural waters, soils and sediments, altering their rates of accumulation, sorption and degradation (Macdonald et al., 2003). Since reactivity, adsorption and accumulation are temperature-dependent processes, climate change can influence every step along the transport and redistribution pathways of organic pollutants (Kallenborn et al., 2012; Macdonald et al., 2003; Schiedek et al., 2007; UNEP, 2010). Hence, many climate change policies

imply changes of several non-climatic exposure patterns known to be related to health (Perez et al., 2015).

Polycyclic aromatic hydrocarbons (PAHs) are a group of SVOCs composed of two or more benzene and/or pentacyclic aromatic rings (Muckian et al., 2007). PAHs may enter the environment from both natural (e.g. plant synthesis, organic matter diagenesis and forest fires) and anthropogenic (e.g., industrial activities, residential heating, power generation, incineration and traffic) sources (Nadal et al., 2009). Generally, anthropogenic factors have a higher impact on PAH distribution in urban areas, whereas natural factors affect their distribution in remote areas. It must be remarked that, as a consequence of the emissions by heavy and light traffic, PAHs have become a major pollutant in urban areas (Jiang et al., 2009; Nadal et al., 2011; Wang et al., 2015).

Some PAHs are resistant to biodegradation and susceptible to bioaccumulation. Although PAHs are present in all environmental compartments (Melnik et al. 2015; Liu et al., 2014), they tend to deposit via dry and wet processes on the soil top layer (Nadal et al., 2004), becoming a special sink due to the PAH affinity to soil organic matter (Aichner et al., 2015; Sweetman et al., 2005). Moreover, PAHs can be transformed to more toxic compounds by chemical reactions such as sulfonation, nitration, photo-oxidation and photodegradation (Ras et al., 2009).

Compound-Specific Isotope Analysis (CSIA) is a valuable tool to control the natural degradation of environmental pollutants, where other natural processes such as dispersion, volatilization or sorption, also occur. Among these non-destructive processes, CSIA is able of discriminating natural degradation reactions. The discrimination is linked to different reaction speeds of light (e.g., ^{12}C , ^1H , ^{35}Cl) and heavy isotopes (e.g., ^{13}C , ^2H , ^{37}Cl). Significant changes in isotope ratios ($^{13}\text{C}/^{12}\text{C}$, $^2\text{H}/^1\text{H}$, $^{37}\text{Cl}/^{35}\text{Cl}$) over time and/or space, can be used to monitor the existence of degradation at contaminated sites (Elsner et al., 2012). Moreover, the enrichment factor $-\epsilon$ - value of a specific degradation process, which relates the amount of hydrogen isotope change with the concentration variation, makes possible to calculate the fraction of compound that has been lost through a specific degradation process. Unfortunately, in the scientific literature information regarding CSIA and PAHs is scarce, with very few approaches. Bergmann et al. (2011) investigated the hydrogen isotopic fractionation

of naphthalene due to biodegradation. Other studies report the hydrogen isotope fractionation of other organic substances, such as acetic acid and atrazine, subjected to light exposure (Hartenbach et al., 2008; Oba and Naraoka, 2007).

As PAHs in soils are highly influenced by temperature and solar radiation (Balmer et al., 2000; Frank et al., 2002; Gong et al., 2001; Xiaozhen et al., 2005). The present study was aimed at estimating the photodegradation rate of PAHs in soils affected by climate change. Laboratory experiments were conducted in a climate chamber considering two climate scenarios in the Mediterranean region. In addition, the hydrogen isotopic composition of some PAHs under study was also investigated to verify any degradation. Since changes on ecotoxicity are expected due to PAH photodegradation and the potential to form reactive intermediates in soil (Gupta and Gupta, 2015; Woo et al., 2009), Microtox® test and PAHs photodegradation by-products identification were carried out in both climate scenarios.

MATERIALS AND METHODS

Photodegradation experiment

Details of the photodegradation experiment, including soil characteristics and contamination procedure, were previously given (Marquès et al., 2016). Briefly, two different soils with opposite characteristics were collected from the A horizon of remotes areas of Catalonia (NE of Spain): a) acidic and coarse-textured Arenosol soil, with granitic origin, and b) fine-textured Regosol soil, formed by sedimentary materials. A layer of 1 mm of soil was formed with 10 g of air-dried soil deployed in uncovered glass Petri dishes. Each soil sample was 10-times spiked with a solution containing 16 US EPA priority PAHs at $100 \mu\text{g mL}^{-1}$ in dichloromethane:benzene (Supelco®, 99.0% purity, Bellefonte, PA, USA). Soil samples were incubated inside a Binder KBWF 240 climate chamber (Binder GmbH, Tuttlingen, Germany). Two climate scenarios were considered. In the base (B) scenario, temperature and light intensity were set at 20°C and 9.6 W m^{-2} , respectively, while in the climate change (CC) scenario, temperature and daylight were 24°C and 24 W m^{-2} , respectively. In both cases, humidity was kept at 40% to minimize any biotic reaction. Further details on the B scenario were previously reported (Marquès et al., 2016). Dark control samples,

covered with an aluminum foil, were exposed to the same environmental conditions in order to differentiate concentration decreases due to slow sorption, volatilization and other degradation processes, from those related to photodegradation. Irradiated samples and dark controls of each soil were removed from the climate chamber on days 1, 2, 3, 4, 5, 6, 7, 14, and 28.

Photodegradation rates for each one of the 16 PAHs were obtained by applying the following equation:

$$L = \frac{C_N - C_t}{C_0} \times 100 \quad (\text{Equation 1})$$

where L is the photodegradation rate (in percentage) at time t, C_N is the concentration of the individual PAH in non-irradiated soil sample at time t, C_t is the concentration of the same PAH in irradiated sample at time t, and C_0 is the initial PAH concentration. In turn, the following equations were used to determine the PAH half-lives:

$$\ln \frac{C_0}{C_t} = k \cdot t \quad (\text{Equation 2})$$

$$T_{1/2} = \frac{\ln 2}{k} \quad (\text{Equation 3})$$

where $T_{1/2}$ is the half-life of the individual PAH (in days), k is the apparent constant reaction rate of the pseudo first order (1/day), t is the exposure time (in days), C_0 is the initial PAH concentration in soil, and C_t is the initial soil concentration of the individual PAH.

PAH extraction and analysis

PAHs were extracted from soil samples with 30 mL of a mixture of hexane/dichloromethane (1:1) (Scharlau Chemie S.A., Barcelona, Spain) by using an ultrasonic bath for 10 min, according to the US EPA method 3550. This step was repeated three times, filtering the solvent after finishing each ultrasonic extraction in order to assure good PAH recoveries. Afterwards, samples were further concentrated with a rotary evaporator, as well as with a gentle stream of purified N_2 . A procedure of quality control/quality assurance was carried out to verify the reported results. A mixture of six labeled hydrocarbons (d_4 -1,4-dichlorobenzene (99.8% purity), d_8 -naphthalene (96.3% purity), d_{10} -acenaphthene (99.8% purity), d_{10} -phenanthrene

(99.3% purity), d₁₂-chrysene (99.8% purity), and d₁₂-perylene (99.5% purity) (all of them provided by Supelco[®], Bellefonte, PA, USA), were used as surrogates. In addition, d₁₀-fluorene (98.3% purity, Supelco[®], Bellefonte, PA, USA), as well as d₁₂-benzo(*a*)pyrene (98.5% purity, Supelco[®], Bellefonte, PA, USA), were used as internal standards for analytical control, being added to samples prior the analyses. A Hewlett-Packard G1099A/MSD5973 equipment with a DB-5 5% Phenyl Methyl Siloxane column (60 m x 0.25 mm x 0.25 μm) was used for quantification of the 16 PAHs. One μL of sample was injected at 310°C in pulsed splitless mode. The transfer line temperature was set at 280°C. The carrier gas was ultra-pure (99.9999%) helium, at a total flow rate of 1.4 mL min⁻¹. The gas chromatograph oven temperature started at 90°C, was increased at 15°C min⁻¹ until 200°C, and at 6°C min⁻¹ up to 320°C, being finally held at 320°C for 20 minutes. The detector was set to quantify the analytes covering specific masses ranging from 40 to 350 atomic mass units (AMU). The mass spectrometer and source temperatures were 150°C and 230°C, respectively. A five-point calibration curve (20, 30, 50, 70 and 80 μg mL⁻¹) was done for PAH quantification.

Microtox[®] test

Soils ecotoxicity was assessed as previously described in chapter 2. Briefly, PAH spiked and blank soils were extracted by using an ultrasonic bath mixture (1:1) of n-hexane 95% (UV-IR-HPLC) PAI-ACS (Panreac, Castellar del Vallès, Barcelona, Spain) and acetone (Reag. Ph. Eur) PA-ACS-ISO (Panreac), following the US EPA method 3550C. Afterwards, soil extracts were further filtered and completely dried with a rotatory evaporator, being finally reconstituted with 2 mL of dimethyl sulfoxide (UV-IR-HPLC-GPC) to a concentration of 2-4% in Microtox[®] diluent (2% NaCl of aqueous solution). The bioluminescent bacteria *V. fischeri* was used to measure the inhibition of light emission when organisms were exposed to soil extract samples, following the ISO 11348-1:2007. EC₅₀ values were estimated as the sample concentration causing 50% of light inhibition on the test organisms.

Metabolites identification

In order to identify PAH metabolites, individual compounds detected in both climate scenarios, B and CC, in the two soils, Arenosol and fine-textured Regosol, were identified using the MS library search NIST 11 (Scientific Instrument Services, Inc., Ringoes, NJ, USA). Possible pathways of such byproducts formed in samples under light exposure, for both soils and climate scenarios, were further studied.

Hydrogen isotope analysis of PAHs

For hydrogen isotope analysis of naphthalene, acenaphthene, fluorene, phenanthrene, anthracene, pyrene and benzo(*a*)pyrene, PAHs were extracted from duplicate samples specifically prepared for this isotopic study. The extraction method was the same as that used for concentration analysis, being the extract dissolved in 62.5 μL of dichloromethane (99.5%, Scharlau Chemie S.A., Barcelona, Spain). To avoid any possible interference with the $\delta^2\text{H}$ analysis, no deuterated PAHs were added to samples. Since the isotope composition of a compound does not depend on its concentration (Elsner et al., 2012), total mass recovery is not crucial for hydrogen isotopes analysis. The hydrogen isotope composition of each of the 7 individual PAHs was analyzed using a gas chromatography-pyrolysis-isotope ratio mass spectrometry system (GC-TC-IRMS), consisting of a Trace GC Ultra equipped with a split/splitless injector, coupled to a Delta V Advantage IRMS (Thermo Scientific GmbH, Bremen, Germany) through a high temperature pyrolysis interface. The column used in the GC-TC-IRMS system was an Agilent Technologies DB-1 column (30 m \times 0.25 mm, 1.0 μm film thickness; Santa Clara, CA, USA). The oven temperature program started at 50°C for 1 min, heated until 160°C at a rate of 25°C min^{-1} , and then up to 320°C at a rate of 3°C min^{-1} , being finally held at 320°C for 20 min. The injector was set to splitless mode at a temperature of 280°C. Helium was used as a carrier gas, with a gas flow rate of 1.0 mL min^{-1} .

Hydrogen isotope ratios are reported according to the international standard Vienna Standard Mean Ocean Water (VSMOW), using the delta notation, $\delta^2\text{H}$ (‰) = $(R/(R_{\text{std}}-1)) \times 1000$; where R and R_{std} are the isotope ratios ($^2\text{H}/^1\text{H}$) of the sample and the standard, respectively. Measurements were run in duplicate, achieving standard

deviations of the duplicates of $\delta^2\text{H}$ values below $\pm 10\%$. The analytical system was daily verified using PAH control standards with known hydrogen isotope ratios, which were determined previously using a Carlo-Erba 1108 (Carlo-Erba, Milano, Italy) elemental analyzer (EA), coupled in continuous flow to a Delta Plus XP isotope ratio mass spectrometer (Thermo Fisher Scientific, Bremen, Germany).

RESULTS AND DISCUSSION

Photodegradation of PAHs

Fig. 1 and Fig. 2 show the concentration changes of naphthalene, anthracene, pyrene, benzo(*a*)pyrene and benzo(*ghi*)perylene, as representatives of 2-, 3-, 4-, 5-, and 6- ringed PAHs, respectively, in Arenosol and fine-textured Regosol soils exposed for 28 days to B and CC scenarios. The complete list of photodegradation rates of the 16 PAHs here analyzed on the 28th day of light exposure is summarized in Table 1. Half-lives for the 16 PAHs in both kinds of soil, and in both simulated scenarios, are depicted in Fig. 3.

Because of methodological difficulties, different solvent extraction procedures were used in both scenarios. A Microwave Extraction System was utilized in the B scenario, while an ultrasonic bath was applied in the CC scenario. Recovery percentages were better in the latter case. Therefore, the initial concentrations of all PAHs were higher in the CC scenario. On the other hand, minor fluctuations in the concentrations were noticed over time. However, since irradiated samples were always compared to dark controls, these changes were not relevant. Three main processes might be related to PAH concentration decreases in soils subjected to the experimental conditions of the current study: volatilization, sorption, and photodegradation (Marquès et al., 2016). However, the contribution of each process was different according to the physicochemical properties of each compound, the texture of each soil, and the climate conditions. In general terms, higher photodegradation rates were noted in PAHs under the CC scenario than under the B scenario in Arenosol soil. In contrast, fewer differences in photodegradation rates were found in fine-textured Regosol soil when both scenarios were compared.

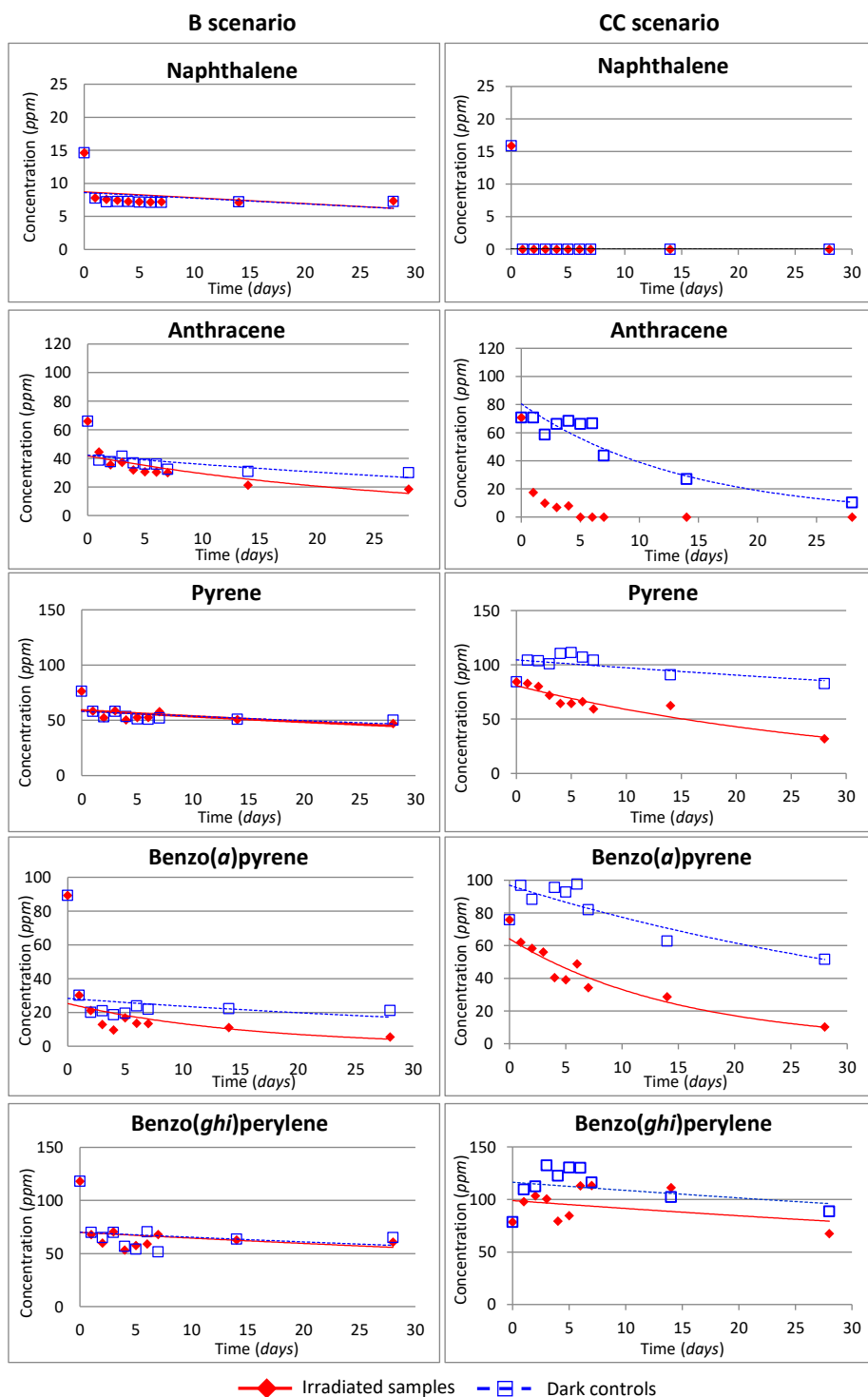


Fig. 1. Concentration trends of some 2-, 3-, 4-, 5-, and 6- ringed PAHs exposed to B and CC scenarios in Arenosol soil. Relative Standard Deviations: naphthalene= 0.36-2.38%; anthracene= 0.48-2.43%; pyrene= 0.43-4.55%; benzo(a)pyrene= 0.04-0.70%; and benzo(ghi)perylene= 0.01-2.64%.

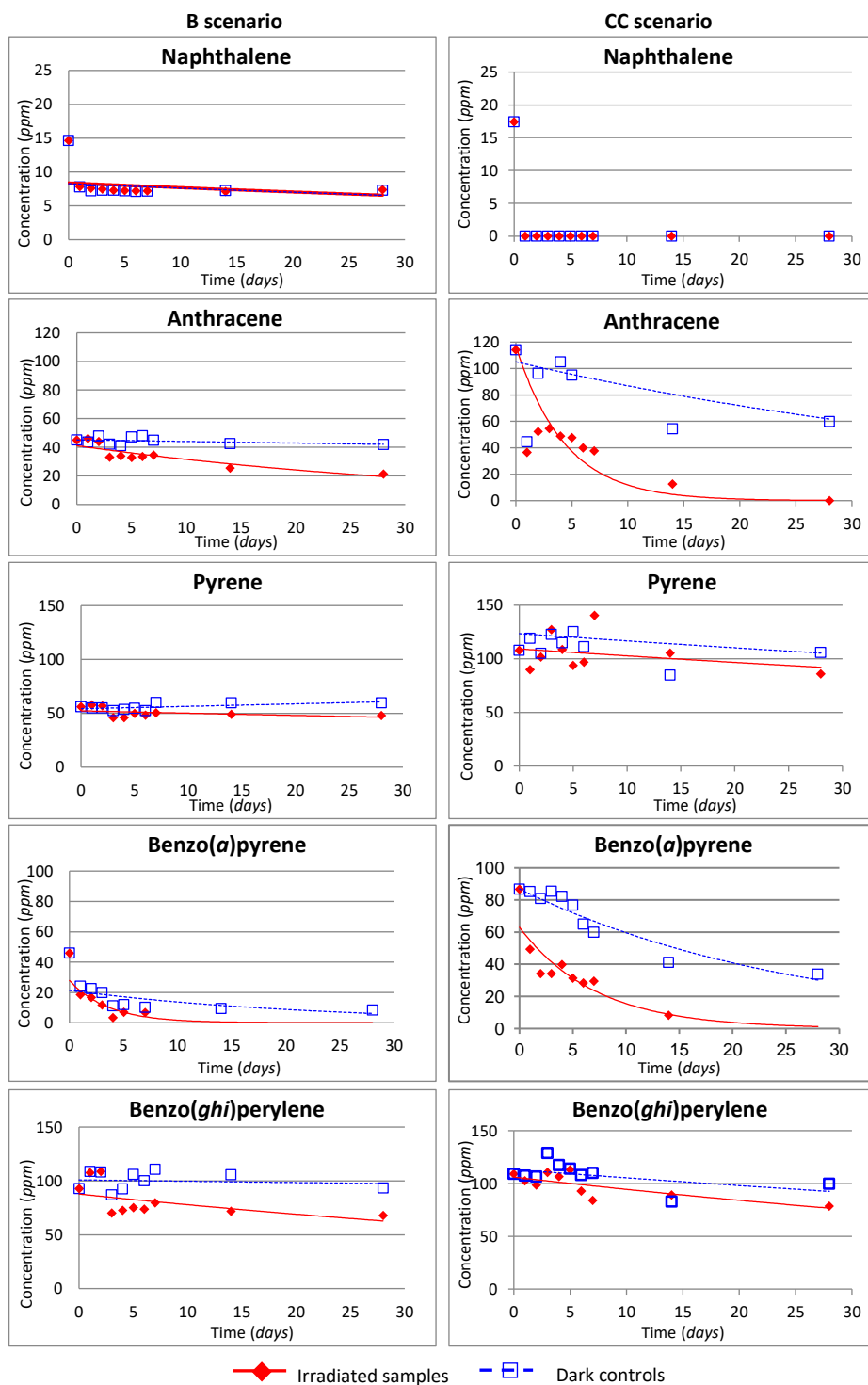


Fig. 2. Concentration trends of some 2-, 3-, 4-, 5-, and 6- ringed PAHs exposed to B and CC scenarios in fine-textured Regosol soil. Relative Standard Deviations: naphthalene= 0.36-2.38%; anthracene= 0.48-2.43%; pyrene= 0.43-4.55%; benzo(a)pyrene= 0.04-0.70%; nd benzo(ghi)perylene= 0.01-2.64%.

In the B scenario, concentrations of naphthalene were the same in irradiated and dark control samples, indicating that it was not photodegraded in any of the soils. In the CC scenario, naphthalene was not detected in any soil sample, either irradiated or dark control, which could be due to the volatilization related to the increase of temperature. These findings agree with those reported by Cabrerizo et al. (2015), who found a higher volatilization of low molecular weight PAHs in correlation with the temperature. Acenaphthylene also dramatically decreased its concentration under CC conditions. However, this reduction was not as quick as that of naphthalene, achieving undetected levels after the 1st and the 7th day of soil incubation, in coarse- and fine-textured soils, respectively. Similarly to naphthalene, volatilization would be playing a key role in the loss of acenaphthylene. In contrast, in the B scenario both compounds could be detected at the end of the experiment in both soils.

Table 1. Photodegradation rates (%) of 16 US EPA priority PAHs in Arenosol and fine-textured Regosol soils under B and CC scenarios.

	Arenosol soil		Fine-textured Regosol soil	
	B scenario*	CC scenario**	B scenario*	CC scenario**
Naphthalene	0	0	0	0
Acenaphthylene	0	0	0	0
Acenaphthene	1.5	21.3 ^a	2	2.6
Fluorene	2.9	15.4 ^c	9.5	7.8
Phenanthrene	11.2	16.0	33.2	30.5
Anthracene	19.7	85.4 ^b	39.8	36.4 ^d
Fluoranthene	0	28.9	12.5	14.1
Pyrene	0	60.1	17.1	18.6
Benzo(a)anthracene	0	41.0	30	34.2
chrysene	0	20.2	30	16.8
Benzo(b+k)fluoranthene	0	20.2	30	16.8
Benzo(a)pyrene	23.0	54.6	4.9 ^c	37.8 ^d
Benzo(ghi)perylene	3.6	27.1	24.6	19.5
Dibenzo(ah)anthracene	2.0	37.0	28.3	23.2
Indeno(123-cd)pyrene	11.7	39.1	68.9	43.2

*T= 20°C; light intensity= 9.6 W m⁻²; ** T= 24°C; light intensity= 24 W m⁻²; Complete degradation after: ^a1 day, ^b4 days, ^c7 days, and ^d14 days.

In Arenosol soil, photodegradation rates of acenaphthene, fluorene, phenanthrene and anthracene in the CC scenario (21.3%, 14.5%, 16.0% and 85.4%,

respectively) were notably higher than those obtained in the B scenario (1.5%, 2.9%, 11.2% and 19.7%, respectively). It evidences that an increase of temperature and light enhances photodegradation. Moreover, only under more extreme conditions, acenaphthene, anthracene and fluorene could not be detected in soil after 1, 4 and 14 days of light exposure, respectively. In contrast to Arenosol soil, similar photodegradation rates were found in fine-textured Regosol soil in both climate scenarios. Acenaphthene, fluorene, phenanthrene and anthracene showed photodegradation rates of 2.0%, 9.5%, 33.2% and 39.8% in the B scenario, while the loss of these compounds in the CC scenario was 2.6%, 7.8%, 30.5% and 36.4%, respectively. However, anthracene was completely photodegraded in soil when increasing the temperature and light intensity after 14 days of incubation. These results are in agreement with those previously reported by Coover and Sims (1987), who found different loss rates of 3-ringed PAHs according to the temperature (10°C, 20°C and 30°C).

In Arenosol soil, fluoranthene, pyrene, benzo(*a*)anthracene + chrysene, and benzo(*b+k*)fluoranthene were highly photodegraded under CC conditions, showing photodegradation rates of 28.9%, 60.1%, 41.0% and 20.2%, respectively. However, no photodegradation was noted for the same PAHs in the B scenario, where soil concentrations remained constant in both irradiated and dark control samples. These results also agree with those of Maliszewska-Kordybach (1993), who identified 4-ringed PAHs as the most sensitive to temperature change. Finally, no differences in photodegradation rates were observed in fine-textured Regosol soil, irrespective of the climate scenario. Zhang et al. (2010) reported a higher photodegradation of pyrene under UV light irradiation in a fine-textured soil, with loss rates of 25% and 35%, at 20°C and 25°C, respectively. In turn, lower rates were observed in both soils (17.1% and 18.6% in Arenosol and Regosol, respectively), probably because of differences in the light spectrum.

Benzo(*a*)pyrene, benzo(*ghi*)perylene, dibenzo(*ah*)anthracene and indeno(123-*cd*)pyrene presented a similar pattern to that of 3-ringed PAHs. The increase of temperature and light intensity enhanced the photodegradation of these PAHs in Arenosol soil. Photodegradation rates of benzo(*a*)pyrene, benzo(*ghi*)perylene, dibenzo(*ah*)anthracene and indeno(123-*cd*)pyrene increased from 23.0%, 3.6%, 2.0%

and 11.7% to 54.6%, 27.1%, 37.0% and 39.1%, respectively, after the increase of temperature and light related to the climate change. In fine-textured Regosol soil, these PAHs underwent more similar photodegradation rates under both simulated scenarios. Moreover, benzo(*a*)pyrene was completely lost before finishing the experiment regardless the climate conditions.

Half-lives of PAHs in soils determined on the basis of Equations 2 and 3, confirmed the same trends (Fig. 2). Lower half-lives were noted for the most volatile compounds (e.g., acenaphthylene and acenaphthene), due to their volatilization, as well as for those that were more rapidly photodegraded (e.g., anthracene and benzo(*a*)pyrene). In Arenosol soil, most PAHs presented lower half-lives when simulating the CC scenario, while they were similar in fine-textured Regosol soil in both scenarios.

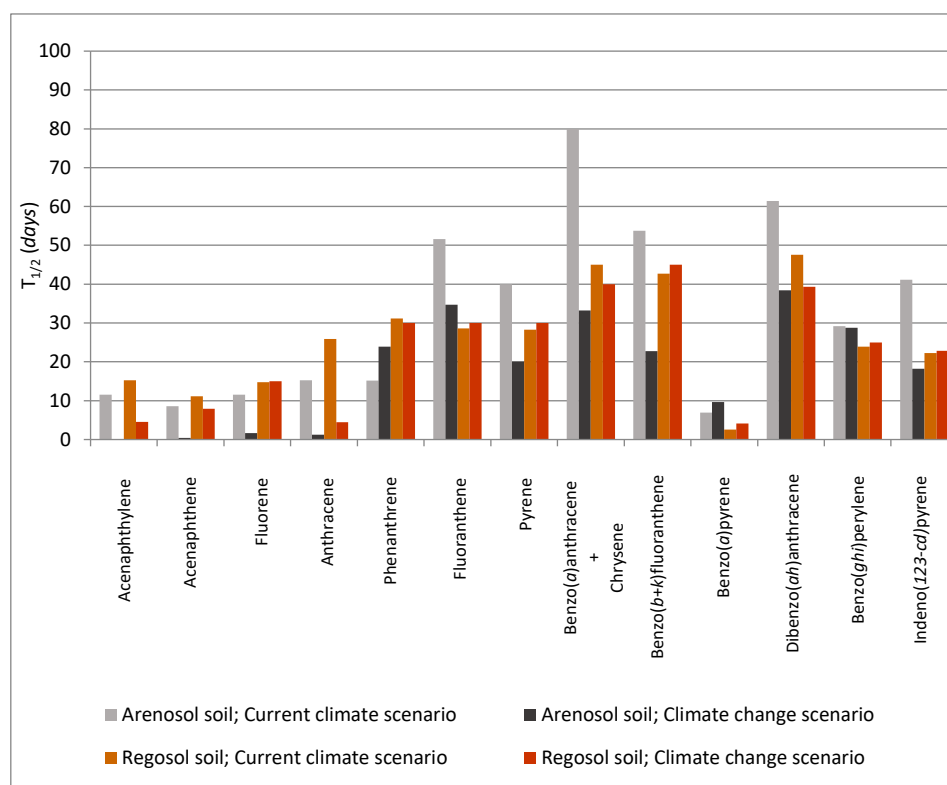


Fig. 3. Half-lives of 16 PAHs exposed to B and CC scenarios in Arenosol and fine-textured Regosol soils.

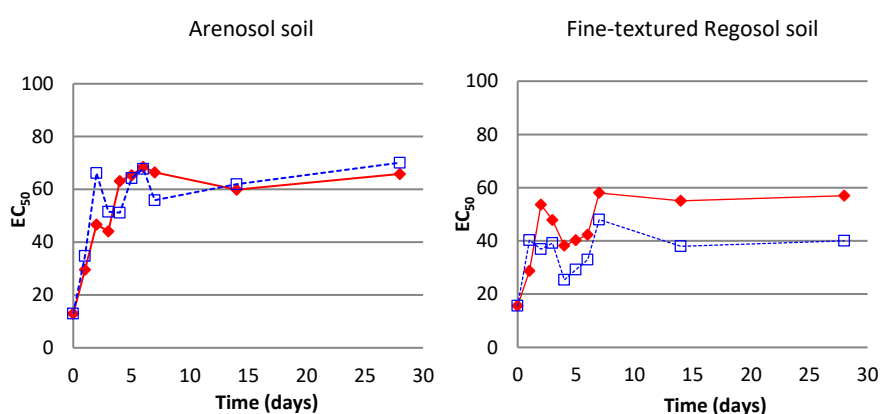
Higher degradation rates of PAHs were found in fine-textured Regosol soil. Soil texture plays a key role in the photodegradation of these chemicals. Xiaozhen et al.

(2005) showed that the photolytic depth increases gradually from sand through silt to clay. Therefore, photochemical reactions may be accelerated when soil particles are smaller. Moreover, it has also been pointed out the important role of the photocatalysts content (manganese, magnesium, zinc, iron and aluminum oxides) in soil over PAH degradation rates (Zhang et al., 2006; Zhao et al., 2004). In contrast to Regosol soil, PAH photodegradation rates clearly increased in Arenosol soil, after applying CC conditions, being probably related to the need of more activation energy (increase of temperature and light intensity) to achieve the photodegradation of the PAHs in Arenosol soil. The higher amount of iron, aluminum and manganese oxides in fine-textured soil than in Arenosol soil, favors PAH photodegradation, even with no increase of temperature and light intensity. This fact highlights the tremendous importance of the soil properties on the PAH degradation, which makes hard compare the current results with those from the scientific literature. The values of volatilization and enhanced degradation of the mid-molecular weight PAHs found in this study were in agreement with those previously reported by a number of investigators. In contrast, the high photodegradation rates led to lower half-lives, in comparison to values from the scientific literature (Coover and Sims, 1987; Maliszewska-Kordybach, 1993; Oleszczuk and Baran, 2003). Furthermore, photodegradation of high molecular weight PAHs contrasts with previous findings in which these compounds had been reported to be very recalcitrant in soil, even when increasing the temperature up to 30°C (Coover and Sims, 1987; Maliszewska-Kordybach, 1993). In the present study, benzo(*a*)pyrene was more easily photodegraded when increasing the temperature under light exposure (Zhang et al., 2006). Nonetheless, it must be remarked that not only temperature, but also light intensity, were adjusted. Consequently, the current results might differ from others reported in the scientific literature, in which temperature was the only controlled parameter. It has been suggested that there might be a synergistic effect of PAH photodegradation when both temperature and light intensity are increased (Nadal et al., 2006). Anyhow, the assessment of two simultaneous variables makes more difficult the comparability between studies.

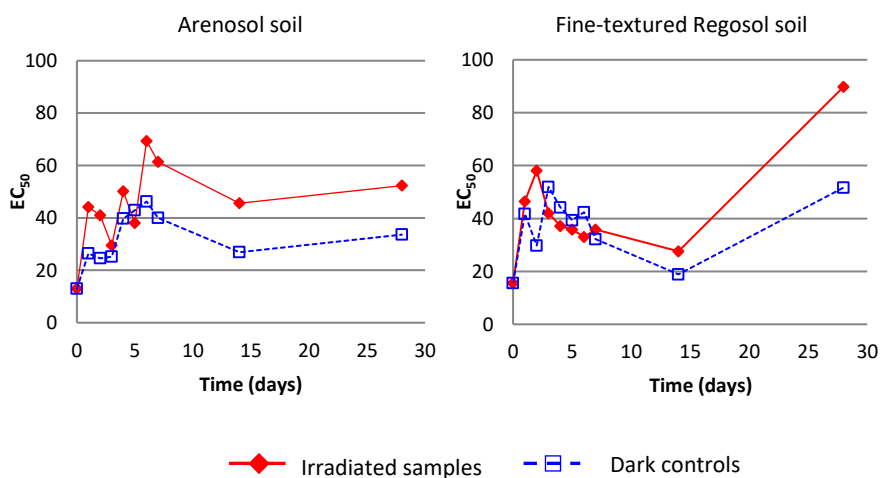
Ecotoxicity: Microtox® test

Under current climate conditions, irradiated and dark control samples showed a similar ecotoxicity trend in Arenosol soil. By contrast, irradiated samples were more detoxified than dark controls in fine-textured soil. These differences between both soils agreed with concentrations results, since higher photodegradation rates were shown in fine-textured soil than in Arenosol soil when the current Mediterranean scenario was simulated.

a) B scenario



b) CC scenario



◆ Irradiated samples -□- Dark controls

Fig. 4. Ecotoxicity trend in Arenosol and fine-textured Regosol soil under B and CC scenarios.

Contrary to the current climate scenario, irradiated samples became more detoxified than dark controls in Arenosol soil under the simulation of the climate change scenario. In fact, PAHs found in this kind of soil were more photodegraded when the temperature and light intensity increased. In fine-textured Regosol soil, EC₅₀ of irradiated samples and dark controls did not show many differences until 14th day of exposure, being afterwards irradiated samples more detoxified. Regardless of the soil and climate scenario, EC₅₀ oscillations in irradiated samples, which in turn were more pronounced in climate change scenario, might probably be related to the formation of PAHs photodegradation by-products.

Identification of PAH metabolites

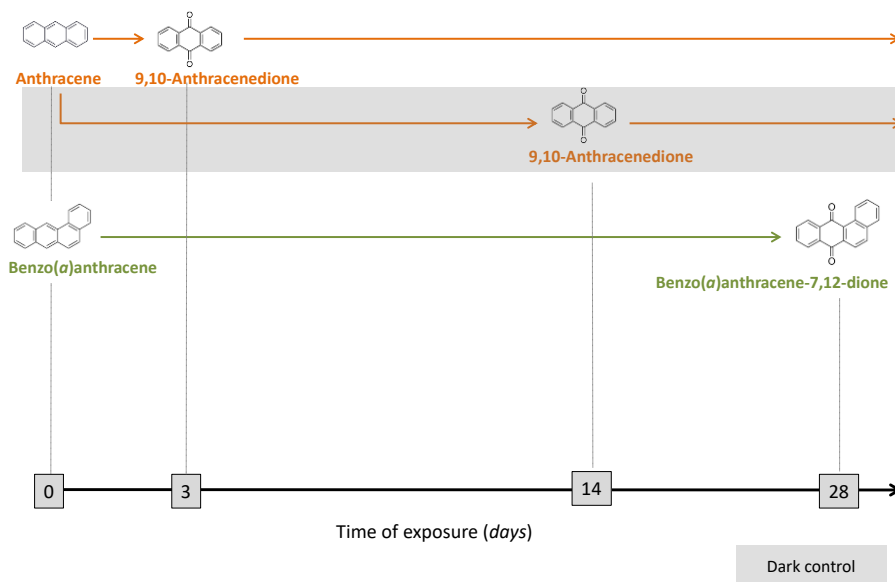
PAH metabolites were identified in irradiated samples and dark controls of both soils and under both climate scenarios (Table 2). Potential pathways for their formation are shown in Fig. 5 and Fig. 6.

Table 2. Information about identified metabolites in both soils and climate scenarios.

	m/z	T _R (min)	Arenosol soil				Fine-textured Regosol soil				
			B scenario*		CC scenario**		B scenario*		CC scenario**		
			RAD	DC	RAD	DC	RAD	DC	RAD	DC	
Benzophenone	182	12.40	x	x	x	x	x	x	x	x	x
9H-fluorene,9-methylene	252	6.72	x	x				x	x		
Methyl dehydroabietate	299	14.45	x	x				x	x		
1,2-dihydrobenzo(b)fluoranthene	253	16.86	x	x				x	x	x	x
2,3-dihydrofluoranthene	202	12.22	x	x				x	x		
Acetophenone	120	6.93			x	x				x	x
Benzaldehyde,3-hydroxy-4-methoxy	151	9.85			x	x				x	x
Benzeneacetic acid	136	8.22			x	x				x	x
2,6-dimethylbenzaldehyde	133	7.95								x	x
9,10-anthracenedione	208	16.85	x	x	x	x	x	x	x	x	x
7H-benzanthrene / 11H-benzo(b)fluorene	281	20.32								x	x
Benzo(a)anthracene-7,12-dione	258	24.98	x		x			x		x	
1-acenaphthenol	168	12.91								x	
2-naphthalenecarboxaldehyde	184	16.20								x	
Naphthalic anhydride	198	17.74			x					x	
9H-fluoren-9-one	180	13.88			x						
1(2H)-acenaphthylenone	168	12.93			x						

RAD= irradiated sample; DC= dark control; *T= 20°C; light intensity= 9.6 W m⁻²; ** T= 24°C; light intensity= 24 W m⁻²

a) Arenosol soil



b) Fine-textured Regosol soil

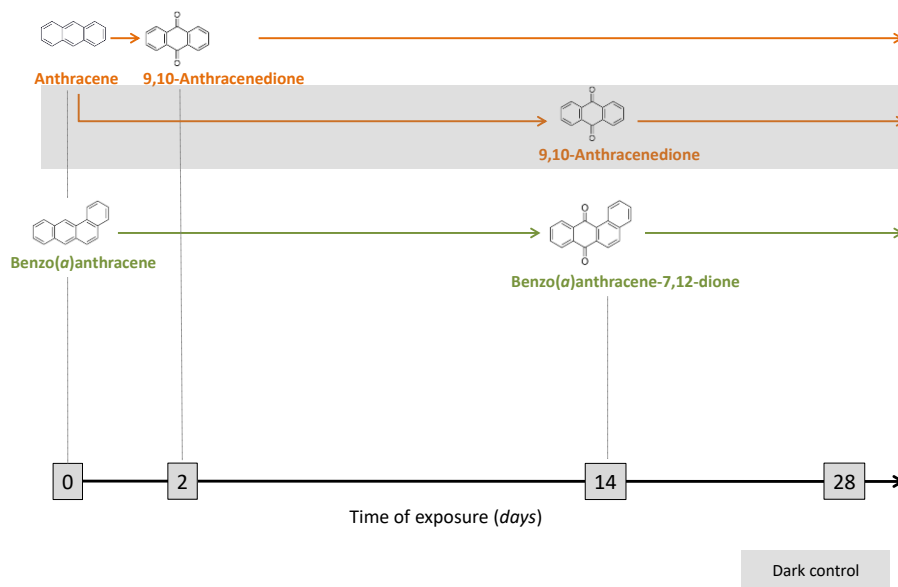
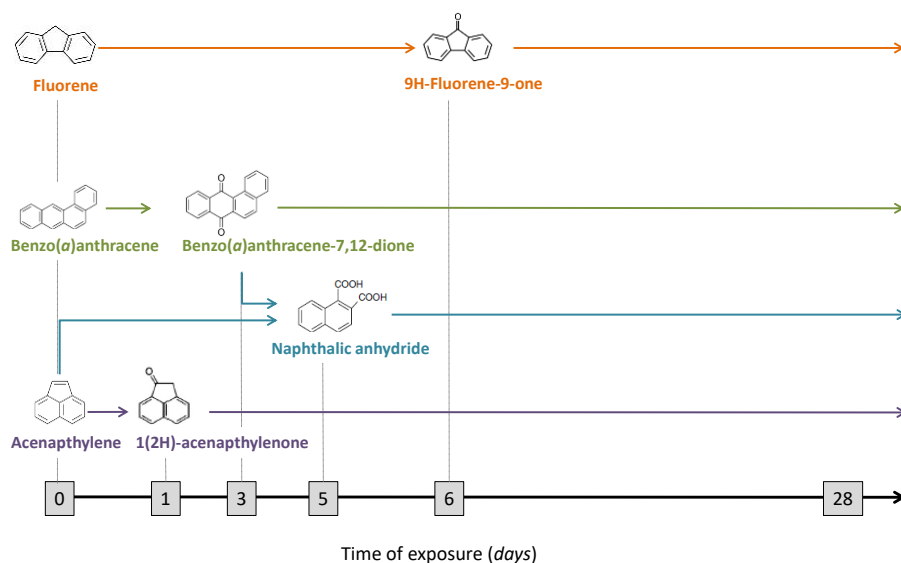


Fig. 5. Photodegradation by-products of PAHs in a) Arenosol soil and b) fine-textured Regosol soil, under the B scenario.

a) Arenosol soil



b) Fine-textured Regosol soil

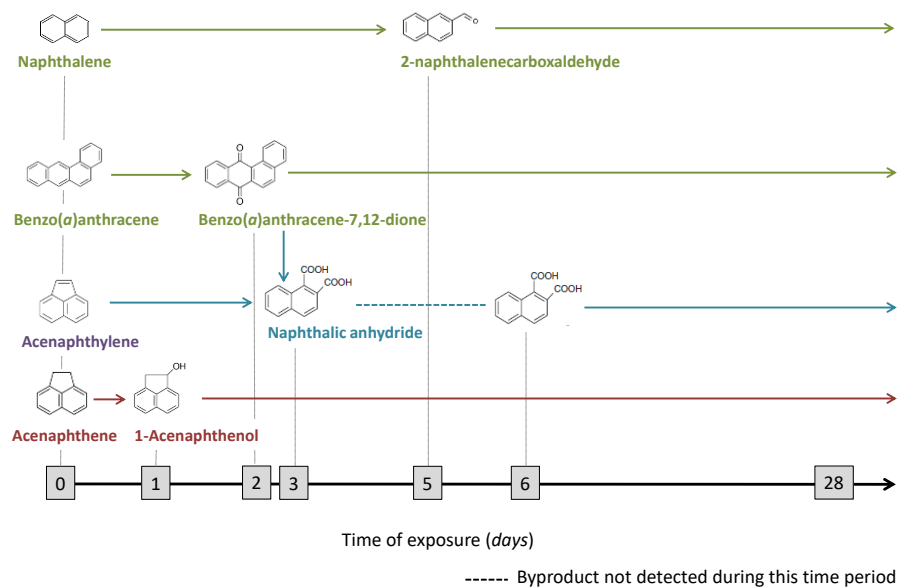


Fig. 6. Photodegradation by-products of PAHs in a) Arenosol soil and b) fine-textured Regosol soil, under the CC scenario.

Up to 7 metabolites were identified when simulating the B climate scenario (Fig. 4). Benzo(*a*)anthracene-7,12-dione was only found in soils exposed to light, while 9,10-anthracenedione was formed under light and darkness conditions. The oxidation of anthracene and benzo(*a*)anthracene may lead to the formation of 9,10-anthracenedione and benzo(*a*)anthracene-7,12-dione, respectively, as a consequence of photodegradation or other degradation processes (Cajthaml et al., 2006; Gabriel et al., 2004; Woo et al., 2009). 9,10-anthracenedione was found after 2 and 3 days of light exposure in fine-textured Regosol and Arenosol soils, respectively. It was also found in dark controls after 14 days of soil incubation, showing that unknown degradation processes could be also occurring in the dark. In addition, light could also enhance the oxidation of anthracene, leading to a quicker formation of 9,10-anthracenedione. Although concentrations indicated that benzo(*a*)anthracene was only photodegraded in fine-textured Regosol soil, benzo(*a*)anthracene-7,12-dione was identified not only in fine-textured Regosol soil, after 14 days, but also unexpectedly in Arenosol soil after 28 days of light exposure. Therefore, a slight degradation could be also happening in Arenosol soil.

The same metabolites that were found in the B scenario, were also identified under CC conditions (Fig. 5). 9,10-anthracenedione was found just the first day of incubation in both kinds of soil, in both irradiated samples and dark controls. Benzo(*a*)anthracene-7,12-dione was identified after 2 and 3 days of light exposure in fine-textured Regosol and Arenosol soils, respectively. It suggests that the formation of benzo(*a*)anthracene-7,12-dione could depend on soil texture and climate conditions. In contrast to concentration data, the increase of temperature and light intensity enhanced by-products formation in Regosol soil. Overall, these results clearly show the need to jointly evaluate the levels of the 16 priority US EPA PAHs together with those of the metabolites, when assessing the photodegradation of these organic compounds. As PAHs in soil can be influenced by a number of processes (e.g. volatilization and/or sorption/desorption), the presence of metabolites makes clear the degradation of parental compounds.

The increase of the temperature, as well as the light intensity, led to the formation of new metabolites under CC conditions (Fig. 5). Acenaphthylene and benzo(*a*)anthracene-7,12-dione could have been transformed into naphthalic

anhydride (Cajthaml et al., 2006), which was detected after 3 and 5 days of light exposure in fine-textured Regosol and Arenosol soils, respectively. However, it was not detected between the 3rd and the 6th day in fine-textured Regosol soil, being the most plausible hypothesis the generation/degradation dynamics of this metabolite. According to Microtox[®] results, the occurrence of naphthalic anhydride matches with the occasionally toxicity increase in irradiated samples. However, there is not available data on naphthalic anhydride and that fact should be further studied. There were some by-products that were formed depending on the soil. In Arenosol soil, acenaphthylene and fluorene, which were completely lost before finishing the experiment, may be oxidized and transformed into oxy-PAHs. Woo et al. (2009) reported that the photodegradation of acenaphthylene leads to the formation of 1(2H)-acenaphthylenone. On the other hand, Acevedo et al. (2011) stated that fluorene leads to the formation of 9H-fluorene-9-one when studying PAH biodegradation. In the present study, the oxygen consumption of soils was negligible, disregarding any biodegradation process. Hence, the occurrence of such metabolite on the 7th day of light exposure might come from the oxidation of fluorene, being light a key parameter.

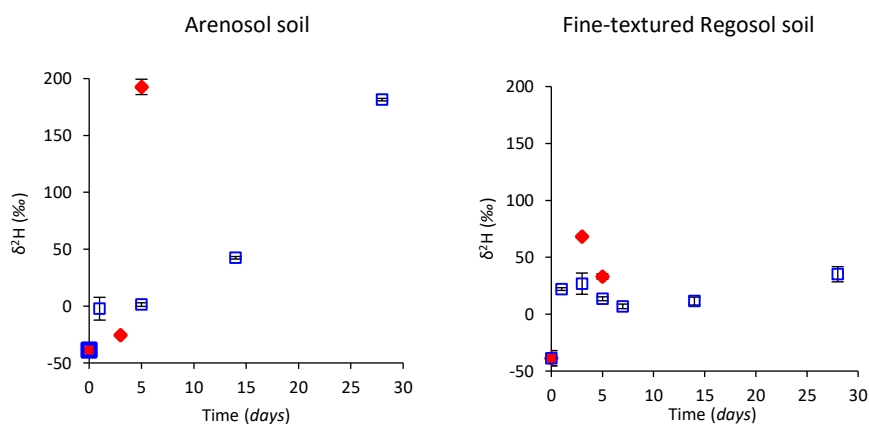
Since the 1st day, light exposure might have hydroxylized acenaphthene by attaching an -OH radical, ultimately generating acenaphthenol (Woo et al., 2009). Furthermore, naphthalene oxidation might have generated 2-naphthalenecarboxaldehyde, after 5 days in fine-textured soil, therefore disregarding volatilization as the only process occurring in Regosol soil. However, these findings still need further confirmation.

The intermediate chemicals identified in the present study were quinones, ketones and aldehydes, whose high stability allows a higher resistance to degradation. However, although undetected, it cannot be discarded that intermediate compounds with lower stability may be formed, but quickly degraded. Moreover, the experiment was focused on the assessment of the 16 US EPA priority PAHs, whereas the identification and description of PAH metabolites might be somehow biased.

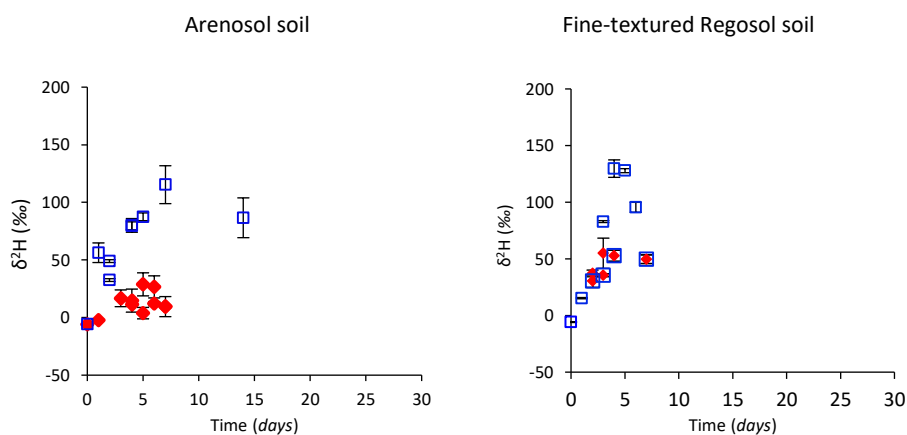
Hydrogen isotopes of PAHs

In a context of climate change, benzo(*a*)pyrene showed a significant hydrogen isotope fractionation over time in both Arenosol and fine-textured Regosol soils (Fig. 7). Additionally, a significant enrichment in ^2H in benzo(*a*)pyrene was also observed in dark controls from both types of soil.

a) B scenario



b) CC scenario



◆ Irradiated samples □ Dark controls

Fig. 7. Hydrogen isotope composition of benzo(*a*)pyrene under (a) B and (b) CC scenarios over time in the Arenosol fine-textured Regosol soil. Error bars represent the standard deviation between analytical duplicates.

In Arenosol soil, benzo(*a*)pyrene in irradiated soil samples experienced hydrogen isotopic fractionation, with a change of hydrogen isotopic composition from -6‰ to +29‰ (Fig. 6b), after 5 days of experiment. In Regosol soil, a similar variation in hydrogen isotopic composition of benzo(*a*)pyrene was obtained (from -6‰ to +55‰ after 3 days of experiment, Fig. 6b). These results are in agreement with concentration data, confirming the degradation of benzo(*a*)pyrene under climate change conditions. Hydrogen isotopic changes of benzo(*a*)pyrene in dark controls (from -6‰ to +115‰ after 7 days of incubation in Arenosol soil, and from -6‰ to +129‰ after 4 days of incubation in Regosol soil, Fig. 6b) confirm its degradation in the dark, which is in agreement with the formation of metabolites under these conditions. Although none of the metabolites was linked to benzo(*a*)pyrene, non-stable byproducts could have been generated, but also quickly degraded. Therefore, the presence of unknown degradation processes of PAHs, occurring also in the dark, was confirmed from two lines of evidence: 1) metabolites formation from other PAHs, and 2) hydrogen isotopic fractionation of benzo(*a*)pyrene (Fig. 6). Since it could mean an important pathway of PAH loss in soil, the degradation of benzo(*a*)pyrene in the dark should be further studied.

When comparing the hydrogen isotope fractionation of benzo(*a*)pyrene under light in both climate scenarios, a similar increasing tendency was observed. However, a higher degree of hydrogen isotope fractionation was achieved in the B scenario (Fig. 6a). In Arenosol soil, after 5 days of irradiation, the total hydrogen isotopic change was 232‰ and 35‰ in the B and CC scenarios, respectively. In fine-textured Regosol soil, after 3 days, the hydrogen isotope fractionation of benzo(*a*)pyrene in the B and CC scenarios was 107‰ and 55‰, respectively. These results indicate a less hydrogen isotope discrimination under CC conditions.

Contrastingly, global warming might lead a higher hydrogen isotope fractionation in the darkness. In Arenosol soil, a total fractionation of 121‰ was achieved after 7 days in the CC scenario, while that in the B scenario was only 81‰. Finally, in Regosol soil, the fractionation was 136‰ vs. 74‰ in the CC and B scenarios, respectively.

The differences in the degree of hydrogen isotope fractionation between the different soils and climate conditions, including darkness conditions, suggest that hydrogen isotope fractionation could discriminate different types of degradation.

Unfortunately, the presence of other processes occurring along the experiment such as volatilization and sorption, made impossible to calculate the degree of isotopic enrichment factor (ϵ value). To obtain the specific ϵ value of each degradation process, further studies should be designed to avoid other processes that may affect concentration variation.

With respect to the other six PAHs analyzed during the isotopic study (namely, naphthalene, acenaphthene, fluorene, phenanthrene, anthracene and pyrene), naphthalene and acenaphthene were not detected. Therefore, no isotopic effects could be assessed for these two particular hydrocarbons. On the other hand, due to its interference with the deuterated fluorene used as internal standard for analytical control, fluorene could not be properly detected. Finally, phenanthrene, anthracene and pyrene did not show any hydrogen isotope fractionation. According to the basis of isotopic fractionation (Elsner et al., 2012), the absence of isotopic effects on these three PAHs could be associated to low isotopes discrimination during the bond breakage produced by photodegradation. Further investigations should also confirm this hypothesis.

CONCLUSIONS

Climate change is able to impact on the photodegradation of PAHs depending on the exposure time, the molecular weight of each compound, and the soil texture. According to the results of the present study, when increasing the temperature and light intensity, low molecular weight PAHs are more rapidly volatilized. Moreover, medium and high molecular weight PAHs showed higher photodegradation rates in Arenosol soil, while their rates remained constant in fine-textured Regosol soil, regardless of the climate scenario. The important role of the required activation energy was confirmed, as it favours the photodegradation reactions in different kinds of soil. The content of photocatalysts in Arenosol soil needs more temperature and light intensity to enhance the photodegradation of PAHs. In turn, photocatalysts in fine-textured Regosol soil are able of fostering the photodegradation of PAHs under any climate condition. It was also noted that the formation of PAH metabolites, as a consequence of light exposure, takes place through different pathways, being the oxidation of parent compounds the most relevant. In the CC scenario, the formation

of by-products was clearly favoured in comparison with data from the B scenario, in which the amount of detected metabolites was notably lower. Consequently, in a more or less near future, although humans might be exposed to lower environmental concentrations of PAHs, they could be exposed to new PAH metabolites, which may be even more toxic (Ras et al., 2009).

Finally, hydrogen isotope results confirm that benzo(*a*)pyrene is degraded in a CC scenario, in both light and darkness. The differences in the degree of hydrogen isotopic fractionation, according to the different climate conditions and types of soil, indicate the suitability of hydrogen isotopes to distinguish different degradation processes. Moreover, the significant hydrogen isotopic change obtained in the different case-studies emphasizes the great potential of CSIA as a powerful tool to monitor PAH degradation in the field. Furthermore, the degradation of benzo(*a*)pyrene without light intervention requires additional investigations, since it could be a potentially relevant pathway of PAH loss in soil.

Acknowledgements

This study was financially supported by the Spanish Ministry of Economy and Competitiveness, through the projects CTM2012-33079, CGL2011-29975-C04-01 and CGL2014-57215-C4-1-R, and by the Catalan Government, through the projects 2014SGR90 and 2014SGR1456. Montse Marquès received a PhD fellowship from AGAUR (Commissioner for Universities and Research of the Department of Innovation, Universities and Enterprise of the “Generalitat de Catalunya” and the European Social Fund).

References

- Acevedo, F., Pizzul, L., Castillo, M. d. P., Cuevas, R., Diez, M. C., 2011. Degradation of polycyclic aromatic hydrocarbons by the Chilean white-rot fungus *Anthracophyllum discolor*. *J. Hazard. Mater.* 185, 212-219.
- Aichner, B., Bussian, B. M., Lehnik-Habrink, P., Hein, S., 2015. Regionalized concentrations and fingerprints of polycyclic aromatic hydrocarbons (PAHs) in German forest soils. *Environ. Pollut.* 203, 31-39.
- Armitage, J. M., Quinn, C. L., Wania, F., 2011. Global climate change and contaminants-an overview of opportunities and priorities for modelling the

- potential implications for long-term human exposure to organic compounds in the Arctic. *J. Environ. Monit.* 13, 1532-1546.
- Balmer, M. E., Goss, K.-U., Schwarzenbach, R. P., 2000. Photolytic transformation of organic pollutants on soil surfaces: an experimental approach. *Environ. Sci. Technol.* 34, 1240-1245.
- Bangash, R. F., Passuello, A., Hammond, M., Schuhmacher, M., 2012. Water allocation assessment in low flow river under data scarce conditions: A study of hydrological simulation in Mediterranean basin. *Sci. Total Environ.* 440, 60-71.
- Bergmann, F. D., Abu Laban, N. M. F. H., Meyer, A. H., Elsner, M., Meckenstock, R. U., 2011. Dual (C, H) isotope fractionation in anaerobic low molecular weight (Poly)aromatic hydrocarbon (PAH) degradation: potential for field studies and mechanistic implications. *Environ. Sci. Technol.* 45, 6947-6953.
- Cabrerizo, A., Galbán-Malagón, C., Vento, S. D., Dachs, J., 2015. Sources and fate of polycyclic aromatic hydrocarbons in the Antarctic and Southern Ocean atmosphere. *Global Biogeochem. Cycl.* 28, 1424-1436.
- Cajthaml, T., Erbanová, P., Sasek, V., Moeder, M., 2006. Breakdown products on metabolic pathway of degradation of benz[a]anthracene by a ligninolytic fungus. *Chemosphere* 64, 560-564.
- Coover, M. P., Sims, R. C., 1987. The effect of temperature on polycyclic aromatic hydrocarbon persistence in an unacclimated agricultural soil. *Hazard. Waste Hazard. Mater.* 4, 69-82.
- Cubasch, U., Wuebbles, D., Chen, D., Facchini, M. C., Frame, D., Mahowald, N., Winther, J. G., Introduction. In: T. F. Stocker, D. Qin, G.K. Plattner, et al., Eds., *Climate Change 2013: The Physical Science Basis. Contribution of Working Group I to the Fifth Assessment Report of the Intergovernmental Panel on Climate Change.* Cambridge University Press, Cambridge, United Kingdom and New York, NY, USA, 2013, pp. 119-158.
- Elsner, M., Jochmann, M. A., Hofstetter, T. B., Hunkele, D., Bernstein, A., Schmidt, T. C., Schimmelmann, A., 2012. Current challenges in compound-specific stable isotope analysis of environmental organic contaminants. *Anal. Bioanal. Chem.* 403, 2471-2491.
- Frank, M. P., Graebing, P., Chib, J. S., 2002. Effect of soil moisture and sample depth on pesticide photolysis. *J. Agric. Food Chem.* 50, 2607-2614.
- Gabriel, J., Baldrian, P., Verma, P., Cajthaml, T., Merhautová, V., Eichlerová, I., Stoytchev, I., Trnka, T., Stopka, P., Nerud, F., 2004. Degradation of BTEX and PAHs by Co(II) and Cu(II)-based radical-generating systems. *Appl. Catal. B Environ.* 51, 159-164.
- Giorgi, F., 2006. Climate change hot-spots. *Geophys. Res. Lett.* 33, L08707.
- Gong, A., Ye, C., Wang, X., Lei, Z., Liu, J., 2001. Dynamics and mechanism of ultraviolet photolysis of atrazine on soil surface. *Pest Manage. Sci.* 57, 380-385.
- Gupta, H., Gupta, B., 2015. Photocatalytic degradation of polycyclic aromatic hydrocarbon benzo[a]pyrene by iron oxides and identification of degradation products. *Chemosphere* 138, 924-931.
- Hartenbach, A., Hofstetter, T., Tentscher, T., Canonica, S., Berg, M., Schwarzenbach, A., 2008. Hydrogen, and nitrogen isotope fractionation during light-induced transformations of atrazine. *Environ. Sci. Technol.* 42, 7751-7756.
- IPCC, 2013. *Climate Change 2013: The Physical Science Basis. Contribution of Working Group I to the Fifth Assessment Report of the Intergovernmental Panel on Climate*

- Change. Cambridge University Press, Cambridge, United Kingdom and New York, NY, USA.
- Jiang, Y. F., Wang, X. T., Wang, F., Jia, Y., Wu, M. H., Sheng, G. Y., Fu, J. M., 2009. Levels, composition profiles and sources of polycyclic aromatic hydrocarbons in urban soil of Shanghai, China. *Chemosphere* 75, 1112–1118.
- Kallenborn, R., Halsall, C., Dellong, M., Carlsson, P., 2012. The influence of climate change on the global distribution and fate processes of anthropogenic persistent organic pollutants. *J. Environ. Monit.* 14, 2854-2869.
- Lamon, L., Valle, M. D., Critto, A., Marcomini, A., 2009. Introducing an integrated climate change perspective in POPs modelling, monitoring and regulation. *Environ. Pollut.* 157, 1971-1980.
- Liu, L. Y., Kukučka, P., Venier, M., Salamova, A., Klánová, J., Hites, R. A., 2014. Differences in spatiotemporal variations of atmospheric PAH levels between North America and Europe: Data from two air monitoring projects. *Environ. Int.* 64, 48-55.
- Macdonald, R. W., Mackay, D., Li, Y.F., Hickie, B., 2003. How will global climate change affect risks from long-range transport of Persistent Organic Pollutants? *Hum. Ecol. Risk Assess.* 9, 643-660.
- Maliszewska-Kordybach, B., 1993. The effect of temperature on the rate of disappearance of polycyclic aromatic hydrocarbons from soils. *Environ. Pollut.* 79, 15-20.
- Manciocco, A., Calamandrei, G., Alleva, E., 2014. Global warming and environmental contaminants in aquatic organisms: The need of the etho-toxicology approach. *Chemosphere* 100, 1-7.
- Mariotti, A., Pan, Y., Zeng, N., Alessandri, A., 2015. Long-term climate change in the Mediterranean region in the midst of decadal variability. *Clim. Dyn.* 44, 1437–1456.
- Marquès, M., Bangash, R. F., Kumar, V., Sharp, R., Schuhmacher, M., 2013. The impact of climate change on water provision under a low flow regime: A case study of the ecosystems services in the Francoli river basin. *J. Hazard. Mater.* 263, Part 1, 224-232.
- Marquès, M., Mari, M., Audí-Miró, C., Sierra, J., Soler, A., Nadal, M., Domingo, J.L., 2016. Photodegradation of polycyclic aromatic hydrocarbons in soils under a climate change base scenario. *Chemosphere*, in press.
- Melnyk, A., Dettlaff, A., Kuklińska, K., Namieśnik, J., Wolska, L., 2015. Concentration and sources of polycyclic aromatic hydrocarbons (PAHs) and polychlorinated biphenyls (PCBs) in surface soil near a municipal solid waste (MSW) landfill. *Sci. Total Environ.* 530-531, 18-27.
- Muckian, L., Grant, R., Doyle, E., Clipson, N., 2007. Bacterial community structure in soils contaminated by polycyclic aromatic hydrocarbons. *Chemosphere* 68, 1535–1541.
- Nadal, M., Mari, M., Schuhmacher, M., Domingo, J. L., 2009. Multi-compartmental environmental surveillance of a petrochemical area: Levels of micropollutants. *Environ. Int.* 35, 227-235.
- Nadal, M., Marquès, M., Mari, M., Domingo, J. L., 2015. Climate change and environmental concentrations of POPs: A review. *Environ Res.* 143, 177-185.
- Nadal, M., Schuhmacher, M., Domingo, J. L., 2004. Levels of PAHs in soil and vegetation samples from Tarragona County, Spain. *Environ. Pollut.* 132, 1-11.

- Nadal, M., Schuhmacher, M., Domingo, J. L., 2011. Long-term environmental monitoring of persistent organic pollutants and metals in a chemical/petrochemical area: Human health risks. *Environ. Pollut.* 159, 1769-1777.
- Nadal, M., Wargent, J. J., Jones, K. C., Paul, N. D., Schuhmacher, M., Domingo, J. L., 2006. Influence of UV-B radiation and temperature on photodegradation of PAHs: Preliminary results. *J. Atmos. Chem.* 55, 241-252.
- Noyes, P. D., McElwee, M. K., Miller, H. D., Clark, B. W., Van Tiem, L. A., Walcott, K. C., Erwin, K. N., Levin, E. D., 2009. The toxicology of climate change: Environmental contaminants in a warming world. *Environ. Int.* 35, 971-986.
- Oba, Y., Naraoka, H., 2007. Carbon and hydrogen isotope fractionation of acetic acid during degradation by ultraviolet light. *Geochem. J.* 41, 103-110.
- Oleszczuk, P., Baran, S., 2003. Degradation of individual polycyclic aromatic hydrocarbons (PAHs) in soil polluted with aircraft fuel. *Pol. J. Environ. Stud.* 12, 431-437.
- Perez, L., Trüeb, S., Cowie, H., Keuken, M. P., Mudu, P., Ragetti, M. S., Sarigiannis, D. A., Tobollik, M., Tuomisto, J., Vienneau, D., Sabel, C., Künzli, N., 2015. Transport-related measures to mitigate climate change in Basel, Switzerland: A health-effectiveness comparison study. *Environ. Int.* 85, 111-119.
- Philippart, C. J. M., Anadón, R., Danovaro, R., Dippner, J. W., Drinkwater, K. F., Hawkins, S. J., Oguz, T., O'Sullivan, G., Reid, P. C., 2011. Impacts of climate change on European marine ecosystems: Observations, expectations and indicators. *J. Exp. Mar. Biol. Ecol.* 400, 52-69.
- Ras, M. R., Marcé, R. M., Cuadras, A., Mari, M., Nadal, M., Borrull, F., 2009. Atmospheric levels of polycyclic aromatic hydrocarbons in gas and particulate phases from Tarragona Region (NE Spain). *Int. J. Environ. Anal. Chem.* 89, 543-556.
- Sánchez-Canales, M., López Benito, A., Passuello, A., Terrado, M., Ziv, G., Acuña, V., Schuhmacher, M., Elorza, F. J., 2012. Sensitivity analysis of ecosystem service valuation in a Mediterranean watershed. *Sci. Total Environ.* 440, 140-153.
- Schiedek, D., Sundelin, B., Readman, J. W., Macdonald, R. W., 2007. Interactions between climate change and contaminants. *Mar. Pollut. Bull.* 54, 1845-1856.
- Schröter, D., Cramer, W., Leemans, R., Prentice, I. C., Araújo, M. B., Arnell, N. W., Bondeau, A., Bugmann, H., Carter, T. R., Gracia, C. A., De La Vega-Leinert, A. C., Erhard, M., Ewert, F., Glendining, M., House, J. I., Kankaanpää, S., Klein, R. J. T., Lavorel, S., Lindner, M., Metzger, M. J., Meyer, J., Mitchell, T. D., Reginster, I., Rounsevell, M., Sabaté, S., Sitch, S., Smith, B., Smith, J., Smith, P., Sykes, M. T., Thonicke, K., Thuiller, W., Tuck, G., Zaehle, S., Zierl, B., 2005. Ecology: Ecosystem service supply and vulnerability to global change in Europe. *Science*. 310, 1333-1337.
- Sweetman, A. J., Valle, M. D., Prevedouros, K., Jones, K. C., 2005. The role of soil organic carbon in the global cycling of persistent organic pollutants (POPs): interpreting and modelling field data. *Chemosphere* 60, 959-972.
- Terrado, M., Acuña, V., Ennaanay, D., Tallis, H., Sabater, S., 2014. Impact of climate extremes on hydrological ecosystem services in a heavily humanized Mediterranean basin. *Ecol. Indic.* 37, Part A, 199-209.
- UNEP, Climate Change and POPs; Predicting the Impacts. Report of the UNEP/AMAP expert group. United Nations Environmental Programme, 2010, pp. 65.

- Wang, C., Wu, S., Zhou, S., Wang, H., Li, B., Chen, H., Yu, Y., Shi, Y., 2015. Polycyclic aromatic hydrocarbons in soils from urban to rural areas in Nanjing: Concentration, source, spatial distribution, and potential human health risk. *Sci. Total Environ.* 527-528, 375-383.
- Woo, O. T., Chung, W. K., Wong, K. H., Chow, A. T., Wong, P. K., 2009. Photocatalytic oxidation of polycyclic aromatic hydrocarbons: Intermediates identification and toxicity testing. *J. Hazard. Mater.* 168, 1192-1199.
- Wu, X., Lu, Y., Zhou, S., Chen, L., Xu, B., 2016. Impact of climate change on human infectious diseases: Empirical evidence and human adaptation. *Environ. Int.* 86, 14-23.
- Xiaozhen, F., Boa, L., Aijun, G., 2005. Dynamics of solar light photodegradation behavior of atrazine on soil surface. *J. Hazard. Mater.* B117, 75-79.
- Zhang, L., Li, P., Gong, Z., Oni, A., 2006. Photochemical behavior of benzo[a]pyrene on soil surfaces under UV light irradiation. *J. Environ. Sci.* 18, 1226-1232.
- Zhang, L., Xua, C., Chena, Z., Li, X., Li, P., 2010. Photodegradation of pyrene on soil surfaces under UV light irradiation. *J. Hazard. Mater.* 173, 168-172.
- Zhao, X., Quan, X., Zhao, Y., Zhao, H., Chen, S., Chen, J., 2004. Photocatalytic remediation of γ -HCH contaminated soil induced by α -Fe₂O₃ and TiO₂. *J. Environ. Sci.* 16, 938-941.

DISCUSSION CHAPTER 4

These results confirm that the expected increase of temperature and light intensity, resulting from climate change, will impact on the fate and behaviour of PAHs once they are deposited on surface soils. Exposure time, environmental parameters (e.g., temperature and light intensity), molecular weight of each hydrocarbon and soil texture were identified as the key parameters.

LMW PAHs were more quickly volatilized in both soils (Arenosol and fine-textured Regosol) with the increment of temperature and light intensity. Medium and high molecular weight PAHs showed higher photodegradation rates in Arenosol soil surface when the climate change scenario was set. Photodegradation rates were: phenanthrene (11.2 and 16%), anthracene (19.7 and 85.4%), benzo(*a*)pyrene (23 and 54.6%) and indeno(*123-cd*)pyrene (11.7 and 39.1%), as representative compounds, in the current and climate change scenario, respectively. In contrast, no difference was found in fine-textured soil, regardless the temperature and radiation increase.

As previously mentioned, metal oxides may act as photocatalysts of PAHs. Although we found that iron oxide is not the only responsible photocatalyzing PAHs degradation, it is evident photocatalysis occurs in Regosol soil, being probably caused by interactions of different soil components. Thus, a possible explanation for the enhancement of PAHs photodegradation in Arenosol soil in the climate change scenario could be its lower content of photocatalysts, which eventually result in a higher activation energy requirement. This is, they require higher temperature and light intensity to be photodegraded. On the other hand, PAHs photodegradation in fine-textured soil was not temperature - and light - dependent, possibly because of the higher content of metal oxides in this soil. Hence, a higher temperature and light intensity (climate change scenario) does not mean a higher photodegradation of PAHs, since the required activation energy was already achieved in the B scenario.

The hydrogen isotope results confirmed that benzo(*a*)pyrene was degraded in a CC scenario, as it occurred in the B scenario, under light and in the darkness. Therefore, the degradation of benzo(*a*)pyrene without light intervention requires additional investigations, since it could be a potentially relevant pathway of PAH loss in soil.

The increase of temperature and light intensity clearly enhanced the formation of by-products, in terms of required energy and number of by-products, in both soils. Some of the identified by-products are known to own a higher toxicity than their parent PAHs.

Despite PAHs have shown sensitivity to temperature and light exposure at laboratory scale, it is evident that intensity of solar radiation is, by far, higher. Consequently, lab-scale results might be underestimating photodegradation rates occurring in the environment. To solve this gap, a field experiment was conducted using the same design but assuming the occurrence of other degradation processes like biodegradation.

CHAPTER 5

Solar radiation as a swift pathway for PAH photodegradation: A field study

Montse Marquès ^{a,b}, Montse Mari ^{a,b}, Jordi Sierra ^c,

Martí Nadal ^a, José L. Domingo ^a

^a Laboratory of Toxicology and Environmental Health, School of Medicine, IISPV, Universitat Rovira i Virgili, Sant Llorenç 21, 43201 Reus, Catalonia, Spain.

^b Environmental Engineering Laboratory, Departament d'Enginyeria Química, Universitat Rovira i Virgili, Av. Països Catalans 26, 43007 Tarragona, Catalonia, Spain.

^c Laboratory of Soil Science, Faculty of Pharmacy, Universitat de Barcelona, Av. Joan XXIII s/n, 08028 Barcelona, Catalonia, Spain.

Science of the Total Environment. 581–582 (2017) 530–540.

ABSTRACT

The photodegradation of polycyclic aromatic hydrocarbons (PAHs) may be an important degradation pathway of PAHs in regions with a high solar radiation. The present investigation was aimed at studying the photodegradation of PAHs after their deposition on surface soils with different textures. Photodegradation by-products were also identified and semi-quantified, as well as correlated with the decrease of parent compounds. The experiment was performed by deploying soil samples spiked with a mixture of the 16 US EPA priority PAHs in a methacrylate box, exposed to solar radiation for 7 days, meaning a solar energy of 102.6 MJ m^{-2} . As hypothesized, the individual PAHs were volatilized, sorbed and/or photodegraded, depending on their physicochemical properties, as well as the soil characteristics. Low and medium molecular weight PAHs were more sorbed and photodegraded in fine-textured Regosol soil, while a higher volatilization was observed in the coarse-textured Arenosol soil. In contrast, high molecular weight PAHs were more photodegraded in Arenosol soil. Especially low half-lives were noted for anthracene and benzo(*a*)pyrene, agreeing with previous findings at laboratory scale. Nine by-products were identified, including oxy-, nitro- and hydro-PAHs, whose toxic and mutagenic potential might be higher than the 16 priority PAHs.

Keywords: Polycyclic aromatic hydrocarbons (PAHs), soil, solar radiation, photodegradation, by-products

INTRODUCTION

Polycyclic aromatic hydrocarbons (PAHs) form a group of over 200 different organic compounds with two or more fused aromatic rings (Domingo and Nadal, 2015). Since some PAHs have been classified as carcinogenic and teratogenic, this family of pollutants has reached a considerable international concern (Chen et al., 2016). PAHs may enter the environment from both natural (e.g., plant synthesis, organic matter diagenesis, and forest fires) and anthropogenic (e.g., industrial activities, residential heating, power generation, incineration, and traffic) sources (Nadal et al., 2009). Once released to the atmosphere, gas phase PAHs are able to travel long distances before their deposition. Because of their low solubility and hydrophobic nature, high molecular weight (HMW) PAHs tend to be sorbed to particulates, being also widely transported through atmospheric routes. Consequently, they may mean a hazard, not only to human populations living in urban areas, but also to natural ecosystems (Augusto et al., 2015; Hu et al., 2014; Hung et al., 2005; Nadal et al., 2011; Ohkouchi et al., 1999).

As organic molecules, PAHs may undergo various natural processes such as biodegradation, chemical transformation, and photolysis reactions (Jia et al., 2015). It has been suggested that the photolysis of PAHs on soil surfaces plays an important role in the environmental fate of these chemicals (EL-Saeid et al., 2015). Upon light irradiation, PAHs can absorb light energy to reach photo-excited states. Therefore, they react with molecular oxygen and coexisting chemicals to produce reactive oxygen species (ROS) and other reactive intermediates, such as oxygenated PAHs and free radicals (Fu et al., 2012).

The photodegradation of organic compounds in various environmental matrices has been largely studied, mostly for remediation purposes. One of the applications is the use of light lamps to remove antibiotics in water (Batchu et al., 2014; Ge et al., 2010; Pereira et al., 2007). Regarding PAHs, most photodegradation investigations have been performed at laboratory scale by means of artificial light (Gupta and Gupta, 2015; Marquès et al., 2016a; Marquès et al., 2016b; Zhang et al., 2008; Zhang et al., 2006; Zhang et al., 2010). Natural sunlight, whose intensity is notably higher than that emitted by laboratory lamps, has been used to study the photodegradation in air of different organic compounds such as organophosphate pesticides (Borrás et al.,

2015), aromatic compounds (Pereira et al., 2015), organochlorines (Vera et al., 2015), and herbicides (Muñoz et al., 2014). However, there is a gap in the knowledge of the natural photodegradation of PAHs in soils and other environmental matrices.

It has been hypothesized that PAHs photodegradation would be higher and faster under solar radiation than under lab-controlled light lamps. Consequently, PAHs by-products, which may be even more toxic than their parent compounds, can be more easily generated (Ras et al., 2009). The evaluation of PAHs degradation products is highly valuable to assess human health risks derived from exposure to such compounds, which are not considered so far by environmental regulations.

This study was aimed at assessing the photodegradation of the 16 US EPA priority PAHs under solar radiation in two types of soils frequently found in the Mediterranean region, as it naturally occurs. In addition, PAHs photodegradation by-products were identified and semi-quantified. The current results were finally compared to those obtained in a previous study performed at laboratory scale (Marquès et al., 2016a; Marquès et al., 2016b).

MATERIALS AND METHODS

Experiment design: photodegradation of PAHs

Details of soil characteristics, as well as contamination procedure, were recently reported (Marquès et al., 2016b). Briefly, two different soils were collected from the A horizon of remotes areas of Catalonia (NE of Spain): a) an acidic and coarse-textured Arenosol soil, with granitic origin, and b) a fine-textured Regosol soil, formed by sedimentary materials. Ten grams of air-dried soil were weighed and deployed in uncovered glass Petri dishes of 7 cm of diameter. Each soil sample was spiked with a solution containing the 16 US EPA priority PAHs from Supelco® (Bellefonte, PA, USA) (naphthalene 99.3% purity, acenaphthylene 99.2% purity, acenaphthene 99.3% purity, fluorene 98.2% purity, phenanthrene 97.6% purity, anthracene 99.0% purity, fluoranthene 99.5% purity, pyrene 98.9% purity, benzo(*a*)anthracene 98.5% purity, chrysene 97.4% purity, benzo(*b*)fluoranthene 97.3% purity, benzo(*k*)fluoranthene 99.5% purity, benzo(*a*)pyrene 95.0% purity, dibenzo(*ah*)anthracene 99.0% purity, benzo(*ghi*)perylene 99.4% purity, and indeno(123-*cd*)pyrene 99.7% purity), leading to

an individual concentration of $2.5 \mu\text{g g}^{-1}$ of soil, and a $\Sigma 16$ PAHs concentration of $40 \mu\text{g g}^{-1}$ of soil.

The present study was carried out in a UV-light permeable methacrylate box placed on the roof of the School of Chemical Engineering, Universitat Rovira i Virgili, Tarragona (Catalonia, Spain). Although the methacrylate box protected the samples from the wind, it allowed the penetration of the whole light spectrum coming from solar radiation. The box owned eight holes of 2 cm of diameter, which facilitated the exchange of air and softened any temperature increase. The temperature inside the box was registered by using the temperature data logger EBI 300 (Ebro®, Ingolstadt, Germany) with 30 minutes of time-span. Once the samples were contaminated with PAHs, they were deployed inside the methacrylate box and exposed to sunlight. In addition to irradiated samples, dark controls were performed by covering half of samples with aluminum foil. The experiment was conducted during late boreal winter, from 8 to 15 March 2016. Triplicates of irradiated samples and dark controls of each soil were removed from the methacrylate box after the following exposure times: 0.5, 1, 2, 3, 6, 24, 48, 72, 96 and 168 hours. Simultaneously, environmental parameters such as precipitation, humidity and global solar irradiance were continuously monitored in a meteorological station located nearby (Constantí, Tarragona, Spain).

PAH extraction and analysis

The methodology for the extraction and analysis of PAHs in soils was previously reported (Marquès et al., 2016a). Briefly, 30 mL of hexane/dichloromethane (1:1) (Scharlau Chemie S. A., Barcelona, Spain) were added to soil samples. Then, each sample was 3-times subjected to an ultrasonic bath programmed for 10 min. After each step, the solvent was filtered. Subsequently, the extract was slowly concentrated with a rotatory evaporator down to 2 mL, and finally with a gentle stream of purified N_2 (99.9999%). In addition to irradiated and dark control samples, 10 g of soil free of PAHs were also extracted and used as blank soil samples. Analytes were quantified by using a gas chromatograph (Hewlett-Packard G1099A/MSD5973) coupled to a mass spectrometer (MSD5973). Separations were achieved on a DB-5 5% phenyl methyl siloxane column (60 m x 0.25 mm x 0.25 μm). A volume of 1 μL of sample was injected at 310°C in pulsed splitless mode, while the transfer line temperature was 280°C . The

initial column temperature was 90°C, being increased at a rate of 15°C min⁻¹ up to 200°C, and then at 6°C min⁻¹ until 325°C, being this temperature held for 20 min. Ultra-pure helium (99.9999%) was the carrier gas at a flow rate of 1.4 mLmin⁻¹. PAHs were quantified by means of a five-point calibration curve (20, 30, 50, 70, 80 µg mL⁻¹). In order to allow the identification of PAHs degradation products as a second step of the experiment, the mass spectrometer was set at full scan mode.

Quality control

To assess any potential loss, a mixture of 6 labeled hydrocarbons (d₄-1,4-dichlorobenzene (99.8% purity), d₈-naphthalene (96.3% purity), d₁₀-acenaphthene (99.8% purity), d₁₀-phenanthrene (99.3% purity), d₁₂-chrysene (98.8% purity), and d₁₂-perylene (99.5% purity)), provided by Supelco® (Bellefonte, PA, USA), was spiked to soil samples before extraction. In turn, two individual deuterated PAHs, also from Supelco® (d₁₀-fluorene (98.3% purity) and d₁₂-benzo(a)pyrene (98.5% purity)), were added to samples before GC-MS analyses.

Naphthalene and d₈-naphthalene were highly volatilized after being spiked in the soil, finding very low recoveries in both cases. Therefore, the results of naphthalene were not included and further investigated. The recoveries of the remaining PAHs ranged 54-106% and 76-117% in Arenosol and fine-textured Regosol soil, respectively. A complete list including recoveries of each hydrocarbon in both soils is summarized in Annex 4 (Table S1).

Identification of PAHs degradation products

Potential PAHs by-products, generated as a consequence of soil exposure to solar radiation, were identified by using the MS library search NIST 11 (Scientific Instrument Services, Inc., Ringoes, NJ, USA). Based on the similarity of their mass spectra with those in the library, only compounds fitting with a high probability (>90%) were confirmed. Afterwards, identified compounds were semi-quantified by considering peak areas of the degradation product divided by the peak area of the corresponding internal standard (A/AI). In addition, the correlations between their formation and the degradation of their parent compounds were graphically assessed. Finally, kinetics of

PAHs by-products were plotted, including corresponding equations and coefficients of determination, when each relative peak area was statistically different from others (Fig. 1).

Statistical analysis

XLSTAT Statistical Software for Excel was used to evaluate statistically the results. Significant differences in the changes of PAH levels with time were assessed by comparing results for irradiated and non-irradiated samples, applying a repeated analysis of variance (ANOVA). In addition, the same statistics test was performed to assess significant differences between by-products relative peak areas. Probability levels were considered as statistically significant at $p < 0.05$.

RESULTS AND DISCUSSION

Meteorological data

The average air temperature inside the box throughout the whole experiment was 14.4°C , with values ranging from 1.5 to 40.6°C . The mean global solar energy was 0.6 MJ m^{-2} , showing maximum irradiance peaks of 1.4 MJ m^{-2} . As expected, there was some correlation between temperature and solar irradiance. Temperature versus irradiance and environmental humidity versus precipitation are shown in Annex 4 (Fig. S1 and Fig. S2, respectively). The solar energy doses over the experiment, associated to an exposure time of 0.5, 1, 2, 3, 6, 24, 48, 72, 96 and 168 hours, were 2.7, 4.1, 6.7, 8.6, 10.1, 12.4, 28.3, 47.9, 67.9 and 102.6 MJ m^{-2} , respectively. In consequence, the total solar energy to which PAHs were exposed at the end of the experiment was 102.6 MJ m^{-2} .

PAH photodegradation and half-lives

The photodegradation (%) was estimated by considering the impact of the sunlight exposure, as a difference between irradiated samples and dark controls when they were statistically different. In contrast, the half-life indicates the loss speed of a chemical exposed to solar radiation as well as to other co-occurring processes, such as volatilization, sorption or unknown degradation processes. The experiment was


performed with dried soils. Consequently, the availability of water was scarce. However, since the experiment was conducted in the field, it cannot be disregarded that the increase of environmental humidity might have induced other degradation processes, such as the biological oxidation of PAHs. Nevertheless, such process is not light-dependent and it may occur under the sunlight or in the darkness.

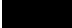
Photodegradation (%) and half-lives of the 16 PAHs at three representative exposure times (24 h, 48 h, 168 h) and solar energy doses (12.4 MJ m^{-2} , 47.9 MJ m^{-2} and 102.6 MJ m^{-2}), are summarized in Table 1. Details on the concentration trends of 16 PAHs in irradiated samples and dark controls are provided as Annex 4 (Fig. S3). The photodegradation (%) of acenaphthylene, anthracene, pyrene, benzo(*a*)pyrene and benzo(*ghi*)perylene, as representatives of different molecular weight PAHs, in Arenosol and fine-textured Regosol soils, are depicted in Fig. 1. The kinetics were calculated only when photodegradation (%) showed statistical differences over time. In Arenosol soil, the photodegradation of anthracene, pyrene, benzo(*a*)pyrene and benzo(*ghi*)perylene was clearly adjusted to lineal kinetics, showing R^2 of 0.74, 0.91, 0.73 and 0.91, respectively. By contrast, in fine-textured Regosol soil, only acenaphthylene was able to be adjusted to exponential trend with an acceptable R^2 (0.73).

Three main processes are related to the fate of PAHs on surface soils: volatilization, sorption, and photodegradation (Marquès et al., 2016a; Marquès et al., 2016b). Their importance depends not only on the physicochemical properties of each hydrocarbon, but also on the soil texture. Volatilization was the most important process for low molecular weight (LMW) PAHs, whose initial levels were low and followed a decreasing tendency in both sets of samples, under light and in the darkness. It suggests that volatilization of LMW PAHs is the key process leading to a reduction of concentration. On the other hand, photodegradation was more remarkable for medium molecular weight (MMW) and high molecular weight (HMW) PAHs. LMW and MMW PAHs tended to undergo a higher photodegradation in fine-textured Regosol soil than in Arenosol soil. In contrast, HMW compounds (4-, 5-, and 6- ringed PAHs) were more easily photodegraded in Arenosol soil, with percentages up to 70%. In addition, photodegradation trends of PAHs found in Arenosol soil were still increasing at the end of the experiment, while in fine-textured soil the maximum

Table 1. Photodegradation and half-lives of PAHs under study in Arenosol and fine-textured Regosol soil.

	Arenosol soil				Fine-textured Regosol soil			
	Photodegradation (%)			Half-life (days)	Photodegradation (%)			Half-life (days)
Exposure time (h)	24	72	168		24	72	168	
Solar energy ($MJ m^{-2}$)	12.4	47.9	102.6		12.4	47.9	102.6	
Acenaphthylene	50.0 ± 1.7			0.3 ± 0.05	63.7 ± 6.3		0.5 ± 0.1	
Acenaphthene		63.6 ± 18.2		0.9 ± 0.2	48.6 ± 14.8	54.7 ± 11.5	0.9 ± 0.2	
Fluorene		44.4 ± 1.7	45.6 ± 8.2	2.9 ± 0.3		52.0 ± 15.5	61.0 ± 9.8	
Phenanthrene			34.6 ± 2.2	8.7 ± 1.4		37.1 ± 5.3	38.0 ± 2.4	
Anthracene	22.6 ± 4.7	45.2 ± 3.9	60.8 ± 9.1	1.9 ± 0.3	48.3 ± 14.3	57.3 ± 3.3	57.3 ± 6.5	
Fluoranthene		10.3 ± 3.6	38.3 ± 2.7	4.5 ± 0.5		33.5 ± 18.2	53.7 ± 11.0	
Pyrene		48.0 ± 7.2	61.1 ± 3.7	5.4 ± 2.0		29.3 ± 13.2	39.5 ± 6.8	
Benzo(a)anthracene		41.6 ± 5.6	50.3 ± 3.5	7.8 ± 4.9		34.9 ± 6.5	33.7 ± 6.6	
Chrysene		36.2 ± 5.5	45.5 ± 6.1	8.7 ± 1.1		9.6 ± 1.0	13.5 ± 6.0	
Benzo(b)fluoranthene			26.8 ± 1.9	17.2 ± 4.2		20.2 ± 1.8	22.4 ± 6.6	
Benzo(k)fluoranthene				15.9 ± 2.1		20.7 ± 0.6	26.4 ± 7.5	
Benzo(a)pyrene	35.2 ± 8.1	60.9 ± 1.3	69.7 ± 3.3	2.9 ± 0.1	28.6 ± 8.9	32.6 ± 9.7	32.7 ± 4.2	
Benzo(ghi)perylene		21.8 ± 3.2	33.7 ± 3.4	3.1 ± 0.4		28.6 ± 9.4	23.0 ± 5.7	
Dibenzo(ah)anthracene		25.8 ± 2.8	38.6 ± 2.3	8.3 ± 0.2		23.3 ± 3.6	21.7 ± 5.5	
Indeno(123-cd)perylene		31.7 ± 3.0	37.8 ± 1.4	5.4 ± 0.2		26.5 ± 3.5	26.8 ± 5.0	

 No significant differences between irradiated samples and dark controls ($p > 0.05$).

 Concentration of irradiated sample < limit of quantification (loq).

level was generally reached with 47.9 MJ m⁻² of solar energy dose (72h of exposure in the present experiment) (Table 1 and Fig. 1). Consequently, most compounds presented lower half-lives in Arenosol soil, regardless their final percentage of photodegradation.

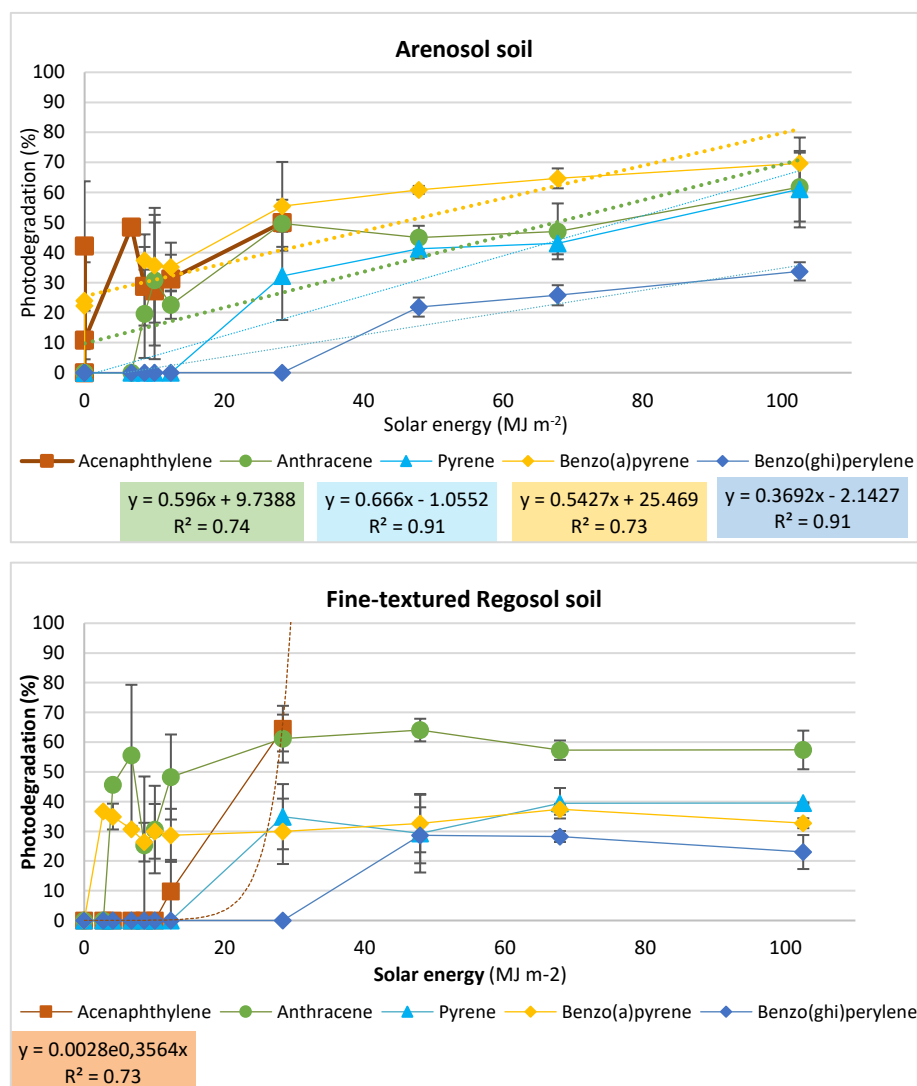


Fig. 1. Photodegradation trends of acenaphthylene, anthracene, pyrene, benzo(a)pyrene and benzo(ghi)perylene in Arenosol soil (above) and fine-textured Regosol soil (below). Bars indicate standard deviations between photodegradation calculated in three pairs of samples (irradiated samples and dark controls).

*Photodegradation was not calculated when statistical differences between irradiated samples and dark controls were found, which was pointed out as 0 in the present Fig. ** Kinetics were adjusted only when statistical differences between the first and the last photodegradation value were found.

The concentrations of acenaphthylene and acenaphthene dramatically decreased after soil contamination, as a consequence of the important role of volatilization for the loss of those PAHs. However, differences between irradiated and dark control samples indicated the impact of sunlight exposure, suggesting that photodegradation also occurred. In Arenosol soil, acenaphthylene and acenaphthene under solar radiation could not be detected when the solar energy was low (28.3 and 67.9 MJ m⁻², respectively), leading to a final photodegradation of 50% and 64%, respectively (half-lives: 7.2 and 21.6h, respectively). In turn, the decrease of these PAHs in fine-textured Regosol soil was softer, being both above the limit of detection of 47.9 MJ m⁻² (72h of exposure). Since Regosol soils own a fine texture, they have an enhanced capacity to adsorb chemicals. The differences of PAH loss between irradiated and dark control samples, led to a similar accumulated photodegradation (64% and 55% for acenaphthylene and acenaphthene, respectively).

Despite phenanthrene, fluoranthene, benzo(*ghi*)perylene, dibenzo(*ah*)anthracene and indeno(*123-cd*)perylene own a different number of aromatic rings, they behaved similarly in Arenosol soil. Their photodegradation at the end of the experiment ranged between 34% and 39% (half-lives: 3.1 – 8.7 days). Benzo(*a*)anthracene and chrysene showed a final photodegradation of 50% and 45%, and half-lives of 7.8 and 8.7 days, respectively, in Arenosol soil. Similarly, fluoranthene in fine-textured Regosol soil presented a photodegradation of 53.7% and a half-life of 9.9 days. In contrast, chrysene was more resistant to solar radiation, showing only a slight photodegradation (13%) and high half-life (11.2 days) under the maximum solar energy dose (102.6 MJ m⁻²).

As isomer compounds, benzo(*b*)fluoranthene and benzo(*k*)fluoranthene presented half-lives of 17.2 and 15.9 days, being the most resistant PAHs to be photodegraded in Arenosol soil. However, benzo(*b*)fluoranthene levels of irradiated samples and dark controls were only significantly different at the end of the experiment. In turn, benzo(*k*)fluoranthene in irradiated samples and dark controls were not statistically different during the whole experiment ($p > 0.05$), and consequently, photodegradation did not take place.

The remaining PAHs showed a similar degree of photodegradation in fine-textured Regosol soil, with a slight decrease of the photodegradation percentage

when the molecular weight increased. Benzo(*a*)anthracene underwent photodegradation of 34% at the end of the experiment, being the half-lives estimated in 6.6 days. In addition to this 4-ringed PAH, benzo(*b*)fluoranthene and benzo(*k*)fluoranthene presented 22% and 26% of photodegradation, respectively (half-lives: 8.4 and 9.2 days, respectively). Phenanthrene, together with chrysene, was the most resistant to photodegradation in this kind of soil, with half-lives around 13.0 days. Concentrations of those MMW and HMW PAHs in irradiated and non-irradiated samples showed significant differences ($p < 0.5$) at 28.3 MJ m^{-2} (48h of exposure). Finally, the photodegradation of dibenzo(*ah*)anthracene, indeno(*123-cd*)perylene and benzo(*ghi*)perylene ranged between 22% and 27% at the end of the experiment, without finding statistical differences when solar energy was below 47.9 MJ m^{-2} (72h of exposure). Unlike Arenosol soil, fine-textured Regosol soil might have sorbed HMW PAHs more easily. Because of the small particle size of these soils, light cannot penetrate, reducing the photodegradation of LMW and MMW PAHs.

Fluorene, anthracene, pyrene and benzo(*a*)pyrene, with 3, 4 and 5 aromatic rings, were the PAHs presenting the highest photodegradation. Fluorene was especially sensitive to solar exposure in fine-textured soil, showing a 60% of total photodegradation, although its half-life was not particularly low (7.4 days), and finding significant differences between samples and controls ($p < 0.05$) with a solar energy dose higher than 28.3 MJ m^{-2} (48h of exposure). In turn, fluorene in Arenosol soil experienced a slightly lower total photodegradation (46%) as well as lower half-life (2.9 days), while statistical differences were noted slightly later (47.9 MJ m^{-2} ; 72h of exposure). Anthracene showed a final photodegradation and half-lives of 61% and 1.9 days, in Arenosol, while it was up to 54% and 2.6 days in fine-textured Regosol soils, showing significant differences between samples and controls when reached a solar energy impact of 6.7 MJ m^{-2} and 4.9 MJ m^{-2} , respectively, at a short exposure time (2h and 1h, respectively). In Arenosol soil, the concentration of fluorene and anthracene dramatically decreased over the time, not only in soils subjected to solar radiation, but also those in the darkness. In addition to volatilization, other degradation processes could be occurring in dark controls. On the other hand, in fine-textured Regosol soil, fluorene and anthracene probably experienced fewer changes in the darkness, as the concentrations of these compounds were constant with time. Pyrene

showed 61% of final photodegradation in Arenosol soil, while it was found to be 39% in fine-textured soil. However, half-lives were not extremely low, being 5 and 7 days, respectively, and significant differences between irradiated and non-irradiated samples were noted with 28.3 MJ m^{-2} of solar energy dose (48h of exposure in the present study). In turn, benzo(*a*)pyrene was the highest photodegraded PAHs in Arenosol soil (70%), being 2-times the photodegradation speed observed in fine-textured Regosol soil (33%) at the end of the experiment. Moreover, minor differences were noted in the estimated half-lives (2.9 and 2.3 days, respectively). The levels of benzo(*a*)pyrene, as it occurred with fluorene and anthracene in Arenosol soil, remarkably decreased with time in all soils, both under solar radiation and in the darkness, which was probably due to simultaneously unknown degradation processes occurring without light condition. However, only a solar energy dose of 2.7 MJ m^{-2} was required to show statistically significant differences between benzo(*a*)pyrene in irradiated samples and dark controls, which means after half an hour of exposure in the present field study.

Finally, the high sensitivity of anthracene, pyrene and benzo(*a*)pyrene to solar radiation could be somehow related to the use of these PAHs to estimate molecular diagnostic ratios (MDRs) as a function of distance. After travelling long distances, anthracene/(anthracene+phenanthrene) is halved while benzo(*a*)pyrene/benzo(*ghi*)perylene and fluoranthene/(fluoranthene+pyrene) are doubled (Katsoyiannis and Breivik, 2014).

Comparing results: lab scale vs. field study

The photodegradation of PAHs has been widely studied at laboratory scale by means of natural or UV light lamps (Gupta and B, 2015; Marquès et al., 2016a; Marquès et al., 2016b; Zhang et al., 2008b; Zhang et al., 2010; Zhang et al., 2006b). Recently, we performed a similar experiment with soils subjected to artificial light in a climate chamber (Marquès et al., 2016a), considering various climate scenarios in terms of temperature (20°C and 24°C), light intensity (9.6 and 24 W m^{-2}) and energy dose (0.48 and 1.21 MJ m^{-2}). The results of the current study indicate that PAH photodegradation is higher and quicker in the field than in lab-controlled tests, showing all the chemicals a shorter half-life (Fig. 2). In the laboratory, LMW PAHs were

only volatilized. By contrast, in natural conditions, not only volatilization, but also photodegradation could be detected as relevant degradation pathways. Half-lives of MMW and HMW PAHs ranged between 3 and 80 days in soils exposed to artificial light exposure. In turn, in the field experiment, they were remarkably lower, with half-life values from 7 hours to 18 days.

Despite the photodegradation speed was more important in the field, concentration trends of the individual PAHs were similar in the lab and in the field. Especially low half-lives of anthracene and benzo(*a*)pyrene were found, resulting from their sensitivity to light exposure and also other co-occurring degradation processes. Moreover, benzo(*a*)anthracene, chrysene, benzo(*b*)fluoranthene and dibenzo(*ah*)anthracene were among the most resistant to photodegradation in both tested soils.

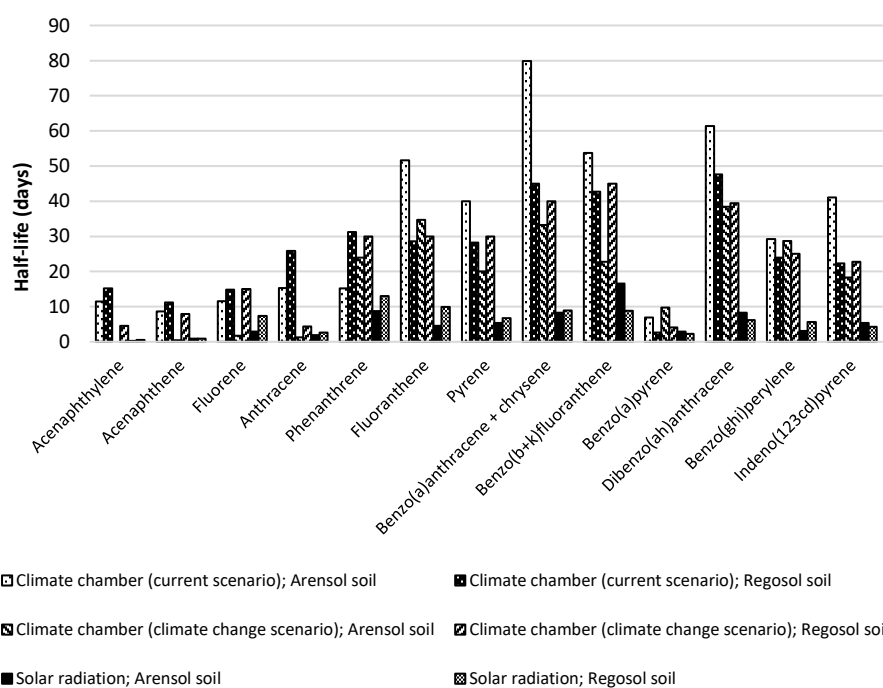


Fig. 2. Comparison between half-lives of PAHs when simulating different climate scenarios at lab scale (adapted from chapter 4) and the current experiment in the field, for both tested soils.

With respect to differences between soils, the higher content of iron, manganese and aluminum oxides in fine-textured Regosol soil, was pointed out as a key factor

when both temperature and radiation are low, as these photocatalysts enhance photodegradation reactions (Marquès et al., 2016b). In contrast, they had a very minor role when temperature and light intensity were increased (Marquès et al., 2016a). As expected, a similar pattern was found in the field experiment. Thus, the content of oxides in Regosol soil did not lead to an enhancement of PAH photodegradation. As above-mentioned, the coarse-texture of Arenosol soil facilitates a higher light penetration, leading to a higher photodegradation.

Identification of PAHs by-products

The occurrence of PAH degradation by-products in irradiated samples and dark controls was also investigated. However, potential by-products either generated under radiation or in the darkness, were not here considered, being focused on by-products formed only when solar radiation is present. Fig. 3 shows a number of potential degradation pathways due to degradation of PAHs in soil samples exposed to solar radiation. Up to 9 PAH degradation compounds were detected in the samples exposed to a solar energy dose of 102.6 MJ m^{-2} (7 days of solar exposure in the present study). Table 2 shows a list of identified by-products, CAS number, match with NIST library, retention time, diagnostic ions and relative peak areas over the experiment. In addition, relative peak areas of PAHs by-products and corresponding native PAHs, including kinetics (equation and coefficient of determination) are depicted in Fig 4. A number of aldehydes, oxy- PAHs, hydro-PAHs and nitro-PAHs were formed. Five of them were already identified in our previous study performed at lab scale (Marquès et al., 2016a). Nevertheless, they were more quickly generated under solar radiation. Moreover, degradation reactions stepped forward by causing the formation of new nitro- and hydro-PAHs.

Oxidation reactions are viewed as the most effective in chemical degradation (Ukiwe et al. 2013). However, some authors have suggested that photochemical reactions may also aid oxidative reaction processes. The most oxidation reactions in the environment are initiated by oxidants such as peroxides (H_2O_2), ozone (O_3) and hydroxyl radicals generated by photochemical processes. Ozone may attack double bonds directly or it can form reactive hydroxyl radicals (which attack double bonds) by decomposing water. The reaction proceeds with complex pathways producing

numerous intermediates. In agreement to our findings, the final reaction products include a mixture of ketones, quinones, aldehydes, phenols and carboxylic acids for both oxidants.

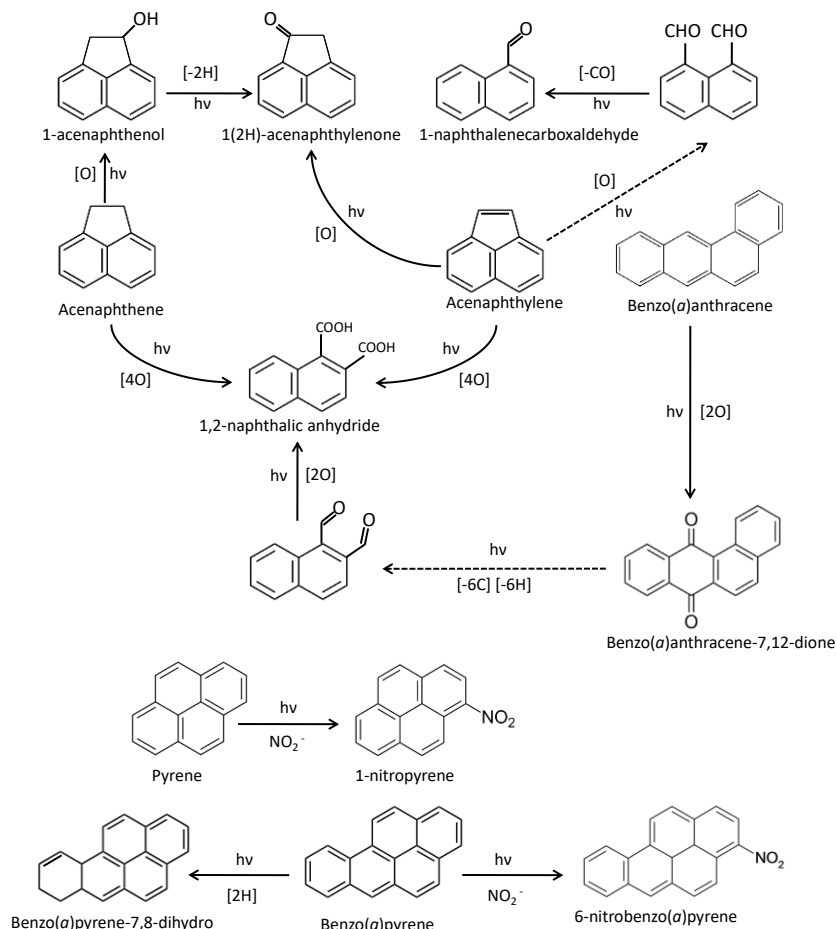
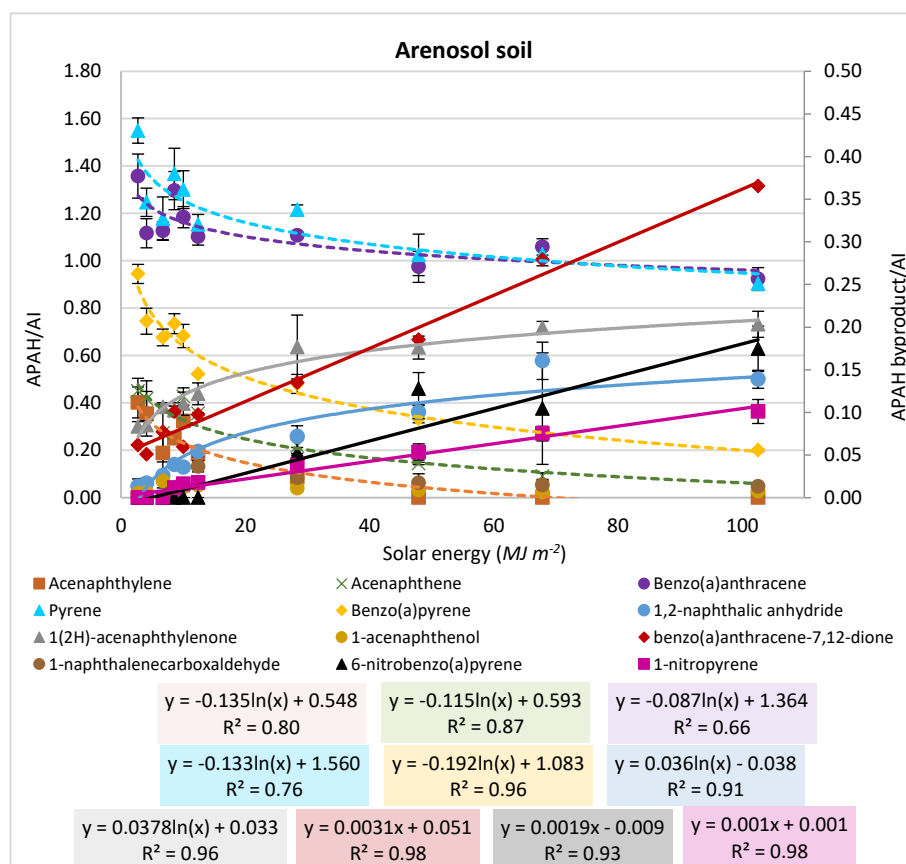


Fig. 3. Potential degradation pathways due to degradation of PAHs in soil samples exposed to solar radiation. *Dashed arrow drives to a non-detected intermediate although its presence is necessary for the formation of the following by-product.

Benzo(a)anthracene-7,12-dione, 1-acenaphthenol and 1-naphthalenecarboxaldehyde were formed with a solar energy dose of 2.7 MJ m^{-2} in Arenosol and fine-textured Regosol soil. It would be linked to the degradation of benzo(a)anthracene, acenaphthene and acenaphthylene, respectively (Cajthaml et al., 2006; Marquès et al., 2016a; Riva et al., 2016; Woo et al., 2009). There was a clear relationship between the degradation of benzo(a)anthracene and the formation of its

by-product, benzo(*a*)anthracene-7,12-dione, in both soils. Benzo(*a*)anthracene-7,12-dione trend was adjusted to a lineal kinetics ($R^2 = 0.98$ and $R^2 = 0.95$ in Arenosol and fine-textured Regosol soil, respectively). In contrast, any relationship could be found between the formation of 1-naphthalenecarboxaldehyde and the degradation of acenaphthylene in Arenosol soil. Although in fine-textured Regosol soil, 1-naphthalenecarboxaldehyde was poorly detected, a relative quantification could not be done.



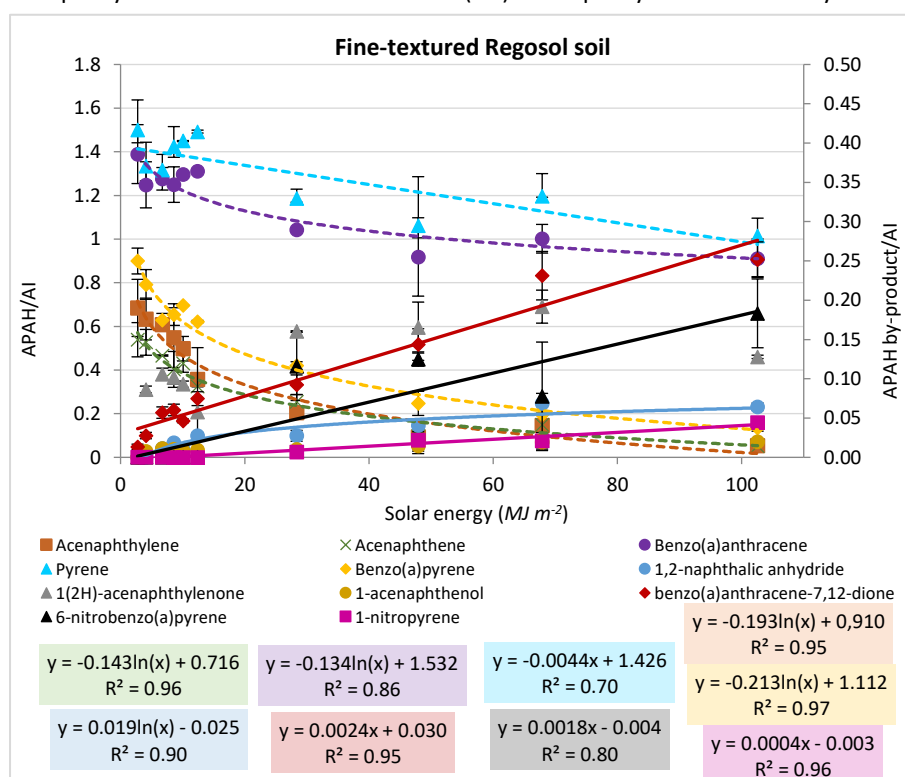
A/AI: the area response of each compound relative to an internal standard.

Fig. 4. PAHs concentrations vs corresponding by-products trends in soils under study.

A clear inverse correlation in the concentrations of 1-acenaphthenol and acenaphthene was noted in fine-textured Regosol soil. Acenaphthene decreased, while 1-acenaphthenol increased throughout the whole experiment. In Arenosol

soil, 1-acenaphthenol was firstly formed, and then its concentration slightly decreased and finally it was kept constant, probably due to soil dynamics. In this case, soil textures might be playing a key role. The coarse texture may enhance the light penetration, facilitating a quicker formation of 1-acenaphthenol in Arenosol soil. However, the texture and the low organic matter content of this soil do not allow the sorption of this by-product, favoring its volatilization and degradation.

Similarly, 1(2H)-acenaphthylene was generated as a consequence of acenaphthylene and 1-acenaphthenol oxidation (Ghosal et al., 2016; Woo et al., 2009). Again, generation processes depended on soil texture. 1(2H)-acenaphthylene was formed with 2.7 MJ m⁻² of solar energy in Arenosol soil (half an hour of exposure), while almost the double of solar dose (4.1 MJ m⁻²) was required in fine-textured Regosol soil. Correlations between the degradation of the acenaphthylene and the formation of the 1(2H)-acenaphthylene were very clear in



A/AI: the area response of each compound relative to an internal standard.

Fig. 4. (Continuation) PAHs concentrations vs corresponding by-products trends in soils under study.

Arenosol soil, being adjusted to logarithmical kinetics ($R^2= 0.96$). By contrast, its trend is not clear in fine-textured Regosol soil since statistical differences over the experiment were not found. 1,2-naphthalic anhydride was formed after half an hour (2.7 MJ m^{-2}) and two hours (6.7 MJ m^{-2}) of exposure, in Arenosol and fine-textured Regosol soil, respectively. Potential precursors may be acenaphthylene, acenaphthene and benzo(*a*)anthracene-7,12-dione (Cajthaml et al., 2006; Marquès et al., 2016a; Zhou and Wenger, 2013), and it showed a logarithmical increasing trend in both soils ($R^2= 0.91$ and $R^2= 0.90$ in Arenosol and fine-textured Regosol soil, respectively).

At the end of the experiment, after soils had been exposed to a solar energy dose of 102.6 MJ m^{-2} , benzo(*a*)pyrene-7,8-dihydro was detected in Arenosol soil, being likely generated after the degradation of benzo(*a*)pyrene. As the experiment lasted only 7 days, no more information could be retrieved regarding the fate of benzo(*a*)pyrene-7,8-dihydro in soils.

With respect to nitro-PAHs, 1-nitropyrene and 6-nitrobenzo(*a*)pyrene were detected in both soils. 1-nitropyrene was generated after only 3 h of exposure (8.6 MJ m^{-2}) in Arenosol soil, while 6-nitrobenzo(*a*)pyrene was formed with 28.3 MJ m^{-2} of solar energy dose (48h of exposure in the present study). It was on that exposure time and solar energy dose when 1-nitropyrene and 6-nitrobenzo(*a*)pyrene were formed in fine-textured Regosol soil. Both nitro-PAHs experienced a lineal kinetics increase, showing relatively good R^2 values in both soils (0.98 and 0.96 for 1-nitropyrene, and 0.93 and 0.80 for 6-nitrobenzo(*a*)pyrene, in Arenosol and fine-textured Regosol soil, respectively). The formation of nitrated and oxygenated derivatives may occur through photo-reactions of PAHs with oxidative species such as ozone, hydroxyl and nitrate radicals, under UV radiation (Walgraeve et al., 2010; Zhang et al., 2011). In addition, the presence of NO_x radicals in soils can accelerate the formation of nitro-PAHs (Pham et al., 2015), by reacting with pyrene and benzo(*a*)pyrene. Sugiyama et al. (2001) demonstrated that nitrite (NO_2^-) and nitrate (NO_3^-) ions are sources of nitrated pyrenes in the presence of metallic oxides, which act as photocatalysts. Both tested soils contained nitrates, aluminum, iron and manganese oxides (Marquès et al., 2016b), which could have a key role on the formation of nitro-PAHs. Nitro-PAHs

Table 2. By-product names, CAS number, match with NIST library (method of identification), retention time, diagnostic ions and relative abundance of the peaks at an exposure time and solar energy dose.

	By product name	CAS number	Match with NIST library (%) ^a	Retention time (min) ^a	Diagnostic ions	Relative response area (A/AI) ^{b,c}										
						Time (h)										
						0	0.5	1	2	3	6	24	48	72	96	168
						Solar energy (MJ m ⁻²)										
0	2.7	4.1	6.7	8.6	10.1	12.4	28.3	47.9	67.9	102.6						
Arenosol	1(2H)-Acenaphthyleneone	2235-15-6	92	11.139	168 140 113	nd	0.08 ± 0.01	0.08 ± 0.01	0.11 ± 0.005	0.10 ± 0.005	0.11 ± 0.01	0.12 ± 0.01	0.18 ± 0.04	0.18 ± 0.01	0.20 ± 0.01	0.20 ± 0.02
	1-acenaphthenol	6306-07-6	96	11.190	169 141 115	nd	0.01 ± 0.001	0.01 ± 0.003	0.02 ± 0.01	0.01 ± 0.003	0.01 ± 0.01	0.01 ± 0.004	0.01 ± 0.003	0.01 ± 0.001	0.01 ± 0.0003	0.01 ± 0.001
	1-Naphthalenecarboxaldehyde	66-99-9	90	14.160	184 155 127	nd	nd	nd	nd	0.01 ± 0.01	0.01 ± 0.01	0.04 ± 0.01	0.02 ± 0.004	0.02 ± 0.01	0.01 ± 0.01	0.01 ± 0.003
	1,2-naphthalic anhydride	81-84-5	93	16.605	198 154 126	nd	0.01 ± 0.01	0.02 ± 0.01	0.03 ± 0.002	0.04 ± 0.004	0.04 ± 0.005	0.05 ± 0.01	0.07 ± 0.01	0.10 ± 0.01	0.16 ± 0.02	0.14 ± 0.01
	Benzo(a)pyrene-7,8-dihydro	17573-23-8	91	19.261	254 239 126	nd	nd	nd	nd	nd	nd	nd	nd	nd	nd	0.03 ± 0.03
	Benzo(a)anthracene-7,12-dione	2498-66-0	92	26.391	258 230 202	nd	0.06 ± 0.003	0.05 ± 0.003	0.08 ± 0.01	0.10 ± 0.003	0.06 ± 0.04	0.10 ± 0.01	0.13 ± 0.03	0.19 ± 0.003	0.28 ± 0.04	0.37 ± 0.03
	1-nitropyrene	5522-43-0	96	26.705	247 201 100	nd	nd	nd	nd	0.01 ± 0.004	0.02 ± 0.002	0.02 ± 0.002	0.04 ± 0.01	0.05 ± 0.01	0.08 ± 0.01	0.10 ± 0.01
	6-nitrobenzo(a)pyrene	63041-90-7	90	36.984	297 267 239	nd	nd	nd	nd	nd	nd	nd	0.05 ± 0.02	0.13 ± 0.02	0.10 ± 0.07	0.17 ± 0.03
Regosol	1(2H)-Acenaphthyleneone	2235-15-6	91	11.147	168 140 113	nd	nd	0.09 ± 0.004	0.11 ± 0.01	0.10 ± 0.01	0.09 ± 0.004	0.06 ± 0.08	0.16 ± 0.001	0.17 ± 0.03	0.19 ± 0.02	0.13 ± 0.002
	1-acenaphthenol	6306-07-6	95	11.189	169 141 115	nd	nd	0.01 ± 0.003	0.01 ± 0.002	0.01 ± 0.001	0.01 ± 0.001	0.01 ± 0.002	0.01 ± 0.004	0.01 ± 0.002	0.02 ± 0.004	0.02 ± 0.003
	1,2-naphthalic anhydride	81-84-5	96	16.579	198 154 126	nd	nd	nd	0.01 ± 2E-5	0.02 ± 0.002	0.01 ± 0.002	0.03 ± 0.004	0.03 ± 0.01	0.04 ± 0.01	0.07 ± 0.01	0.06 ± 0.005
	Benzo(a)anthracene-7,12-dione	2498-66-0	98	26.391	258 230 202	nd	0.01 ± 0.003	0.03 ± 0.004	0.06 ± 0.01	0.06 ± 0.01	0.05 ± 0.002	0.07 ± 0.01	0.09 ± 0.01	0.14 ± 0.02	0.23 ± 0.03	0.25 ± 0.02
	1-nitropyrene	5522-43-0	98	26.705	247 201 100	nd	nd	nd	nd	nd	nd	nd	0.01 ± 0.01	0.02 ± 0.001	0.02 ± 0.01	0.04 ± 0.005
	6-nitrobenzo(a)pyrene	63041-90-7	90	36.984	297 267 239	nd	nd	nd	nd	nd	nd	nd	0.12 ± 0.04	0.13 ± 0.01	0.08 ± 0.07	0.18 ± 0.04

^aAverage of all samples; ^bA/AI: the area response of each compound relative to an internal standard; ^cAverage of three replicates; nd: non-detected.

generally exhibit higher mutagenicity and carcinogenicity than their parent PAHs showing toxic effects for human health (Kameda, 2011; Nascimento et al., 2015). Some nitro-PAHs act directly as mutagens and carcinogens on living organisms. In mammals, these chemicals may have a strong genotoxic potential, being similar to or even higher than that of benzo(*a*)pyrene (Busby et al., 1988; Onduka et al., 2015; Wislocki et al., 1986). 1-nitropyrene has been pointed out as a mutagenic substance in many bacterial and mammalian assay systems, as well as tumorigenic in experimentation animals (Hirose et al., 1984; McGregor et al., 1994; Rosenkranz and Mermelstein, 1983; Rosenkranz and Mermelstein, 1985; Watt et al., 2007). In general terms, HMW nitro-PAHs tend to be resistant to photodegradation, partly due to their strong adsorption to soil organic matter, low solubility, large molecular size and polar character of the nitro group (Kielhorn et al., 2003). In addition, 6-nitrobenzo(*a*)pyrene has been found as a potential NO donor due to its low stability, inducing DNA strand breaks upon photoirradiation (Fukuhara et al., 2001).

Oxy-PAHs show a relatively high persistence, being usually formed in the practice of remediation of PAH contaminated soils. Because of their polarity, oxy-PAHs are more mobile in the environment than PAHs, showing a high tendency to spread from contaminated sites via surface water and groundwater (Lundstedt et al., 2007). Furthermore, they are also very bioavailable compounds (Arp et al., 2014). Benzo(*a*)anthracene-7,12-dione induces similar or more elevated genotoxic responses than their respective parent PAHs (Dasgupta et al., 2014; Gurbani et al., 2013). Its DNA damage is in fact comparable to that produced by a well-known environmental mutagen, benzo(*a*)pyrene, in fish embryos (Dasgupta et al., 2014).

Because of the lack of regulations and standardized methods for their analysis, oxy- and nitro-PAHs are seldom included in monitoring and risk assessment programs (Lundstedt et al., 2014). However, recent investigations on some of these by-products have provided valuable information on their environmental occurrence and human toxicity (Jörundsdóttir et al., 2014; Pinto et al., 2014; Qiao et al., 2014). Therefore, environmental and health risks associated to exposure to these by-products is evident. Since there is a gap on the environmental regulation of PAHs, it has been recently suggested that the original list of 16 US EPA priority PAHs should be enlarged by including, at least, 10 oxy-PAHs, 10 nitro-PAHs and 6 amino-PAHs

(Andersson and Achten, 2015). Some of these PAH derivatives have been here identified as photodegradation by-products. Anyhow, further investigations on their fate and behavior should be conducted, paying especial attention to chemicals whose parent compounds are not only toxic, but also very photosensitive, like benzo(*a*)pyrene.

CONCLUSIONS

Although environmental parameters are continuously changing in the field, our results demonstrate the real high degree of PAHs photodegradation occurring in the field during the late boreal winter, being their half-lives considerably shorter than ones usually reported at lab scale. Thus, solar radiation exposure has been found to be an important pathway for PAHs loss as well as by-products formation.

LMW PAHs tended to leave quickly the soil through volatilization. Photodegradation was more remarkable for LMW and MMW PAHs in fine-textured Regosol soil, whereas this pathway played only a role for HMW PAHs in Arenosol soil samples. Although those differences between both soils were very low, photodegradation of PAHs in fine-texture Regosol soil might have reached the maximum level after 7 days of exposure, while in Arenosol soil was probably still increasing over time. High photodegradation rates were reported for fluorene in fine-textured Regosol soil, and anthracene, pyrene and benzo(*a*)pyrene in both soils. Low half-lives were especially estimated for anthracene and benzo(*a*)pyrene, while chrysene, benzo(*b*)fluoranthene and benzo(*k*)fluoranthene were the most resistant PAHs to solar radiation. The decrease in darkness of anthracene, fluorene, fluoranthene and benzo(*ghi*)perylene in Arenosol soil and benzo(*a*)pyrene in both soils indicated that other degradation processes, which should be further studied, are simultaneously occurring.

Although the photodegradation of PAHs deposited on surface soils in highly irradiated regions might cause a decrease of the human exposure to such compounds, a number of by-products are also generated, including a variety of aldehydes, oxy-, hydroxy- and nitro-PAHs. Some of them (e.g., 1-naphthalenecarboxaldehyde, 1,2-naphthalic anhydride, 1-acenaphthenol, 1(2H)-acenaphthylenone, and benzo(*a*)anthracene-7,12-dione) were already identified in photodegradation

experiments performed at laboratory scale. However, their formation is occurring faster in the field, and their concentrations increase as that of their parent compounds decrease over time. Moreover, other nitro-PAHs (1-nitropyrene and 6-nitrobenzo(*a*)pyrene) and hydroxy-PAHs (benzo(*a*)pyrene-7,8-dihydro) were also detected throughout the experiment. Although few differences were found between soils, up to three metabolites were more quickly generated in Arenosol soil. Specifically, the highest photodegradation of pyrene in Arenosol soil than in fine-textured Regosol soil might cause the quicker formation of 1-nitropyrene in Arenosol soil as well. In addition, benzo(*a*)pyrene-7,8-dihydro was only found in Arenosol and fine-textured Regosol soil, respectively. Some of these photodegradation by-products, such as 1-nitropyrene and 6-nitrobenzo(*a*)pyrene, which are not currently monitored and regulated in risk assessment programs, could drive to an increase in human health risk since they exhibit a high mutagenic potential (Gurbani et al., 2013).

Acknowledgements

This study was supported by the Spanish Ministry of Economy and Competitiveness (Mineco), through the project CTM2012-33079. Montse Marquès received a PhD fellowship from AGAUR (Commissioner for Universities and Research of the Department of Innovation, Universities and Enterprise of the “Generalitat de Catalunya” and the European Social Fund). The authors are indebted to Dr. Irene Maijó for her excellent guidance and assistance in GC-MS analysis.

References

- Andersson J.T., Achten C., 2015. Time to say goodbye to the 16 EPA PAHs? Toward an up-to-date use of PACs for environmental purposes. *Polycyclic Aromat. Compd.* 35, 330-354.
- Arp H.P.H., Lundstedt S., Josefsson S., Cornelissen G., Enell A., Allard A.-S., Kleja D.B., 2014. Native Oxy-PAHs, N-PACs, and PAHs in historically contaminated soils from Sweden, Belgium, and France: Their soil-porewater partitioning behavior, bioaccumulation in *Enchytraeus crypticus*, and bioavailability. *Environ. Sci. Technol.* 48, 11187–11195.
- Augusto S., Sierra J., Nadal M., Schuhmacher M., 2015. Tracking polycyclic aromatic hydrocarbons in lichens: It's all about the algae. *Environ. Pollut.* 2015, 441-445.

- Batchu S.R., Panditi V.R., O'Shea K.E., Gardinali P.R., 2014. Photodegradation of antibiotics under simulated solar radiation: Implications for their environmental fate. *Sci. Total Environ.* 470-471, 299-310.
- Borrás E., Ródenas M., Vázquez M., Vera T., Muñoz A., 2015. Particulate and gas-phase products from the atmospheric degradation of chlorpyrifos and chlorpyrifos-oxon. *Atmos. Environ.* 123, 112-120.
- Busby W.J., Stevens E., Kellenbach E., Cornelisse J., Lugtenburg J., 1988. Dose-response relationships of the tumorigenicity of cyclopenta(cd)pyrene, benzo(a)pyrene and 6-nitrochrysene in a newborn mouse lung adenoma bioassay. *Carcinogenesis* 9, 741-746.
- Cajthaml T., Erbanová P., Šašek V., Moeder M., 2006. Breakdown products on metabolic pathway of degradation of benzo(a)anthracene by a ligninolytic fungus. *Chemosphere* 64, 560-564.
- Chen F., Tan M., Ma J., Zhang S., Li G., Qu J., 2016. Efficient remediation of PAH-metal co-contaminated soil using microbial-plant combination: A greenhouse study. *J. Hazard. Mater.* 302, 250-261.
- Dasgupta S., Cao A., Mauer B., Yan B., Uno S., McElroy A., 2014. Genotoxicity of oxy-PAHs to Japanese medaka (*Oryzias latipes*) embryos assessed using the comet assay. *Environ. Sci. Pollut. Res.* 21, 13867-13876.
- Domingo J.L., Nadal M., 2015. Human dietary exposure to polycyclic aromatic hydrocarbons: A review of the scientific literature. *Food Chem. Toxicol.* 86, 144-153.
- EL-Saeid M.H., Al-Turki A.M., Nadeem M.E.A., Hassanin A.S., Al-Wabel M.I., 2015. Photolysis degradation of polyaromatic hydrocarbons (PAHs) on surface sandy soil. *Environ. Sci. Pollut. Res.* 22, 9603-9616.
- Fu P.P., Xia Q., Sun X., Yu H., 2012. Phototoxicity and environmental transformation of polycyclic aromatic hydrocarbons (PAHs)-light-induced reactive oxygen species, lipid peroxidation, and DNA damage. *J. Environ. Sci. Health Part C Environ. Carcinog. Ecotoxicol. Rev.* 30, 1-41.
- Fukuhara K., Kurihara M., Miyata N., 2001. Photochemical generation of nitric oxide from 6-nitrobenzo(a)pyrene. *J. Am. Chem. Soc.* 123, 8662-8666.
- Ge L., Chen J., Wei X., Zhang S., Qiao X., Cai X., Xie Q., 2010. Aquatic photochemistry of fluoroquinolone antibiotics: kinetics, pathways, and multivariate effects of main water constituents. *Environ. Sci. Technol.* 44.
- Ghosal D., Ghosh S., Dutta T., Ahn Y., 2016. Current State of Knowledge in Microbial Degradation of Polycyclic Aromatic Hydrocarbons (PAHs): A Review. *Front. Microbiol.* 7, 1369.
- Gupta H., B G., 2015. Photocatalytic degradation of polycyclic aromatic hydrocarbon benzo[a]pyrene by iron oxides and identification of degradation products. *Chemosphere* 138, 924-931.
- Gupta H., Gupta B., 2015. Photocatalytic degradation of polycyclic aromatic hydrocarbon benzo[a]pyrene by iron oxides and identification of degradation products. *Chemosphere*.
- Gurbani D., Bharti S.K., Kumar A., Pandey A.K., Ana G.R.E.E., Verma A., Khan A.H., Patel D.K., Mudiam M.K.R., Jain S.K., Raja Royf A.D., 2013. Polycyclic aromatic hydrocarbons and their quinones modulate the metabolic profile and induce DNA damage in human alveolar and bronchiolar cells. *Int. J. Hyg. Environ. Health* 216, 553-565.

- Hirose M., Lee M.S., Wang C.Y., King C.M., 1984. Induction of rat mammary gland tumors by 1-nitropyrene, a recently recognized environmental mutagen. *Cancer Res.* 44, 1158-1162.
- Hu N.-J., Huang P., Liu J.-H., Ma D., Shi X.-F., Mao J., Liu Y., 2014. Characterization and source apportionment of polycyclic aromatic hydrocarbons (PAHs) in sediments in the Yellow River Estuary, China. *Environ. Earth Sci.* 71, 873-883.
- Hung H., Blanchard P., Halsall C.J., Bidleman T.F., Stern G.A., Fellin P., Muir D.C.G., Barrie L.A., Jantunen L.M., Helm P.A., Ma J., Konoplev A., 2005. Temporal and spatial variabilities of atmospheric polychlorinated biphenyls (PCBs), organochlorine (OC) pesticides and polycyclic aromatic hydrocarbons (PAHs) in the Canadian Arctic: Results from a decade of monitoring. *Sci. Total Environ.* 342, 119-144.
- Jia H., Li L., Chen H., Zhao Y., Li X., Wang C., 2015. Exchangeable cations-mediated photodegradation of polycyclic aromatic hydrocarbons (PAHs) on smectite surface under visible light. *J. Hazard. Mater.* 287, 16-23.
- Jörundsdóttir H.Ó., Jensen S., Hylland K., TorFredrikHolth, Gunnlaugsdóttir H., Svavarsson J., Ólafsdóttir Á., El-Taliawy H., Rigét F., Strand J., Nyberg E., Bignert A., KatrinS.Hoydal, Halldórsson H.P., 2014. Pristine Arctic: Background mapping of PAHs, PAH metabolites and inorganic trace elements in the North-Atlantic Arctic and sub-Arctic coastal environment. *Sci. Total Environ.* 493, 719-728.
- Kameda T., 2011. Atmospheric Chemistry of Polycyclic Aromatic Hydrocarbons and Related Compounds. *J. Health Sci.* 57, 504-511.
- Katsoyiannis A., Breivik K., 2014. Model-based evaluation of the use of polycyclic aromatic hydrocarbons molecular diagnostic ratios as a source identification tool. *Environ. Pollut.* 184, 488-494.
- Kielhorn J., Wahnschaffe U., Mangelsdorf I. Environmental Health Criteria 229: Selected nitro- and nitro-oxy-polycyclic aromatic hydrocarbons. *Environ. Health Criter.* 229, 2003, pp. i-480.
- Lundstedt S., Bandowe B.A.M., Wilcke W., Boll E., Christensen J.H., Vila J., Grifoll M., Faure P., Biache C., Lorgeoux C., Larsson M., Irgum K.F., Ivarsson P., Ricci M., 2014. First intercomparison study on the analysis of oxygenated polycyclic aromatic hydrocarbons (oxy-PAHs) and nitrogen heterocyclic polycyclic aromatic compounds (N-PACs) in contaminated soil. *Trends Anal. Chem.* 57, 83-92.
- Lundstedt S., White P.A., Lemieux C.L., Lynes K.D., Lambert I.B., Öberg L., Haglund P., Tysklind M., 2007. Sources, Fate, and Toxic Hazards of Oxygenated Polycyclic Aromatic Hydrocarbons (PAHs) at PAH-Contaminated Sites. *Ambio* 36.
- Marquès M., Mari M., Audí-Miró C., Sierra J., Soler A., Nadal M., Domingo J.L., 2016a. Climate change impact on the PAH photodegradation in soils: Characterization and metabolites identification. *Environ. Int.* 89-90, 155-165.
- Marquès M., Mari M., Audí-Miró C., Sierra J., Soler A., Nadal M., Domingo J.L., 2016b. Photodegradation of polycyclic aromatic hydrocarbons in soils under a climate change base scenario. *Chemosphere* 148, 495-503.
- McGregor W.G., Maher V.M., McCormick J.J., 1994. Kinds and locations of mutations induced in the hypoxanthine-guanine phosphoribosyltransferase gene of human T-lymphocytes by 1-nitrosopyrene, including those caused by V(D)J recombinase. *Cancer Res.* 54, 4207-4213.

- Muñoz A., Vera T., Ródenas M., Borrás E., Mellouki A., Treacy J., Sidebottom H., 2014. Gas-phase degradation of the herbicide ethalfuralin under atmospheric conditions. *Chemosphere* 95, 395-401.
- Nadal M., Mari M., Schuhmacher M., Domingo J.L., 2009. Multi-compartmental environmental surveillance of a petrochemical area: Levels of micropollutants. *Environ. Int.* 35, 227-235.
- Nadal M., Schuhmacher M., Domingo J.L., 2011. Long-term environmental monitoring of persistent organic pollutants and metals in a chemical/petrochemical area: Human health risks. *Environ. Pollut.* 159, 1769-1777.
- Nascimento P.C., Gobo L.A., Bohrer D., Carvalho L.M., Cravo M.C., Leite L.F.M., 2015. Determination of oxygen and nitrogen derivatives of polycyclic aromatic hydrocarbons in fractions of asphalt mixtures using liquid chromatography coupled to mass spectrometry with atmospheric pressure chemical ionization. *J. Sep. Sci.* 38, 4055-4062.
- Ohkouchi N., Kawamura K., Kawahata H., 1999. Distribution of threeto seven-ring polycyclic aromatic hydrocarbons on the deep sea floor in the central Pacific. *Environ. Sci. Technol.* 33, 3086-3090.
- Onduka T., Ojima D., Mochida K.I., Koyama J., Fujii K., 2015. Reproductive toxicity of 1-nitronaphthalene and 1-nitropyrene exposure in the mummichog, *Fundulus heteroclitus*. *Ecotoxicology* 24, 648-656.
- Pereira K.L., Hamilton J.F., Rickard A.R., Bloss W.J., Alam M.S., Camredon M., Ward M.W., Wyche K.P., Muñoz A., Vera T., Vázquez M., Borrás E., Ródenas M., 2015. Insights into the Formation and Evolution of Individual Compounds in the Particulate Phase during Aromatic Photo-Oxidation. *Environ. Sci. Technol.* 49, 13168-13178.
- Pereira V.J., Weinberg H.S., Linden K.G., Singer P.C., 2007. UV degradation kinetics and modeling of pharmaceutical compounds in laboratory grade and surface Water via direct and indirect photolysis at 254 nm. *Environ. Sci. Technol.* 41, 1682-1688.
- Pham C.T., Tang N., Toriba A., Hayakawa K., 2015. Polycyclic Aromatic Hydrocarbons and Nitropolycyclic Aromatic Hydrocarbons in atmospheric particles and soil at a traffic site in Hanoi, Vietnam. *Polycyclic Aromat. Compd.* 35, 355-371.
- Pinto M., Costa P.M., Louro H., Costa M.H., Lavinha J., Caeiro S., Silva M.J., 2014. Determining oxidative and non-oxidative genotoxic effects driven by estuarine sediment contaminants on a human hepatoma cell line. *Sci. Total Environ.* 478, 25-35.
- Qiao M., Qi W., Liu H., Qu J., 2014. Oxygenated, nitrated, methyl and parent polycyclic aromatic hydrocarbons in rivers of Haihe River System, China: Occurrence, possible formation, and source and fate in a water-shortage area. *Sci. Total Environ.* 481, 178-185.
- Ras M.R., Marcé R.M., Cuadras A., Mari M., Nadal M., Borrull F., 2009. Atmospheric levels of polycyclic aromatic hydrocarbons in gas and particulate phases from Tarragona Region (NE Spain). *Int. J. Environ. Anal. Chem.* 89, 543-556.
- Riva M., Healy R.M., Tomaz S., Flaud P.-M., Perraudin E., Wenger J.C., Villenave E., 2016. Gas and particulate phase products from the ozonolysis of acenaphthylene. *Atmos. Environ.* 142, 104-113.
- Rosenkranz H.S., and Mermelstein R., 1983. Mutagenicity and genotoxicity of nitroarenes. All nitro-containing chemicals were not created equal. *Mutat. Res/Rev. Genet.* 114, 217-267.

- Rosenkranz H.S., Mermelstein R., 1985. The genotoxicity, metabolism, and carcinogenicity of nitrated polycyclic aromatic hydrocarbons. *J. Environ. Sci. Health Part C Environ. Carcinog. Rev.* 3, 221-272.
- Sugiyama H., Watanabe T., Hirayama T., 2001. Nitration of pyrene in metallic oxides as soil components in the presence of indoor air, nitrogen dioxide gas, nitrite ion, or nitrate ion under xenon irradiation. *J. Health Sci.* 47, 28-35.
- Ukiwe L.N., Egereonu U.U., Njoku P.C., Nwoko C.I.A., Allinor J.I., 2013. Polycyclic Aromatic Hydrocarbons Degradation Techniques: A Review *Int. J. Chem.* 5, 43-55.
- Vera T., Borrás E., Chen J., Coscollá C., Daële V., Mellouki A., Ródenas M., Sidebottom H., Sun X., Yusá V., Zhang X., Muñoz A., 2015. Atmospheric degradation of lindane and 1,3-dichloroacetone in the gas phase. Studies at the EUPHORE simulation chamber. *Chemosphere* 138, 112-119.
- Walgraeve C., Demeestere K., Dewulf J., Zimmermann R., Langenhove H.V., 2010. Oxygenated polycyclic aromatic hydrocarbons in atmospheric particulate matter: Molecular characterization and occurrence. *Atmos. Environ.* 44, 1831-1846.
- Watt D.L., Utzat C.D., Hilario P., Basu A.K., 2007. Mutagenicity of the 1-Nitropyrene-DNA Adduct N-(Deoxyguanosin-8-yl)-1-aminopyrene in Mammalian Cells. *Chem. Res. Toxicol.* 20, 1658-1664.
- Wislocki P.G., Bagan E.S., Lu A.Y.H., Dooley K.L., Fu P.P., Han-Hsu H., Beland F.A., Kadlubar F.F., 1986. Tumorigenicity of nitrated derivatives of pyrene, benzo(a)anthracene, chrysene and benzo(a)pyrene in the newborn mouse assay. *Carcinogenesis* 7, 1317-1322.
- Woo O.T., Chung W.K., Wong K.H., Chow A.T., P.K.Wong. 2009. Photocatalytic oxidation of polycyclic aromatic hydrocarbons: Intermediates identification and toxicity testing. *J. Hazard. Mater.* 168, 1192-1199.
- Zhang L., Li P., Gong Z., Li X., 2008. Photocatalytic degradation of polycyclic aromatic hydrocarbons on soil surfaces using TiO₂ under UV light. *J. Hazard. Mater.* 158, 478-484.
- Zhang L., Li P., Gong Z., Oni A., 2006a. Photochemical behavior of benzo[a]pyrene on soil surfaces under UV light irradiation. *J. Environ. Sci.* 18, 1226-1232.
- Zhang L., Xua C., Chena Z., Li X., Li P., 2010. Photodegradation of pyrene on soil surfaces under UV light irradiation. *J. Hazard. Mater.* 173, 168-172.
- Zhang Y., Yang B., Gan J., Liu C., Shu X., Shu J., 2011. Nitration of particle-associated PAHs and their derivatives (nitro-, oxy-, and hydroxy-PAHs) with NO₃ radicals. *Atmos. Environ.* 45, 2515-2521.
- Zhou S., Wenger J.C., 2013. Kinetics and products of the gas-phase reactions of acenaphthylene with hydroxyl radicals, nitrate radicals and ozone. *Atmos. Environ.* 75, 103-112.

DISCUSSION CHAPTER 5

Working at laboratory scale is suitable to control environmental conditions and to avoid other degradation processes, such as biodegradation. However, the impact by light exposure may be easily underestimated because the intensity achieved by light lamps is, by far, lower than that natural. In order to investigate PAHs photodegradation in a more realistic scenario, the same experiment conducted in a climate chamber was repeated in the field, under natural conditions.

In the field experiment, faster volatilization of LMW PAHs in both soils than that previously reported in the climate chamber, was observed. Photodegradation was more remarkable for LMW and MMW PAHs in fine-textured Regosol soil, whereas this pathway played only a role for HMW PAHs in Arenosol soil samples. Although differences between soils were very low, the photodegradation of PAHs in fine-texture Regosol soil might have reached the maximum level after 7 days of exposure. In contrast, it could continue to increase after the end of the study in Arenosol soil. High photodegradation rates were reported for fluorene in fine-textured Regosol soil, as well as anthracene, pyrene, and benzo(*a*)pyrene, in both soils. Low half-lives were especially estimated for anthracene and benzo(*a*)pyrene, while chrysene, benzo(*b*)fluoranthene and benzo(*k*)fluoranthene were the most resistant PAHs to solar radiation. In the darkness, some PAHs, such as anthracene, fluorene, fluoranthene and benzo(*ghi*)perylene, in Arenosol soil, and benzo(*a*)pyrene, in both soils were also degraded. It indicates that other degradation processes, which should be further studied, were simultaneously occurring.

According to our results, the photodegradation of PAHs deposited on surface soils in highly irradiated regions may be significant, causing a decrease of their environmental levels. This leads to a reduction of the human exposure to these compounds. Several photodegradation by-products are also generated, including a variety of aldehydes, oxy-, hydro- and nitro-PAHs. In addition to those identified at laboratory scale, whose photodegradation was more enhanced, other nitro-PAHs (1-nitropyrene and 6-nitrobenzo(*a*)pyrene), hydro-PAHs (benzo(*a*)pyrene-7,8-dihydro) were also detected throughout the experiment. Although few differences were found between soils, 3 by-products were more quickly generated in Arenosol soil. Specifically, 1-nitropyrene was formed from the photodegradation of pyrene,

especially in Arenosol soil. In turn, benzo(*a*)pyrene-7,8-dihydro was only found in Arenosol. The attachment of oxy- and nitro- radicals decrease the lipophilic character of PAHs, enhancing their bioavailability, and consequently, increasing their hazard. Importantly, some of these photodegradation by-products, such as 1-nitropyrene and 6-nitrobenzo(*a*)pyrene, which are not currently monitored and regulated in risk assessment programs, exhibit a high mutagenic potential.

CHAPTER 6

Polycyclic aromatic hydrocarbons (PAHs) and trace elements in Arctic soils: A case-study in Svalbard

Montse Marquès ^{a,b}, Montse Mari ^{a,b}, Jordi Sierra ^{b,c},

Tatiana Drotikova ^{d,e}, Roland Kallenborn ^{d,e},

Martí Nadal ^a, José L. Domingo ^a

^a Laboratory of Toxicology and Environmental Health, School of Medicine, IISPV, Universitat Rovira i Virgili, Sant Llorenç 21, 43201 Reus, Catalonia, Spain.

^b Environmental Engineering Laboratory, Departament d'Enginyeria Química, Universitat Rovira i Virgili, Av. Països Catalans 26, 43007 Tarragona, Catalonia, Spain.

^c Laboratory of Soil Science, Faculty of Pharmacy, Universitat de Barcelona, Av. Joan XXIII s/n, 08028 Barcelona, Catalonia, Spain.

^d University Centre in Svalbard (UNIS), Arctic Technology Department, Longyearbyen, Norway.

^e Department of Chemistry, Biotechnology and Food Science (IKBM), Norwegian University of Life Sciences (NMBU), Ås, Norway.

Environmental Research. Submitted.

ABSTRACT

This study was aimed at assessing the occurrence of polycyclic aromatic hydrocarbons (PAHs) and trace elements in soils from Pyramiden (Central Spitsbergen, Svalbard Archipelago). Due to long-range atmospheric transport, local geology, previous coal mining extractions, and the stack emissions of two operative power plants at this settlement, those soils might be a sink of pollutants during the free-ice season. Fieldwork was carried out in late summer of 2014 by collecting 8 top-layer soil samples, whose content of 16 US EPA priority PAHs and potentially toxic elements (As, Be, Cd, Co, Cr, Cu, Hg, Mn, Mo, Ni, Pb, Sn, Tl, V, Zn) was determined. PAH levels showed a similar profile with pyrogenic molecular diagnostic ratios (MDRs) in most samples. The highest levels of PAHs and trace elements were found in sampling sites located near two power plants and downwind, being their concentrations even higher than typical threshold values. Two different indices, the Pollution Load Index (PLI) and the Geoaccumulation Index (I_{geo}), were calculated to determine the environmental status of Svalbard soils, in terms of metal pollution. Those samples collected in the area adjacent to the power plants were pointed out as moderately polluted by Hg. The significant correlations between the concentrations of some contaminants (e.g., naphthalene, phenanthrene, Mn, Pb, V, Cu, Zn, Tl and Be) and the organic matter content would suggest that soil properties play a key role for pollutant retention in the Arctic. Furthermore, the correlations between $\Sigma 16$ PAHs and some elements (e.g., Hg, Pb, Zn and Cu) indicates that the main source of contamination is anthropogenic, although the contribution of the local geology should not be disregarded.

Keywords: Svalbard, soil, pollution, polycyclic aromatic hydrocarbons, trace elements.

INTRODUCTION

Environmental studies in remote areas are useful not only to identify transportation routes of chemical pollutants, but also to assist in the environmental risk assessment (Bazzano et al., 2015). Polar areas, both Arctic and Antarctica, are potential receptors of organic compounds and trace elements due to the long-range transport capacity of these substances to be deposited far away their emission sources (Bargagli, 2016; Ge et al., 2016; Nadal et al., 2015; Turetta et al., 2016). Although remote areas are the least disturbed habitats on the Earth, they are not free of being impacted by environmental pollution. Some of these high-latitude regions, such as the Svalbard archipelago, own settlements with industrial development and existing coal mining centers (Abramova et al., 2014), which have become a potential local source of pollution.

In the northern part of Isfjorden (Billefjorden, Svalbard), an abandoned Russian settlement and coal-mining town called Pyramiden is located. Pyramiden was founded by Sweden in 1910, and sold to the Soviet Union in 1927. In 1983, agricultural soil was begun to be imported to supplement the thin layer of soils, which were characterized by a poor content of nutrients. It enabled the establishment of imported grasses as part of an “ecological action”. Despite of the unknown exact origin of these soils, they were classified as chernozem sourced from southern European Russia or Ukraine (Coulson et al., 2015). In 1998, Pyramiden was closed, although the infrastructure is still in place. Nowadays, the human impact is related to the coal and diesel combustion carried out in two different power plants, as well as traffic, harbor and heliport activity derived from tourism and research. This area has a tundra climate, and even in the summer, the ambient temperatures are very low.

Polycyclic aromatic hydrocarbons (PAHs) and trace elements, such as mercury, are among the most harmful pollutants derived from human activities and coal-mining extraction. In fact, PAHs have been widely found in Svalbard atmosphere (Cecinato et al., 2000), water (Polkowska et al., 2011; Ruman et al., 2014), biota (Carrasco-Navarro et al., 2015; Nahrgang et al., 2013; Szczybelski et al., 2016; Wang et al., 2009), sediments (Konovalov et al., 2010; Sapota et al., 2009; van den Heuvel-Greve et al., 2016), snow (Abramova et al., 2016), and soils (Gulińska et al., 2003; Wang et al., 2009). In addition, there are recent findings of trace elements in air particulate matter

(Bazzano et al., 2015; Bazzano et al., 2016), sea water (Bazzano et al., 2014), biota (Fenstad et al., 2016; Węgrzyn et al., 2016), marine particulate and sediments (Ardini et al., 2016; Frankowski and Ziōła-Frankowska, 2014), ice (Lehmann et al., 2016; Łokas et al., 2016), and soils (Gulińska et al., 2003; Krajcarová et al., 2016; Wojtuń et al., 2013).

Because of the deep snow and ice cover of Svalbard, the content of environmental pollutants has not been widely studied in the soil matrix. However, contaminants can be accumulated in the snow, and be transferred to soil through ice-snow melting (Perrette et al., 2013). In addition, Pyramiden soils are ice-free for almost 5 months every year (Koroleva, 2014), being pollutants able to be deposited on the soil surface. The present study was aimed at examining the presence of 16 US EPA priority PAHs and trace elements in soil samples from Svalbard, as well as to assess potential sources of contamination.

MATERIALS AND METHODS

Sampling campaign

A soil sampling campaign was carried out in Pyramiden (Spitsbergen, Svalbard archipelago) in September 2-4, 2014. Seven soils (P1-P7) were sampled in Pyramiden town, while one soil sample (P8) was collected in a background area, at 2 km from any potential emission source (Fig. 1). Soil samples were collected from the surface layer (0-5 cm depth), kept in polyethylene bags, and immediately covered with aluminum foil. Afterwards, they were dried at 30°C to avoid the loss of volatile compounds. Once their weight was stable (± 0.001 g), soil samples were sieved through a 2-mm mesh screen to standardize particle size. Finally, soil samples were kept again in polyethylene bags and placed in the freezer until further treatment. Qualitative data and physicochemical properties of all collected soils are included in Table 1.

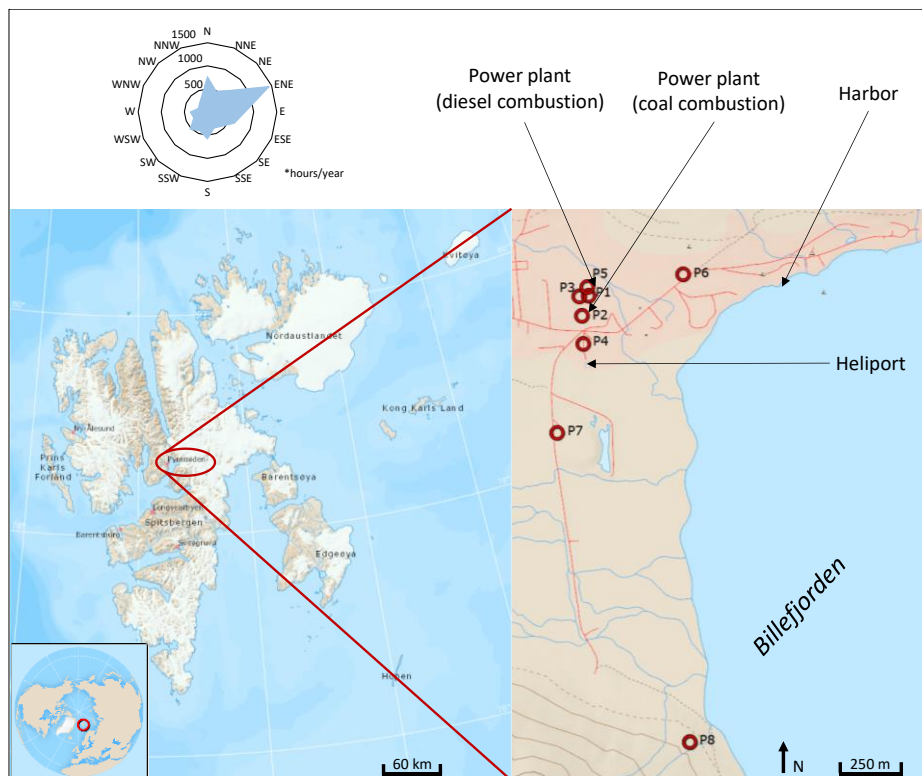


Fig. 1. Localization of soil sampling sites in Pyramiden (Spitsbergen, Svalbard archipelago).

Analytical procedure

PAHs

Briefly, PAHs were extracted with dichloromethane:hexane (1:1) (Scharlau Chemie S. A., Barcelona, Spain) by performing three 10-min subsequent extractions with ultrasonic bath. The resulting extracts were filtered and further concentrated with a rotatory evaporator. Afterwards, a Solid Phase Extraction (SPE), adapted from Khan et al. (2015) and Lundstedt et al. (2014), was conducted. Firstly, 6 mL DSC-18 cartridges containing 500 mg of silica (Supelco®, Bellefonte, PA, USA) were conditioned with 10 mL of hexane. Secondly, the sample extract was run, followed by 9 mL of dichloromethane:hexane (1:9), and finally, with 8 mL of dichloromethane. Finally, all extracts were concentrated with a gentle stream of N_2 (99.9999%). Samples were run in a 7890A Series gas chromatograph coupled to a 7000 GCQqQ (Agilent Technologies), equipped with a J&W Scientific DB-XLB chromatographic column (30 m

x 0.25 mm i.d., 0.25 μm film) (Agilent Technologies). A volume of 1 μL of sample was automatically injected into a split/splitless inlet in splitless mode, being kept at 280°C of temperature. Helium (99.999% purity) was used as a carrier gas, at a flow rate of 1.2 mL min^{-1} in constant mode. The oven program was set at an initial temperature of 80°C, increased to 320°C at a rate of 10°C min^{-1} , and held at 320°C for 22 min. Total running time was 46 min. Ionization was done by electronic impact (EI), with an electron energy of 70 eV and a source temperature of 230°C. Mass spectra data were recorded after a solvent delay of 3 min. The QqQ analyzer operated in MRM mode, under the conditions shown in Table S1 (Annex 5).

Trace elements

The contents of arsenic (As), beryllium (Be), cadmium (Cd), cobalt (Co), chromium (Cr), copper (Cu), mercury (Hg), manganese (Mn), molybdenum (Mo), nickel (Ni), lead (Pb), thallium (Tl), tin (Sn), vanadium (V) and zinc (Zn) were analyzed by inductively coupled plasma-mass spectrometry (ICP-MS) (Perkin Elmer Elan 6000), using rhodium (Rh) as internal standard. One-half of soil was digested with 5 mL of nitric acid (65% Suprapur, E. Merck, Darmstadt, Germany) in hermetic Teflon vessels. Samples were pre-digested for 8 h at room temperature, and subsequently they were heated at 80°C for 8 h. Once cooled down, the solutions were filtered and made up to 25 mL with ultrapure water. Finally, the extracts were maintained at -20°C until further metal analysis. Additional details of the determination of trace elements are provided elsewhere (Nadal et al., 2011; Rovira et al., 2010; Vilavert et al., 2015).

Quality assurance and quality control (QA/QC)

Triplicates of soil samples were spiked with PAHs in order to assess the method performance by reporting the average PAH recoveries and their reproducibility (standard deviations). The standard mixture contained the following 16 US EPA priority PAHs: naphthalene (99.7% of purity), acenaphthylene (99.4% of purity), acenaphthene (99.3% of purity), fluorene (98.7% of purity), phenanthrene (98.0% of purity), anthracene (99.0% of purity), fluoranthene (99.5% of purity), pyrene (99.2% of purity), benzo(a)anthracene (98.5% of purity), chrysene (97.4% of purity),

benzo(*b*)fluoranthene (97.3% of purity), benzo(*k*)fluoranthene (99.5% of purity), benzo(*a*)pyrene (96.7% of purity), dibenzo(*ah*)anthracene (98.3% of purity), benzo(*ghi*)perylene (99.4% of purity), and indeno(123-*cd*)pyrene (99.0% of purity). Due to chromatographic limitations, benzo(*b*)fluoranthene and benzo(*k*)fluoranthene were quantified together as benzo(*b+k*)fluoranthene. In order to determine any potential laboratory contamination, extraction blanks were also performed. PAH recoveries were ranged between 43% and 123%, while those of surrogates were $46\pm 14\%$, $63\pm 10\%$, $85\pm 21\%$ and $64\pm 14\%$ for d₁₀-acenaphthene, d₁₀-phenanthrene, d₁₂-chrysene and d₁₂-perylene, respectively. Two compounds, d₁₀-fluorene and d₁₂-benzo(*a*)pyrene, were used as internal standards, being added prior to the chemical analysis. The calibration curve for PAH quantitation covered concentrations from 0.5 to 100 µg mL⁻¹. The limits of quantification (LOQs) of the individual PAHs were in the range 2-70 pg g⁻¹ of dry weight.

Regarding trace elements, background levels were also determined in blank samples and standards, which were inserted in every batch. Loamy clay 1 (National Institute of Standards and Technology, USA) was used as certified reference material to check the accuracy of the method. Metal recoveries were ranged between 86% and 106% (Zn and Co, respectively). The limits of detection (LODs) of trace elements were in the range 0.03-0.50 mg kg⁻¹ of dry weight.

Statistical analysis

Pearson correlations were calculated by using XLSTAT 2016 (Addinsoft SARL™, Paris, France), with a significance value set at $p < 0.05$.

RESULTS AND DISCUSSION

Soils characterization

Qualitative information and results of the soil characterization are summarized in Table 1. All the soil samples collected in Pyramiden and surrounding area were non-saline, alkaline (pH between 7.2 and 8.01) and calcareous. Most of them (P1, P2, P4, P5, P6 and P7) were coarse-textured, while P3 and P8 were fine-textured, with a notable content of silt and clay, respectively. A relatively higher content of organic

matter was found in 3 locations (2.25%, 4.68% and 4.08% in P3, P6 and P7, respectively) in comparison with the remaining sampling sites. In turn, nitrate contents were low, being ranged 4.2-29.6 mg kg⁻¹.

Table 1. Characterization of soils collected in Pyramiden (Svalbard Archipelago).

	P1	P2	P3	P4	P5	P6	P7	P8
Human activity	Power plants	Power plants In front coal-based power plant	Power plants	Power plant Traffic Heliport	Power plants In front diesel-based power plant	Harbor	No visible	No visible
GPS coordinates	78.655°N 16.337°E	78.654°N 16.336°E	78.655°N 16.336°E	78.653°N 16.336°E	78.655°N 16.337°E	78.655°N 16.355°E	78.650°N 16.331°E	78.639°N 16.354°E
Level above the sea (m)	9	7	9	7	9	20	10	43
pH ^a	8.01	7.74	7.85	7.44	7.60	7.63	7.17	7.61
Electrical conductivity at 25°C (μS cm ⁻¹) ^a	1105	189	308	1145	170	1506	719	102
Oxidizable C ^b (%)	0.86	0.39	1.30	0.52	0.25	2.71	2.36	0.25
Organic Matter ^b (%)	1.48	0.67	2.25	0.90	0.42	4.68	4.08	0.42
Texture: sand/silt/clay ^c (%)	85/9/6	88/7/5	62/26/12	83/8/9	73/21/6	72/21/7	84/11/5	67/14/19
CaCO ₃ ^d	c ⁺⁺	c ⁺⁺	c ⁺⁺	c ⁺⁺	c ⁺⁺	c ⁺	c ⁺	c ⁺
NO ₃ ^{-e} (mg kg ⁻¹)	6.8	6.6	5.5	4.2	5.2	6.8	29.6	6.1

^a Aqueous extracts 1:2.5; ^b Organic Carbon by Walkley-Black method; ^c sedimentation method; ^d qualitative method: 0 < c+ < 10% and 10 ≤ c++ < 20%; ^e Extracted in soil to water ratio 1:10 elutriates and quantified by ion chromatography (Dionex D-300; Chromeleon software v6.80).

PAHs

The concentrations of the individual 16 US EPA priority PAHs, the total amount, the sum of 7 carcinogenic PAHs, as well as the levels expressed as benzo(*a*)pyrene equivalents (BaP_{eq}), are listed in Table 2, together with the limit of quantification (LoQ) of each hydrocarbon. All the studied PAHs were above detection limits, except for acenaphthylene, acenaphthene and anthracene in blank soil (P8). P3 was, by far, the

most contaminated site, showing a $\Sigma 16$ PAH concentration of $11600 \mu\text{g kg}^{-1}$ of dry soil. P1 and P3 sampling sites were closely located each other, being both near two power plants (coal- and diesel-fired). However, the PAH values registered in P3 were much higher. As P3 was located downwind, it would indicate that prevailing winds (ENE and N) have a critical impact on the deposition of PAHs near the power plants. In addition, P6 and P7 sampling sites also presented notably high concentrations of PAHs (6370 and $2350 \mu\text{g kg}^{-1}$ of dry soil, respectively). P6 is located 500 m upwind the power plants, and close to the harbor. In turn, P7 is in a zone with no visible human activity, but downwind the 2 power plants, which are located at a distance of 600 m. Contrastingly, the lowest value of PAHs in soil was found in the background point (P8), being quantified in $52.8 \mu\text{g kg}^{-1}$ of dry soil. Therefore, the concentration of $\Sigma 16$ PAHs near the power plants was almost 220-times higher than that in the background area, evidencing the local impact of these facilities.

Since there is a lack of threshold levels in Svalbard, as well as in Norway, target and intervention values for soil remediation from the Netherlands were used for comparison purposes (ESdat, 2000). According to the Dutch legislation, the sum of 10 PAHs (naphthalene, anthracene, phenanthrene, fluoranthene, benzo(*a*)anthracene, chrysene, benzo(*a*)pyrene, benzo(*ghi*)perylene, benzo(*k*)fluoranthene, and indeno(123-*cd*)pyrene) should not exceed 1 mg kg^{-1} , which is the target value for soils with an organic matter content below 10%. Three sampling sites (P3, P6, and P7) showed levels above this target value (8.33 , 5.63 and 2.07 mg kg^{-1} , respectively). However, PAH levels did not exceed the intervention values, set at a level of 40 mg kg^{-1} (Table 2).

To the best of our knowledge, there exist only two scientific publications reporting soil concentrations of PAHs in Svalbard (Gulińska et al., 2003; Wang et al., 2009). Because the Arctic surface is often covered by snow and ice, most of the scientific literature is focused on PAHs in snow, instead of soil. However, some spots are free of ice and snow in the summer, making easier the deposition of PAHs directly onto soil. Furthermore, ice and snow melting might be mean an addition input of PAHs to soil, in addition to that occurred through air deposition.

The current concentrations of $\Sigma 16$ PAHs in soils were clearly higher than those previously found by other researchers. In the first study, Gulińska et al. (2003) found

Table 2. Concentration of PAHs in soils ($\mu\text{g kg}^{-1}$ of dry soil) sampled in Pyramiden (Svalbard) and reference values.

	Naphthalene	Acenaphthylene	Acenaphthene	Fluorene	Phenanthrene	Anthracene	Fluoranthene	Pyrene	Benzo(a)anthracene	Chrysene	Benzo(b+k)fluoranthene	Benzo(a)pyrene	Dibenzo(a,h)anthracene	Indeno(123-cd)pyrene	Benzo(ghi)perylene	$\Sigma 16$ PAHs	$\Sigma 7$ carc. PAHs	$\Sigma 10$ PAHs	$\Sigma \text{BaP}_{\text{eq}}$
P1	133	12.1	5.88	14.5	139	19.2	95.5	79.0	52.2	60.2	100	53.6	9.43	24.8	38.6	837	349	666	82.0
P2	66.9	6.10	2.64	6.07	69.2	5.68	22.0	20.4	12.3	15.2	20.6	10.7	2.47	5.12	10.5	276	79.6	228	14.4
P3	622	333	43.4	108	1250	315.5	2360	1960	849	1160	1450	846	114	132	72.7	11600	5312	8330	1255
P4	182	2.79	2.59	7.79	156	3.5	19.7	25.2	15.2	30.3	39.9	15.3	10.1	12.7	47.2	571	156	502	33.8
P5	40.9	2.83	1.23	2.97	45.3	3.11	13.2	13.0	7.79	9.54	16.11	6.55	2.89	5.45	14.7	186	63.5	155	12.8
P6	2290	57.1	31.6	134	1840	44.35	356	314	118	311	328	162	45.9	67.4	271	6370	1261	5620	281
P7	893	19.7	14.0	93.5	707	18.71	93.3	91.0	47.3	108	104	44.3	14.6	15.9	84.6	2350	387	2060	81.1
P8 (background)	31.9	<LoQ	<LoQ	0.74	10.3	<LoQ	0.80	0.95	0.80	1.59	1.95	0.69	0.66	0.74	1.68	52.8	6.80	49.4	1.80
Mean ¹	604	62.0	14.5	52.32	601	58.57	422	358	157	242	294	163	28.5	37.6	77.0	3170	1087	2203	221
LoQ	0.02	0.02	0.05	0.02	0.01	0.06	0.002	0.003	0.01	0.01	0.004	0.07	0.03	0.05	0.07	-	-	-	-
Gulinska et al. (2003) ²	42-48	NA	8-14	10-12	24-45	Nd-69	1.8-28	8-109	ND-18	Nd-22	ND-19	ND-18	1-12	ND-28	ND-9.8	-	-	-	-
Gulinska et al. (2003) ³	42	NA	12	12	42	ND	23	8	ND	ND	9	3	1	3	3	158	16	120.5	-
Wang et al. (2009)	12	0.4	3	10	59	5	10	10	7	10	18	7	0.5	3	3	157	38.5	125	13.48

¹ calculated without considering P8 (blank soil); ² Range of all sampling sites; ³ Soil collected in Pyramiden; LoQ= Limit of Quantification; NA= No Analysed; ND= Non-Detected.

7 carc. PAHs= chrysene, benzo(b)fluoranthene, benzo(k)fluoranthene, benzo(a)pyrene, indeno(123-cd)pyrene, dibenzo(a,h)anthracene.

10 PAHs= naphthalene, anthracene, phenanthrene, fluoranthene, benzo(a)anthracene, chrysene, benzo(a)pyrene, benzo(ghi)perylene, benzo(k)fluoranthene, indeno(123-cd)pyrene.

that the total level of $\Sigma 16$ PAHs in a sample of soil collected in Pyramiden was $158 \mu\text{g kg}^{-1}$ of dry soil. In July and August 2007, Wang et al. (2009) collected samples of surface soil, moss and reindeer dung from 12 sites at Ny-Ålesund, Svalbard. The mean concentration of PAHs in soil was $157 \mu\text{g kg}^{-1}$ of dry soil, with levels ranging from 37 to $324 \mu\text{g kg}^{-1}$ of dry soil.

PAH levels in soil samples collected in Svalbard were also compared with data regarding zones surrounding other power plants. Our results were of the same order of magnitude as those found in the vicinity of a coal-fired power station in Plomin, Croatia (Medunić et al., 2016). In addition, they fell in the upper part of the range in comparison to levels found in soils surrounding coal-fired power plants in Xuzhou, China ($165\text{-}3495 \mu\text{g kg}^{-1}$ of dry soil), the Yangtze River Delta region, China ($285\text{-}504 \mu\text{g kg}^{-1}$ of dry soil), or Korba, India ($7\text{-}2100 \mu\text{g kg}^{-1}$ of dry soil) (Kumar et al., 2014; Ma et al., 2016; Wang et al., 2017).

The contribution of each individual PAH to the sum of 16 PAHs is depicted in Fig. 2. Naphthalene and phenanthrene were the most abundant PAHs, showing an average contribution of 33% and 25%. Therefore, similar emission sources might be responsible for PAH contamination in the area of study. However, the PAH profile was different in P3, where fluoranthene and pyrene were the most important contributors to the total concentration (20% and 17%, respectively). The contribution of naphthalene increased with the distance to the power plants. Naphthalene was identified as the most abundant hydrocarbon in the sampling site (P8), probably due its capacity to travel long distance. Low molecular weight PAHs may be present far away the potential emission sources, being ubiquitous in the environment. In turn, high molecular weight PAHs, which are more associated to the particulate matter, tend to be more deposited close to emission sources (Nadal et al., 2009).

According to the International Agency for Research on Cancer (IARC), benzo(a)pyrene is a carcinogenic substance to humans, being classified as Group 1. Due to this carcinogenic potential, it is a good indicator for the assessment of the health risks associated to the exposure of environmental PAHs (Domínguez-Morueco et al., 2015). Since the 16 US EPA priority PAHs do not have the same toxicity, the levels of PAH mixtures are sometimes expressed in terms of BaP_{eq} concentrations (Albuquerque et al., 2016), which are calculated by summing the values obtained after

multiplying the value of each individual PAH by the corresponding toxicity equivalency factor (TEF), according to the following equation:

$$\text{BaP}_{\text{eq}} = \sum_{i=1}^n \text{PAH}_i \times \text{TEF}_i$$

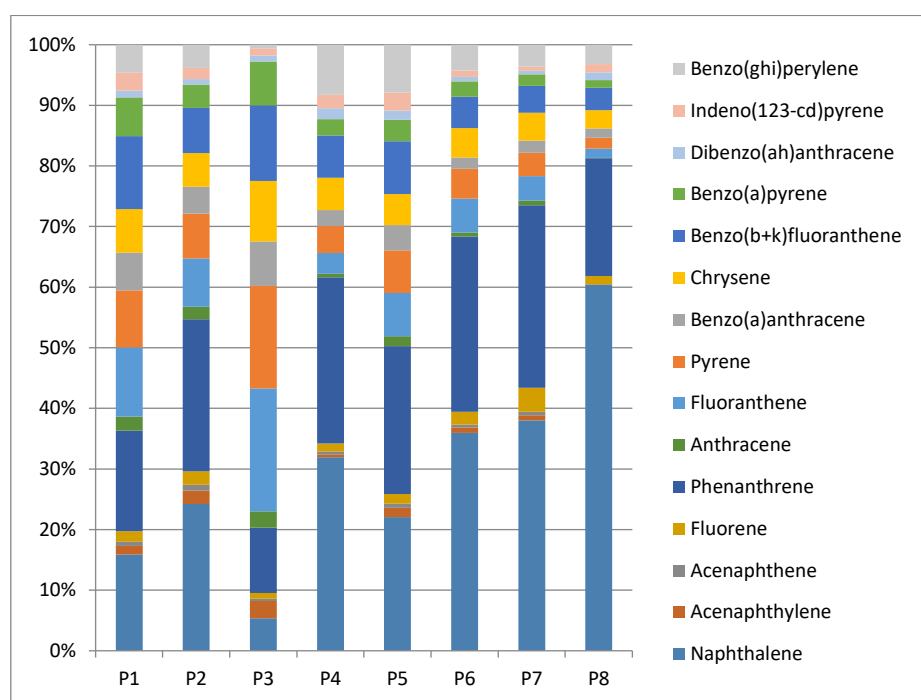


Fig. 2. Contribution (%) of each PAH to the $\Sigma 16$ PAHs.

TEFs reported by Nadal et al. (2004), and adapted from Nisbet and LaGoy (1992) and Larsen and Larsen (1998), were here applied. The BaP_{eq} concentrations of PAHs in each sampling site are summarized in Table 2. As expected, P3 showed the highest value ($1255 \mu\text{g BaP}_{\text{eq}} \text{kg}^{-1}$), being almost 700-times higher than the value in the background site ($1.80 \mu\text{g BaP}_{\text{eq}} \text{kg}^{-1}$). Considering the 7 sampling points in Pyramiden, the mean PAH concentration in soils was calculated in $221 \mu\text{g BaP}_{\text{eq}} \text{kg}^{-1}$. This is a relatively high amount in comparison to data from other impacted areas, such as a chemical/petrochemical zone in Tarragona, Spain (Nadal et al., 2004), the industrial city of Changzhi, China (Liu et al., 2017) or several residential areas in Sahibabad-Ghaziabad, India (Kumar et al., 2016). Despite naphthalene and phenanthrene were

the most abundant PAHs, their contribution to the $\Sigma\text{BaP}_{\text{eq}}$ was low (6.4% in average). In contrast, benzo(*a*)pyrene and dibenzo(*ah*)anthracene, whose contribution to $\Sigma 16$ PAHs was low (mean: 4.8%), had the greatest impact to $\Sigma\text{BaP}_{\text{eq}}$, with an aggregated contribution of 77%. The importance of heavy PAHs in the total concentration of PAHs is a new evidence that, although Svalbard is located in a remote area of the planet, it is affected by local pollution, mainly associated to the presence of power plants.

In order to assess potential emission sources of PAHs, Molecular Diagnostic Ratios (MDRs) are sometimes applied to a number of environmental matrices, including soils (Tobiszewski and Namieśnik, 2012). MDR calculations ($\text{Ant}/\text{Ant}+\text{Phe}$, $\text{Flt}/\text{Flt}+\text{Pyr}$, $\text{BaA}/\text{BaA}+\text{Chry}$, and $\text{IP}/\text{IP}+\text{BghiP}$) for the 8 soils collected in Svalbard, including typically reported values for some specific processes, are summarized in Table 3. As expected, most of these ratios pointed out combustion sources as the main contributor of PAHs in the area under study. Specifically, $\text{Flt}/\text{Flt}+\text{Pyr}$, $\text{BaA}/\text{BaA}+\text{Chry}$ and $\text{IP}/\text{IP}+\text{BghiP}$ showed a PAH pyrogenic origin, linking pollution to incomplete combustion of organic material. Contrastingly, $\text{BaA}/\text{BaA}+\text{Chry}$ in P4, P6, P7 and P8 presented a mixed source profile (pyrogenic and petrogenic). However, the petrogenic origin is not an unlikely scenario, due to the local geology and coal-mining extraction carried out in the past. Although these ratios have been satisfactorily used to identify emission sources (Agarwal et al., 2009; Plachá et al., 2009), atmospheric photoreactions prior to chemical deposition, may easily change the PAH profile (Tobiszewski and Namieśnik, 2012). In addition, $\text{Ant}/\text{Ant}+\text{Phe}$ pointed out a petrogenic source in 5 out of 7 sampling locations (P2, P4, P5, P6 and P7). However, which is less likely according to the location of those sampling sites, very close to power stations. In the past, Brändli et al. (2008) already questioned the applicability of $\text{Ant}/\text{Ant}+\text{Phe}$ ratio, since phenanthrene and naphthalene are also generated in soils by biogenic processes (Cabrerizo et al., 2011). Moreover, phenanthrene is more depleted by microbial degradation in comparison to anthracene (Enell et al., 2005; Sabaté et al., 2006), while anthracene is more quickly photodegraded than phenanthrene (Marquès et al., 2017). The different behavior between pairs of PAHs may affect diagnostic ratios. Moreover, the high photoactivity expected in soils from high latitudes, especially during the midnight sun season, may lead to the formation of PAH oxidation products, and subsequently, nitrated derivatives (Marquès et al., 2017).

Table 3. Diagnostic ratios of soils collected soils in Pyramiden (Svalbard) and typical reported values for particular processes.

	P1	P2	P3	P4	P5	P6	P7	P8	Petrogenic ²	Pyrogenic ²
Ant/Ant+Phe	0.12	0.08	0.20	0.02	0.06	0.02	0.03	0.03 ¹	<0.1	>0.1
Flt/(Flt + Pyr)	0.55	0.52	0.55	0.44	0.50	0.53	0.51	0.46	<0.4	>0.4
BaA/(BaA + Chry)	0.46	0.45	0.42	0.33	0.45	0.28	0.30	0.33	<0.2	>0.35
IP/(IP + BghiP)	0.39	0.33	0.64	0.21	0.27	0.20	0.16	0.31	<0.2	>0.2

¹ Anthracene concentration was considered LoQ/2; ² Katsoyiannis et al. (2011); Ant= anthracene; Phen=phenanthrene; Flt= fluoranthene; Pyr= pyrene; BaA= benzo(a)anthracene; Chry= chrysene; IP= indeno(123-cd)pyrene; BghiP= benzo(ghi)perylene.

Trace elements

The concentrations of trace elements in samples of soil collected in Svalbard are summarized in Table 4. All the elements showed values above their respective LODs. In general terms, the average content of trace elements was lower than the World Soil Average (WSA) (Kabata-Pendias, 2011). In addition, mean concentrations were also below the Target Values reported in the Netherlands (TVN) (ESdat, 2000) (Fig. 3). However, there existed some particular exceptions. Beryllium was found in higher amounts than the threshold value in P6 and P7 sites (1.25 and 1.61 mg kg⁻¹, respectively, being >1.1 mg kg⁻¹). In addition, Hg, Mn, Ni and Zn punctually exceeded the WSA. The levels of Hg were 0.28, 0.17 and 0.10 in P3, P6 and P7, respectively, higher than 0.07 mg kg⁻¹, which is the WSA. Manganese showed the highest values in P1 and P8 (494 and 513 mg kg⁻¹, respectively), while Ni exceeded WSA in P3 and P7 (32.9 and 30.5 mg kg⁻¹, respectively). Finally, Zn in P3 and P6 (100.1 and 120 mg kg⁻¹, respectively), and Co in P3 and P6 (10.2 and 10.6 mg kg⁻¹, respectively), were also above the TVN. The remaining trace elements (As, Cd, Cr, Cu, Mo, Sn, Tl and V) showed values below both WSA and TVN, in all the sampling points.

Table 4. The content of trace elements in soils (mg kg⁻¹) sampled in Pyramiden (Svalbard) and scientific data.

	As	Be	Cd	Co	Cr	Cu	Hg	Mn	Mo	Ni	Pb	Sn	Tl	V	Zn
P1	3.50	0.72	0.23	8.43	15.9	14.8	0.03	494	0.48	21.4	13.4	0.10	0.08	13.1	62.7
P2	2.71	0.66	0.21	8.75	16.5	14.2	0.01	350	0.42	22.5	11.9	0.05	0.09	13.6	55.5
P3	4.81	0.77	0.26	10.2	24.9	30.4	0.28	307	0.76	32.9	23.3	0.40	0.13	16.6	101
P4	3.12	0.70	0.16	8.42	13.8	18.0	0.01	347	0.35	22.2	10.6	0.05	0.12	14.2	59.7
P5	2.96	0.75	0.24	8.91	17.6	14.5	0.01	353	0.42	23.7	12.2	0.10	0.09	14.2	57.3
P6	2.58	1.25	0.27	7.90	15.6	22.6	0.17	202	0.35	22.3	25.8	0.20	0.28	17.9	120
P7	2.22	1.61	0.22	10.6	32.0	31.4	0.10	95.5	0.46	30.5	16.9	0.79	0.18	22.1	77.6
P8 (background)	1.22	0.45	0.05	3.88	8.99	10.8	0.01	513	0.12	10.5	4.84	0.01	0.16	8.19	15.9
Mean ¹	3.13	0.92	0.23	9.04	19.5	20.8	0.09	307	0.46	25.1	16.3	0.24	0.14	15.9	76.2
WSA ²	6.83	1.34	0.41	11.3	59.5	38.9	0.07	490	1.1	29	27	2.5	0.5	129	70
TVN ³	29	1.1	0.8	9	100	36	0.3	-	3	35	85	-	1	42	140
Gulińska et al. (2003)	0.03-0.2	0.0068-0.044	0.001-0.02	0.06-0.3	0.11-0.78	0.12-1.19	NA	20-80	0.00005-0.06	0.2-1	0.1-9	0.00004-0.42	0.0006-0.011	0.04-0.75	1.0-13
Wojtuń et al. (2013)	NA	NA	0.05-0.4	13-60	16-47	17-92	0.01-0.25	240-1450	NA	12.0-78	9.0-38	NA	NA	NA	70-300
Krajcarová et al. (2016)	4.46	NA	6.04	13.8	40.4	37.3	0.025	600	17.7	36.4	-	NA	NA	NA	0.08

NA= No Analyzed ² Kabata-Pendias (2011); ³ ESdat (2000)

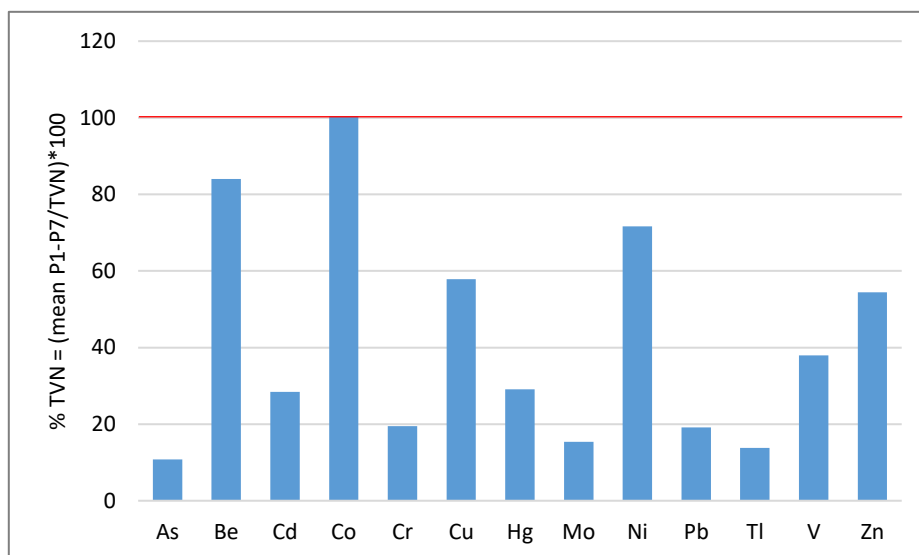


Fig. 3. Trace elements occurrence in Pyramiden soils (mean value of P1-P7) relative to their corresponding TVN. The red line shows TVN (in %).

*Not calculated for Mn and Sn because corresponding TVN values are not reported in ESdat (2000).

As it occurred with PAHs, the number of studies addressing the occurrence of trace element in polar soils is limited, being a good portion of them focused on Svalbard. Findings reported by Santos et al. (2005) when studying concentrations of some trace elements in Antarctica are in the same range as those here reported, with the exception of Ni and Mo which are two and one orders of magnitude higher and lower, respectively, in the present study. Wojtuń et al. (2013) reported levels of 35 topsoil samples (depth of 0-3 cm) from the SW of Svalbard while Krajcarová et al. (2016) analyzed the top soil (>5 cm) and deeper soil (5-10 cm) of 13 localities in the vicinity of Pyramiden and its surroundings. One decade before, Gulińska et al. (2003) showed trace elements concentrations of the uppermost 20 cm of 8 soils collected in Pyramiden as well. Despite all those studies and the present applied different methods of analysis, similar results should be provided (Pavličková et al., 2003; Sastre et al., 2002). In fact, present results are in the same range as those reported by Wojtuń et al. (2013). Trace elements under study were also comparable to Krajcarová et al. (2016), with the exception of Zn which was currently found in three orders of magnitude higher, and Cd and Mo one and two orders of magnitude lower, respectively. By contrast, results reported by Gulińska et al. (2003) are much lower

than ours, and even other published results and the world average values of metal contents in soils.

In turn, trace elements concentrations were aimed at comparing to those levels found around other power plants. Present results were in the same order as those also reported by Minkina et al. (2017) and Noli and Tsamos (2016) with the exception of Cr, which was found in one order of magnitude higher in those both studies performed in the surroundings of a Russian and Greek power plants. As, Cr and Ni concentrations from soils collected around a power plant from Turkey (Özkul, 2016) were one order of magnitude higher than ours. Finally, Hg concentrations here reported was lower by far than Hg levels found in a wide Spanish sampling campaign to assess the impact of several coal-fired power plants.

As for PAHs, the number of studies addressing the occurrence of trace elements in polar soils is very limited. However, most of them have been performed in Svalbard soils. Wojtuń et al. (2013) investigated the concentrations of trace elements in 35 topsoil samples (depth of 0-3 cm) from the SW of Svalbard, while Krajcarová et al. (2016) analyzed the top soil (>5 cm) and deeper soil (5-10 cm) in 13 sites surrounding Pyramiden. A few years before, Gulińska et al. (2003) studied the levels of trace elements in the uppermost 20 cm of soils collected in Pyramiden. Despite analytical methods were sometimes different, very similar results were obtained in all those studies, when compared to our data. The current concentrations of trace elements in Svalbard soils were actually of the same order of magnitude as those reported by Wojtuń et al. (2013), and comparable to those observed by Krajcarová et al. (2016), with only a few exceptions (e.g., Zn, Cd and Mo). By contrast, they are not in agreement with those published by Gulińska et al. (2003), who observed metal contents much lower than the rest of studies, and even lower than world average values. For comparison purposes, Santos et al. (2005) reported similar concentrations to those recently found in Svalbard, when studying trace elements in Antarctica, with the only exceptions of Ni and Mo. Because of the presence of power plants as important emission sources of chemical pollution, values were also compared with data from the scientific literature regarding areas impacted by power stations. Our results were very similar to those found by Minkina et al. (2017) and Noli and Tsamos (2016) in the surroundings of facilities in Russia and Greece, respectively. In turn, As,

Cr and Ni concentrations from soils collected around a power plant from Turkey were one order of magnitude higher than those found in Svalbard (Özkul, 2016). Finally, Hg concentrations here reported were much lower than soils levels found in a wide Spanish investigation to assess the impact of several coal-fired power plants (Rodríguez Martín and Nanos, 2016).

Two methods, the pollution load index (PLI) and the geoaccumulation index (I_{geo}), are widely applied formulas to classify the environmental degree of pollution in a specific area (Adama et al., 2016; Akoto et al., 2016; Krajcarová et al., 2016; Tian et al., 2017; Zarei et al., 2014). Such parameters are calculated according to the following formulas:

$$CF = C_m / B_m$$

$$PLI = \sqrt[n]{CF_1 \cdot CF_2 \cdot \dots \cdot CF_n}$$

$$I_{geo} = \log_2 (C_m / 1.5 \cdot B_m)$$

Where CF is the Concentration Factor, C_m is the measured concentration of the trace element m, B_m is the geochemical background of the trace element m, taken from the World Soil Average (Kabata-Pendias, 2011), and n is the number of trace elements under study.

The results of both PLI and I_{geo} indexes are summarized in Table 5, which also gives in detail the categories of classification for each one. Soil values above the unity (PLI>1) are considered as polluted, while PLI<1 is linked to non-polluted soils. Regarding to the I_{geo} parameter, Müller (1969) provided an identification and classification of soil pollution level into seven grades (Table 5). The specific value resulting from I_{geo} calculations for each element and sampling site, is included in Table S2 (Annex 5). According to I_{geo} values, P6 was slightly polluted by Zn and Hg (0.19 and 0.66 I_{geo} grades, respectively), while soil from P3 was moderately polluted by Hg (1.41 I_{geo} grade). These two sampling sites, as well as P7, were identified as the locations showing the highest PLI values (0.63, 0.52 and 0.55 in P3, P6 and P7, respectively). However, all of them were lower than 1, being all sites classified as “unpolluted”, according to the PLI. Finally, as expected, P8 presented the lowest PLI, with a value of 0.17.

Table 5. Grades of geoaccumulation index (Igeo) and the pollution load index (PLI) for all the sampling points.

Sampling point / element	Zn	Cd	Hg	As	V	Cr	Pb	Ni	Mn	Co	Sn	Tl	Be	Mo	PLI
P1	1	1	1	1	1	1	1	1	1	1	1	1	1	1	0.38
P2	1	1	1	1	1	1	1	1	1	1	1	1	1	1	0.31
P3	1	1	3	1	1	1	1	1	1	1	1	1	1	1	0.63
P4	1	1	1	1	1	1	1	1	1	1	1	1	1	1	0.32
P5	1	1	1	1	1	1	1	1	1	1	1	1	1	1	0.35
P6	2	1	2	1	1	1	1	1	1	1	1	1	1	1	0.52
P7	1	1	1	1	1	1	1	1	1	1	1	1	1	1	0.55
P8	1	1	1	1	1	1	1	1	1	1	1	1	1	1	0.17
Grade Igeo	Pollution status														
1	Unpolluted														
2	Slightly polluted														
3	Moderately polluted														
4	Moderatedly to strongly polluted														
5	Strongly polluted														
6	Strongly to extremely polluted														
7	Extremely polluted														
Grade PLI	Pollution status														
<1	Unpolluted														
>1	Polluted														

Correlation of PAHs and trace elements

Pearson correlations were performed between the levels of PAHs and those of trace elements, as well as with the organic matter content (Table S3; Annex 5). The results showed strong correlations between $\Sigma 16$ PAHs and some metals, such as Hg (0.989; $p < 0.01$), Pb (0.836; $p < 0.01$), Zn (0.769; $p < 0.05$) and Cu (0.730; $p < 0.05$), indicating a common source. It would highlight that the power plants operating in Svalbard are the main responsible of the chemical pollution in the area of study, at least in terms of PAHs and trace elements. However, notable differences between sampling sites were also found, and they cannot be explained only by the distance to the power plants. With respect to that, the organic content of soils would play a key role, as it showed a strong, significant correlation with some PAHs (i.e., naphthalene and phenanthrene) and trace elements (i.e., Mn, Pb, V, Cu, Zn, Tl and Be). Although the distance from the facilities to P1, P2, P3 and P5 sites was similar, P3 soil presented

not only the highest concentrations of PAHs, but also the highest content of organic matter among them (2.25%). In turn, despite P6 and P7 were located far away combustion processes, PAHs also occurred in relatively high concentrations. This increase could be partly due to the high accumulation capacity of soils with a high content of organic matter (4.68 and 4.08% in P6 and P7, respectively). Soil organic matter clearly plays a key role in the adsorption/retention of pollutants by soils. Finally, the specific impact of local geology and previous coal extraction should be further assessed.

CONCLUSIONS

The results of the present investigation revealed that Pyramiden (Svalbard) soils are affected by environmental pollution, primarily from local emission sources. In addition, there is a potential impact of coal deposits and extraction activities carried out in the past. Concentrations of $\Sigma 16$ PAHs reached up to $11\,600\ \mu\text{g kg}^{-1}$, being more than 200-times higher than values from a soil sample collected in a background site ($52.8\ \mu\text{g kg}^{-1}$). When expressed in terms of BaP_{eq} , the difference was even higher, being the levels 700-fold higher in the surroundings of the power stations. Furthermore, the concentrations of Hg in soils from the vicinity of the power plant were very close to threshold levels (0.28 vs. $0.3\ \text{mg kg}^{-1}$), according to Dutch Target Values. The application of the PLI pointed out that those soils were moderately polluted by Hg, with levels 4-times higher than the World Soil Average. Despite any differences in the total amount of $\Sigma 16$ PAHs in soils, all the samples showed a similar profile, being associated to a common, pyrogenic source.

These results strongly suggest the importance of environmental monitoring in remote areas of the planet. Moreover, this kind of actions should be a priority for regulators in areas where non-sustainable local emission sources are located. The complementarity of using other environmental matrices, such as air, ice/snow and biota, should be further considered. In addition, it must be highlighted that high PAH levels may lead to the formation of oxy- and nitro-PAHs, whose toxic/carcinogenic potential may be even higher than the parental compounds. Therefore, the assessment of emerging PAH derivatives is extremely important, especially in areas potentially vulnerable to soil radiation.

Aknowledgements

This study was supported by the Spanish Ministry of Economy and Competitiveness (Mineco), through the project CTM2012-33079. Montse Marquès received a PhD fellowship from AGAUR (Commissioner for Universities and Research of the Department of Innovation, Universities and Enterprise of the “Generalitat de Catalunya” and the European Social Fund) and the research mobility fellowship from NILS Science and Sustainability (ES07 – EEA Grants) ABEL-IM-2014A. The authors are indebted to Jessica Birkeland for field trip organization, Dr. Renato Igor da Silva Alves for his help with samples treatment, and Dr. Rosa Ras for her excellent guidance and assistance in GC-QqQ analysis.

References

- Abramova, A., Chernianskii, S., Marchenko, N., Terskaya, E., 2016. Distribution of polycyclic aromatic hydrocarbons in snow particulates around Longyearbyen and Barentsburg settlements, Spitsbergen. *Polar Rec.* 52, 645-659.
- Abramova, A., Marchenko, N., Terskaya, E., Comparative analysis of human impact on the environment in Arctic settlements Longyearbyen and Barentsburg (Spitsbergen). *Arct. Front.*, Tromsø, Norway, 2014.
- Adama, M., Esena, R., Fosu-Mensah, B., Yirenya-Tawiah, D., 2016. Heavy metal contamination of soils around a hospital waste incinerator bottom ash dumps site. *J. Environ. Public Health.* ID 8926453, 6 pages.
- Agarwal, T., Khillare, P. S., Shridhar, V., Ray, S., 2009. Pattern, sources and toxic potential of PAHs in the agricultural soils of Delhi, India. *J. Hazard. Mater.* 163, 1033-1039.
- Akoto, O., Nimako, C., Asante, J., Bailey, D., 2016. Heavy metals enrichment in surface soil from abandoned waste disposal sites in a hot and wet tropical area. *Environ. Process.* 3, 747-761.
- Abuquerque, M., Coutinho, M., Borrego, C., 2016. Long-term monitoring and seasonal analysis of polycyclic aromatic hydrocarbons (PAHs) measured over a decade in the ambient air of Porto, Portugal. *Sci. Total Environ.* 543, 439-448.
- Ardini, F., Bazzano, A., Rivarolo, P., Soggia, F., Terol, A., Grotti, M., 2016. Trace elements in marine particulate and surface sediments of Kongsfjorden, Svalbard Islands. *Rend. Lincei-sci Fis.* 27, 183-190.
- Bargagli, R., 2016. Atmospheric chemistry of mercury in Antarctica and the role of cryptogams to assess deposition patterns in coastal ice-free areas. *Chemosphere.* 163, 202-208.
- Bazzano, A., Ardini, F., Becagli, S., Traversi, R., Udisti, R., Cappelletti, D., Grotti, M., 2015. Source assessment of atmospheric lead measured at Ny-Ålesund, Svalbard. *Atmos. Environ.* 113, 20-26.
- Bazzano, A., Ardini, F., Grotti, M., Malandrino, M., Giacomino, A., Abollino, O., Cappelletti, D., Becagli, S., Traversi, R., Udisti, R., 2016. Elemental and lead

- isotopic composition of atmospheric particulate measured in the Arctic region (Ny-A° lesund, Svalbard Islands). *Rend. Lincei-sci Fis.* 27, 73-84.
- Bazzano, A., Rivarolo, P., Soggia, F., Ardini, F., Grotti, M., 2014. Anthropogenic and natural sources of particulate trace elements in the coastal marine environment of Kongsfjorden, Svalbard. *Mar. Chem.* 163, 28-35.
- Brändli, R. C., Bucheli, T. D., Ammann, S., Desaulles, A., Keller, A., Blum, F., Stahel, W. A., 2008. Critical evaluation of PAH source apportionment tools using data from the Swiss soil monitoring network. *J. Environ. Monit.* 10, 1278-1286.
- Cabrero, A., Dachs, J., Moeckel, C., Ojeda, M.-J., Caballero, G., Barcelo, D., Jones, K. C., 2011. Ubiquitous net volatilization of polycyclic aromatic hydrocarbons from soils and Parameters influencing their Soil-air partitioning. *Environ. Sci. Technol.* 45, 4740-4747.
- Carrasco-Navarro, V., Jæger, I., Honkanen, J. O., Kukkonen, J. V. K., Carroll, J., Camus, L., 2015. Bioconcentration, biotransformation and elimination of pyrene in the arctic crustacean *Gammarus setosus* (Amphipoda) at two temperatures. *Mar. Environ. Res.* 110, 101-109.
- Cecinato, A., Mabilia, R., Marino, F., 2000. Relevant organic components in ambient particulate matter collected at Svalbard Islands (Norway). *Atmos. Environ.* 34, 5061-5066.
- Coulson, S. J., Fjellberg, A., Melekhina, E. N., Taskaeva, A. A., Lebedeva, N. V., Belkina, O. A., Seniczak, S., Seniczak, A., Gwiazdowicz, D. J., 2015. Microarthropod communities of industrially disturbed or imported soils in the High Arctic; the abandoned coal mining town of Pyramiden, Svalbard. *Biodivers. Conserv.* 24, 1671-1690.
- Domínguez-Morueco, N., Augusto, S., Trabalón, L., Pocurull, E., Borrull, F., Schuhmacher, M., Domingo, J. L., Nadal, M., 2015. Monitoring PAHs in the petrochemical area of Tarragona County, Spain: comparing passive air samplers with lichen transplants. *Environ. Sci. Pollut. Res.*
- Enell, A., Reichenberg, F., Ewald, G., Warfvinge, P., 2005. Desorption kinetics studies on PAH-contaminated soil under varying temperatures. *Chemosphere.* 61, 1529-1538.
- ESdat, Circular on target values and intervention values for soil remediation. Annex A. Environmental Guidelines and Standards, 2000.
- Fenstad, A. A., Bustnes, J. O., Lierhagen, S., Gabrielsen, K. M., Öst, M., Jaatinen, K., Hanssen, S. A., Moe, B., Jenssen, B. M., Krøkje, Å., 2016. Blood and feather concentrations of toxic elements in a Baltic and an Arctic seabird population. *Mar. Pollut. Bull.* 114, 1152-1158.
- Frankowski, M., Ziota-Frankowska, A., 2014. Analysis of labile form of aluminum and heavy metals in bottom sediments from Kongsfjord, Isfjord, Hornsund fjords. *Environ. Earth Sci.* 71, 1147-1158.
- Ge, L., Li, J., Na, G., Chen, C.-E., Huo, C., Zhang, P., Yao, Z., 2016. Photochemical degradation of hydroxy PAHs in ice: Implications for the polar areas. *Chemosphere.* 155, 375-379.
- Gulińska, J., Rachlewicz, Szczuciński, W., Barańkiewicz, D., Kózka, M., Bulska, E., Burzyk, M., 2003. Soil contamination in high Arctic areas of human impact, central Spitsbergen, Svalbard. *Pol. J. Environ. Stud.* 12, 701-707.
- Kabata-Pendias, A., 2011. Trace elements in soils and plants. Taylor & Francis Group, Boca Raton, FL.

- Katsoyiannis, A., Sweetman, A. J., Jones, K. C., 2011. PAH molecular diagnostic ratios applied to atmospheric sources: A critical evaluation using two decades of source inventory and air concentration data from the UK. *Environ. Sci. Technol.* 45, 8897–8906.
- Khan, M. F., Latif, M. T., Lim, C. H., Amil, N., Jaafar, S. A., Dominick, D., Nadzir, M. S. M., Sahani, M., Tahir, N. M., 2015. Seasonal effect and source apportionment of polycyclic aromatic hydrocarbons in PM_{2.5}. *Atmos. Environ.* 106, 178-190.
- Konovalov, D., Renaud, P. E., Berge, J., Voronkov, A. Y., Cochrane, S. K. J., 2010. Contaminants, benthic communities, and bioturbation: Potential for PAH mobilisation in Arctic sediments. *Chem. Ecol.* 26, 197-208.
- Koroleva, N., 2014. Phytosociological evaluation of terrestrial habitat types in Pyramiden area (Svalbard, Norway). *Czech Polar Rep.* 4, 193-211.
- Krajcarová, L., Novotný, K., Chattová, B., Elster, J., 2016. Elemental analysis of soils and *Salix polaris* in the town of Pyramiden and its surroundings (Svalbard). *Environ. Sci. Pollut. Res.* 23, 10124–10137.
- Kumar, B., Verma, V. K., Kumar, S., Sharma, C. S., 2014. Polycyclic aromatic hydrocarbons in residential soils from an Indian city near power plants area and assessment of health risk for human population. *Polycycl. Aromat. Compd.* 34, 191-213.
- Kumar, B., Verma, V.K., Tyagi, J., Sharma, C.S., Akolkar, A.B., 2016. Occurrence and source apportionment of polycyclic aromatic hydrocarbons in urban residential soils from National Capital Region, Uttar Pradesh, India. *Polycycl. Aromat. Compd.* 36, 729-744.
- Larsen, J. C., Larsen, P. B., Chemical carcinogens. In: E. E. Hester, R. R. Harrison, (Eds.), *Air Pollution and Health*. The Royal Society of Chemistry, Cambridge, U.K., 1998, pp. 33-56.
- Lehmann, S., Gajek, G., Chmiel, S., Polkowska, Ž., 2016. Do morphometric parameters and geological conditions determine chemistry of glacier surface ice? Spatial distribution of contaminants present in the surface ice of Spitsbergen glaciers (European Arctic). *Environ. Sci. Pollut. Res.* 23, 23385–23405.
- Liu, G., Guo, W., Niu, J., An, X., Zhao, L., 2017. Polycyclic aromatic hydrocarbons in agricultural soils around the industrial city of Changzhi, China: characteristics, spatial distribution, hotspots, sources, and potential risks. *J. Soil. Sedim.* 17, 229-239.
- Łokas, E., Zaborska, A., Kolicka, M., Rozycki, M., Zawierucha, K., 2016. Accumulation of atmospheric radionuclides and heavy metals in cryoconite holes on an Arctic glacier. *Chemosphere.* 160, 162-172.
- Lundstedt, S., Bandowe, B. A. M., Wilcke, W., Boll, E., Christensen, J. H., Vila, J., Grifoll, M., Faure, P., Biache, C., Lorgeoux, C., Larsson, M., Frech Irgum, K., Ivarsson, P., Ricci, M., 2014. First intercomparison study on the analysis of oxygenated polycyclic aromatic hydrocarbons (oxy-PAHs) and nitrogen heterocyclic polycyclic aromatic compounds (N-PACs) in contaminated soil. *Trends Anal. Chem.* 57, 83-92.
- Ma, J., Zhang, W., Chen, Y., Zhang, S., Feng, Q., Hou, H., Chen, F., 2016. Spatial variability of PAHs and microbial community structure in surrounding surficial soil of coal-fired power plants in Xuzhou, China. *Int. J. Environ. Res. Public Health.* 13, 878.

- Marquès, M., Mari, M., Sierra, J., Nadal, M., Domingo, J. L., 2017. Solar radiation as a swift pathway for PAH photodegradation: A field study. *Sci. Total Environ.*
- Medunić, G., Ahel, M., Mihalić, I. B., Srček, V. G., Kopjare, N., Fiket, Ž., TomislavBituh, Mikac, I., 2016. Toxic airborne S, PAH, and trace element legacy of the superhigh-organic-sulphur Raša coal combustion: Cytotoxicity and genotoxicity assessment of soil and ash. *Sci. Total Environ.* 566-567, 306-319.
- Minkina, T. M., Mandzhieva, S. S., Chaplygin, V. A., Bauer, T. V., Burachevskaya, M. V., Nevidomskaya, D. G., Sushkova, S. N., Sherstnev, A. K., Zamulina, I. V., 2017. Content and distribution of heavy metals in herbaceous plants under the effect of industrial aerosol emissions. *J. Geochem. Explor.* 174, 113-120.
- Müller, G., 1969. Index of geoaccumulation in sediments of the Rhine River. *GeoJournal.* 2, 108-118.
- Nadal, M., Mari, M., Schuhmacher, M., Domingo, J. L., 2009. Multi-compartmental environmental surveillance of a petrochemical area: Levels of micropollutants. *Environ. Int.* 35, 227-235.
- Nadal, M., Marquès, M., Mari, M., Domingo, J. L., 2015. Climate change and environmental concentrations of POPs: A review. *Environ. Res.* 143, 177-185.
- Nadal, M., Schuhmacher, M., Domingo, J. L., 2004. Levels of PAHs in soil and vegetation samples from Tarragona County, Spain. *Environ. Pollut.* 132, 1-11.
- Nadal, M., Schuhmacher, M., Domingo, J. L., 2011. Long-term environmental monitoring of persistent organic pollutants and metals in a chemical/petrochemical area: Human health risks. *Environ. Pollut.* 159, 1769-1777.
- Nahrgang, J., Brooks, S. J., Evenset, A., Camus, L., Jonsson, M., Smith, T. J., Lukina, J., Frantzen, M., Giarratano, E., Renaud, P. E., 2013. Seasonal variation in biomarkers in blue mussel (*Mytilus edulis*), Icelandic scallop (*Chlamys islandica*) and Atlantic cod (*Gadus morhua*)—Implications for environmental monitoring in the Barents Sea. *Aquat. Toxicol.* 127, 21-35.
- Nisbet, I., LaGoy, P., 1992. Toxic equivalency factors (TEFs) for polycyclic aromatic hydrocarbons (PAHs). *Regul. Toxicol. Pharmacol.* 16, 290-300.
- Noli, F., Tsamos, P., 2016. Concentration of heavy metals and trace elements in soils, waters and vegetables and assessment of health risk in the vicinity of a lignite-fired power plant. *Sci. Total Environ.* 563-564, 377-385.
- Özkul, C., 2016. Heavy metal contamination in soils around the Tunçbilek Thermal Power Plant (Kütahya, Turkey). *Environ. Monit. Assess.* 188, 284.
- Page, A. L., R.H, M., D.R, K., 1985. Methods of soil analysis. Part 2. Chemical and microbiological properties. American Society of Agronomy & Soil Science Society of America, Madison, Wisconsin, USA.
- Pavličková, J., Zbiral, J., Čižmarová, E., Kubáň, V., 376:118–, A. B. C., doi:10.1007/s00216-003-1845-x, 2003. Comparison of aqua regia and HNO₃ - H₂O₂ procedures for extraction of TI and some other elements from soils. *Anal. Bioanal. Chem.* 376, 118-125.
- Perrette, Y., Poulenard, J., Durand, A., Quiers, M., Malet, E., Fanget, B., Naffrechoux, E., 2013. Atmospheric sources and soil filtering of PAH content in karst seepage waters. *Org. Geochem.* 65, 37-45.
- Plachá, D., Raclavská, H., Matýsek, D., Rummeli, M. H., 2009. The polycyclic aromatic hydrocarbon concentrations in soils in the Region of Valasske Mezirici, the Czech Republic. *Geochem. Trans.* 10, 12-33.

- Polkowska, Ż., Cichała-Kamrowska, K., Ruman, M., Koziół, K., Krawczyk, W. E., Namieśnik, J., 2011. Organic pollution in surface waters from the Fuglebekken basin in Svalbard, Norwegian Arctic. *Sensors*. 11, 8910-8929.
- Rodríguez Martín, J.A., Nanos, N., 2016. Soil as an archive of coal-fired power plant mercury deposition. *J. Hazard. Mater.* 308, 131-138.
- Rovira, J., Mari, M., Nadal, M., Schuhmacher, M., Domingo, J. L., 2010. Environmental monitoring of metals, PCDD/Fs and PCBs as a complementary tool of biological surveillance to assess human health risks. *Chemosphere*. 80, 1183-1189.
- Ruman, M., Szopinska, M., Kozak, K., Lehmann, S., Polkowska, Z., 2014. The research of the contamination levels present in samples of precipitation and surface waters collected from the catchment area Fuglebekken (Hornsund, Svalbard Archipelago). *AIP Conf. Proc.* 1618, 297.
- Sabaté, J., Viñas, M., Solanas, A. M., 2006. Bioavailability assessment and environmental fate of polycyclic aromatic hydrocarbons in biostimulated creosotecontaminated soil. *Chemosphere*. 63, 1648-1659.
- Santos, I. R., Silva-Filho, E. V., Schaefer, C. E. G. R., Albuquerque-Filho, M. R., Campos, L. S., 2005. Heavy metal contamination in coastal sediments and soils near the Brazilian Antarctic Station, King George Island. *Mar. Pollut. Bull.* 50, 185-194.
- Sapota, G., Wojtasik, B., Burska, D., Nowiński, K., 2009. Persistent Organic Pollutants (POPs) and Polycyclic Aromatic Hydrocarbons (PAHs) in surface sediments from selected fjords, tidal plains and lakes of the North Spitsbergen. *Pol. Polar Res.* 30, 59-76.
- Szczybelski, A. S., Heuvel-Greve, M. J. v. d., Kampen, T., Wang, C., Brink, N. W. v. d., Koelmans, A. A., 2016. Bioaccumulation of polycyclic aromatic hydrocarbons, polychlorinated biphenyls and hexachlorobenzene by three Arctic benthic species from Kongsfjorden (Svalbard, Norway). *Mar. Pollut. Bull.* 112, 65-74.
- Tian, K., Huang, B., Xing, Z., Hu, W., 2017. Geochemical baseline establishment and ecological risk evaluation of heavy metals in greenhouse soils from Dongtai, China. *Ecol. Indic.* 72, 510-520.
- Tobiszewski, M., Namieśnik, J., 2012. PAH diagnostic ratios for the identification of pollution emission sources. *Environ. Pollut.* 162, 110-119.
- Turetta, C., Zangrando, R., Barbaro, E., Gabrieli, J., Scalabrin, E., Zennaro, P., Gambaro, A., Toscano, G., Barbante, C., 2016. Water-soluble trace, rare earth elements and organic compounds in Arctic aerosol. *Rend. Lincei-sci Fis.* 27, 95-103.
- van den Heuvel-Greve, M. J., Szczybelski, A. S., van den Brink, N. W., Kotterman, M. J. J., Kwadijk, C. J. A. F., Evenset, A., Murk, A. J., 2016. Low organotin contamination of harbour sediment in Svalbard. *Polar Biol.* 39, 1699-1709.
- Vilavert, L., Nadal, M., Schuhmacher, M., Domingo, J. L., 2015. Two decades of environmental surveillance in the vicinity of a waste incinerator: Human health risks associated with metals and PCDD/Fs. *Arch. Environ. Contam. Toxicol.* 69, 241-253.
- Wang, J., Zhang, X., Ling, W., Liu, R., Liu, J., Kang, F., Gao, Y., 2017. Contamination and health risk assessment of PAHs in soils and crops in industrial areas of the Yangtze River Delta region, China. *Chemosphere*. 168, 976-987.
- Wang, Z., Ma, X., Na, G., Lin, Z., Ding, Q., Yao, Z., 2009. Correlations between physicochemical properties of PAHs and their distribution in soil, moss and reindeer dung at Ny-Ålesund of the Arctic. *Environ. Pollut.* 157, 3132-3136.

- Węgrzyn, M., Wietrzyk, P., Lisowska, M., Klimek, B., Nicia, P., 2016. What influences heavy metals accumulation in arctic lichen *Cetrariella delisei* in Svalbard. *Polar Sci.* 10, 532-540.
- Wojtuń, B., Samecka-Cymerman, A., Kolon, K., Kempers, A. J., Skrzypek, G., 2013. Metals in some dominant vascular plants, mosses, lichens, algae, and the biological soil crust in various types of terrestrial tundra, SW Spitsbergen, Norway. *Polar Biol.* 36, 1799–1809.
- Zarei, I., Pourkhabbaz, A., Khuzestani, R. B., 2014. An assessment of metal contamination risk in sediments of Hara Biosphere Reserve, southern Iran with a focus on application of pollution indicators. *Environ. Monit. Assess.* 186, 6047-6060.

DISCUSSION CHAPTER 6

Long Range Atmospheric Transport (LRAT) is a well known property of POPs, and also some PAHs and Hg, which may reach and be deposited in Polar regions. Pollutants can accumulate in snow and ice-packs, but also remobilized due to climate change. The increasing trend of average temperatures during the last century is causing a slow melting of glaciers. Depending on the physicochemical properties of those pollutants, they might be transported through atmospheric and ocean routes, or be *in-situ* degraded. However, the increase of human activities in remote areas is currently leading to an increase of environmental pollution in less disturbed regions. The exposure of temperature- and light- sensitive pollutants (e.g., PAHs), to sunlight makes easier their degradation and the formation of PAHs by-products. Consequently, the monitoring of pollution in Polar regions is highly valuable to establish the current level of pollution and further assess the potential impact of climate change.

Pyramiden (Central Spitsbergen, Svalbard Archipelago) is an Arctic settlement fulfilling both aforementioned situations: entrance of pollutants due to LRAT, local contamination derived from coal deposits and previous mining extraction, and currently operative power plants. In addition to PAHs, trace elements were also analyzed to confirm the hypothesis of local pollution sources. In general terms, trace elements in soils were lower than reference values, although some of them (Be, Co, Hg, Mn, Ni and Zn) punctually exceeded threshold levels. The sampling sites with the $\Sigma 16$ PAHs concentrations also presented the greatest values of trace elements. The high concentrations of PAHs and trace elements in soils were found to be dependent on the distance to the power plants, the prevailing winds (ENE and N), and the organic matter content. PAHs profiles and MDRs of all sampling points mostly demonstrated a pyrogenic source. In turn, correlations between $\Sigma 16$ PAHs and Hg, Pb, Zn and Cu confirmed the anthropogenic nature of the contamination. Hence, the occurrence of PAHs and trace elements occurrence in Pyramiden might probably be related to the local contamination derived from power plants, although the contribution of coal deposits should not be disregarded.

The significant pollution of the studied area strongly suggests it is important to continue with the environmental monitoring in such remote region. PAHs are able to travel long distances and, therefore, PAHs might be spread around the Arctic. In

addition, the occurrence of PAHs derivatives should be further investigated because they are formed during combustion processes. Finally, PAHs found in soil surface once exposed to light are photodegraded, and in turn, PAHs by-products are generated. Thus, the 24h/day sunlight exposure during the midnight sun season might probably be an important pathway for their formation in the Arctic.

GENERAL DISCUSSION

In recent years, the impact of climate change on the concentrations of persistent organic pollutants (POPs) has become a topic of notable concern. Some PAHs are classified as POPs, according to the Aarhus protocol. Moreover, PAHs are well known photosensitive substances, and hence, potentially vulnerable to climate change.

The present thesis was aimed at investigating the impact of increasing temperature and light intensity on the fate of PAHs, after their deposition on typically Mediterranean soils. The monitoring of PAHs concentrations and ecotoxicity, as well as the identification of PAHs photodegradation by-products, was carried out at laboratory scale by the simulation of 2 climate scenarios: current and extreme (RCP 8.5) for the Mediterranean region, considering estimations from the IPCC. Field experiments were performed to compare lab-controlled and natural conditions. On one hand, the photodegradation of PAHs caused by solar radiation in a Mediterranean area was assessed. On the other hand, PAHs levels were measured in soils collected in Pyramiden (Svalbard Archipelago), as another vulnerable location to climate change.

It was confirmed that the increase of temperature and light intensity due to climate change may impact on the fate of PAHs, by enhancing their volatilization, photodegradation and, in turn, their capability to be transformed into PAHs by-products. Temperature increase led to an acceleration of LMW PAHs volatilization, while soil properties were a key factor controlling the photodegradation of MMW and HMW PAHs. In fine-textured Regosol soil, they underwent similar photodegradation rates, regardless the climate scenario. In contrast, the photodegradation of these PAHs was more significant in Arenosol soil under the climate change scenario. In both soils, the increase of temperature and light intensity enhanced the formation of oxidation PAHs by-products. Microtox® results showed a higher soil detoxification in the climate change scenario than under current climate conditions. However, slight increases of toxicity over the decreasing trend were noted, which may probably be related to the formation of more toxic and bioavailable by-products.

Differences between photodegradation trends of PAHs in Arenosol and fine-textured Regosol soils were explained by the potential role of metal oxides as photocatalysts of PAHs photodegradation. It was hypothesized that the lower the content of metal oxides is, the higher the required activation energy is to achieve a

full PAHs photodegradation. In contrast, higher amounts of metal oxides in soils, such as the fine-textured Regosol soil, do not require a high activation energy to reach a complete photodegradation of PAHs. However, when assessing the role of Fe_2O_3 – the most abundant metal oxide in both tested soils – as a PAHs photocatalyst, it was found that this metal oxide is not the only responsible for PAHs photodegradation. Soil is a complex matrix with several elements (e.g., metal oxides, acid humics, and texture), each one with a different potential role on the PAHs fate.

As expected, PAHs half-lives in the field were significantly shorter than at laboratory scale due to the higher temperatures and intensity of radiation. In addition, the wider spectra of sunlight than that of light lamps may enhance the photodegradation of PAHs. Notwithstanding, the effect of other co-occurring processes (e.g., biodegradation) should not be disregarded. Especially high photodegradation rates and low soil half-lives were noted for fluorene, anthracene, pyrene and benzo(*a*)pyrene. In addition, the formation of some oxidation compounds previously identified at laboratory scale was accelerated, while other photodegradation by-products (e.g., 1-nitropyrene, 6-nitrobenzo(*a*)pyrene, and benzo(*a*)pyrene-7,8-dihydro) were identified.

Interestingly, all tests highlighted the especially high photodegradation rate observed for benzo(*a*)pyrene, regardless of the environmental conditions and tested soils. This fact could be related with the ionization potential (IP) of this compound. IP measures the difficulty of removing an electron or the strength by which an electron is bound, and therefore, provides the degree of reactivity. Benzo(*a*)pyrene is the single hydrocarbon among PAH under study which owns the lowest IP. Therefore, it is the PAH which can be most easily and quickly degraded. This finding highlights the limitation of using this compound as a single marker for PAHs pollution and regulation. Benzo(*a*)pyrene is generally used as a marker of PAHs pollution. However, its differential behaviour with respect to other PAHs requires the need to investigate the co-occurrence of other hydrocarbons, especially in terms of decision-making and policy development. Finally, the electron distribution over the PAH determines the most reactive positions of the molecule, which in turn, agrees with the localization of oxy- and nitro- radicals of by-products here identified.

A soil sampling campaign was carried out in the Arctic, one of the most vulnerable regions to climate change. Polar regions are especially affected by POP contamination, because of the LRAT capacity of these environmental contaminants. In addition, local emission spotlights may increase pollution levels in these areas. Substantially high PAHs levels were found in soils collected in Svalbard. This showed mostly pyrogenic sources of contamination and significant correlations with trace elements. Coal- and diesel- based power plants were pointed out as the important sources of soil pollution, although the contribution of coal deposits due to the local geology should not be disregarded. As a consequence of the wide light exposure during midnight sun season and the increase of solar intensity, especially that belonging to UV-B radiation, temperature- and radiation- dependent changes linked to the climate change may involve PAHs changes in surface soils and the generation of PAHs by-products.

The physicochemical properties of PAHs and the soil properties are key factors determining the PAHs fate in surface soils. Climate change conditions will enhance the volatilization of LMW PAHs and the photodegradation of MMW and HMW PAHs in soils with coarse texture and low metal oxides content. While volatilization and photodegradation are expected to decrease of PAHs concentrations in surface soils, oxidation and nitrification reactions may arise the levels of oxy- and nitro- PAHs. These PAHs derivatives own lower lipophilicity, and therefore, higher mobility and bioavailability. Furthermore, they are potentially more toxic than their parent PAHs. Unfortunately, these PAHs by-products are unregulated and environmental surveillance programs do not usually monitor they occurrence, being 16 US EPA priority PAHs the most commonly assessed. As the regulation of PAHs derivatives is very important, it would be necessary to develop new procedures considering different climate projections.

CONCLUSIONS

Specific conclusions

1. Physicochemical properties of each PAH and soil properties are the 2 key factors regulating PAHs photodegradation in soils.
2. Climate change will enhance the volatilization of LMW PAHs in either Arenosol or fine-textured Regosol soil, and the photodegradation of MMW and HMW PAHs in Arenosol soil.
3. Oxidation reactions were accelerated under a climate change scenario, being the photodegradation by-products more diversely formed than in the current Mediterranean environmental conditions.
4. Volatilization, sorption and photodegradation of PAHs in surface soils led to a decrease of PAHs concentrations, and therefore, soils were detoxified over time. The toxic decline was more remarkable in the climate change scenario. However, punctual increases of toxicity, which were related with the formation of more bioavailable and toxic photodegradation by-products, were noted.
5. Fe_2O_3 has a role on the photocatalysis of the most photosensitive PAHs (e.g., fluorene, phenanthrene and benzo(*a*)pyrene). However, other components of soil, which is a complex matrix with several elements (different metal oxides, humic acids and a specific texture), are also involved on PAHs fate in surface soils.
6. Higher photodegradation rates, lower PAHs half-lives and a wider range of PAHs by-products were reported in the field than at lab scale.
7. Benzo(*a*)pyrene was the most degraded compound in all experiments. This fact agrees with its low ionization potential, and therefore, the high reactivity of this compound. Consequently, there is a clear limitation in the use and regulation of benzo(*a*)pyrene as a single indicator for PAHs pollution.
8. Because of the local geology, previous coal-mining extraction, and power plants located in Pyramiden (Svalbard archipelago, Arctic), soils were greatly polluted by PAHs and some trace elements. The light exposure during midnight sun season, and the increase of temperature and light intensity due to the climate change, may enhance PAHs photodegradation, leading to an increase in by-products occurrence.

9. There is a clear need to include PAHs derivatives in environmental surveillance programs and regulations, as their occurrence will arise as a consequence of the climate change.

General conclusion

The expected increase of temperature and light intensity derived from climate change will impact differently on the fate of PAHs depending on soil characteristics. LMW PAHs will be more easily volatilized, while the photodegradation of MMW and HMW will be enhanced in soils with coarse texture and low metal oxides content. In addition, a wide range of PAHs by-products will be more rapidly formed. The emergence of PAHs photodegradation derivatives in soils poses a hazard for the ecosystems and human health due to their potential bioavailability and/or toxicity, becoming their regulation and monitoring even more necessary in a climate change context.

REFERENCES

REFERENCES

- Abdel-Shafy, H. I., Mansour, M. S. M., 2016. A review on polycyclic aromatic hydrocarbons: Source, environmental impact, effect on human health and remediation. *Egypt. J. Petrol.* 25, 107-123.
- Amjadian, K., Sacchi, E., Mehr, M. R., 2016. Heavy metals (HMs) and polycyclic aromatic hydrocarbons (PAHs) in soils of different land uses in Erbil metropolis, Kurdistan Region, Iraq. *Environ. Monit. Assess.* 188, 605.
- Augusto, S., Pereira, M. J., Máguas, C., Branquinho, C., 2013. A step towards the use of biomonitors as estimators of atmospheric PAHs for regulatory purposes. *Chemosphere* 92, 626-632.
- Balmer, M. E., Goss, K.-U., Schwarzenbach, R. P., 2000. Photolytic transformation of organic pollutants on soil surfaces - An experimental approach. *Environ. Sci. Technol.* 34, 1240-1245.
- Bangash, R. F., Passuello, A., Hammond, M., Schuhmacher, M., 2012. Water allocation assessment in low flow river under data scarce conditions: A study of hydrological simulation in Mediterranean basin. *Sci. Total Environ.* 440, 60-71.
- Bertilsson, S., Widenfalk, A., 2002. Photochemical degradation of PAHs in freshwaters and their impact on bacterial growth – influence of water chemistry. *Hydrobiologia* 469, 23-32.
- Borrás, E., Ródenas, M., Vázquez, M., Vera, T., Muñoz, A., 2015. Particulate and gas-phase products from the atmospheric degradation of chlorpyrifos and chlorpyrifos-oxon. *Atmos. Environ.* 123, 112-120.
- Cabrerizo, A., Dachs, J., Moeckel, C., Ojeda, M.-J., Caballero, G., Barceló, D., Jones, K. C., 2011. Ubiquitous net volatilization of Polycyclic Aromatic Hydrocarbons from soils and parameters influencing their soil air partitioning. *Environ. Sci. Technol.* 45, 4740-4747.
- Cai, J. J., Song, J. H., Lee, Y., Lee, D. S., 2014. Assessment of climate change impact on the fates of polycyclic aromatic hydrocarbons in the multimedia environment based on model prediction. *Sci. Total Environ.* 470-471, 1526-1536.
- Cuadras, A., Rovira, E., Marcé, R. M., Borrull, F., 2016. Lung cancer risk by polycyclic aromatic hydrocarbons in a Mediterranean industrialized area. *Environ. Sci. Pollut. Res.* 23, 23215-23227.
- Chao, H. R., Huang, H. L., Hsu, Y. C., Lin, C. W., Lin, D. Y., Gou, Y. Y., Chen, K. C., 2014. Impact of brominated POPs on the neurodevelopment and thyroid hormones of young children in an indoor environment-A review. *Aerosol Air Qual. Res.* 14, 1320-1332.
- de Bruyn, W. J., Clark, C. D., Ottelle, K., Aiona, P., 2012. Photochemical degradation of phenanthrene as a function of natural water variables modeling freshwater to marine environments. *Mar. Pollut. Bull.* 64, 532-538.
- Domingo, J. L., 2012. Polybrominated diphenyl ethers in food and human dietary exposure: A review of the recent scientific literature. *Food Chem. Toxicol.* 50, 238-249.
- EPA, 2017. Polycyclic Aromatic Hydrocarbons (PAHs) Fact Sheet. Viewed 2 February 2017. https://www.epa.gov/sites/production/files/2014-03/documents/pahs_factsheet_cdc_2013.pdf.

- European Commission. Commission Recommendation 2005/108/EC. Off. J. Eur. Comm. L34, 43.
- European Commission. Directive 98/83/EC of the European Parliament and of the Council of 3 November 1998 on the quality of water intended for human consumption. Off. J. Eur. Comm. L330, 32-54.
- European Commission. Directive 2004/107/EC of the European Parliament and of the Council of 15 December 2004 relating to arsenic, cadmium, mercury, nickel and PAH in ambient air. Off. J. Eur. Comm. L 23, 3-16.
- European Commission. Commission Regulation (EC) No 835/2011 of 19 August 2011 amending Regulation (EC) No 1881/2006 as regards maximum levels for polycyclic aromatic hydrocarbons in foodstuffs. Off. J. Eur. Comm. L215, 4-8.
- European Commission. Commission Regulation (EC) No 1881/2006 of 19 December 2006 setting maximum levels for certain contaminants in foodstuffs. Off. J. Eur. Comm. L364, 2-5.
- Fasnacht, M. P., Blough, N. V., 2003. Mechanisms of the aqueous photodegradation of Polycyclic Aromatic Hydrocarbons. *Environ. Sci. Technol.* 37, 5767-5772.
- Frank, M. P., Graebing, P., Chib, J. S., 2002. Effect of soil moisture and sample depth on pesticide photolysis. *J. Agric. Food Chem.* 50, 2607-2614.
- Fu, P. P., Xia, Q., Sun, X., Yu, H., 2012. Phototoxicity and environmental transformation of polycyclic aromatic hydrocarbons (PAHs)-light-induced reactive oxygen species, lipid peroxidation, and DNA damage. *J. Environ. Sci. Health Part C Environ. Carcinog. Ecotoxicol. Rev.* 30, 1-41.
- Gao, J., Ma, C., Xing, S., Zhang, Y., Liu, J., Feng, H., 2016. Particle- and gas-phase PAHs toxicity equivalency quantity emitted by a non-road diesel engine with non-thermal plasma technology. *Environ. Sci. Pollut. Res.* 23, 20017-20026.
- García-Martínez, M. J., Canoira, L., Blázquez, G., Da Riva, I., Alcántara, R., Llamas, J. F., 2005. Continuous photodegradation of naphthalene in water catalyzed by TiO₂ supported on glass Raschig rings. *Chem. Eng. J.* 110, 123-128.
- Gascón, M., Morales, E., Sunyer, J., Vrijheid, M., 2013. Effects of persistent organic pollutants on the developing respiratory and immune systems: A systematic review. *Environ. Int.* 52, 51-65.
- Ghosal, D., Ghosh, S., Dutta, T., Ahn, Y., 2016. Current state of knowledge in microbial degradation of polycyclic aromatic hydrocarbons (PAHs): A review. *Front. Microbiol.* 7, 1369.
- Giorgi, F., Lionello, P., 2008. Climate change projections for the Mediterranean region. *Glob. Planet. Chang.* 63, 90-104.
- Gong, A., Ye, C., Wang, X., Lei, Z., Liu, J., 2001. Dynamics and mechanism of ultraviolet photolysis of atrazine on soil surface. *Pest Manage. Sci.* 57, 380-385.
- Grandjean, P., Landrigan, P., 2006. Developmental neurotoxicity of industrial chemicals. *The Lancet* 368, 2167-78.
- Grung, M., Petersen, K., Fjeld, E., Allan, I., Christensen, J. H., Malmqvist, L. M. V., Meland, S., Rannekleiv, S., 2016. PAH related effects on fish in sedimentation ponds for road runoff and potential transfer of PAHs from sediment to biota. *Sci. Total Environ.* 566-567, 1309-1317.
- Gulińska, J., Rachlewicz, Szczuciński, W., Barańkiewicz, D., Kózka, M., Bulska, E., Burzyk, M., 2003. Soil contamination in high Arctic areas of human impact, central Spitsbergen, Svalbard. *Pol. J. Environ. Stud.* 12, 701-707.

- Gupta, H., Gupta, B., 2015. Photocatalytic degradation of polycyclic aromatic hydrocarbon benzo(a)pyrene by iron oxides and identification of degradation products. *Chemosphere* 138, 924-931.
- Gusev, A., MacLeod, M., Bartlett, P., 2012. Intercontinental transport of persistent organic pollutants: A review of key findings and recommendations of the task force on hemispheric transport of air pollutants and directions for future research. *Atmos. Pollut. Res.* 3, 463-465.
- Haritash, A. K., Kaushik, C. P., 2009. Biodegradation aspects of Polycyclic Aromatic Hydrocarbons (PAHs): A review. *J. Hazard. Mater.* 169, 1-15.
- Hung, H., MacLeod, M., Guardans, R., Scheringer, M., Barra, R., Harner, T., Zhang, G., 2013. Toward the next generation of air quality monitoring: Persistent organic pollutants. *Atmos. Environ.* 80, 591-598.
- IARC, 2013. Air Pollution and Cancer. Chapter 7: Polycyclic Aromatic Hydrocarbons in ambient air and cancer. International Agency for Research on Cancer, Lyon, France.
- IARC, 2017. IARC Monographs on the Evaluation of Carcinogenic Risks to Humans. International Agency for Research on Cancer, Lyon, France.
- IPCC, 2013. Climate Change 2013: The Physical Science Basis. Contribution of Working Group I to the Fifth Assessment Report of the Intergovernmental Panel on Climate Change. Cambridge University Press, Cambridge, United Kingdom and New York, NY, USA. pp. 1535.
- Jacobs, L. E., Weavers, L. K., Chin, Y., 2008. Direct and indirect photolysis of polycyclic aromatic hydrocarbons in nitrate-rich surface waters. *Environ. Toxicol. Chem.* 27, 1643-1648.
- Jayawardena, A. W., 2014. Climate change - is it the cause or the effect? *KSCE J. Civ. Eng.* 19, 359-365.
- Jia, H., Zhao, J., Li, L., Li, X., Wang, C., 2014. Transformation of polycyclic aromatic hydrocarbons (PAHs) on Fe(III)-modified clay minerals: Role of molecular chemistry and clay surface properties. *Appl. Catal., B* 154-155, 238-245.
- Jing, L., Chen, B., Zhang, B., Zheng, J., Liu, B., 2014. Naphthalene degradation in seawater by UV irradiation: The effects of fluence rate, salinity, temperature and initial concentration. *Mar. Pollut. Bull.* 81, 149-156.
- Kallenborn, R., Halsall, C., Dellong, M., Carlsson, P., 2012. The influence of climate change on the global distribution and fate processes of anthropogenic persistent organic pollutants. *J. Environ. Monit.* 14, 2854-2869.
- Keyte, I. J., Harrison, R. M., Lammel, G., 2013. Chemical reactivity and long-range transport potential of polycyclic aromatic hydrocarbons – a review. *Chem. Soc. Rev.* 42, 9333.
- Kim, S., Park, J., Kim, H. J., Lee, J. J., Choi, G., Choi, S., Kim, S., Kim, S. Y., Moon, H. B., Kim, S., Choi, K., 2013. Association between several persistent organic pollutants and thyroid hormone levels in serum among the pregnant women of Korea. *Environ. Int.* 59, 442-448.
- Law, R., Brant, J., Kirby, M., Lee, J., Morris, D., Rees, J., Guidelines for the environmental monitoring and impact assessment associated with subsea oil releases and dispersant use in UK waters. Technical Guideline No. 08 - Processing and analysis of water, biota and sediment samples for the determination of hydrocarbon contamination using gas chromatography - mass spectrometry. Science Series Technical Report, Vol. 153, Cefas, Lowestoft, 2014.

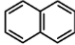
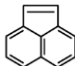
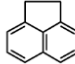
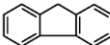
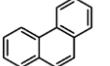
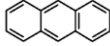
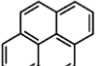
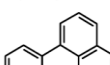
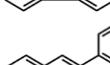
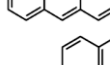
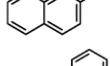
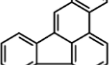
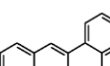
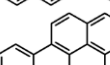
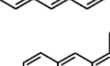
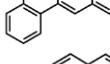
- Li, A., Tanabe, S., Jiang, G., Giesy, J. P., Lam, P. K. S., 2011. Persistent organic pollutants in Asia: Sources, distributions, transport and fate. *Developments in Environmental Science*. Elsevier Science. pp. 842.
- Luo, L., Wang, P., Lina, L., Luana, T., Keb, L., Fung Yee Tam, N., 2014. Removal and transformation of high molecular weight polycyclic aromatic hydrocarbons in water by live and dead microalgae. *Process Biochem.* 49, 1723-1732.
- Ma, W. L., Li, Y. F., Sun, D. Z., Qi, H., 2009. Polycyclic aromatic hydrocarbons and polychlorinated biphenyls in topsoils of Harbin, China. *Arch. Environ. Contam. Toxicol.* 57, 670-678.
- Ma, Y., Xie, Z., Yang, H., Möller, A., Halsall, C., Cai, M., Sturm, R., Ebinghaus, R., 2013. Deposition of polycyclic aromatic hydrocarbons in the North Pacific and the Arctic. *J. Geophys. Res.* 118, 5822-5829.
- Majumdar, D., Rajaram, B., Meshram, S., Suryawanshi, P., Chalapati Rao, C. V., 2017. Worldwide distribution of polycyclic aromatic hydrocarbons in urban road dust. *Int. J. Environ. Sci. Tech.* 14, 397-420.
- Manzetti, S., 2013. Polycyclic Aromatic Hydrocarbons in the environment: Environmental fate and transformation. *Polycyclic Aromat. Compd.* 33, 311-330.
- Mu, X., Zhu, X., Wang, X., An Emission Inventory of Polycyclic Aromatic Hydrocarbons in China. EGU, Vol. 17. EGU General Assembly. Geophysical Research Abstracts, 2015.
- Muñoz, A., Vera, T., Ródenas, M., Borrás, E., Mellouki, A., Treacy, J., Sidebottom, H., 2014. Gas-phase degradation of the herbicide ethalfluralin under atmospheric conditions. *Chemosphere* 95, 395-401.
- Nadal, M., Schuhmacher, M., Domingo, J. L., 2004. Levels of PAHs in soil and vegetation samples from Tarragona County, Spain. *Environ. Pollut.* 132, 1-11.
- Nadal, M., Schuhmacher, M., Domingo, J. L., 2011. Long-term environmental monitoring of persistent organic pollutants and metals in a chemical/petrochemical area: Human health risks. *Environ. Pollut.* 159, 1769-1777.
- Nadal, M., Wargent, J. J., Jones, K. C., Paul, N. D., Schuhmacher, M., Domingo, J. L., 2006. Influence of UV-B radiation and temperature on photodegradation of PAHs: Preliminary results. *J. Atmos. Chem.* 55, 241-252.
- Nielsen, K., Kalmykova, Y., Strömvall, A.-M., Baun, A., Eriksson, E., 2015. Particle phase distribution of polycyclic aromatic hydrocarbons in stormwater — Using humic acid and iron nano-sized colloids as test particles. *Sci. Total Environ.* 532, 103-111.
- Noyes, P. D., McElwee, M. K., Miller, H. D., Clark, B. W., Van Tiem, L. A., Walcott, K. C., Erwin, K. N., Levin, E. D., 2009. The toxicology of climate change: Environmental contaminants in a warming world. *Environ. Int.* 35, 971-986.
- Pereira, K. L., Hamilton, J. F., Rickard, A. R., Bloss, W. J., M.S, A., Camredon, M., Ward, M. W., Wyche, K. P., Muñoz, A., Vera, T., Vázquez, M., Borrás, E., Ródenas, M., 2015. Insights into the formation and evolution of individual compounds in the particulate phase during aromatic photo-oxidation. *Environ. Sci. Technol.* 49, 13168-13178.
- Perra, G., Renzi, M., Guerranti, C., Focardi, S. E., 2009. Polycyclic aromatic hydrocarbons pollution in sediments: distribution and sources in a lagoon system (Orbetello, Central Italy). *Transit. Water. Bull.* 3, 45-58.
- Pierzynski, G., Sims, J., Vance, G., 2000. *Soils and environmental quality*, Second Edition. CRC Press, Boca Raton, FL.

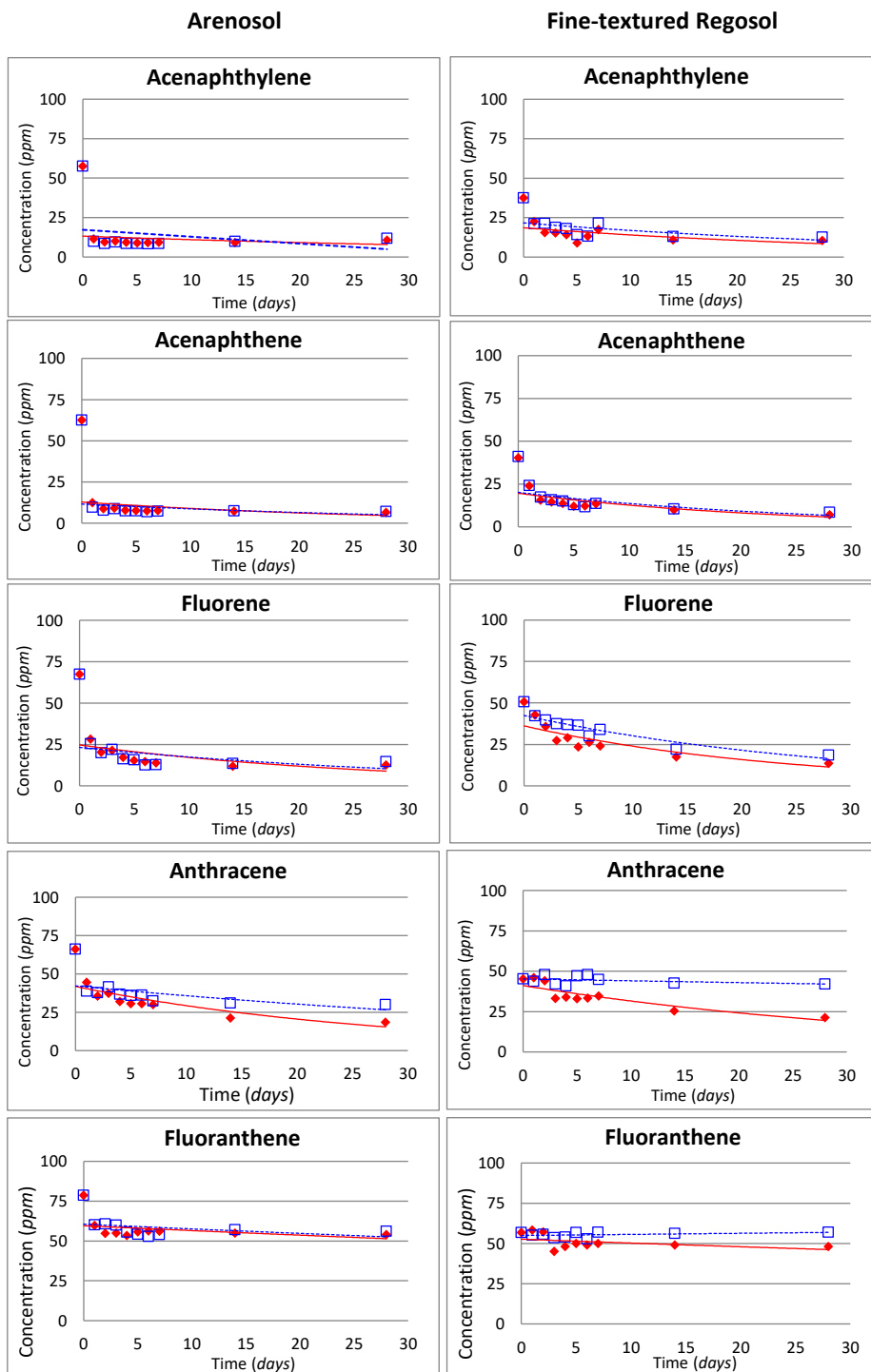
- Rivas, F. J., Beltran, F. J., Acedo, B., 2000. Chemical and photochemical degradation of acenaphthylene. Intermediate identification. *J. Hazard. Mater.* B75, 89-98.
- Sánchez-Canales, M., López Benito, A., Passuello, A., Terrado, M., Ziv, G., Acuña, V., Schuhmacher, M., Elorza, F. J., 2012. Sensitivity analysis of ecosystem service valuation in a Mediterranean watershed. *Sci. Total Environ.* 440, 140-153.
- Schiedek, D., Sundelin, B., Readman, J. W., Macdonald, R. W., 2007. Interactions between climate change and contaminants. *Mar. Pollut. Bull.* 54, 1845-1856.
- Schröter, D., Cramer, W., Leemans, R., Prentice, I. C., Araújo, M. B., Arnell, N. W., Bondeau, A., Bugmann, H., Carter, T. R., Gracia, C. A., de La Vega-Leinert, A. C., Erhard, M., Ewert, F., Glendining, M., House, J. I., Kankaanpää, S., Klein, R. J. T., Lavorel, S., Lindner, M., Metzger, M. J., Meyer, J., Mitchell, T. D., Reginster, I., Rounsevell, M., Sabaté, S., Sitch, S., Smith, B., Smith, J., Smith, P., Sykes, M. T., Thonicke, K., Thuiller, W., Tuck, G., Zaehle, S., Zierl, B., 2005. Ecology: Ecosystem service supply and vulnerability to global change in Europe. *Science* 310, 1333-1337.
- Serreze, M. C., Barry, R. G., 2011. Processes and impacts of Arctic amplification: a research synthesis. *Glob. Planet. Chang.* 77, 85-96.
- Shemer, H., Linden, K. G., 2007. Aqueous photodegradation and toxicity of the polycyclic aromatic hydrocarbons fluorene, dibenzofuran, and dibenzothiophene. *Water Res.* 41, 853-861.
- Siciliano, S. D., Laird, B. D., Lemieux, C. L., 2010. Polycyclic aromatic hydrocarbons are enriched but bioaccessibility reduced in brown field soils adhered to human hands. *Chemosphere* 80, 1101-1108.
- Singh, P., Mondal, K., Sharma, A., 2013. Reusable electrospun mesoporous ZnO nanofiber mats for photocatalytic degradation of polycyclic aromatic hydrocarbon dyes in wastewater. *J. Colloid Interface Sci.* 394, 208-215.
- Stogiannidis, E., Laane, R., 2014. Source characterization of polycyclic aromatic hydrocarbons by using their molecular indices: An overview of possibilities. *Rev. Environ. Contam. Toxicol.* 234, 49-133.
- Tao, S., Shen, H., Wang, R., HUANG, Y., Global PAH emission inventory. College of Urban and Environmental Sciences, Peking University, 2012.
- Teran, T., Lamon, L., Marcomini, A., 2012. Climate change effects on POPs' environmental behaviour: A scientific perspective for future regulatory actions. *Atmos. Pollut. Res.* 3, 466-476.
- Terrado, M., Acuña, V., Ennaanay, D., Tallis, H., Sabater, S., 2014. Impact of climate extremes on hydrological ecosystem services in a heavily humanized Mediterranean basin. *Ecol. Indic.* 37, 199-209.
- Thavamani, P., Megharaj, M., Krishnamurti, G. S. R., McFarland, R., Naidu, R., 2011. Finger printing of mixed contaminants from former manufactured gas plant (MGP) site soils: implications to bioremediation. *Environ. Int.* 37, 184-189.
- Tobiszewski, M., Namieśnik, J., 2012. PAH diagnostic ratios for the identification of pollution emission sources. *Environ. Pollut.* 162, 110-119.
- van der Bilt, W. G. M., Bakke, J., Vasskog, K., D'Andrea, W. J., Bradley, R. S., Ólafsdóttir, S., 2015. Reconstruction of glacier variability from lake sediments reveals dynamic Holocene climate in Svalbard. *Quatern. Sci. Rev.* 126, 201-218.
- Vera, T., Borrás, E., Chen, J., Coscollá, C., Daële, V., Mellouki, A., Ródenas, M., Sidebottom, H., Sun, X., Yusá, V., Zhang, X., Muñoz, A., 2015. Atmospheric

- degradation of lindane and 1,3-dichloroacetone in the gas phase. Studies at the EUPHORE simulation chamber. *Chemosphere* 138, 112-119.
- Vijayalakshmi, K. P., Suresh, C. H., 2008. Theoretical studies on the carcinogenicity of polycyclic aromatic hydrocarbons. *J. Comput. Chem.* 29, 1808-1817.
- Vingiani, S., Nicola, F. D., Purvis, W. O., Concha-Graña, E., Muniategui-Lorenzo, S., López-Mahía, P., Giordano, S., Adamo, P., 2015. Active biomonitoring of heavy metals and PAHs with mosses and lichens: A case study in the cities of Naples and London. *Water Air Soil Pollut.* 226:240.
- Wang, C., Wang, X., Gong, P., Yao, T., 2014. Polycyclic aromatic hydrocarbons in surface soil across the Tibetan Plateau: Spatial distribution, source and airesoil exchange. *Environ. Pollut.* 184, 138-144.
- Wojtuń, B., Samecka-Cymerman, A., Kolon, K., Kempers, A. J., Skrzypek, G., 2013. Metals in some dominant vascular plants, mosses, lichens, algae, and the biological soil crust in various types of terrestrial tundra, SW Spitsbergen, Norway. *Polar Biol.* 36, 1799-1809.
- Xia, X., Li, G., Yang, Z., Chen, Y., Huang, G. H., 2009. Effects of fulvic acid concentration and origin on photodegradation of polycyclic aromatic hydrocarbons in aqueous solution: Importance of active oxygen. *Environ. Pollut.* 157, 1352-1359.
- Xiaozhen, F., Boa, L., Aijun, G., 2005. Dynamics of solar light photodegradation behavior of atrazine on soil surface. *J. Hazard. Mater.* B117.
- Yu, H., 2002. Environmental carcinogenic polycyclic aromatic hydrocarbons: Photochemistry and phototoxicity. *J. Environ. Sci. Health Part C Environ. Carcinog. Ecotoxicol. Rev.* 20, 149-183.
- Zelinkova, Z., Wenzl, T., 2015. The occurrence of 16 EPA PAHs in food - A review. *Polycyclic Aromat. Compd.* 35, 248-284.
- Zhang, G., Pan, Z., Wang, X., Mo, X., Li, X., 2015. Distribution and accumulation of polycyclic aromatic hydrocarbons (PAHs) in the food web of Nansi Lake, China. *Environ. Monit. Assess.* 187, 173.
- Zhang, L., Li, P., Gong, Z., Li, X., 2008. Photocatalytic degradation of polycyclic aromatic hydrocarbons on soil surfaces using TiO₂ under UV light. *J. Hazard. Mater.* 158, 478-494.
- Zhang, L., Xua, C., Chena, Z., Li, X., Li, P., 2010. Photodegradation of pyrene on soil surfaces under UV light irradiation. *J. Hazard. Mater.* 173, 168-172.
- Zhang, L. H., Li, P. J., Gong, Z. Q., Oni, A. A., 2006. Photochemical behavior of benzo[a]pyrene on soil surfaces under UV light irradiation. *J. Environ. Sci.* 18, 1226-1232.
- Zhang, Y., Tao, S., 2009. Global atmospheric emission inventory of polycyclic aromatic hydrocarbons (PAHs) for 2004. *Atmos. Environ.* 43, 812-819.

ANNEX

ANNEX 1 – Supporting information chapter 2**Table S1.** Physico-chemical properties of the 16 US EPA priority PAHs.

Compound	Structure	CAS n.	MW	Log K_{ow}	Vapor Pressure (at 25°C)
Naphthalene		91-20-3	128	3.37	0.087 mm Hg
Acenaphthylene		208-96-8	152	4.00	9.12×10^{-4} mm Hg
Acenaphthene		83-32-9	154	3.92	2.5×10^{-3} mm Hg
Fluorene		86-73-7	166	4.18	3.2×10^{-4} mm Hg
Phenanthrene		85-01-8	178	4.57	1.21×10^{-4} mm Hg
Anthracene		120-12-7	178	4.54	2.67×10^{-6} mm Hg
Pyrene		120-00-0	202	5.18	4.5×10^{-6} mm Hg
Fluoranthene		206-44-0	202	5.22	9.22×10^{-6} mm Hg
Benzo(a)anthracene		56-55-3	228	5.91	1.54×10^{-7} mmHg
Chrysene		218-01-9	228	5.91	6.23×10^{-9} mm Hg
Benzo(b)fluoranthene		205—99-2	252	5.80	5.0×10^{-7} mm Hg
Benzo(k)fluroanthene		207-08-9	252	6.00	9.7×10^{-10} mm Hg
Benzo(a)pyrene		50-32-8	252	5.91	5.49×10^{-9} mm Hg
Dibenzo(ah)anthracene		53-70-3	278	6.75	9.55×10^{-10} mm Hg
Indeno(123-cd)pyrene		193-39-5	276	6.50	1.3×10^{-10} mm Hg
Benzo(ghi)perylene		191-24-2	276	6.50	1.0×10^{-10} mm Hg



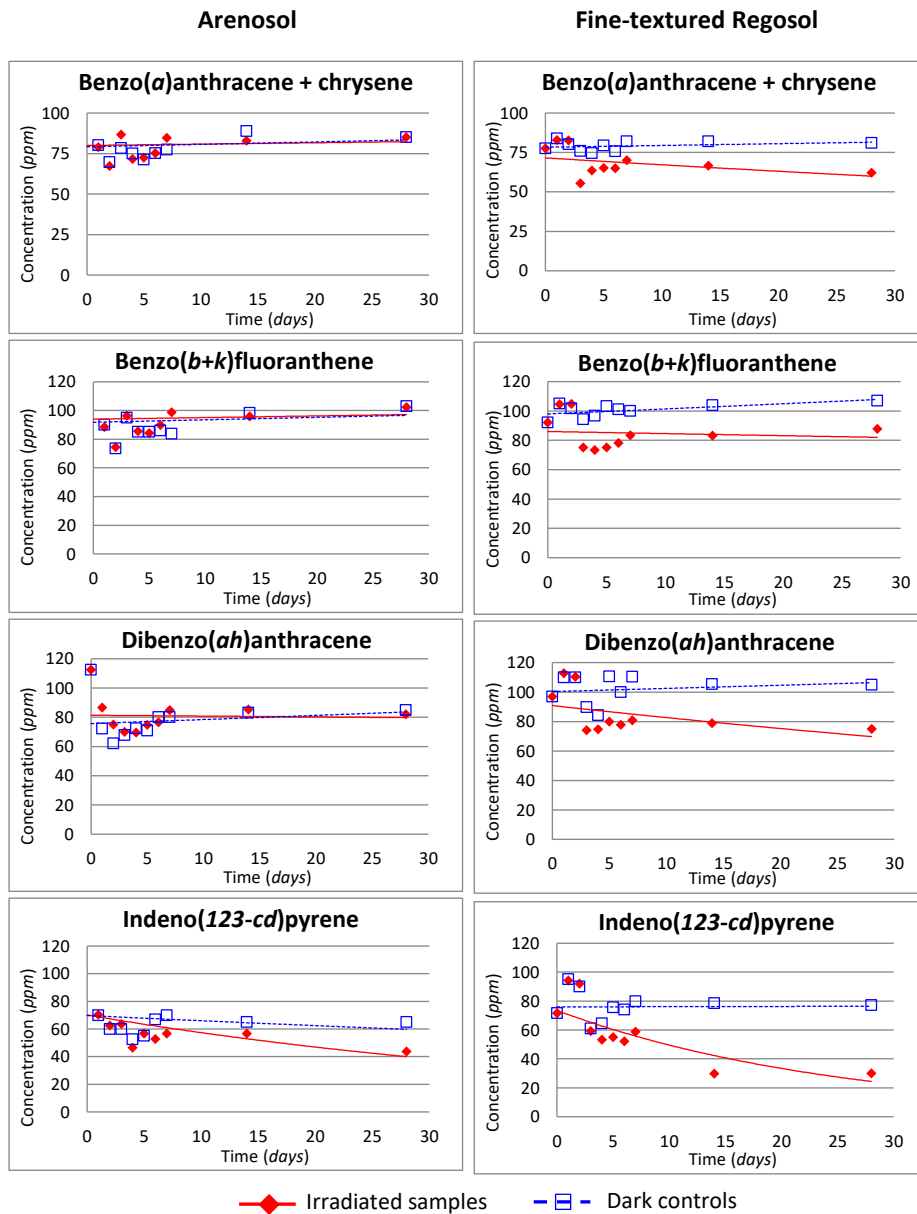
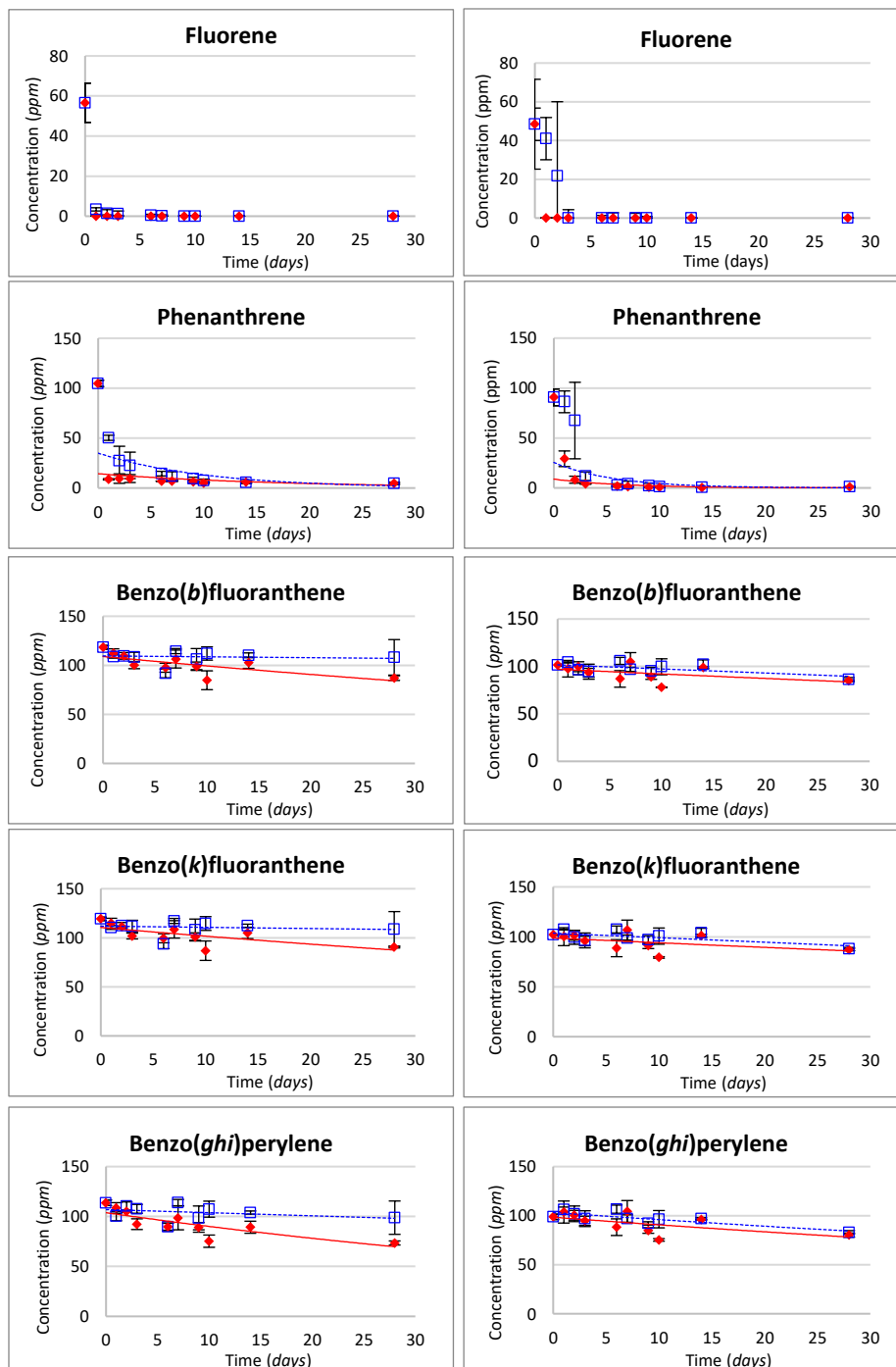


Fig. S1. Concentration of various PAHs in irradiated and dark control soil samples.

ANNEX 2 – Supporting information chapter 3

Oxide Absence (OA)

Oxide Presence (OP)



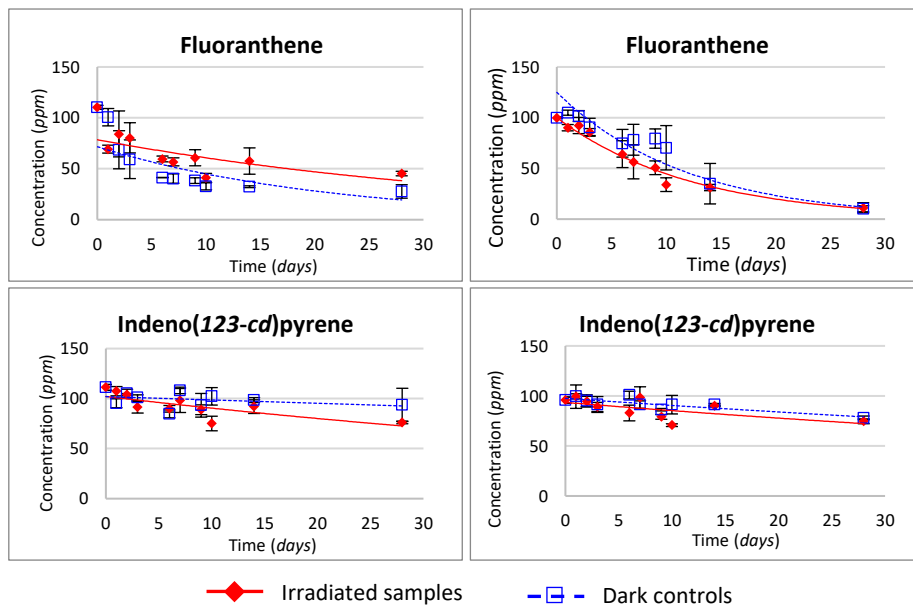


Fig S1. Concentration trend of some 3-, 4-, 5-, and 6-ringed PAH in the absence (OA) and presence (OP) of Fe_2O_3 . Error bars represent the average Standard deviations (SD) of triplicates.

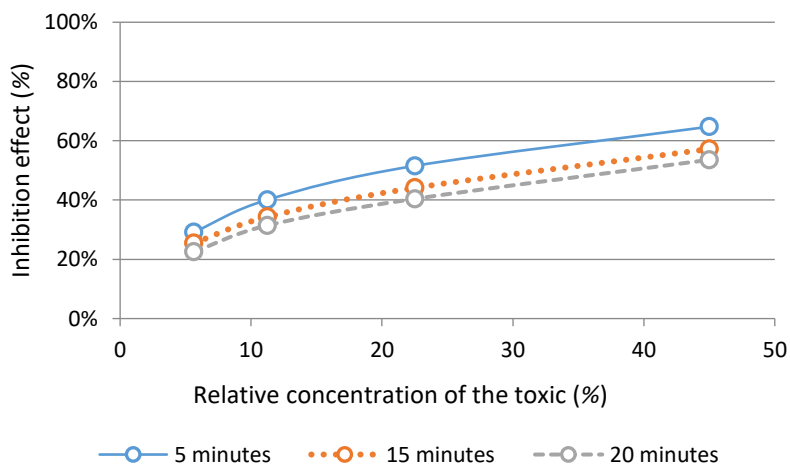
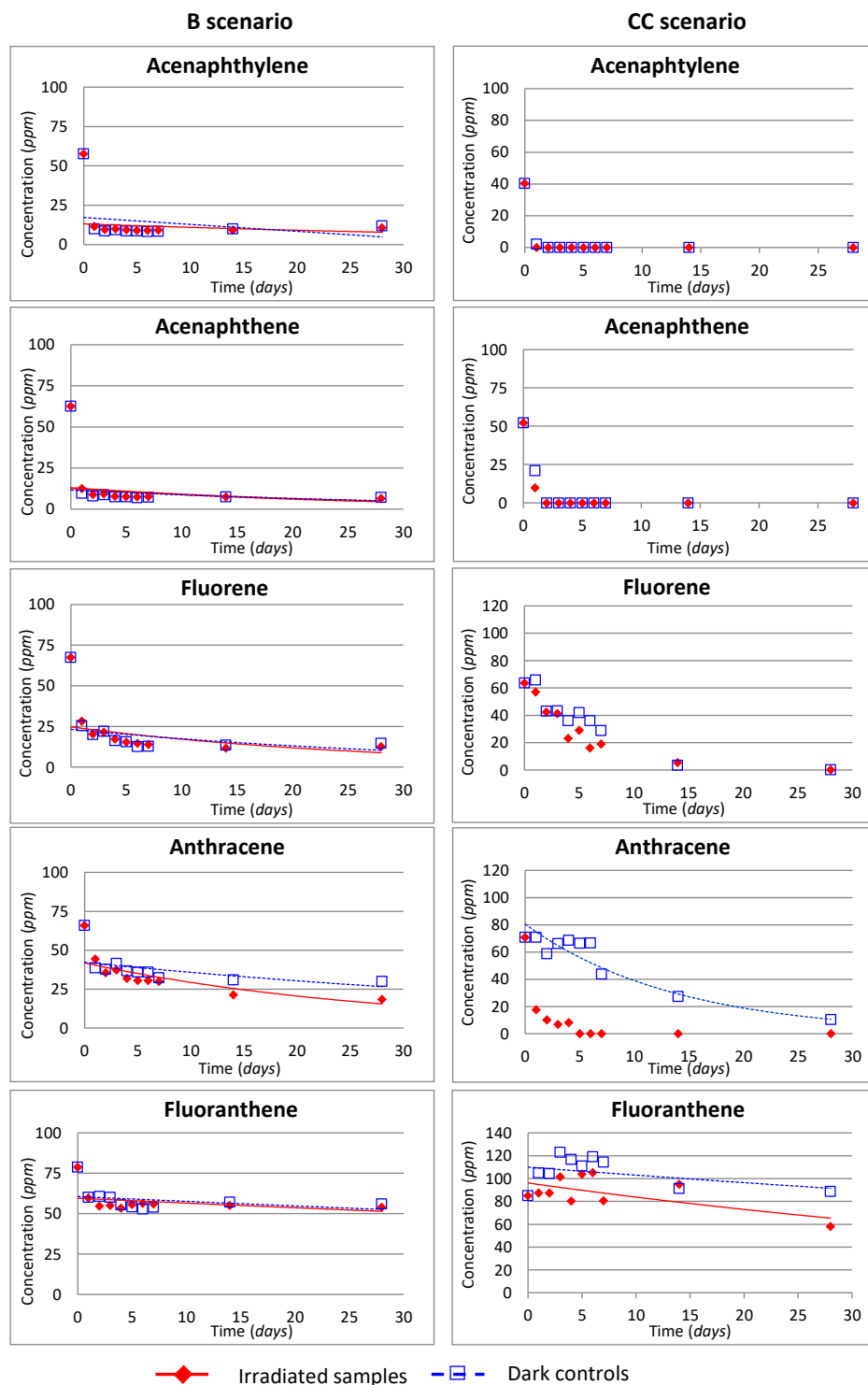


Fig S2. Toxicity values at different times of exposure, according to the Microtox[®] test.

ANNEX 3 – Supporting information chapter 4



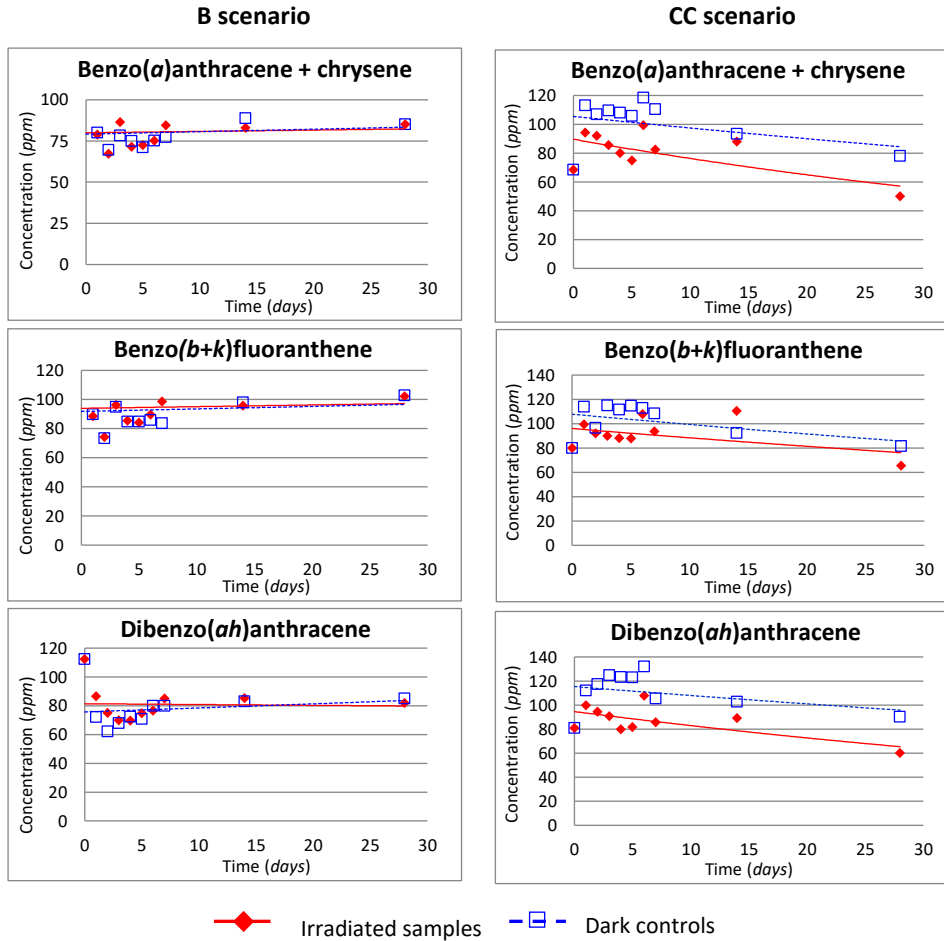
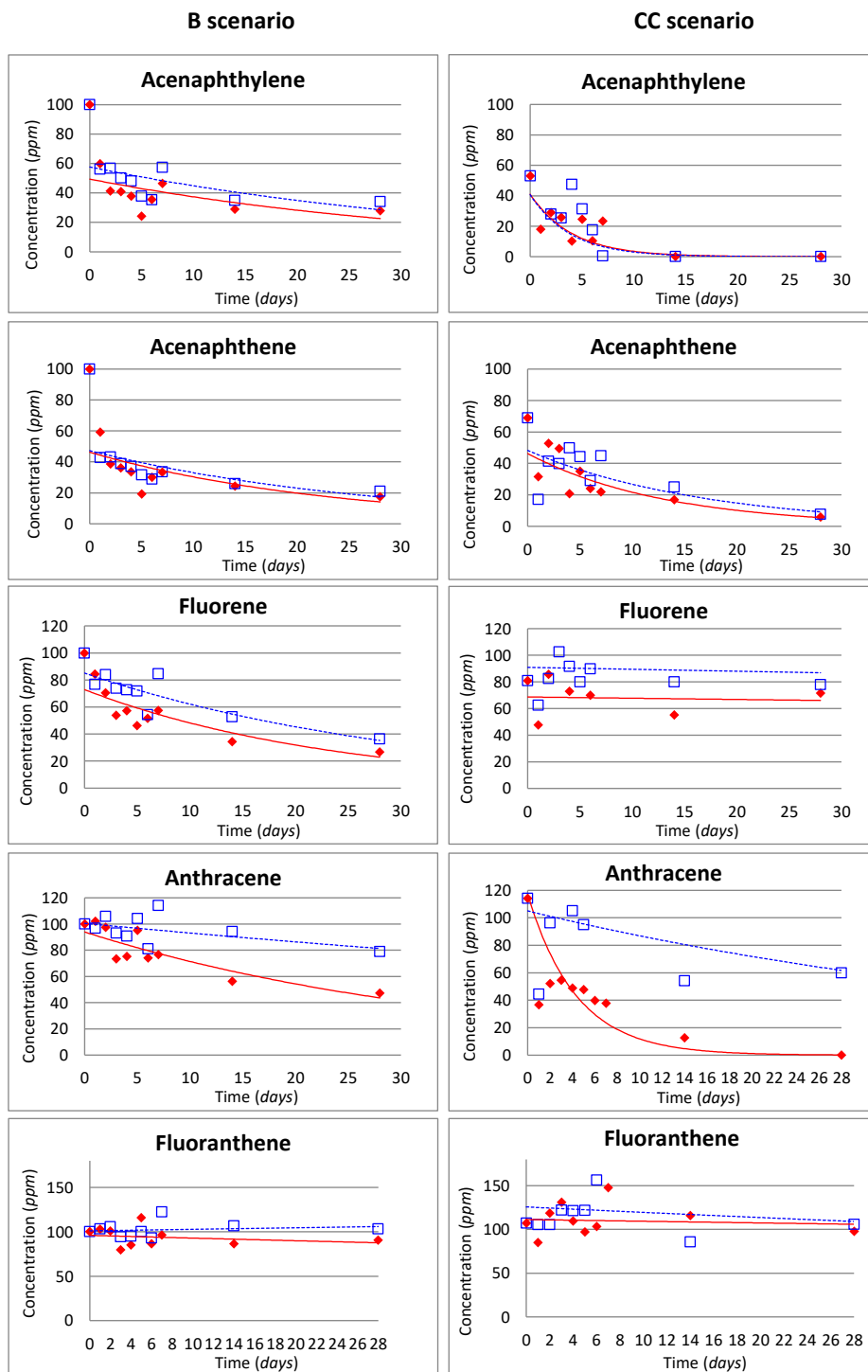


Fig. S1. Concentration trends of various PAHs in irradiated and dark controls in Arenosol soil.



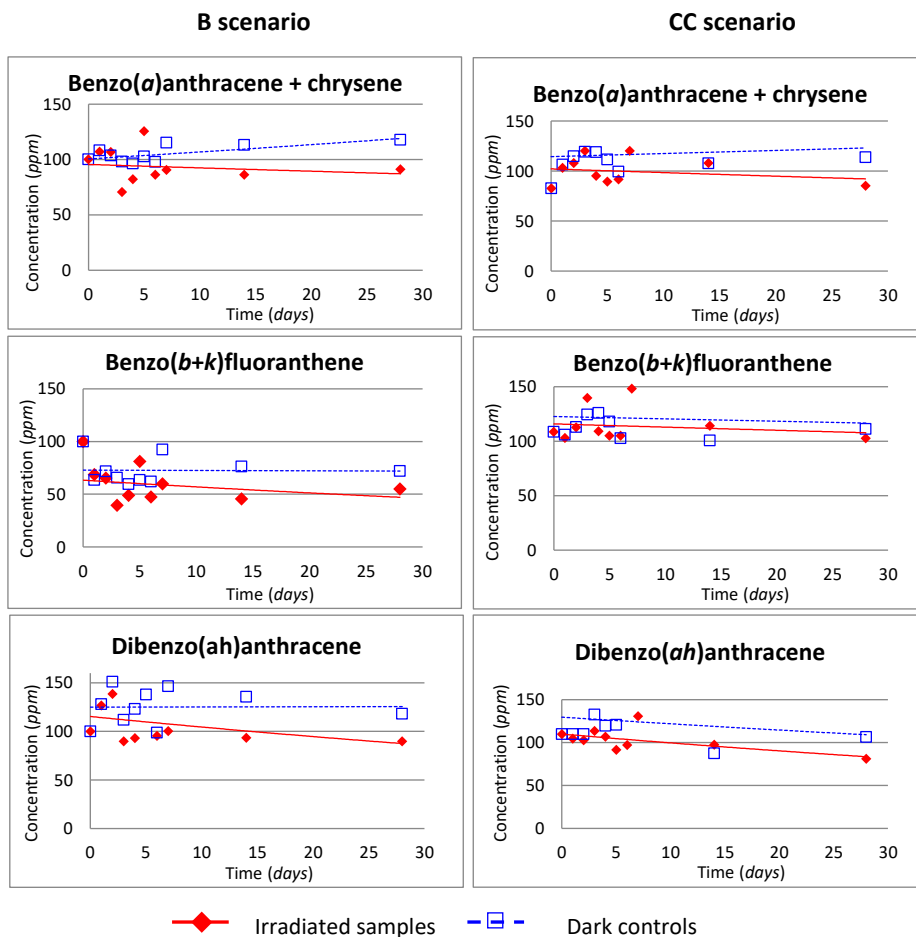


Fig. S2. Concentration trends of various PAHs in irradiated and dark controls in fine-textured Regosol soil.

ANNEX 4 – Supporting information chapter 5**Table S1.** Recoveries (%) of each PAH and and labeled PAH in Arenosol and fine-textured Regosol soil.

	Arenosol	Fine-textured Regosol
Naphthalene	34.5 ± 12.6	35.4 ± 27.2
Acenaphthylene	54.4 ± 6.3	75.5 ± 7.4
Acenaphthene	73.6 ± 9.6	88.2 ± 3.6
Fluorene	82.0 ± 8.4	96.8 ± 8.0
Phenanthrene	87.4 ± 7.9	102 ± 8.5
Anthracene	75.0 ± 6.2	97.0 ± 11.9
Fluoranthene	87.8 ± 7.5	101 ± 9.4
Pyrene	87.6 ± 7.3	102 ± 9.9
Benzo(<i>a</i>)anthracene	91.5 ± 11.0	102 ± 2.6
Chrysene	96.1 ± 12.6	107 ± 0.9
Benzo(<i>b</i>)fluoranthene	94.1 ± 10.2	105 ± 3.9
Benzo(<i>k</i>)fluoranthene	94.9 ± 9.3	104 ± 2.4
Benzo(<i>a</i>)pyrene	83.8 ± 8.0	94.1 ± 7.6
Benzo(<i>ghi</i>)perylene	97.8 ± 11.2	109 ± 7.0
Dibenzo(<i>ah</i>)anthracene	106 ± 11.6	117 ± 5.4
Indeno(<i>123-cd</i>)pyrene	102 ± 11.1	110 ± 4.9
<i>d</i> ₈ -naphthalene	25.7 ± 12.1	30.3 ± 25.5
<i>d</i> ₁₀ -acenaphthene	94.3 ± 10.6	110 ± 1.1
<i>d</i> ₁₀ -phenanthrene	119 ± 7.5	134 ± 20.1
<i>d</i> ₁₂ -chrysene	96.6 ± 10.9	104 ± 3.1
<i>d</i> ₁₂ -perylene	82.0 ± 5.8	83.8 ± 4.3

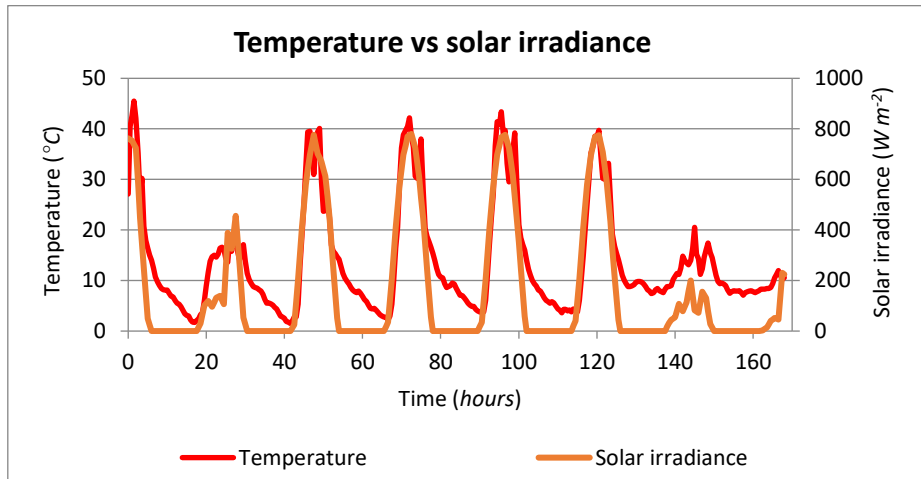


Fig. S1. Temperature and global solar irradiance over the experiment.

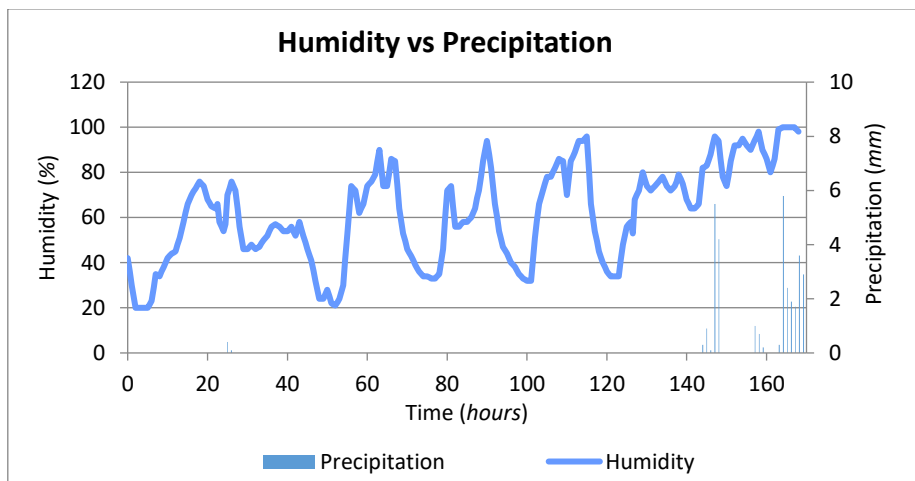
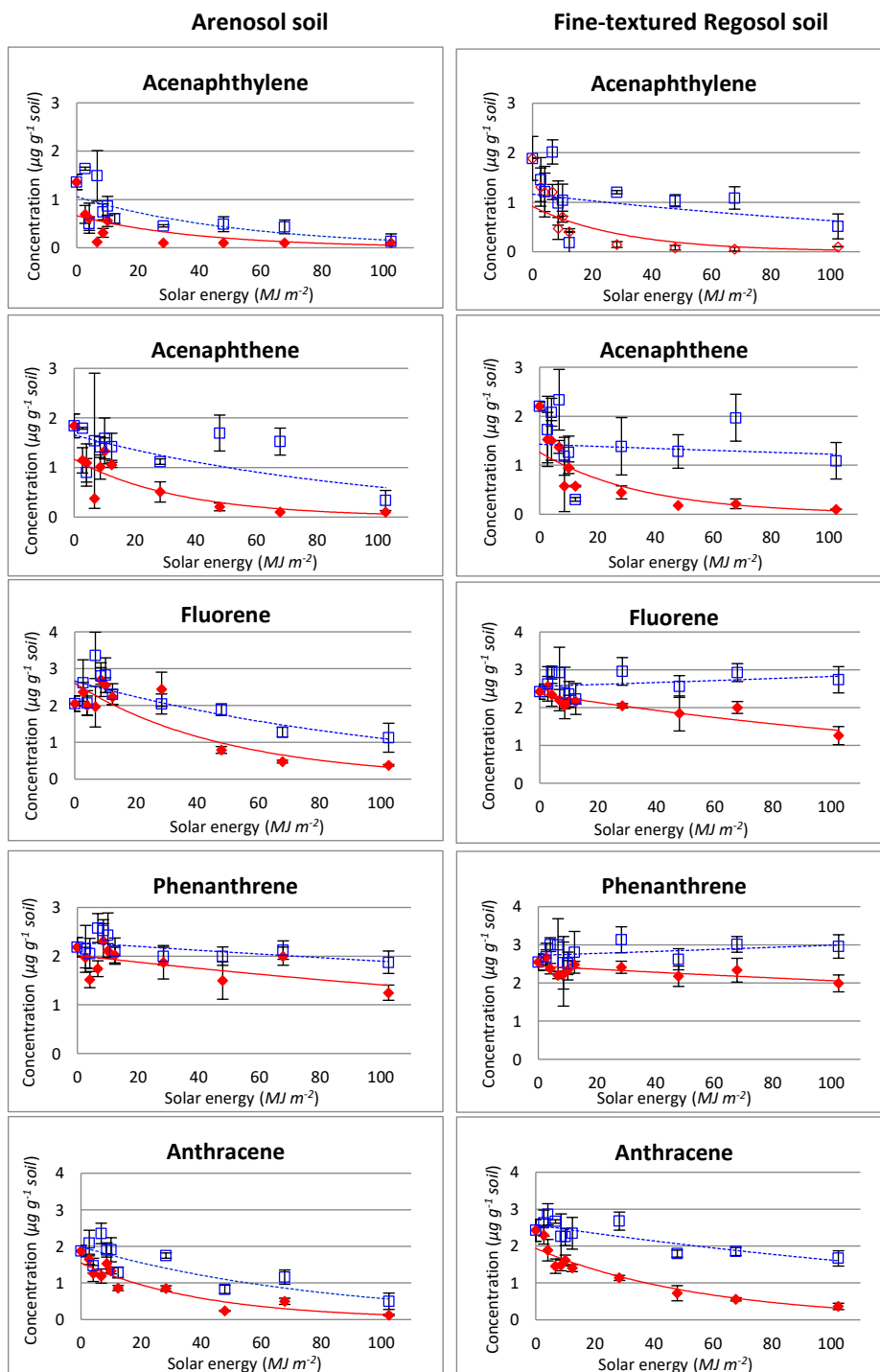
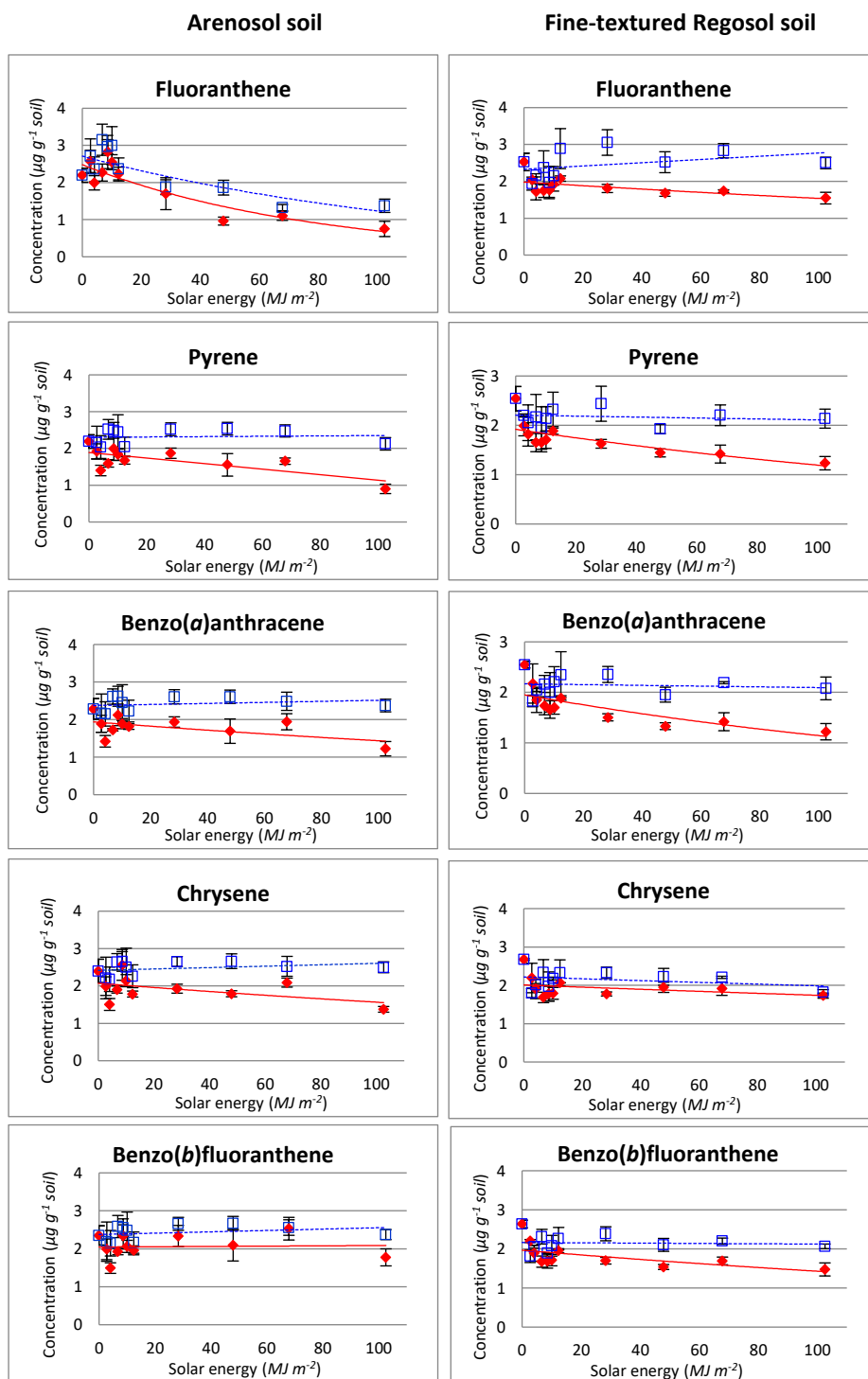


Fig. S2. Humidity and precipitation over 1 the experiment.



◆ Irradiated samples □ Dark controls



◆ Irradiated samples □ Dark controls

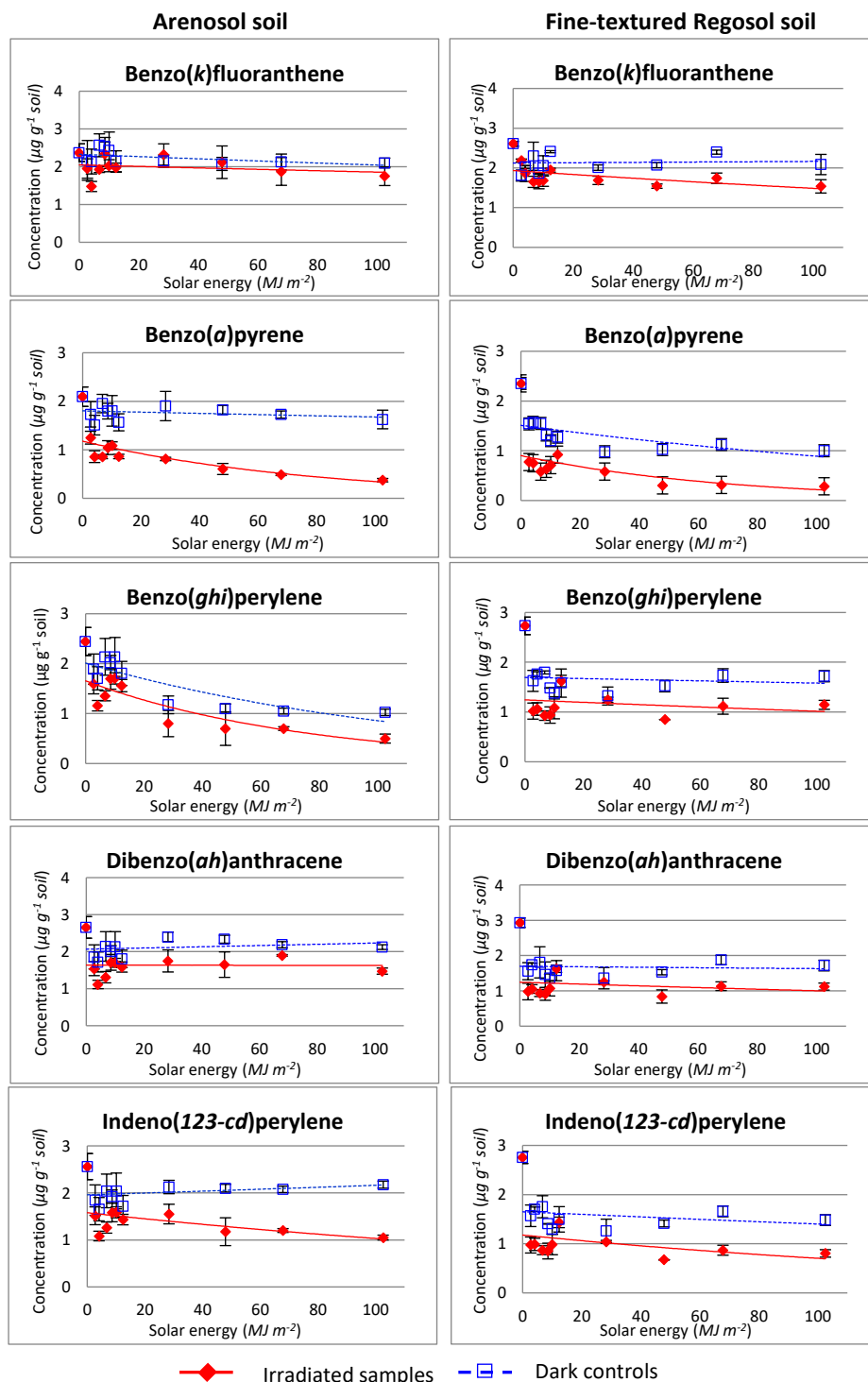


Fig. S3. Concentration trends of 16 PAHs under study in Arenosol soil (left) and fine-textured Regosol soil (right). Each point is the average of triplicates of samples. Bars indicate standard deviations between them.

ANNEX 5 – Supporting information chapter 6

Table S1. Retention time and quantitative and qualitative transitions acquired for the studied compounds, with collision energy (CE) and dwell time applied.

Compound	rT (min)	Segment	Precursor ion (m/z)	Product ion (m/z)	Dwell time (ms)	CE (V)	Relat. Response (%)
d ₄ -1,4-Dichlorobenzene	3.34	1	150	115	100	10	100
				87	100	10	0.6
				78	100	40	85.3
d ₈ -Naphthalene	5.48	2	136	108	50	30	100
				84	50	30	54.1
				82	50	30	41.8
Naphthalene	5.53	2	128	102	50	30	100
				78	50	30	61.1
				77	50	30	51.1
Acenaphthylene	9.20	3	152	151	100	20	100
				150	100	30	38.5
				126	100	30	38.1
d ₁₀ -Acenaphthene	9.55	4	164	162	50	30	100
				160	50	30	51.4
				134	50	50	8.9
Acenaphthene	9.64	4	153	152	50	20	100
				151	50	40	17.5
				77	50	40	10.6
d ₁₀ -Fluorene (IS)	10.89	5	174	172	50	30	100
				170	50	40	94.4
				122	50	30	78.3
Fluorene	10.97	5	166	165	50	20	100
				139	50	40	5.6
				115	50	40	8.0
d ₁₀ -Phenanthrene	13.30	6	188	160	50	30	100
				184	50	30	67.3
				158	50	40	60.0
Phenanthrene	13.37	6	178	152	50	30	100
				176	50	40	89.2
				151	50	40	65.0
Anthracene	13.52	6	178	152	50	30	100
				176	50	40	89.2
				151	50	40	65.0
Fluoranthene	16.43	7	202	200	150	40	100
				201	150	30	96.2
Pyrene	16.98	7	202	200	150	40	100
				201	150	30	96.2

Compound	rT (min)	Segment	Precursor ion (m/z)	Product ion (m/z)	Dwell time (ms)	CE (V)	Relat. Response (%)
Benzo(a)anthracene	20.07	8	228	226	50	40	100
				224	50	60	13.0
				200	50	60	7.8
d ₁₂ -chrysene	20.08	8	240	236	50	40	100
				212	50	30	25.1
				208	50	30	0.8
Chrysene	20.17	8	228	226	50	40	100
				224	50	60	13.0
				200	50	60	7.8
Benzo(b+k)fluoranthene	22.68	9	252	250	100	40	100
	22.69			248	100	60	11.0
	224			100	60	13.2	
Benzo(a)pyrene	23.37	10	252	250	50	40	100
				248	50	60	11.0
				224	50	60	13.2
d ₁₂ -benzo(a)pyrene (IS)	23.48	10	264	260	50	40	100
				236	50	40	23.6
				232	50	60	17.5
d ₁₂ -perylene	23.52	10	264	260	50	40	100
				236	50	40	14.2
				232	50	60	10.0
Dibenzo(ah)anthracene	25.85	11	278	276	50	40	100
				274	50	60	16.7
				250	50	60	6.5
Indeno(123-cd)pyrene	25.89	11	276	274	50	40	100
				275	50	30	43.0
				272	50	60	8.8
Benzo(ghi)perylene	26.60	11	276	274	50	40	100
				275	50	30	43.0
				272	50	60	8.8

Table S2. Geoaccumulation index (Igeo) for all sampled soils.

	Cu	Zn	Cd	Hg	As	V	Cr	Pb	Ni	Mn	Co	Sn	Tl	Be	Mo
P1	-1.98	-0.74	-1.44	-2.01	-1.55	-3.88	-2.48	-1.60	-1.02	-0.57	-1.01	-5.27	-3.15	-1.48	-1.79
P2	-2.04	-0.92	-1.55	-3.30	-1.92	-3.83	-2.43	-1.77	-0.95	-1.07	-0.95	-6.36	-3.13	-1.61	-1.98
P3	-0.94	-0.06	-1.24	1.41	-1.09	-3.54	-1.84	-0.80	-0.40	-1.26	-0.73	-3.22	-2.56	-1.39	-1.13
P4	-1.70	-0.81	-1.93	-2.96	-1.71	-3.77	-2.70	-1.93	-0.97	-1.08	-1.01	-6.35	-2.68	-1.51	-2.25
P5	-2.01	-0.87	-1.33	-2.97	-1.79	-3.77	-2.34	-1.73	-0.88	-1.06	-0.93	-5.17	-3.04	-1.42	-1.96
P6	-1.37	0.19	-1.19	0.66	-1.99	-3.43	-2.52	-0.65	-0.97	-1.86	-1.10	-4.25	-1.42	-0.68	-2.23
P7	-0.89	-0.44	-1.49	-0.04	-2.20	-3.13	-1.48	-1.26	-0.51	-2.94	-0.67	-2.24	-2.07	-0.32	-1.84
P8	-2.44	-2.72	-3.49	-3.80	-3.07	-4.56	-3.31	-3.07	-2.05	-0.52	-2.13	-8.32	-2.19	-2.17	-3.81



UNIVERSITAT
ROVIRA i VIRGILI